12/2-9-96 950(1)

DOE/METC-96/1021, Vol. 2
(DE96000552)

Proceedings of the Environmental Technology Through Industry Partnership Conference Volume II

Vijendra P. Kothari

October 1995

U.S. Department of Energy
Office of Environmental Management
Office of Science and Technology
Morgantown Energy Technology Center
Morgantown, West Virginia

Disclaimer

DOE/METC-96/1021, Vol. 2
(CONF-9510108)
(DE96000552)

Proceedings of the Environmental Technology Development Through Industry Partnership Conference Volume II

Technical Coordinator
Vijendra P. Kothari

Sponsored by

U.S. Department of Energy
Morgantown Energy Technology Center
P.O. Box 880
Morgantown, WV 26507-0880
(304) 285-4764
FAX (304) 285-4403/4469
http://www.metc.doe.gov/

October 3-5, 1995

Contents

Volume I

Session 1 — Opening Session

Poster Session I

Session 2 — Mixed Waste Characterization, Treatment, and Disposal Focus Area

Session 3 — Decontamination and Decommissioning Focus Area

* **No paper was submitted.**

Volume II

Poster Session II

Session 4 — Contaminant Plume Containment and Remediation, and Landfill Stabilization Focus Areas

Appendices

* **No paper was submitted.**

Poster Session II

PII.1 The LASI High-Frequency Ellipticity System

Ben K. Sternberg (BKS@MGE.ARIZONA.EDU; 602-621-2439)
Mary M. Poulton (MARY@BLUE.MGE.ARIZONA.EDU; 602-621-8391)
Laboratory for Advanced Subsurface Imaging
Dept. of Mining & Geological Engineering
Mines Bldg. #12, Room 229
University of Arizona
Tucson, AZ 85721

Abstract

A high-frequency, high-resolution, electromagnetic (EM) imaging system has been developed for environmental geophysics surveys. Some key features of this system include: (1) rapid surveying to allow dense spatial sampling over a large area, (2) high-accuracy measurements which are used to produce a high-resolution image of the subsurface, (3) measurements which have excellent signal-to-noise ratio over a wide bandwidth (31 kHz to 32 MHz), (4) large-scale physical modeling to produce accurate theoretical responses over targets of interest in environmental geophysics surveys, (5) rapid neural network interpretation at the field site, and (6) visualization of complex structures during the survey.

Introduction to EM System

Ground Penetrating Radar (GPR) has been shown to be a powerful tool for environmental investigations. Unfortunately, in many areas the attenuation of radar energy is much too great for radar to be effective. In the southwestern United States, for example, the depth of penetration of radar energy in basin-fill sediments is typically only one meter. In order to reliably obtain a usable depth of penetration for environmental investigations, it is necessary to use lower frequencies than are normally used in GPR investigations.

A high-frequency EM imaging system that overcomes the depth restrictions of ground penetrating radars is being developed for the frequency range 31 kHz to 32 MHz. The system is an extension of an existing imaging system which has a frequency range of 30 Hz to 30 kHz (Sternberg et al., 1991). The 31 kHz-to-32 MHz frequency range is necessary to provide high resolution over the range of depths that are of interest in environmental geophysics surveys.

High-Resolution Subsurface Electromagnetic Imaging System

Figure 1 shows a block diagram of the high-frequency EM imaging system. We currently transmit 11 frequencies sequentially in binary steps over the range 31 kHz to 32 MHz. The transmitter uses a sinusoidal signal supplied from the receiver via a fiber-optic cable. The signal is amplified by a power amplifier and sent to a narrow-band tuned transmitter coil. The

Research sponsored by the U.S. Department of Energy's Morgantown Energy Technology Center, under Contract No. DE-AC21-92MC29101-A001 with the Laboratory for Advanced Subsurface Imaging; Dept. of Mining & Geological Engineering; Mines Bldg. #12, Room 229; Univ. of Arizona; Tuscon, AZ 85721.

signal is amplified by a power amplifier and sent to a narrow-band tuned transmitter coil. The tuning is automatically controlled with digital signals supplied via a second fiber-optic cable from the receiver. Fiber-optic cables are required to avoid interference from the transmitter directly into the receiver as would occur if a metallic wire were used between the transmitter and receiver.

The signals are received at transmitter/receiver separations of generally 2 to 8 meters using a tuned three-axis receiving coil. The signals from each axis are amplified by a preamplifier on the coil frame, conveyed to programmable filters and programmable amplifiers, and then digitized by a 100 MHz digitizing oscilloscope. The programmable filters, amplifiers and tuning are all controlled automatically via RS232 interface from an environmentally sealed and ruggedized computer. A waveform generator provides a calibration signal to the calibration coil located on the receiver coil. A second channel on the waveform generator provides the signal for the transmitter through the fiber-optic link. The digitizer and waveform generator are controlled via GPIB interface. The waveform generator and digitizer are precisely synchronized through a timing clock connection. The data from the receiver coil are signal-averaged, filtered and relayed to an interpretation workstation via an RF telemetry link. The interpretation workstation is located in a remote recording truck. The workstation uses neural networks (described in a later section) and displays the data for interpretation in the field.

The receiver modules are mounted on an all-terrain vehicle (ATV) (Figure 2a). The transmitter modules are mounted on a second ATV (Figure 2b). These ATVs are 6-wheel drive, amphibious vehicles, and can handle extremely rough terrain. The transmitter coil is located on a boom in front of one ATV. Ahead of or off to the side of the transmitter ATV is the receiver ATV with the receiver coil located on a boom extending out the back.

We have chosen to calculate ellipticity of the magnetic field from the observed magnetic field quantities. Hoversten (1981), in a comparison of time- and frequency-domain EM sounding techniques, showed that the frequency-domain ellipticity measurement is superior to any other frequency-domain or time-domain measurement for EM soundings. He also showed that "the ellipticity measurement provides smaller parameter standard errors than the time-domain data". "In addition, the model parameters arrived at through the least squares inverse are much less correlated with each other when ellipticity is used."

We define H_x as the component of the magnetic field in the direction along the survey line. H_y is in the direction perpendicular to the survey line, and H_z is the vertical component. If the transmitter is emitting a sinusoidally varying signal, the total magnetic field at the receiver will trace an ellipse in the XZ plane as a function of time. The ellipticity is defined as the ratio of the major to minor axes of the ellipse.

$$e = \left| \frac{H_2}{H_1} \right|$$

The ellipticity (e) can be determined directly from measurements of the relative magnitude and phase of the H_x and H_z fields.

$$e = \left| \frac{H_Z \cos\alpha - H_X \sin\alpha}{H_Z \sin\alpha + H_X \cos\alpha} \right|$$

where:

$$\tan(2\alpha) = \frac{2|H_z|\cos[\phi_z - \phi_x]}{1 - |H_z|^2}$$

and ϕ_z and ϕ_x are phases of vertical and horizontal components of the total field. The ellipticity measurement is discussed in Spies and Frischknecht (1991).

A number of novel features are included in the system design:

1) The calibration coil supplies a calibration signal to the receiver coil at the same time that the data are being collected. The calibration coil is coupled equally to all three axes of the receiver coil. It is parallel to the x-axis coil over one quadrant, then follows the y-axis coil for another quadrant, then the z-axis coil for a quadrant, and continues on around completing a closed loop. This allows equal calibration signals on all three receiver axes simultaneously with the data measurement. The cal-coil driver has a high output impedance so that the calibration coil does not interfere with the received signal. Four calibration frequencies are transmitted, which are offset slightly in frequency from the data frequency and surround the data frequency. The system response at the data frequency is then interpolated from these four nearby frequency responses. A key feature is that the calibration is performed simultaneously with the data acquisition, thereby preventing any errors due to drift in the system response, as well as greatly increasing the speed of data acquisition. This procedure is known as AFCAL (Adjacent Frequency CALibration). It is an adaptation of the HASCAL method (High-Accuracy Simultaneous CALibration) described by Sternberg and Nopper (1990).

The motivation for making as high an accuracy measurement as possible is based on previous publications which show that if we were able to obtain unlimited precision in our measurements, we would be able to uniquely determine the variation of conductivity with depth. For example, Fullager (1984) investigated horizontal-loop frequency soundings and demonstrated that these methods "are, in principle, imbued with unlimited resolving power". Unfortunately, only a small amount of error in the measured electromagnetic fields can lead to a large amount of error in the interpreted subsurface resistivity structure. Our goal is to obtain as high-accuracy measurements as possible.

A further requirement for obtaining high resolution is the need to obtain data over a large and densely sampled spatial area and at many frequencies. The entire data acquisition process in this system is totally automated. A complete sounding may be made in less than one minute. Therefore, dense spatial sampling can be obtained, as well as rapid surveys of large areas. The wide bandwidth of this system fulfills the need for many frequencies. Although we certainly will not obtain unlimited resolution, we believe that the approach used in this system will provide greatly increased resolution over the current state-of-the-art.

(2) Both the transmitter and receiver coils have been optimized to obtain highly accurate data over a wide bandwidth. The coils consist of nested segments with increasing area and increasing number of turns in the outer coils for the lower frequencies.

Therefore, adequate sensitivity is obtained over the entire bandwidth. A great deal of effort has gone into the design of these coils; in particular, each coil segment is decoupled from the surrounding nested coils and each coil segment has been optimized for a particular frequency range.

(3) The standard procedure for calculating ellipticity uses just H_z and H_x. However, for high-accuracy measurements we also record the H_y component perpendicular to the transmitter-receiver line and determine the ellipticity from all three vectors. This method uses a mathematical rotation of the observed magnetic fields to the major and minor axes of the ellipse and is described in Bak et al. (1993). Basically, this procedure first determines the azimuth of the electromagnetic field polarization and then determines the ellipticity of this azimuth. The mathematical rotation greatly speeds up the measurement of ellipticity in comparison with mechanically orienting the receiver coils, which is a very time-consuming process. The coil can simply be placed on the ground in any orientation and the rotation algorithm automatically rotates the field components to the major and minor axis values of the magnetic-field ellipse.

(4) This system records in a frequency range which includes effects from both conduction currents and displacement currents. It is difficult to obtain reliable numerical modeling calculations of theoretical responses to complex targets in this frequency range. We have adopted a different procedure which involves the use of full-size physical models. A large modeling tank has been constructed at our test site in Avra Valley, Arizona, west of the University of Arizona campus (Figure 3). The tank is 20 m long by 3 m deep by 6 m wide. The transmitter and receiver coils are kept stationary to avoid variations in response due to background effects. Various targets are then moved in the tank along a profile line under the coils. Repeated measurements are made with the targets at different depths, orientations, and with different types of targets. This allows us to generate a large number of theoretical model responses for data interpretation, including neural network training.

Introduction to Data Interpretation

The two fundamental components of the automated interpretation scheme are the neural networks and the data visualization shell. The data visualization shell provides the user interface to the neural networks, graphs of sounding curves, 1D forward modeling program, images of the data, and interpreted sections The only interaction the user has with the trained neural networks is the selection of the networks to use for the interpretation through the visualization shell.

The data interpretation system makes possible a first-pass, real-time interpretation with neural networks directly in the field. The acquired ellipticity data are transferred immediately after the acquisition computer finishes recording one sounding, via a wireless telemetry system from the acquisition computer on the survey line to the interpretation computer in the truck. Each incoming sounding is automatically stored in the background of the program, and from then on is available for display and interpretation.

The user selects all the networks through which the data should be routed. Each network interpretation is passed to a 1D forward model-

ing program so the ellipticity curves can be compared to the measured data. The fit of each interpreted sounding to the field data is calculated as the mean-squared error for the 11 frequencies in each sounding. The user decides which network gives the best fit and the interpretation is plotted in a 2D section.

We have created 48 separate neural networks to do the 1D interpretation. On a 486 50 MHz PC, the neural network interpretation for one transmitter-receiver separation using 16 networks takes less than one second. To run four networks and compute the forward models for each to find the best fit to the field data takes less than one minute. Currently the interpretation system can only produce 1D interpretations. Time constraints and lack of 3D modeling capability have prevented the creation of a training set for 3D targets under this phase of the work. We hope to be able to implement an object location mode in the next phase of work. We also hope to include networks that use all three transmitter-receiver separations simultaneously.

Neural Network Interpretation

Ellipticity data are transferred from the field data acquisition computer via the RF telemetry link to the data interpretation computer housed in the field truck. The data interpretation consists of neural networks operating in mapping mode (1D) and object location mode (3D, not yet implemented). Our approach to the neural network processing is to divide the interpretation into many parts and use several small networks. The interpretation system currently uses three different transmitter-receiver offsets of 8m, 4m, and 2m. Fifteen separate networks are used for each offset for a total of 45 networks. A total of 29,714 models were used for training. Two network paradigms were used for training, a radial basis function algorithm and a modular neural network algorithm. The networks perform parameter estimation. Each network is capable of producing an interpretation in a few milliseconds on a 486 PC.

Mapping Mode. In mapping mode we have two categories of networks: halfspace nets and layered-earth nets. The piecewise apparent resistivity nets, 10 for each separation, fit a halfspace model to each frequency pair in a sounding. The apparent resistivity nets use all 11 frequencies to fit one halfspace model. The main difference between the two is that if there is a frequency dependence for conductivity, the apparent resistivity nets will do a better job of fitting the data. The halfspace networks are trained on models ranging from 1 to 10,000 ohm meters using a radial basis function algorithm.

The layered-earth networks interpret two- and three-layer models. Each layer-case is further subdivided into resistive-over-conductive or conductive-over-resistive networks depending on the relationship between the first two layers. We found this division to be important in increasing the accuracy of the networks. Modular neural networks are used for the layered-earth interpretations. Many different algorithms were tried but only the modular network could produce accurate enough results for both thickness and resistivity. The estimated model parameters for each selected net are input to a forward-modeling code and ellipticity curves are generated for each. The ellipticity curves are plotted along with the field data and the mean-squared error is calculated for each interpretation versus the field data. The user can then select the best fit model and use that for the interpretation. In Figure 4 we show the fit of a three-layered earth network to a model consisting of a 30 ohm meter layer, 0.4m thick, over a 10 ohm meter layer, 0.6m thick, over a 500 ohm

m layer. The network fit is perfect even though it estimates the lower layer resistivity at 405 ohm m.

Several important issues remain to be resolved prior to final implementation of the neural networks for this frequency range. The effect of the dielectric constant becomes significant from 1 MHz and higher. The modeling code we have used to date does not include a dielectric constant. A new modeling code developed under the DOE VETEM project does have the capability to model a changing dielectric constant at high frequencies but the accuracy of the code has not been fully verified with our system yet. The frequency dependence of both dielectric and conductivity also has not been accounted for directly in our modeling. We have some capability to see the frequency effect on conductivity with our piecewise apparent resistivity networks but have no such capability in the layered-earth networks. If we can verify the accuracy of the program that models dielectric effects then our apparent resistivity networks can be remodeled and trained to output a dielectric constant for each frequency pair.

Object Location Mode. While we have not yet implemented an object location mode in the interpretation system, we have trained two backpropagation neural nets to classify data as target or background and to estimate the location of a target for a 4m transmitter-receiver separation. Training was performed using field data collected in May of 1994 with the prototype system. Nineteen soundings were used as training with 11 ellipticities used as input and the depth and offset of the target relative to the midpoint of the transmitter-receiver midpoint used as output. Location estimates were generally within one to fifteen centimeters. Classification of target vs. background was accomplished with 22 training samples, 6 representing background and 16 representing target responses. Three samples were withheld for testing. The net was 100% accurate for both the training and testing sets. Training time for both networks was under 5,000 iterations. Caution must be exercised in drawing conclusions from this exercise as a very limited training set was used.

Data Visualization Software

The Ellipticity Data Interpretation System (EDIS) was developed based on the Interactive Data Language (IDL) graphics software for WINDOWS on a personal computer (PC). EDIS goes far beyond the built-in routines of IDL; it also uses the IDL capabilities of interacting with DOS based programs, WINDOWS based programs and dynamic link libraries (DLL).

Display capabilities in EDIS are for sounding curves, interpreted sections, and raw ellipticity data. The user may select up to twelve sounding curves to display at one time. The difference between the last two selected curves is automatically displayed on a graph below the sounding curves. Interpreted data are displayed in 2D sections that show the color-coded resistivities. The y-axis of the sections indicates the thicknesses of the interpreted layers. Several sections can be displayed at one time for other offsets or lines. Raw ellipticity data can be displayed versus frequency number or skin depth. Future enhancements to the software will include more image processing capability for the ellipticity images, 3D block models of the ellipticity and interpreted data, file format transformations, improved plotting capability, preprocessing algorithms for 3D objects, and inclusion of tilt angle.

The field data can be displayed and compared to previous stations. Quality control

is performed by comparing combined neural network and forward-modeling results with the field data. After deciding on a particular neural network for the interpretation of a specific station the neural network results will be written to disk and can be used to build up a resistivity or ellipticity section interactively. Several printing options and utilities are also available within EDIS.

Future enhancements to the software will include more image processing capability for the ellipticity images, 3D block models of the ellipticity and interpreted data, file format transformations, improved plotting capability, and preprocessing algorithms for 3D objects.

Field Data

We collected field data over 55 gallon barrels buried at the Avra Valley Geophysical Test Site. Nineteen soundings were collected along profiles over a barrel buried 1.0 m deep and one buried 2.25 m. A 4 m transmitter-receiver offset was used for all of these measurements. A cross-section plot of the recorded ellipticity data over the shallow barrel is shown in Figure 5. This plot is a gridded image of the individual measurements along the profile line and shows the difference between the measurements over the barrel and an assumed background value (at 10 m from the midpoint). The barrel is located at the 0 m mark on this grid and the center of the barrel is at a depth of 1.0 m.

Figure 5 shows a broad diffuse anomaly due to the barrel. Figure 6 shows the results of the neural network interpretation. The neural network accurately predicts the depth and location of the barrel.

With a combination of (1) high-accuracy ellipticity measurements, (2) rapid, closely-spaced, wide-bandwidth soundings, and (3) in-field neural-network interpretation, we have been able to produce an accurate and cost-effective image of buried waste objects. We are currently conducting a series of demonstration surveys to determine the capabilities of this system for mapping buried-waste disposal pits.

Acknowledgments

This research was sponsored by the U.S. Department of Energy's Morgantown Energy Technology Center, under Contract No. DE-AC21-92MC29101 A001. The LASI high-resolution EM systems have evolved over many years. Support for this development has included: Electric Power Research Institute, The Copper Research Center, U.S. Geological Survey, U.S. Bureau of Mines, Department of Energy, U.S. Army, and University of Arizona.

References

Bak, N.H., 1992, Sternberg, B.K., Dvorak, S.L., and Thomas, S.J., 1993, Rapid, high-accuracy electromagnetic soundings using a novel four-axis coil to measure magnetic field ellipticity, J. Applied Geophysics, 30, 235-245.

Fullager, P.K., 1984, A uniqueness theorem for horizontal loop electromagnetic frequency soundings, Geophys. J. R. Astr. Soc., 559-566.

Hoversten, G.M., 1981, A comparison of time and frequency domain EM sounding techniques, Ph.D. Thesis, Univ. of California, Berkeley, 169 p.

Spies, B.R., and Frischknecht, F.C., 1991, Electromagnetic sounding, in: Electromagnetic Methods in Applied Geophysics, Vol. 2, M.N. Nabighian, ed., 285-425.

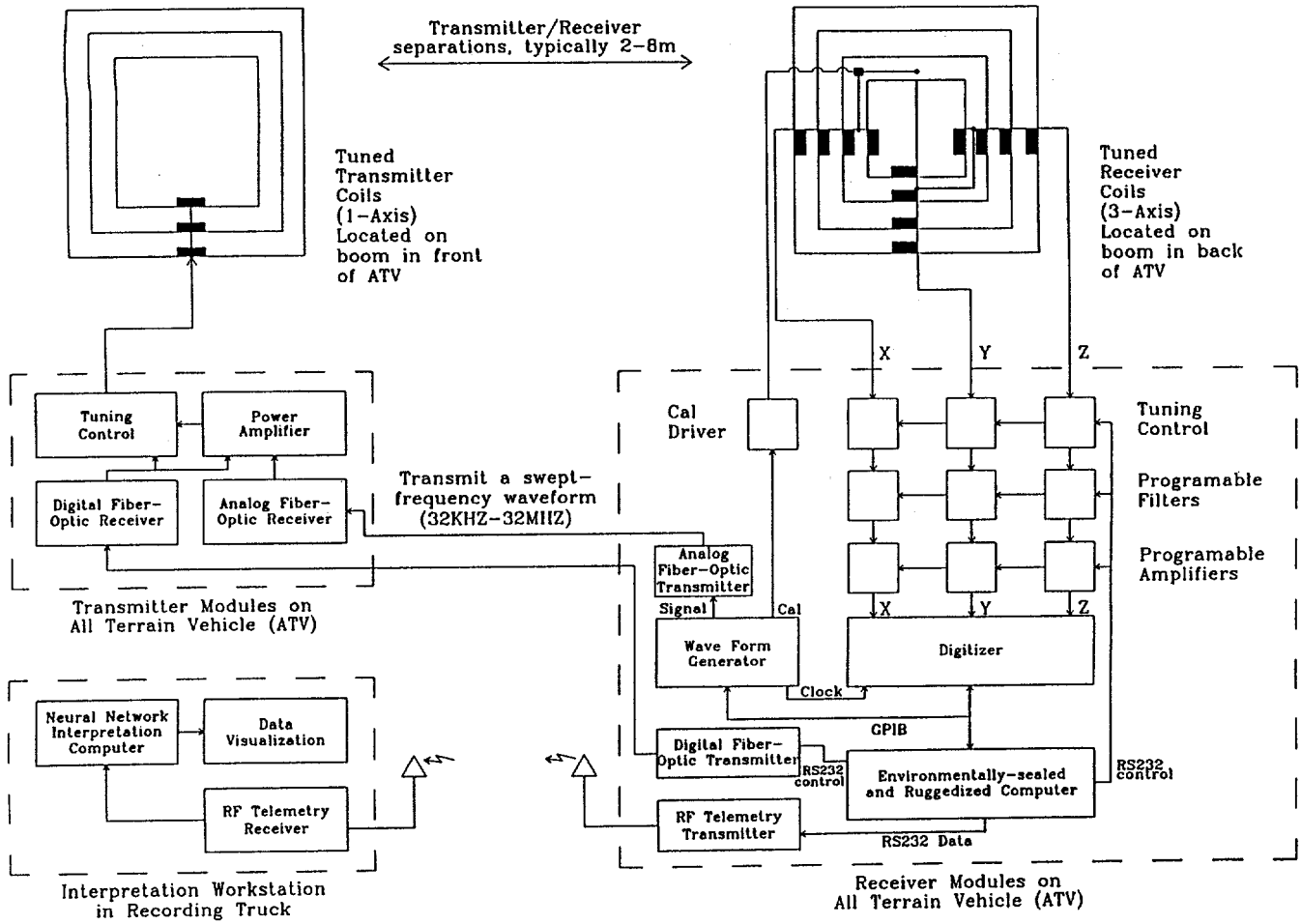

Figure 1. Block diagram of high-resolution ellipticity system.

Sternberg, B.K., and Nopper, R.W., 1990, High-accuracy simultaneous calibration of signal measuring systems, Meas. Sci. Technol., 1, 225-230.

Sternberg, B.K., Thomas, S.J., Bak, N.H., and Poulton, M.M., 1991, High-resolution electromagnetic imaging of subsurface contaminant plumes, EPRI, RP-2485-11, Palo Alto, CA.

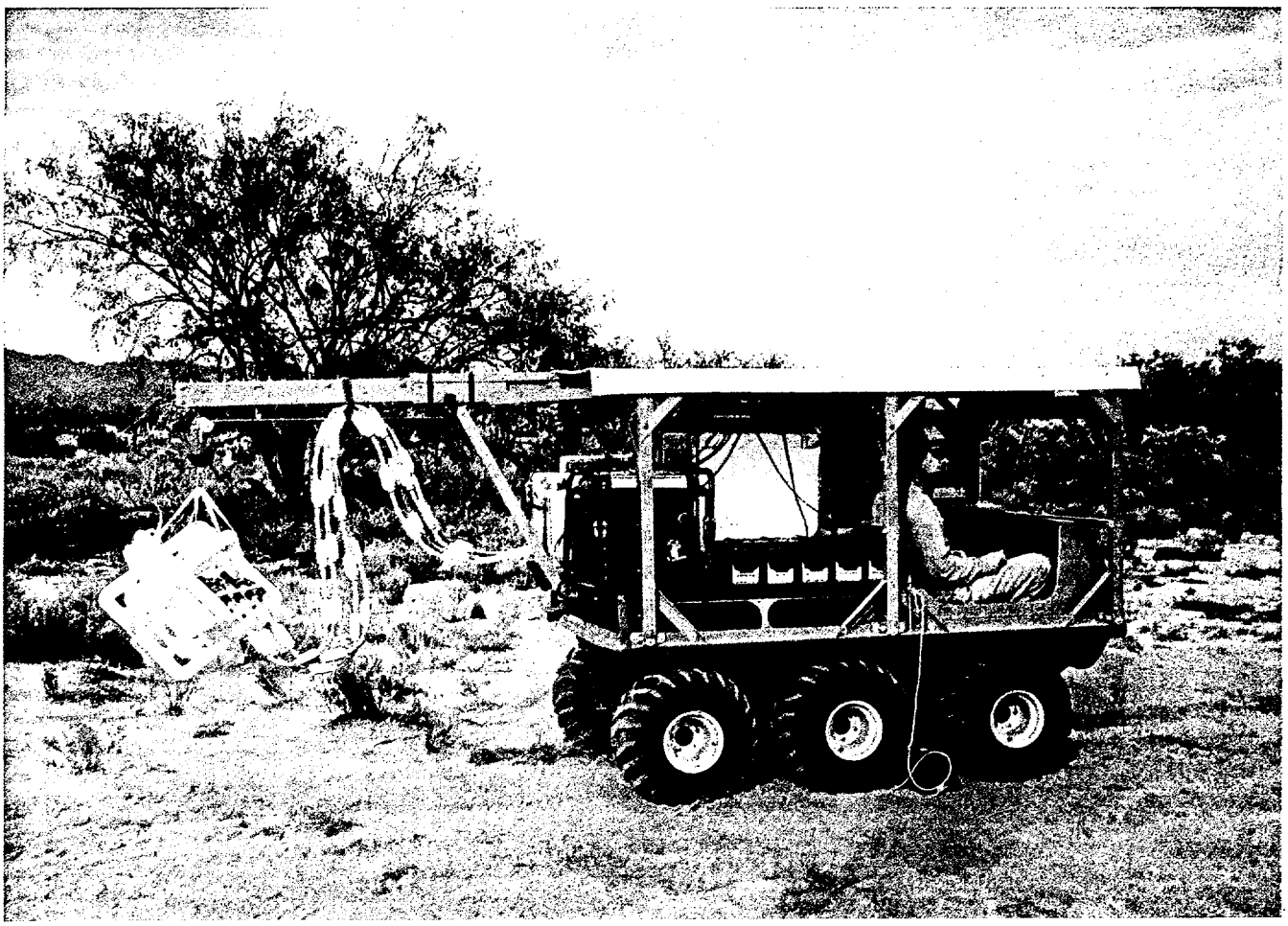

Figure 2a. **Photograph of the amphibious all-terrain field vehicle with the computer enclosure and receiver-module mounted on it.**

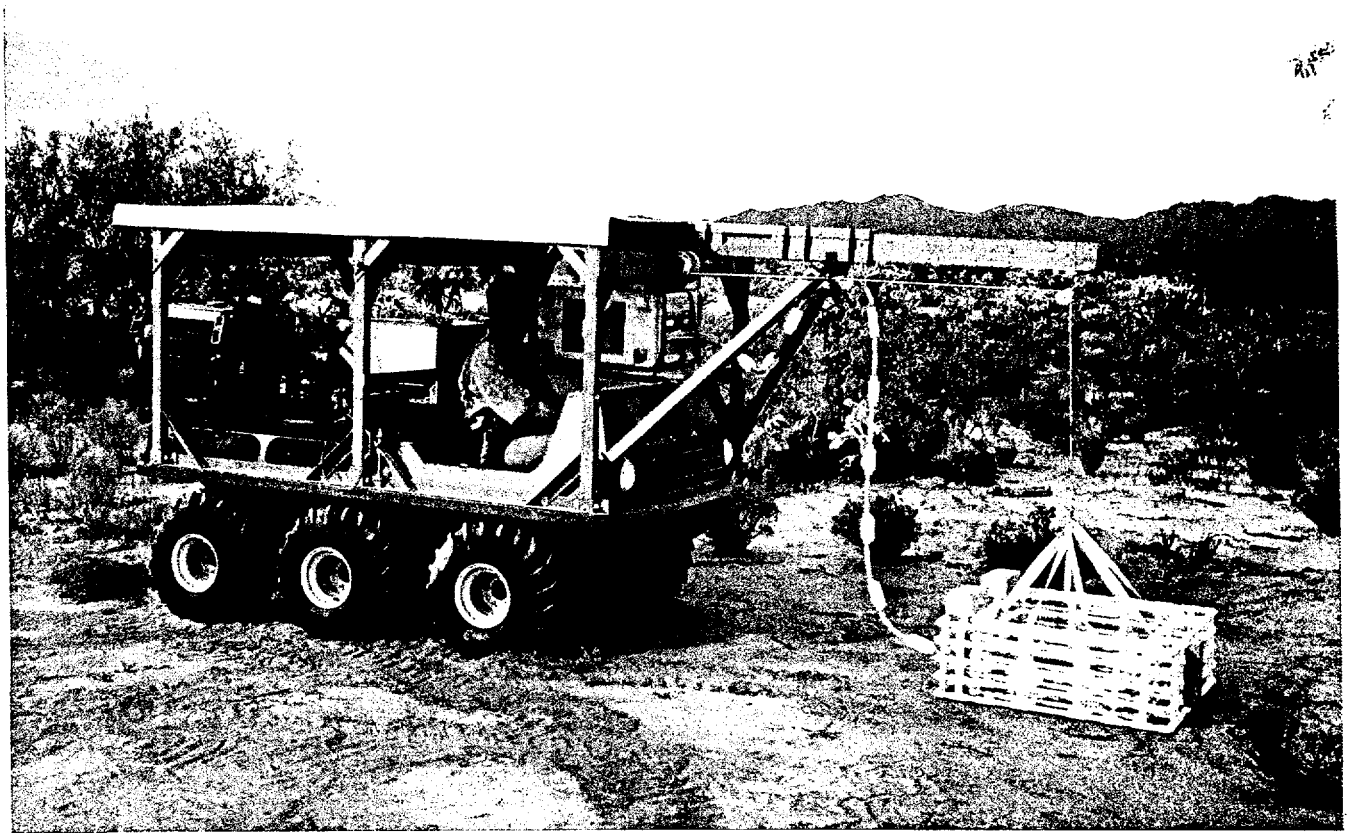

Figure 2b. **Photograph of the transmitter all-terrain vehicle with the transmitting antenna suspended from the boom in front of the ATV.**

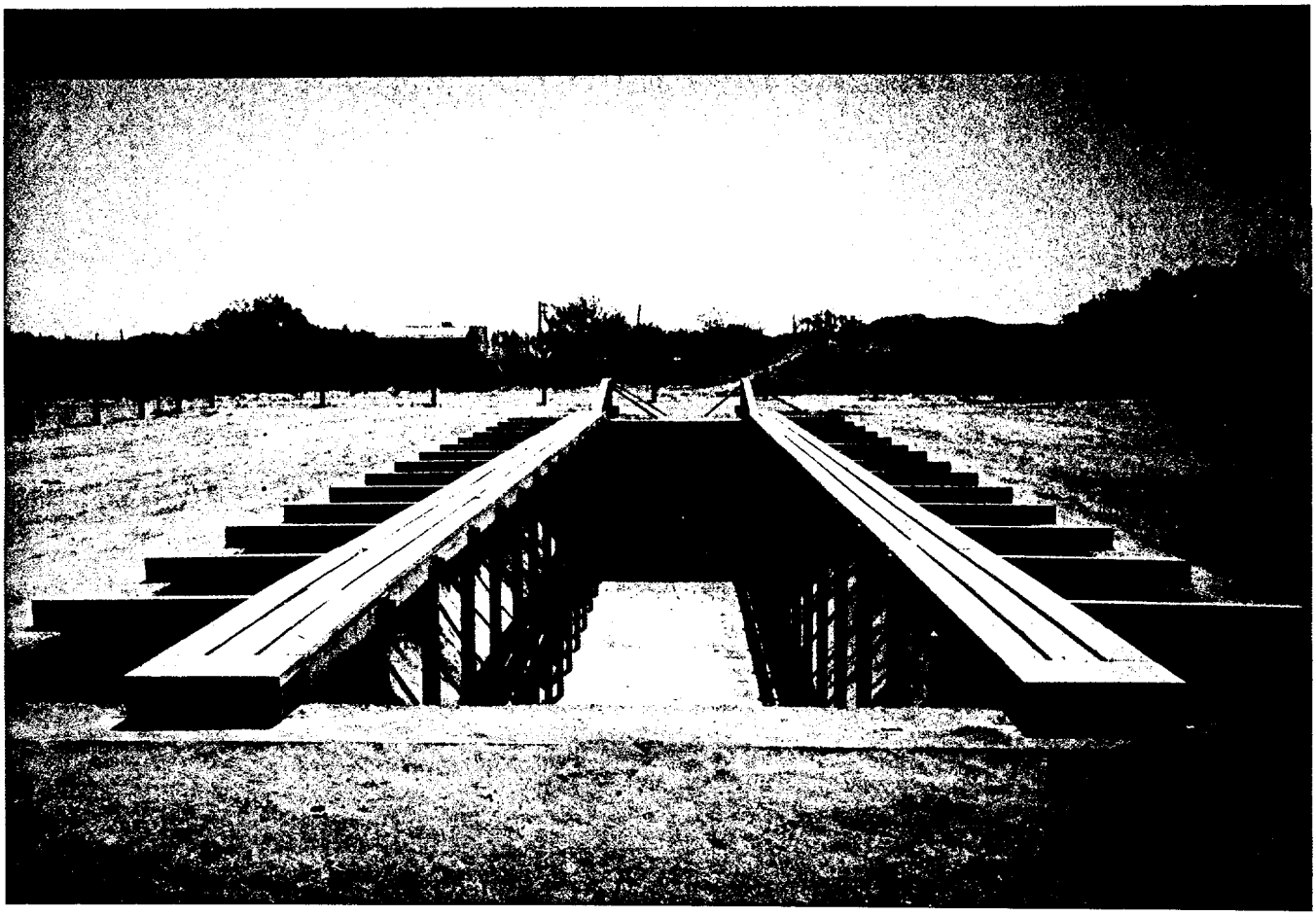

Figure 3. **Photograph of the completed physical modeling facility prior to filling with fluid. A trolley with targets suspended at various depths is moved down the length of the tank during the measurements.**

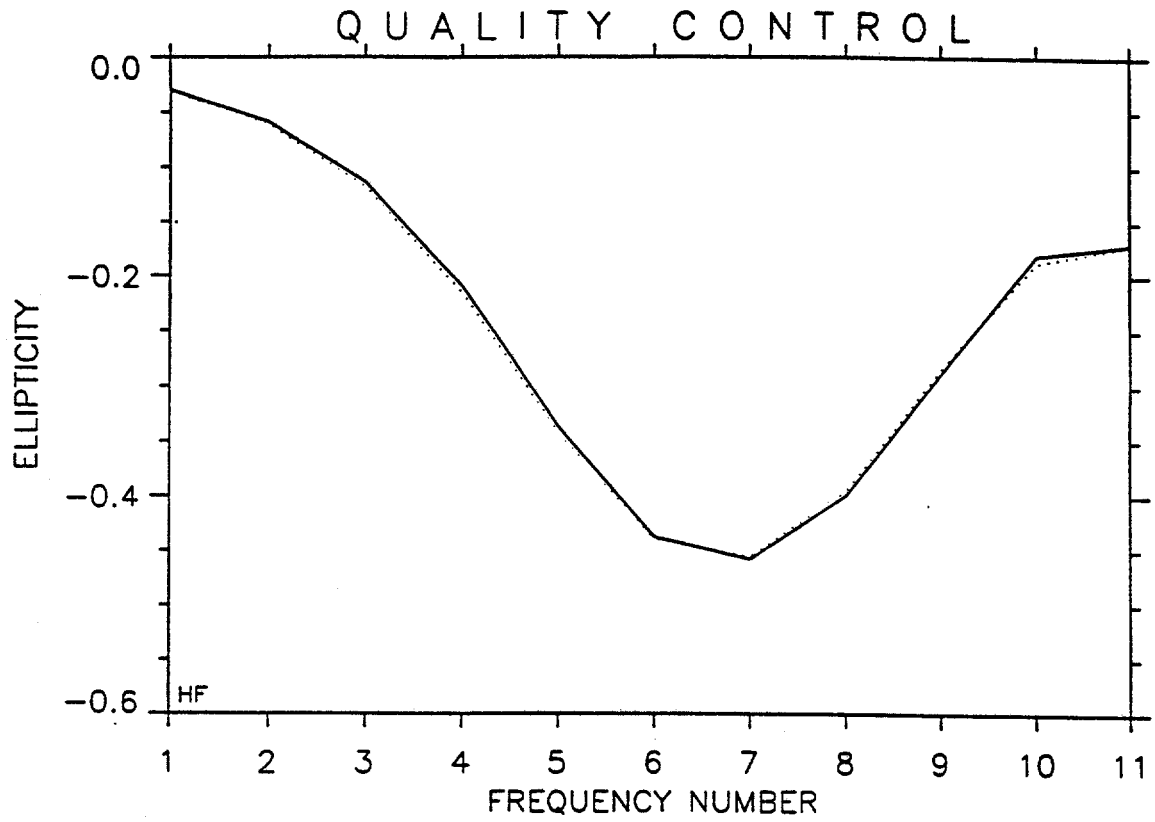

File: AAA003XX Station # 1 Sounding # 1 Quality: 1 X: 2000.00 Y: 0.00

NEURAL NET	RMS–Error	Linestyle	Neural Network Output Values				
Field Data :	0.0	Solid					
Three Layer R/C:	0.00126	Dotted	27.039	10.003	405.576	0.422	0.608

Figure 4. Graph showing the neural net (dotted line) fit of a three-layered earth model to test data (solid line). Desired model is 30 ohm meters over 10 ohm meters over 500 ohm meters with first layer thickness of 0.4m and second layer thickness of 0.6m. The neural net estimated parameters are shown in the lower right of the figure.

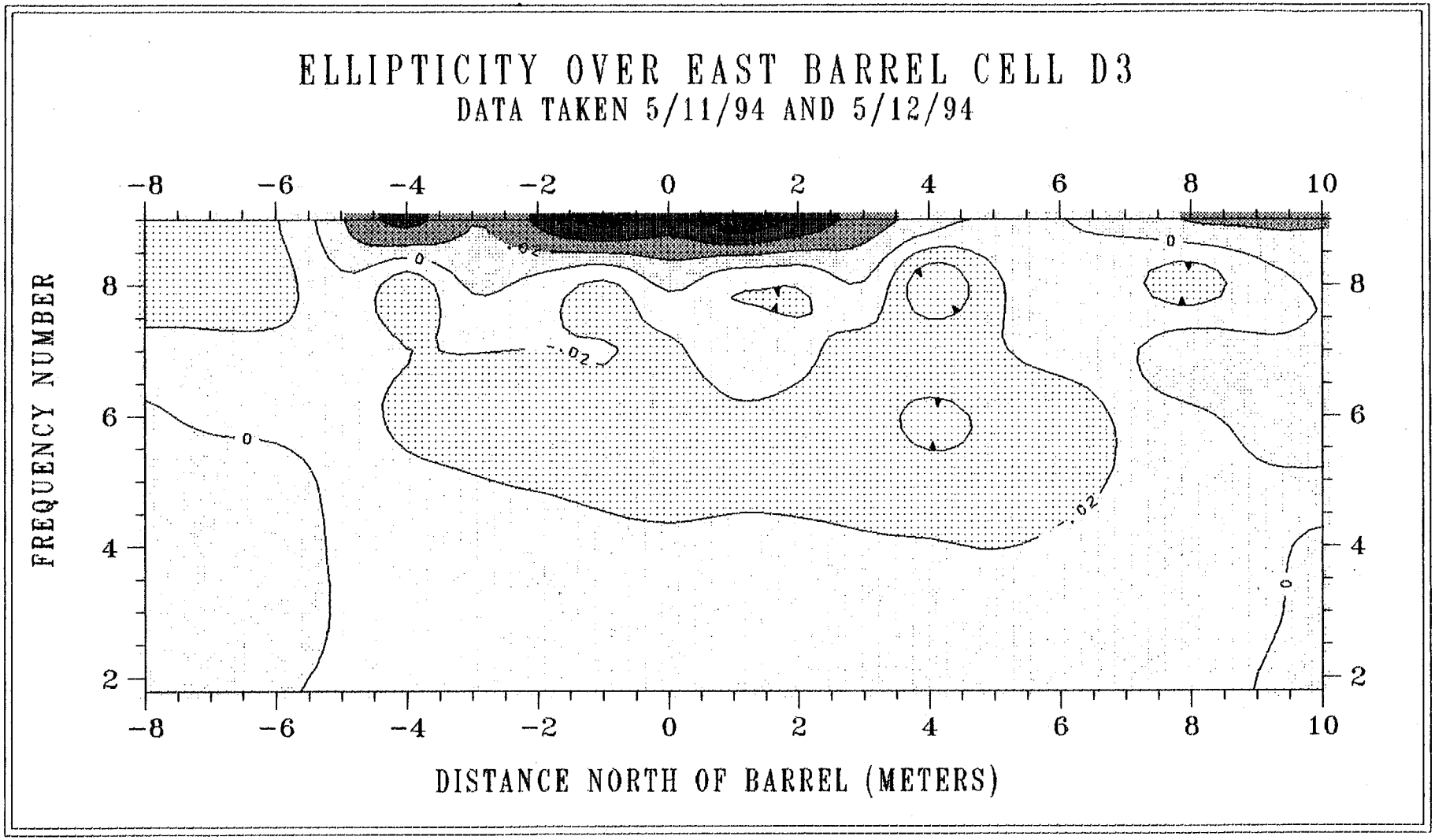

Figure 5. Cross-section plot of ellipticity data over a buried 55-gallon barrel. Log 10 frequency values are plotted on the vertical axis (8 MHz at the top, corresponding to very shallow depth, and 62 kHz at the bottom, corresponding to greater depth). The barrel is located at 0 m offset and 1.0 m depth to the center of the barrel.

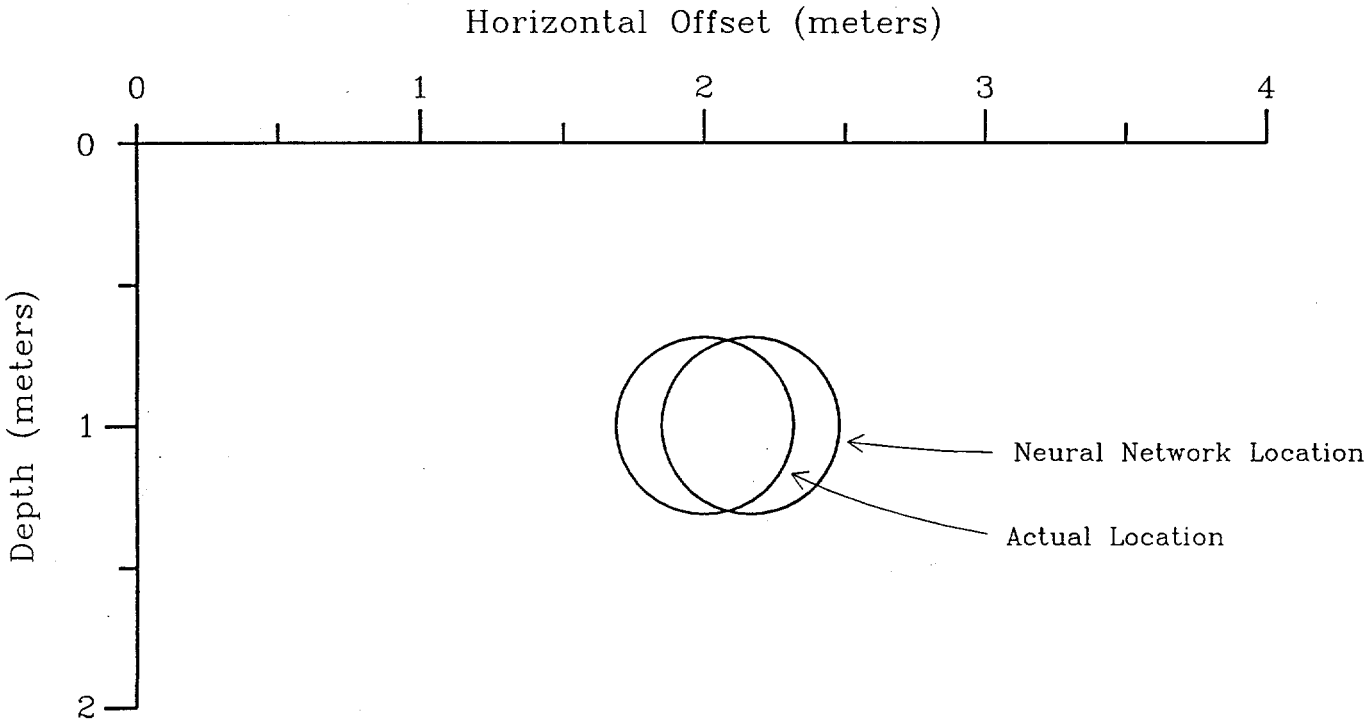

Figure 6. **Comparison of the actual location of one of the buried 55 gal. barrels and the Neural Network interpreted location**

PII.2 Analyze Imagery and Other Data Collected at The Los Alamos National Laboratory

N. David (david@erim.org; 505-982-9180)
Environmental Research Institute of Michigan (ERIM)
1701 Old Pecos Trail
Santa Fe, NM 87505

I. Ginsberg (ginsberg@erim.org; 313-994-1200 X3209)
Environmental Research Institute of Michigan (ERIM)
P.O. Box 134001
Ann Arbor, MI 48113-4001

Introduction

Unfortunately, areas of waste disposal at DOE sites are not all documented and located. There are a number of reasons for this situation: records have been lost or destroyed, the locations were not documented, and memories have been lost. The search of large areas at these sites for buried waste and buried-waste containers is a difficult and expensive problem when using conventional, ground-based methods. Typical conventional methods involve the drilling of wells/boreholes (point sampling), and interpolation is required to obtain the needed areal information.

Drilling for buried waste is expensive, potentially hazardous, and time-consuming, yet accurate interpolation can require a large number of holes per-unit-area. A similar problem is encountered in gaining current information about: the boundaries of toxic waste plumes in the ground, transport pathways, and the composition and concentration of toxic materials.

Research sponsored by the U.S. Department of Energy's Morgantown Technology Center, under Contract DE-AR21-95MC32116 with the Environmental Research Institute of Michigan, P.O. Box 134001, Ann Arbor, MI 48113-4001; (313)994-1200.

The purpose of this effort is to analyze existing imagery data collected under various Department of Energy and other programs. This analyses will be useful for screening, characterization, and monitoring work in the waste site remediation process.

Objectives

With drilling operations costing hundreds of thousands of dollars per hole, the reduction in the number of holes is of great concern. And just as importantly, safety must be a principal consideration when drilling to explore for unknown buried waste. Alternatives to conventional ground-based methods need to be evaluated. To consider alternatives an effort was begun to analyze existing remotely sensed data. By using remote sensing methods to reduce the ground area to be considered, the amount of actual drilling needed can be reduced.

The Los Alamos National Laboratory (LANL) is the initial test facility for the collection of remote sensing data from aircraft and satellite. The remote sensing data includes optical, multispectral, infrared and radar. This technique will survey large areas for underground structures (i.e. pipe lines, buried objects) and disturbed areas which provide information on contaminants and trench

locations. The Environmental Research Institute of Michigan (ERIM) was contracted to collect the data, choose sites of focus and perform special processing developed from defense and intelligence applications. The results have been presented to on-site managers for determining the site specific applications.

Approach

Remote sensing is a technology that is well suited to the surveillance of large areas for detecting and locating buried objects, mapping seepage from buried containers and detecting the boundaries of toxic plumes. Remote sensing provides spatially continuous information to achieve the accurate interpolation of point sampled data.

Image processing and data integration algorithms have been developed and validated under funding by defense and intelligence organizations. They have been applied to the detection of buried objects, vegetation stress, soil moisture and liquid migration, and change detection. The algorithms are based upon phenomenology that is also relevant to the detection, mapping, and monitoring of waste materials. ERIM has integrated these algorithms into a methodology that was applied to waste detection and characterization at DOE sites.

New analysis techniques did not need to be developed and tested to solve DOE waste problems. Many of the chosen sites had archival data available for analysis which include aerial photography, multispectral and infrared imagery, radar imagery, and nuclear radiometry. Those data have been collected by commercial and Government sensors, and span an appreciable time interval. The specific tasks are:

Site Selection and Data Collection: Choose test sites at LANL based on the applicability of remote sensing and availability of prior characterization data at a site. Collect existing imagery and other data for processing and interpretation.

Organization of Technical Workshops: Organize two technical workshops; one to identify problems for study focus and understand the needs from the user's point of view; and a second to review the results with the various technical personnel of the LANL weapon complex sites.

Data Processing and Interpretation: Perform processing of data using the techniques developed for defense and intelligence applications. Based on the results, produce demonstration materials--a brochure detailing the data collection schemes and processing techniques. Integrate the processing techniques with Environmental Restoration Program at LANL, and design a collection scheme for future use at the DOE sites.

Project Description

Status: The Environmental Research Institute of Michigan collected imagery and other data, chose sites of focus and performed special processing. Algorithms were applied to the detection of buried objects, vegetation stress, soil moisture, liquid migration, and change detection, mapping, and monitoring of waste materials.

Potential sites at LANL were chosen as important areas in need of help from remote sensing. Existing imagery from each area was reviewed and site managers collaborated on the concept for solutions. Preliminary processing of imagery was done for many site problems and the most fruitful are being produced in a brochure.

Data Available: Imagery data useful for this project include airborne multispectral Daedalus imagery collected over Los Alamos by EG&G/EM in 1994 and coincident natural color aerial photography; LANDSAT TM, SPOT and 1989 Russian KFA-100 satellite imagery; historical photographs since 1935, ground photos taken during the project and recent orthophotos. Other information includes airborne nuclear (gamma) surveys flown by EG&G/EM in 1994, digital map information, and engineering drawings of burial sites.

Site Selection Criteria: About 10 sites were sought so that at least 3 or 4 would produce useful results. The first technical workshop was held in Los Alamos to invite Los Alamos site managers to suggest and review potential sites. To be a candidate, a site had to satisfy 5 criteria:

1.) The Los Alamos Environmental Restoration Program feels that some problem needs to be solved at the site.

2.) Some problem at the site is amenable to a remote sensing solution, that is, image phenomenology is scientifically possible.

3.) A site manager will take an interest in the project, that is, will take the time and has the knowledge to help find a solution.

4.) Good ground truth is available so that the demonstration products are credible.

5.) Imagery at the right times, wavelengths, resolution, etc., is already available.

Sites Selected: Ten sites were selected at the workshop:

Rofer Site: Detecting and delineating relatively known and unknown trenches.

Mynard Site: Determining location and extent of seepage for septic drain fields and holes, buried cable and firing pits.

Becker Site: Displaying sampling areas by hydrologic category and contaminant concentration.

Glatzmeier Site: Assessing a linear array of circles marked by vegetative damage.

Rofer-2 Site: Detecting buried tubes remaining from hydrologic tests.

Koch Site: Evaluating faults and fractures beneath waste disposal areas, assessing vegetative and thermal anomalies.

Hoard Site: Locating pits and comparing to engineering drawings.

Mason Site: Assessing thermal hot spots in an asphalt cap; locating contaminated trenches, shafts and drains.

Whole Lab: Relating gamma radiation contours to known contaminated areas.

Wheat Site: Locating two old landfills, one known, one unknown.

After the workshop, 3 sites were eliminated. The Glatzmeier Site problem was resolved right after the workshop and was not considered an important enough application. At the Rofer-2 Site, ground disruption by recent environmental work severely degraded possibilities for a demonstration area. At the Wheat site only the low resolution lab-wide coverage was available so existing imagery was inadequate to address the problem.

Analysis Methods: Most of the actual image processing for the paper concentrated on

the Daedalus multispectral imagery. Since this imagery is not as intuitive as simple photographs, the image pre-processing of bands is described below. Once some basic softcopy multispectral images were constructed, a visual procedure was started, analyzing these images along with SPOT, Russian and Landsat satellite images, historical and concurrent aerial photographs, site maps and other ground truth. The phenomenology of the signature of the particular waste site problem guides the special processing of an image. Successful approaches for known trenches and objects are applied to those that are not known. Often no additional image processing or image analysis was needed on any one image, but information from more than one image or map needed to be fused to aid the site managers in assessing a problem. This is especially useful at waste sites when there are conflicting information sources concerning buried waste locations. Data fusion is also discussed below.

Multispectral Image Pre-processing: DOE conducts periodic flights over the waste site areas with aircraft operating the Daedalus AADS 1268 Multispectral Scanner and a 70mm aerial framing camera. These data are collected, analyzed and archived by EG&G/EM. The EG&G/EM data base permitted retrieval of flight logs and imagery of the flight lines covering the pre-selected sites.

A set of flight lines were selected from the collection on 24 June 1994. These included both daytime and pre-dawn collections. The daytime imagery contained eight bands. The nighttime imagery contained only thermal bands (high and low gain channels). Flight lines were collected at an altitude of 1-1.5 km AGL yielding a ground resolution of 2.5-3.75 meters and at 5.5 km providing approximately 14 meter resolution.

The AADS 1268 is capable of recording data in up to 12 spectral bands. The following bands (corresponding to Landsat TM bands) were archived and used for this project:

Daytime Multi-spectral Imagery:

Band 1	0.45-0.52	TM-1
Band 2	0.52-0.60	TM-2
Band 3	0.63-0.69	TM-3
Band 4	0.76-0.90	TM-4
Band 5	1.55-1.85	TM-5
Band 6	2.08-2.35	TM-7
Band 7	8.5-12.5 (low gain 0.5)	TM-6
Band 8	8.5-12.5 (high gain 1.0)	TM-6

Predawn Thermal Imagery (long wave thermal band only):

Band 1	8.5-12.5 (low gain 1.0)	TM-6
Band 2	8.5-12.5 (high gain 2.0)	TM-6

Natural color aerial photography was also collected coincident with all flight lines. This provided very high resolution (estimated at 8-12 inches) with sufficient overlap to permit stereo analysis.

The Daedalus imagery was retrieved off of 8mm exabyte tape using both ERIM software (ERIPS) and commercial software (ENVI/IDL). The sites of interest were identified on the flight lines in softcopy and smaller images of the individual sites were taken from the flight lines. This was done to ease the analysis by reducing the amount of data.

Preliminary Visual Image Analysis for Detection Problems: Imagery was examined for signatures indicating the locations of trenches, other buried objects and contamination problems. The features were identified via site maps provided by Los Alamos. It is expected that detectability is driven by a variety of phenomena, including soil moisture, soil

compaction, soil type, and vegetation type and vigor. Therefore, the first analysis step was a preliminary review of all data, with emphasis on daytime and nighttime thermal and reflective multispectral. The preliminary analysis was visual, using single images, multiple images in a side-by-side presentation, and multi-band or multi-image composites where appropriate (and where the quality of the registration permits). Data transformations such a Tasselled Cap and Principle Components were applied to the multispectral data and day/night thermal data was evaluated for thermal inertia effects. Visual aids such as histograms and scatterplots were also used. Following the preliminary analysis a more detailed analysis was done to better understand the conditions under which the signatures can be detected and to enhance detectability where possible.

Phenomenology: Generally there were three classes of issues;

1.) Locating buried objects or trenches,
2.) Detecting seepage from buried objects, pits or drain fields and
3.) Detecting faults and fractures.

These issues were linked to a set of observables.

Buried objects or trenches usually involve a significant disturbance of the soil which can have a long lasting and often visible effect in the surface. The process of digging up and replacing a large volume of soil creates differences in soil compaction and composition of the disturbed area in contrast to the surrounding undisturbed soil. These differences may result in different drainage over the effected area. Drainage differences result in soil moisture differences which, in turn, may result in vegetation differences (either vigor or type) and thermal differences due to differential evaporative cooling of the surface. In addition, trenches may cause subtle features on the surface either as subsidence due to settling or decay of the buried material or it may leave a mound where excess material is piled on top of the trench.

Seepage from buried objects, pits or drain fields results in soils moisture and nutrient differences which, in turn, may result in vegetation differences (either vigor or type) and thermal differences due to differential evaporative cooling of the surface. This is particularly a problem when the area has an asphalt cap and thermal differences from cracked spots indicate a possible problem.

Faults and fractures also result in soil type and soil moisture differences which may be directly or indirectly observed by assessing vegetative differences. Changes in surface temperature due to differences in soil moisture can often be observed in thermal imagery. If the surface is not directly visible due to vegetative cover, the age type and relative vigor of vegetation can sometimes indicate the location of faults and fractures.

Special Processing:

Burial Site Analysis: Burial sites were searched for evidence of soil or surface disturbances using a side by site comparison of the following band combinations:

(Bands 4,3,2) False Color Composite (looking for vegetation differences)

(Bands 6,4,2) SWIR Composite (looking for soil moisture and vegetation differences)

(Bands 7,6,2) Thermal Composite (looking for thermal anomalies)

(Band 7 or 8) Individual Thermal Bands (looking for warm and cool thermal anomalies

and log stretch which has the effect of stretching the lower valued pixels in the image).

A principal components image was computed for trenches. A three color image of the first three principle components was evaluated for clumps of pixels with unusually large variances. Also, a Tasseled Cap Transform, a special case of principal components, was used to produce estimates of "greenness" and "wetness". The Tasseled Cap Transform is an established process for analysis of Landsat Thematic Mapper imagery. One of the outputs of the Tasseled Cap is a "greenness" transform band which has long been used as an indicator of vegetation vigor and "wetness" which is used as an indicator of vegetative moisture.

A comparison of the daytime and nighttime imagery was conducted to evaluate various areas showing unusual thermal inertia and vegetation stress. The comparison can by made by registering night image to daytime image, using side by side analysis, or using change or difference images.

Stereo analysis of aerial photography has been performed using the conventional mirror stereo scope. Some mounds and evidence of subsidence is visible but difficult to assess due to the vegetation cover.

Analysis of Drain Fields: The drain fields are being evaluated for evidence of vegetation vigor or stress and soil moisture patterns using the same techniques as for buried trenches.

Fault and Fracture Area Analysis: To analyze fault and fracture areas, the multi-spectral images are registered to the geologic map, then examined for spectral features within the known fracture region. The remaining area is searched for similar features

The AADS 1268 data covers the same bands as TM. A modified Tasseled Cap Transform (accounting for the difference in band order) was performed to produce a "greenness" image. The "greenness" image was evaluated to locate areas of vegetation vigor and stress.

Healthy vegetation maintains a relatively uniform temperature (by evaporative cooling). Stressed vegetation often has difficulty regulating its temperature. Ideally one would like to measure the vegetation's temperature at the minimum and maximum solar load (predawn and mid afternoon). A thermal image of the difference in temperature between these two times of day can provide indications of areas of stressed vegetation. While predawn thermal data is available, the daytime imagery was collected mid-morning. Nevertheless severely stressed vegetation might still show a temperature difference. To do this the predawn thermal image is registered to the daytime thermal image, the predawn image is subtracted from the daytime image, and the result is evaluated for vegetated areas with large temperature differences. An overlay is produced registering the results to the geologic map.

Data Fusion to Aid Users: To provide a physiographic representation to the site analysts, layers of information were georeferenced and added. A typical application is to use multiple sources to aid in confirming or denying positions of buried objects. Imagery available in digital form was directly entered as a layer. Maps, diagrams, drawings or photographs not available in digital form were digitized or scanned, depending on the material. Information from georeferenced data bases were added as other layers. Often the layers of information are overlaid on a background image for context and to integrate the geographical features. Four commercially available packages were used--TNT MIPS, ERDAS with ARCINFO and ENVI with ARCINFO. The choice depended the

particular workstation being used and preference of the particular analyst.

Results

Status: The final brochure will cover the remote sensing products that were selected for presentation. Interim products that have been made include the following: delineation of trench and old septic field boundaries using photography, maps and imagery; analysis of thermal signatures in unusual geological strata, asphalt and buried pits; analysis of fault and fracture areas beneath contaminated areas; broad radiological (gamma) data contours overlaid on imagery, compared to site problems; comparison of existing engineering drawings of buried objects with imagery and; use of hydrologic data merged with imagery to aid in soil sampling strategies.

Examples:

Rofer Site: False color or natural color composite with an overlay of suspected trench locations compared to a black and white thermal image showing anomalies; compared to historical photos.

Mynard Site: False color or natural color composite with an overlay of septic drain fields, holes, buried cable and firing pits from diagrams.

Becker Site: Display of hydrologic areas in a watershed and contaminated concentration values used to guide future stratified sampling of uranium, lead and copper.

Koch Site: A multispectral image registered to a geologic map to show faults and fractures; a "greenness" transform image side-by-side with a thermal difference image to assess areas of vegetative stress or vigor.

Hoard Site: Overlay of a detailed engineering drawing of buried pits on a natural color aerial photograph suggesting inaccuracies in the existing information.

Mason Site: Use of pre-dawn data to point out unexplained thermal anomalies in an asphalt cap; demonstrating/denying questionable information about buried trenches and seeps with a multispectral image.

Whole Lab: Overlaying gamma radiation data contours on a SPOT image of the lab, comparing to sites selected for this project, presentation of a Russian KFA-100 image as a newly available data source.

Applications

Economy: Rather than (or in conjunction with) statistical methods, analysis of remotely sensed data will provide information on where waste is located and on where wells should be drilled in order to obtain definitive characterization of waste sites. This would reduce the expense of exploratory drilling and the necessity for fine-gridded sampling.

Accuracy: Remote sensing's capability to provide (relatively) continuous information would be used to extrapolate conditions between wells/boreholes. This would improve the accuracy of information derived from point-sampling, and also would provide better data for waste-flow models.

Safety: In many situations there are risks associated with inadvertently drilling into containers and in working in areas where hazardous waste has migrated to the surface. Such conditions may not be known beforehand. Remote sensing provides the capability to detect and map such hazardous areas prior to beginning clean-up and mitigation.

Future Activities

To demonstrate remote sensing use as a tool for the surveillance of waste disposal at DOE sites requires a three phase process. This project represents Phase I which involves developing examples, by using existing imagery, of how remote sensing products could aid DOE's site restoration efforts. Phase II would optimize the results of the first year by collecting new data. Phase III would develop products at LANL in an operational DOE lab environment and transfer technology to the site restoration people.

Acknowledgements

The authors would like to acknowledge Karl-Heinz Frohne, METC Contracting Officer's Representative (COR) for his technical guidance of this work on contract DE-AR21-95MC32116, EM focus area Decontamination and Decommissioning, period of performance January 30, 1995 - January 30, 1996. The authors would like to acknowledge Richard McQuisten, formerly of DOE/METC for his technical input at project outset.

The authors would also like to acknowledge the scientific contributions of LANL led by Ed Van Eeckhout and of EG&G/EM led by Lee Balick. LANL is contributing the time of its scientists and is funding EG&G scientists as well. The Environmental Restoration Program at LANL also contributed the needed materials and site support for this project.

PII.3 Surfactant-Enhanced Aquifer Remediation at the Portsmouth Gaseous Diffusion Plant

Richard E. Jackson (intera@onr.com; 512-346-2000)
John T. Londergan (intera@onr.com; 512-346-2000)
John F. Pickens (intera@onr.com; 512-346-2000)
INTERA Inc.
Suite 300, 6850 Austin Center Blvd.
Austin, TX 78731

Introduction and Objectives

Many DOE facilities are situated in areas of sand and gravel which have become polluted with dense, non-aqueous phase liquids or DNAPLs, such as chlorinated solvents, from the various industrial operations at these facilities. The presence of such DNAPLs in sand and gravel aquifers is now recognized as the principal factor in the failure of standard ground-water remediation methods, i.e., "pump-and-treat" operations, to decontaminate such systems (Mackay and Cherry, 1989).

The principal objective of this study, as stated in the Statement of Work of the contract (DE-AC21-92MC29111), is to demonstrate that multi-component DNAPLs can be readily solubilized in sand and gravel aquifers by dilute surfactant solutions. The specific objectives of the contract are:

1. to identify dilute surfactants or blends of surfactants in the laboratory that will efficiently extract multi-component DNAPLs from sand and gravel aquifers by micellar solubilization (Phase 1);

2. to test the efficacy of the identified surfactants or blends of surfactants to solubilize *in situ* perchloroethylene (PCE) and trichloroethylene (TCE) DNAPLs by the injection and the subsequent extraction through an existing well or wells at a government-owned contaminated site (Phase 1); and

3. to demonstrate the full-scale operation of this remedial technology at a government-owned contaminated site (Phase 2).

Specific objective number 1 has been completed and reported to DOE (INTERA, 1995). However, the results of the test referred to in specific objective number 2, conducted at Paducah Gaseous Diffusion Plant in 1994, were inconclusive. Following this first test, it was decided by DOE and INTERA to move the test site elsewhere due to difficulties with obtaining core samples of the sand and gravel aquifer containing the DNAPL and with ascertaining the location of the DNAPL relative to the injection well. The solubilization test at the Portsmouth Gaseous Diffusion Plant (PORTS) will constitute the second test of Phase 1 of this contract.

Research sponsored by the U.S.Department of Energy's Morgantown Energy Technology Center, under Contract DE-AC21-92MC29111 with INTERA Inc., Suite 300, 6850 Austin Center Blvd., Austin, TX 78731.

The goal of the interwell DNAPL solubilization test ("surfactant flood") is to test the efficacy of a micellar-surfactant solution to solubilize the DNAPL *in situ.* The test should also demonstrate the ability of Surfactant-Enhanced Aquifer Remediation (SEAR) to enhance the efficiency of conventional pump-and-treat systems in the remediation of DNAPL contamination. SEAR technology uses non-toxic biodegradable surfactants to enhance the solubility of DNAPLs in the subsurface. It is anticipated that the concentrations of trichloroethylene (TCE) and other chlorinated solvents removed during the surfactant flood will be at least an order of magnitude higher than those achieved by simple pump-and-treat operations.

The Field Test Site

The surfactant flood is be undertaken at the X701B site at Portsmouth Uranium Enrichment Plant (PORTS) using 62G as the injection well and BW2G as the extraction well (see Figure 1). The X701B area at PORTS originally contained a holding pond which received liquid wastes, including chlorinated solvents, from industrial operations elsewhere on site.

The X701B area is underlain by lacustrine silts and clays and by deeper alluvium. These Quaternary units lie unconformably on the Sunbury shale which, in turn, overlies the Berea sandstone. The geologic and hydrologic properties of the X701B area are shown in the table below and the hydrostratigraphy of the test site is shown in Figure 2 of this proposal.

Formation	Lithology	Hydraulic Conductivity [cm/s]	Approximate Average Thickness [m]
Minford	Clay	8.1 E-08	4.6
Minford	Silty clay	1.5 E-06	3.0
Gallia	Sand	E-02 to E-03	1.5
Sunbury	Shale	K_v =E-08	3.0
Berea	Sandstone	5.6 E-05	9.1
Bedford	Shale	2.1 E-05	30

The Gallia alluvium was deposited by the ancient Portsmouth river which left abandoned alluvial and fluvio-lacustrine deposits across the PORTS site. Hydraulic conductivities in the Gallia are of the order of 10^{-2} to 10^{-3} cm/s. The Gallia is underlain by the Sunbury shale which is estimated to have a vertical hydraulic conductivity of the order of 10^{-8} cm/s. It is proposed using X701-62G as the injection well and X701-BW2G as the extraction well during the DNAPL solubilization test. Both wells are screened in the Gallia sand and gravel aquifer and are only 5 meters apart. They are shown in Figure 1.

Well BW2G has been producing free-phase DNAPL since at least 1988. The specific gravity of the DNAPL is approximately 1.4 and the viscosity is measured as 4 centipoise. The DNAPL is a multicomponent liquid composed of trichloroethene [TCE], tetrachloroethene [PCE] and a number of minor components including PCBs and 1,1-dichloroethene. The approximate composition of DNAPL from Pumping Well 1 at the X701B area is given in the table below:

Compounds Identified in DNAPL Sample	Quantity [g/L]	Notes
Trichloroethene	12	
Tetrachloroethene	3.6	exceeds initial calibration range
Perchloromethane	0.22	"carbon tetrachloride"
1,1-dichloroethene	0.034	
1,1,2-trichloro-1,2,2-trifluoroethane	1.6	[CFC-113], tentatively identified
1,1,1-trichloroethane	2.3	tentatively identified
1,1,2-trichloroethane	0.12	tentatively identified
toluene	0.028	tentatively identified
xylenes	0.060	tentatively identified
1,2,4-trimethylbenzene	0.080	tentatively identified
polychlorinated biphenyls	820 ug/g [0.08%]	identified as PCB-1254

It should be noted that the chemical analysis only identifies a small fraction of the DNAPL components since the DNAPL weighs about 1400 g. Thus, the listed quantities are probably significantly underestimated, in particular TCE.

The dissolution of this DNAPL by ground waters flowing through the Gallia has led to the development of a long plume of TCE and other components of the DNAPL. The extent of the TCE contamination during 1993 is shown in Figure 3. Recent measurements of TCE indicate that TCE concentrations at the perimeter fence have reached 800 mg/L.

Approach

Future work includes:

- ❑ PORTS site-specific training for INTERA's five-person field staff;

- collaboration with PORTS personnel in the field to collect soil cores from the Gallia aquifer for analysis at the State University of New York at Buffalo (SUNY);
- surfactant screening and other laboratory experiments at SUNY;
- tracer screening and selection at the University of Texas at Austin [UT];
- a pumping test to determine injection/extraction rates during the Fall of 1995;
- test design and permitting during the Winter of 1995-6;
- a partitioning interwell tracer test (PITT; see Jin et al., 1995) prior to the solubilization test to measure the interwell volume of DNAPL;
- an interwell DNAPL solubilization test (see Butler et al., 1995) to solubilize and recover DNAPL from the Gallia aquifer during the Spring of 1996;
- a second PITT, this one following the solubilization test, to measure the quantity of DNAPL remaining in the Gallia;
- analysis and interpretation of the test data; and
- a final report presenting the test results.

Benefits of Applying SEAR

The benefits of SEAR arise from the very high effective solubilities which can be obtained by using dilute surfactant solutions to "solubilize" NAPLs. Because of this enhanced solubilization, it is possible to accelerate the rate of NAPL removal from the subsurface, which in turn reduces overall operations and maintenance costs for any particular pump-and-treat facility. A further advantage of SEAR is that the technology can be superimposed on an existing pump-and-treat systems so that the infrastructure which is invested in the site can be used more efficiently in the future.

Acknowledgments

We appreciate the assistance of Keith Westhusing of DOE Laramie, our COR, in defining the scope of work for this phase of the project and the collaboration of our subcontractors: Dr. John C. Fountain of the State University of New York at Buffalo and Dr. Gary Pope of the University of Texas at Austin. The period of performance of this part of the contract is from August 1, 1995 to December 31, 1996.

References

Butler, G.W., R.E. Jackson, J.F. Pickens and G.A. Pope, 1995. An interwell solubilization test for characterization of nonaqueous-phase liquid zones. Chapter 15 in: *Surfactant-Enhanced Subsurface Remediation: Emerging Technologies*, ACS Symposium Series 594, American Chemical Society, Washington D.C.

INTERA, 1995. The in-situ decontamination of sand and gravel aquifers by chemically-enhanced solubilization of multiple-component DNAPL with surfactant solutions - Phase 1 Final Topical Report: Laboratory and Pilot Field-Scale Testing. Report to DOE/METC by INTERA Inc., Austin, Texas.

Jin, M., M. Delshad, V. Dwarakanath, D.C. McKinney, G.A. Pope, K.Sepehrnoori, C.E. Tilburg and R.E. Jackson, 1995. Partitioning tracer test for detection, estimation and remediation performance assessment of subsurface nonaqueous phase liquids. *Water Resources Research* 31(5):1201-1211.

Mackay, D.M. and J.A. Cherry, 1989. Groundwater contamination: Pump-and-Treat Remediation. *Environmental Science and Technology* 23(6):756-766.

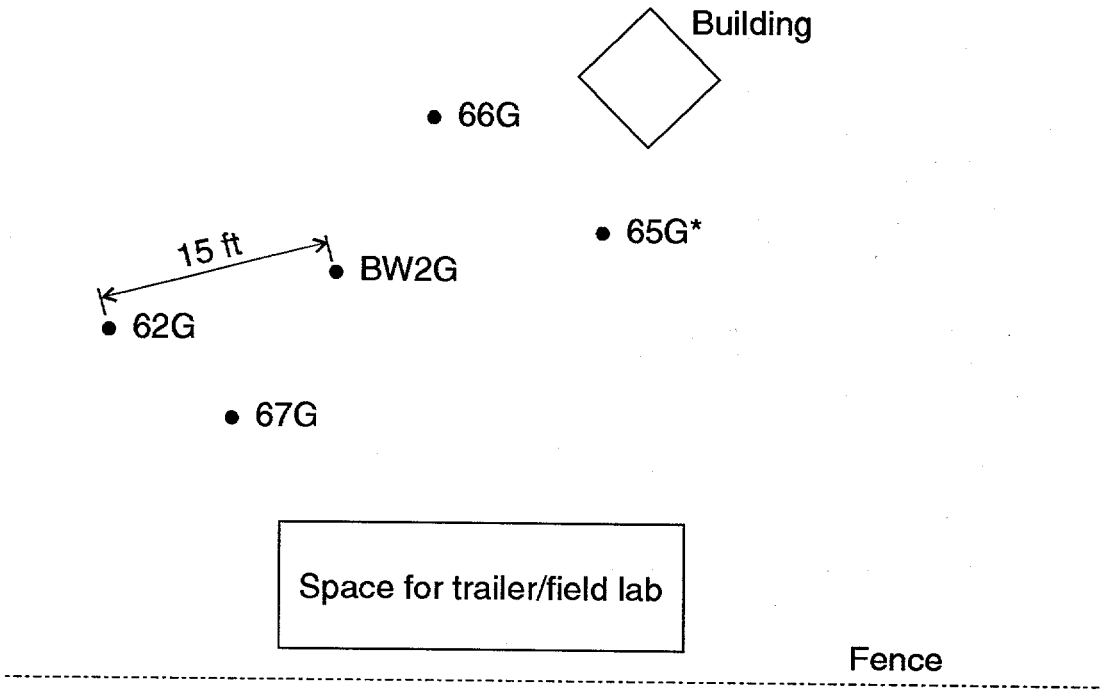

Figure 1 Site Map for the X701B Area, DOE Portsmouth

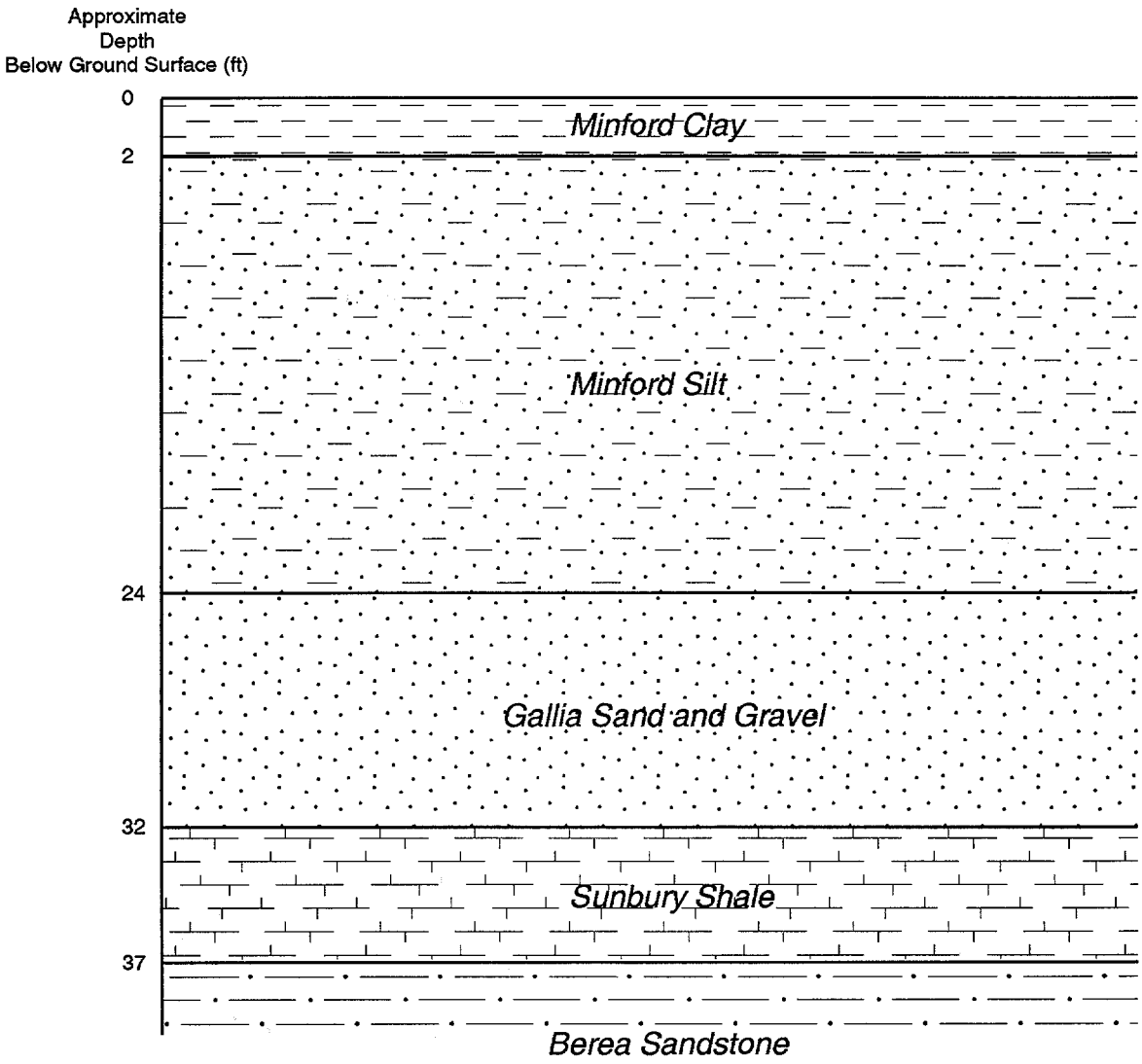

Figure 2 Hydrostratigraphy of the Proposed Test Site, X701B Area.

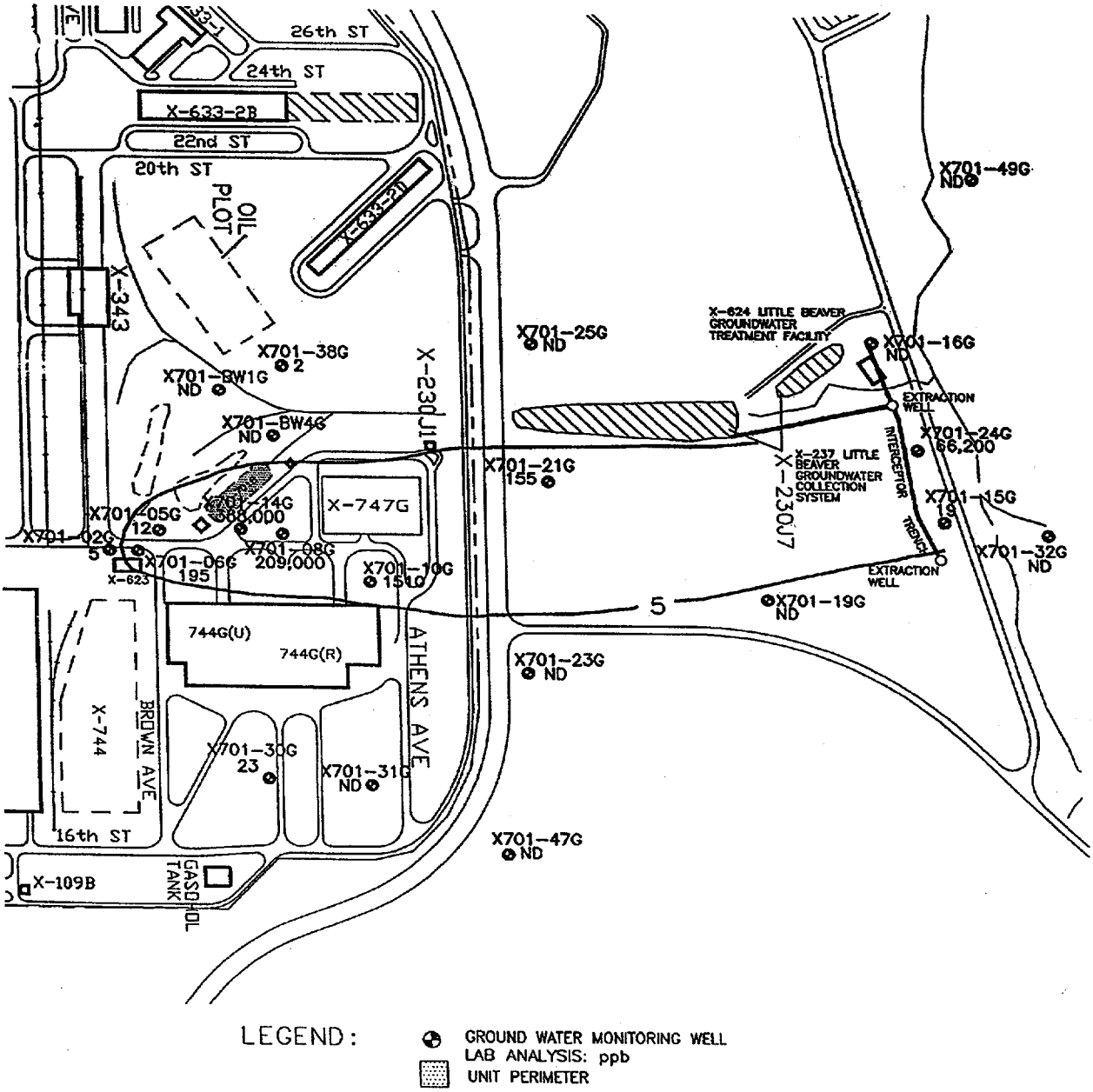

Figure 3 Extent of Trichloroethene Concentration 2nd Quarter 1993

PII.4 Laboratory "Proof of Principle" Investigation for the Acoustically Enhanced Remediation Technology

Joe L. Iovenitti (jli@weiss.com; 510-450-6141)
James W. Spencer, Jr. (jws@weiss.com; 510-450-6000)
Donald G. Hill (dgh@weiss.com; 510-450-6102)
Weiss Associates
5500 Shellmound Street, Suite 100
Emergyville, California 94608-2411

Timothy M. Rynne (trynne@sara.com; 714-373-5509)
John F. Spadaro (jspadaro@sara.com; 714-373-5509)
John Dering (jdering@sara.com; 714-373-5509)
Scientific Applications and Research Associates, Inc
15262 Pipeline Lane
Huntington Beach, California 92649-1136

Introduction

Weiss Associates is conducting a three phase program investigating the systematics of using acoustic excitation fields (AEFs) to enhance the in-situ remediation of contaminated soil and ground water under both saturated and unsaturated conditions.

- Phase I - Laboratory Scale Parametric Investigation
- Phase II - Technology Scaling Study
- Phase III - Large Scale Field Tests

Research sponsored by the U.S. Department of Energy's Morgantown Energy Technology Center, under Contract No. DE-AR21-94MC30360 with Weiss Associates, 5500 Shellmound Street, Emeryville, CA 94608-2411; fax (510) 547-5043; phone (510) 450-6000.

Phase I, the subject of this paper, consisted primarily of a laboratory proof of principle investigation. The field deployment and engineering viability of acoustically enhanced remediation (AER) technology was also examined.

Phase II is a technology scaling study addressing the scale up between laboratory size samples on the order of inches, and the data required for field scale testing, on the order of hundreds of feet.

Phase III will consist of field scale testing at an non-industrialized, non-contaminated site and at a contaminated site to validate the technology.

Summarized herein are the results of the Phase I "proof-of-principle" investigation, and recommendations for Phase II. A general overview of AER technology along with the plan for the Phase I investigation was presented

in Iovenitti et al. (1994). Figure 1 is an example of a possible AER field deployment.

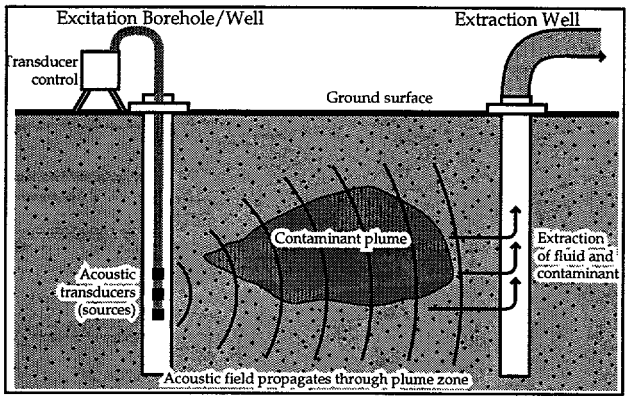

Figure 1. The Acoustically Enhanced Remediation Concept, DOE Contract No. DE-AR21-94MC30360, Phase I.

The primary subcontractor in this effort was Scientific Applications and Research Associates, Inc. Additional subcontractors were Dr. James K. Mitchell of Virginia Polytechnic Institute and State University and Ms. Dorothy Bishop of Lawrence Livermore National Laboratory.

Objectives

The Phase I investigation was focused on non-aqueous phase liquid (NAPL) recovery in low permeability unconsolidated soils with the objectives of (1) evaluating the use of AEFs to increase soil permeability and NAPL mobility, (2) determining the acoustic parameters that maximize fluid and contaminant extraction rates, and (3) evaluating the engineering and field deployablitiy of AER technology.

Phase I primarily investigated the effects of AEFs on the saturated zone which minor emphasis on the unsaturated zone which will be addressed in Phase II.

Addressed by this effort is the need for innovative and improved in-situ remediation methods to (1) expedite clean up of contaminants, (2) expedite clean up of contaminated low permeability soils, (3) reduce clean up time and cost, and (4) diminish human health and ecological risk at contaminated sites.

This program focused on unconsolidated soils because of the large number of remediation sites located in this type of hydrogeologic setting throughout the nation. It also focused on low permeability soil because its remediation is a slow process because of the inherent low permeability and high sorptive capacity.

Approach

To achieve the Phase I objectives, a literature review was conducted, a laboratory test apparatus was constructed with a computerized data acquisition system, sample soil material and NAPL surrogates were obtained, a laboratory testing program, and the engineering and field deployment strategy was evaluated.

Given the inherent difficulties in testing low permeability soil, the test program evaluated changes induced by AEFs on (1) NAPL-recovery in permeable soil and (2) hydraulic conductivity in low permeability soil.

Literature Review

A literature review was conducted to identify prior work related to this study, to develop an awareness of ongoing research and development efforts, and to collect acoustic properties information for use in engineering analysis and modeling. The literature review provided some insight into possible mechanisms controlling AER, measurement techniques, acoustical sources, and the mathematical modeling of their emissions. Theorized potential effects of AER on the solid matrix and

pore fluid based are presented in Figures 2 and 3, respectively. These acoustically generated mechanisms all act towards rendering the remediation process faster and expectedly reduce life-cycle costs.

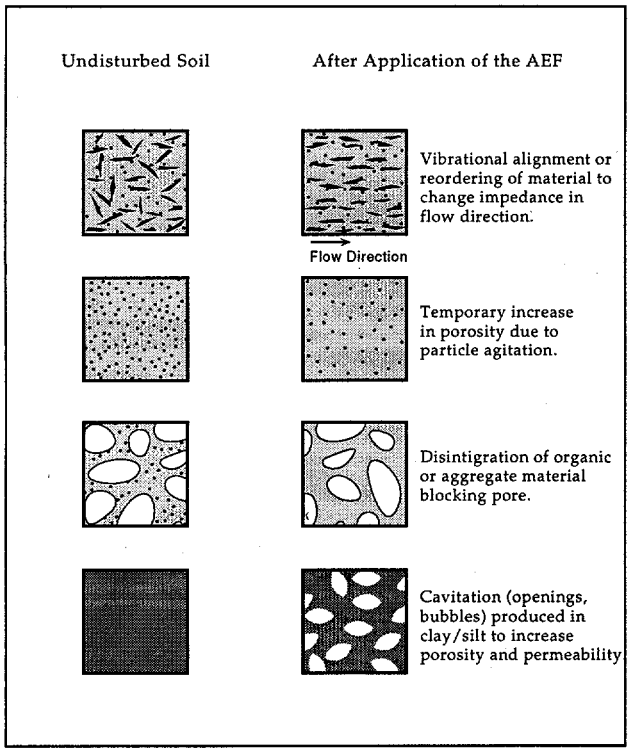

Figure 2. Potential Effects of Acoustic Excitation on Porous Grain Framework, DOE Contract No. DE-AR21-94MC30360, Phase I.

Test Apparatus

Figure 4 is a schematic of the laboratory test apparatus. An electromechanical shaker was used to vibrate a test soil sample, approximately 1.5" diameter and 3.5" long. The sample is encased in a thin, heat-shrink mylar jacket between two end caps that are fitted with screens for fluid flow measurements.

The shaker and sample assembly are enclosed in a sealed chamber pressurized to

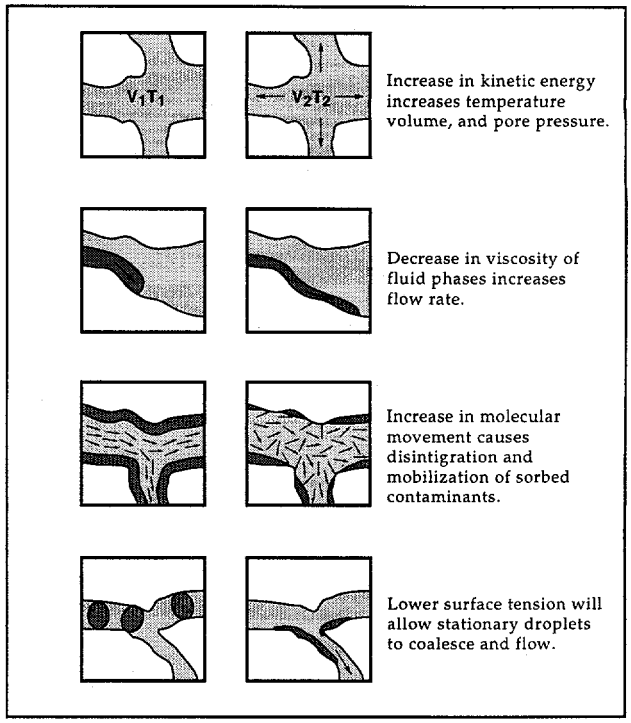

Figure 3. Potential Effects of Acoustic Excitation on Pore Fluids, DOE Contract No. DE-AR21-94MC30360, Phase I.

simulate soil stress at different depths. The wall of the chamber is a Plexiglas cylinder to allow continuous monitoring of the sample condition and the flow of fluids in the inlet and outlet lines.

As the test sample is vibrated, strain in the sample is generated by the inertial loading of the sample due to its own mass and the mass of the top end cap. The sample is instrumented with dynamic pressure transducers, accelerometers, and thermocouples.

The apparatus is capable of generating frequencies between 50 Hz and 10 kHz, strains of 10^{-6} to greater than 10^{-4}, and confining pressures of 10 to 100 psi. The tests were conducted using both manual and computer controls. A data acquisition system with a graphical software interface allowed acquiring, viewing, and storing the data.

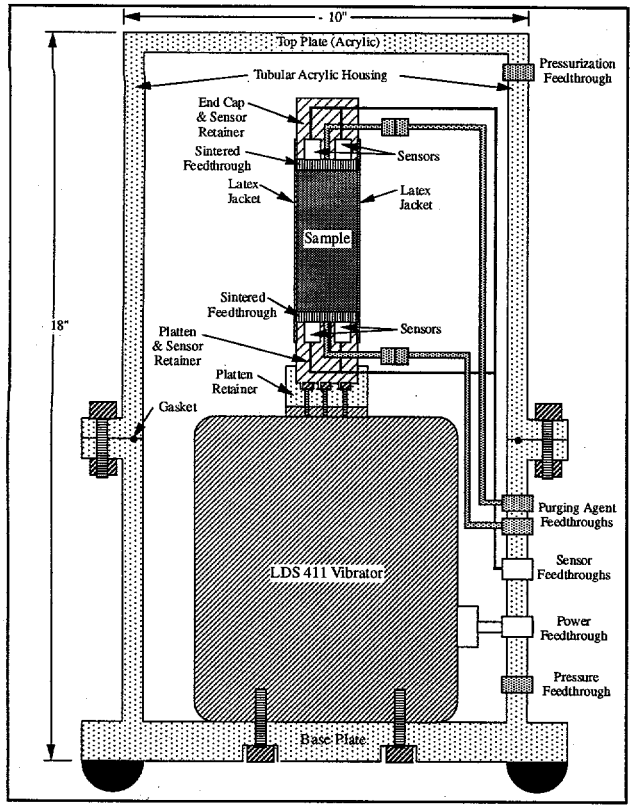

Figure 4. Schematic Cross-Sectional View of the Laboratory Test Cell, DOE Contract No. DE-AR21-94MC30360, Phase I.

Sample Materials and NAPL Surrogates

Four types of soil were tested (1) well-sorted, fine homogeneous sand, (2) poorly-sorted, heterogeneous sand with about 9% silt and clay, (3) silt, and (4) clay. Two NAPL surrogates were used during the testing, canola oil and Soltrol 220. At 70°F, canola oil and Soltrol 220 have a density of 0.9182 and 0. 0.789 g/mL, and a viscosity of 65 and 4.83 centipoise, respectively. These surrogates were chosen because they are relatively non-hazardous and non-toxic.

While both of these surrogates are less dense than water (i.e., LNAPLs), they may also provide a first approximation for denser than water (DNAPL) remediation. This is based upon the observation that Soltrol 130 was the most commonly used fluid by Wilson et al. (1990) in their laboratory investigation of residual liquid organics. Based on this work Cohen and Mercer (1993, p. 4-19) in their evaluation of DNAPLs recommend Soltrol 130 as an ideal fluid for determining residual saturation for a porous media. The densities and viscosities of Soltrol 130 and 220 are comparable for the purposes of this investigation.

Laboratory Tests

Table 1 summarizes the laboratory tests conducted. Each series of tests included baseline conditions without acoustic excitation, and then excited conditions with acoustic excitation either at a single frequency or at a sequence of frequencies between 100 Hz and 10 kHz, and at multiple power levels in addition to the baseline condition. Confining pressures during testing were between 10 and 30 psi.

Table 1. Test Series Summary, DOE Contract No. DE-AR21-94MC30360, Phase I.

Soil Type	Hydraulic Conductivity	Air Permeability	NAPL Extraction Purging Canola Oil with Water	NAPL Extraction Purging Soltrol 220 with Water
Oklahoma Sand	X	X	X	X
Ajax Sand	X	X	X	
Silt	X			
Clay	X			

Results

NAPL-Extraction Tests

The NAPL-extraction tests simulated a ground water-NAPL pump and treat operation. Acoustic excitation resulted in more than 70% improvement in NAPL-recovery relative to baseline conditions in the permeable sands tested. This high degree of recovery was demonstrated during optimization testing in the heterogeneous sand.

Table 2. NAPL Saturations by Various Methods for the Various Tests Conducted, DOE Contract No. DE-AR21-94MC30360, Phase I.

Tests Conducted	Laboratory Tests Measured Residual NAPL Saturation[1,3]			Semi-Logarithmic Extrapolation[2] NAPL Saturation[3] after 100 PV[4] Pump & Treat			Dean Stark Extraction[5]		
	Baseline (FPV[9])	Excited (FPV)	% Improvement[10]	Baseline (FPV)	Excited (FPV)	% Improvement	Baseline (FPV)	Excited (FPV)	% Improvement
Oklahoma Sand/Canola Oil/Water, Test No. 1	0.2746	0.2042	25.64	0.2633	0.1833	30.38	0.1780	0.1740	2.25
Oklahoma Sand/Canola Oil/Water, Test No. 2	0.2015	0.1888	6.30	0.17	0.1483	12.76	0.1623	0.1109	31.67
Oklahoma Sand/Soltrol 220/Water	0.0656	0.0529	19.36	0.068	0.04	41.18	0.1963	0.1490	24.10
Ajax Sand/Canola Oil/Water[6]	0.1766	0.1732	1.93	0.1521	0.1467	3.55			
Ajax Sand/Canola Oil/Water[7]	0.1766	0.1502	14.95	0.1521	0.0933	38.66			
Ajax Sand/Canola Oil/Water(31.05.95 test)[8]	0.1766	0.1264	28.43	0.1521	0.04	73.70			

1 Empirical laboratory results for a simulated pump and treat of a NAPL-contaminated ground water
2 Using Jones and Roszelle (1978) Method
3 Average values from multiple tests
4 Pore volume throughput of water
5 Modified ASTM solvent extraction method a standard laboratory technique for measuring immiscible fluid saturation. in the petroleum industry. Measured NAPL content was divided by the measured porosity of the sample to obtain FPV (see footnote 9).
6 Tests conducted at a single frequency
7 Tests conducted with a sequence of six frequencies
8 Tests conducted with a sequence of eight frequencies and with an increased power level
9 Fractional pore volume occupied by NAPL
10 Acoustically excited NAPL recovery relative to baseline (non-excited) recovery

Table 2 summarizes the results of the NAPL-recovery tests conducted in the order performed for both the homogeneous and heterogeneous sands. Three types of NAPL saturation data are reported in both fractional pore volume and in percent (%) improvement of excited NAPL recovery relative to the baseline recovery:

1. the empirical laboratory pump and treat test results;
2. the semi-logarithmic extrapolation to 100 pore volumes (PVs) throughput of water using the Jones and Roszelle (1978) method; and
3. the Dean Stark extraction results.

The empirical laboratory results represent residual NAPL saturations for the tests conducted. The Jones and Roszelle (1978) data represent a graphical technique whereby the laboratory data is extrapolated to a common throughput of water, in this case 100 PVs. The Dean Stark extraction is a modified ASTM solvent extraction method which is a standard laboratory technique used by the petroleum industry to determine the residual oil and water saturations (Cohen and Mercer, 1993).

Optimization testing in the form of sequential frequency excitation instead of single frequency testing, and changes in power levels, was only performed on the heterogeneous sands.

Acoustic excitation enhanced the recovery of both canola oil and Soltrol 220 from samples of homogeneous sand. The excited condition test results showed relative NAPL-extraction improvements above baseline conditions ranging from 6% to 26% for the empirical laboratory data, and 13% to 41% for the Jones and Roszelle (1978) extrapolation.

The apparent disagreement between the Dean-Stark analyses and the empirical laboratory and the semi-logarithmic extrapolation data for the canola oil homogeneous sand data is paradoxical. Its resolution was beyond the scope of this investigation. The Dean Stark data for the Soltrol 220 test are consistent with the laboratory test % improvement data. No optimization testing was conducted for

homogeneous sand. Time constraints did not allow Dean Stark analyses of the heterogeneous sand.

Hydraulic Conductivity of Clay

Hydraulic conductivity (K_h) testing in fully saturated clays under excited conditions provided a very favorable result. Acoustic excitation induced a two- to four-fold increase in K_h and a possible permanent change in the intrinsic permeability of the clay, post-excitation.

Figure 5 presents the cumulative flow behavior of optimization testing of the clay test sample which had a baseline K_h of 1.35×10^{-8} cm/sec. After two hours of excitation, the sample temperature increased from 71° to 95° F, due to the combined effects of heating from the shaker and anelastic attenuation, and the water flow rate increased nearly six-fold. The acoustically excited hydraulic conductivities peaked at 5.5×10^{-8} cm/sec, which represents over a four-fold increase. The increase in the flow rate was even larger due to the temperature-dependent reduction (about 30 percent) in the viscosity of water. This figure also shows how K_h declined with time. Post acoustic excitation K_h decreased to 1.9×10^{-8} cm/sec which is higher than the original baseline for this test but within the range of the other

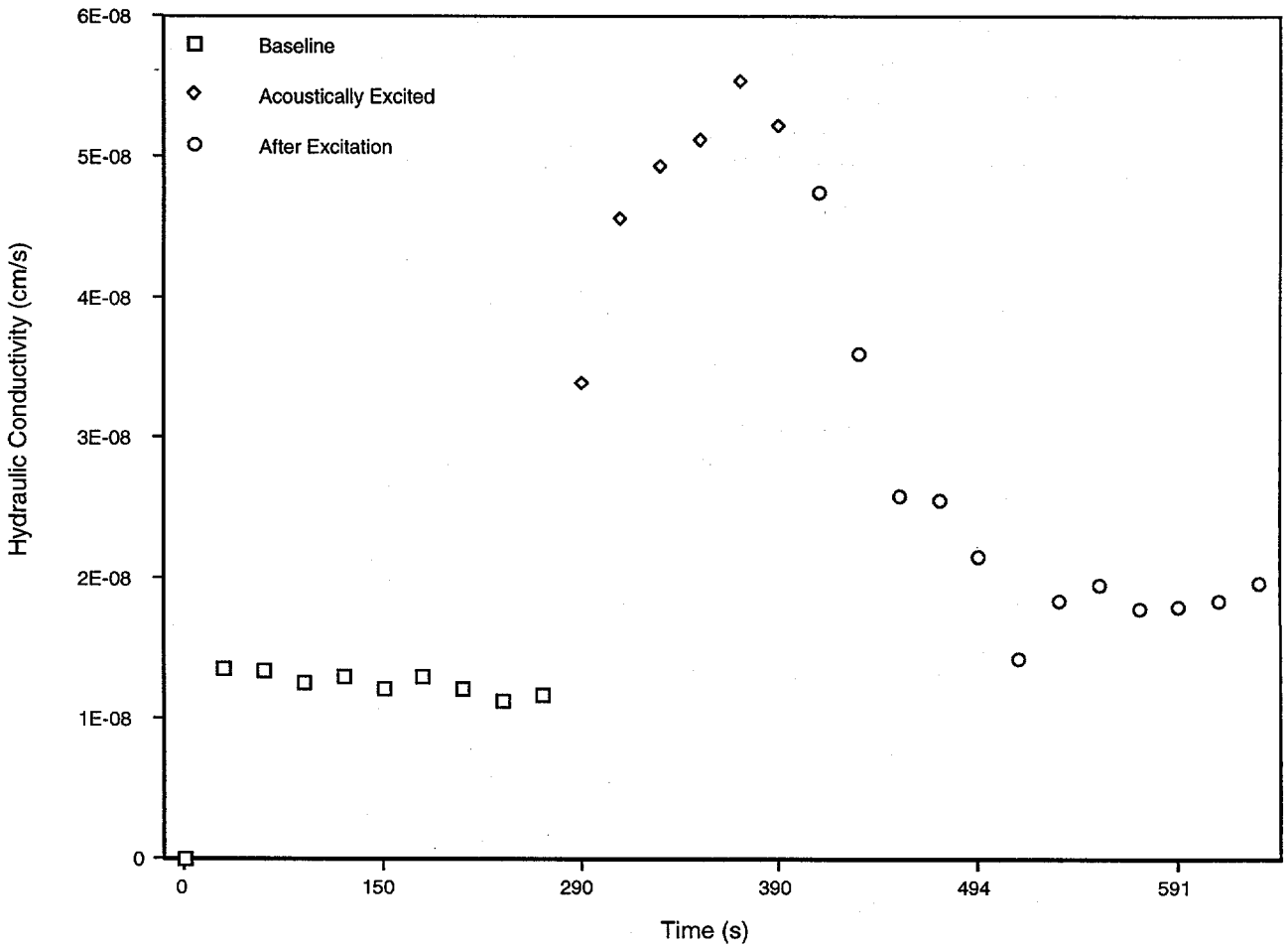

Figure 5. Hydraulic Conductivity of Clay Increased Four-Fold During Excitation, DOE Contract No. DE-AR21-94MC30360, Phase I.

baseline analyses. These data are suggestive, although not conclusive that the post-excitation intrinsic permeability of the clay was increased. Additional testing is required to investigate this effect.

Hydraulic Conductivity of Heterogeneous Sand

Acoustic excitation of fully saturated heterogeneous sand, produced large amounts of muddy water, and the hydraulic conductivity decreased apparently due to the plugging of pores by the mobilized fine-grained particles. During baseline testing, only clear effluent was produced. The mobilization of fines under acoustic excitation is consistent with the finding of Reddi et al. (1993, 1994) except that their work was done under atmospheric conditions. The mobilization of fines would be advantageous for remediation since contaminants tend to be sorbed on the fine-grained sediments. Additional testing will be required to optimize the production of fines while minimizing the tendency to plug pores (see discussion below).

Hydraulic Conductivity of Silt

The hydraulic conductivity testing of one silt sample provided promising results. The prepared sample had a baseline K_h of 9.95×10^{-4} cm/sec and a porosity near 43.5%.

During the baseline measurements, the effluent water was essentially clear. With excitation, milky water was produced, indicating that silt size particles were being mobilized and the K_h of the test sample decreased to 6.4×10^{-4} cm/sec, or about 34% of the pre-excited value. This result is similar to the hydraulic conductivity testing in the heterogeneous sand. With continued excitation of the silt under high power and at a sequence of frequencies, a conductivity increase of about 10% was suggested. It was beyond the scope of this investigation to pursue this promising trend but, these initial data suggests that fines can be mobilized while minimizing the hydraulic conductivity reduction.

Hydraulic Conductivity of Homogeneous Sand

Acoustic excitation of saturated homogeneous sand showed no discernible positive effects relative to baseline conditions. The overall K_h of the sand did decline suggesting some incremental consolidation of the material. This result stands in contrast to those reported by Reddi et al. (1993, 1994) who indicate K_h increases of several orders of magnitude with excitation. However, these authors also reported possible bypass betwwen their test cell wall and ultrasonic horn during their excited measurements.

Laboratory Strain Amplitudes

The laboratory tests described above show that acoustic excitation can (1) increase the NAPL-recovery from permeable soil, and (2) increase the K_h of low permeability soil. An obvious question is whether the acoustical levels required to develop these beneficial effects can be generated in-situ with available acoustic source technologies. To address this issue, estimates of the strain amplitudes developed in the laboratory tests were compared with strain amplitudes that can be generated with available source technologies.

Optimization Testing

Primarily two approaches were pursued for optimization testing (1) increasing acoustic power to the sample, and (2) subjecting the sample to a sequence of frequencies. Extremely encouraging results were obtained during clay

(Figure 5) and heterogeneous sand (Table 2) testing.

Field Deployment Strategy

The Phase I laboratory test results show that the beneficial effects of acoustic excitation are observed when the strain amplitudes are between approximately 10^{-5} and 10^{-4}. These strain amplitudes are within the range that can be developed in-situ with existing source technology, especially if the sources are deployed using a phased array.

The complex geohydrological setting of contaminant plumes makes acoustical excitation of large volumes desirable. Also, given the high cost of installing wells, it is preferable to use a distributed array of acoustic sources. With a distributed array of sources, and:

1. by controlling the phase of the sources, high-power acoustical energy can be directed to various parts of the plume; and

2. by modifying the phase of the sources, high intensity acoustic energy can be focused and swept throughout the contaminant volume.

Figure 6 presents an engineering trade space of acoustical frequency and intensity in comparison with the test regime of our laboratory experiments. Several constraints limit the portion of this trade space where AER should be feasible:

1. strain levels that are too low, roughly below 10^{-6}, will not induce significant remediation enhancement;

2. strain levels that are too high, roughly above 10^{-3}, can lead to soil liquefaction that should be avoided at most remediation sites;

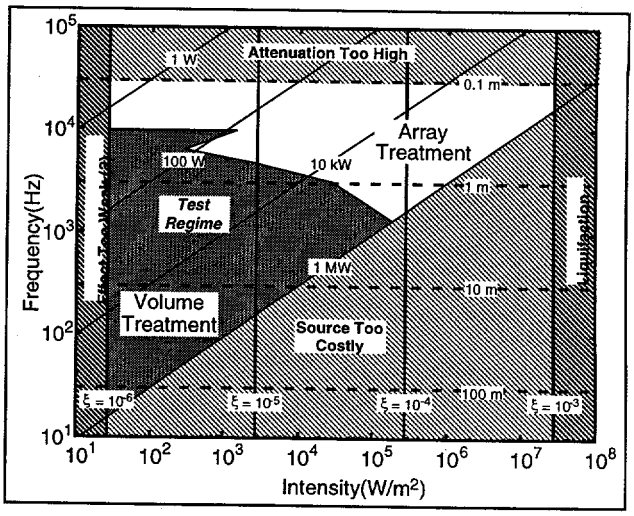

Figure 6. Trade Space of Strain and Field Intensity Compared Against Experimental Test Regime, DOE Contract No. DE-AR21-94MC30360, Phase I.

3. frequencies that are too high, roughly above $3x10^4$ Hz, will not propagate very far in the subsurface; and

4. sources above 1 MW will not be available in the near future, and may ultimately be unaffordable.

The horizontal lines in this figure are different wavelengths of acoustic energy. This highly simplified analysis leaves a roughly triangular region of likely AER operation. For viable and cost-effective deployment of AER technology, the operative frequency, intensity, power, and wavelength regimes will be about 20 Hz to 10 kHz, 30 watts/square meter to $50x10^5$ watts/square meter (10^{-6} to 10^{-4} in strain), 100 W to 1 MW, and wavelengths of about 0.5m to about 50 m, respectively. Strain amplitudes developed during the Phase I testing fall in the upper region of where AER technology appears feasible using existing source technologies.

Several different approaches to field implementation were examined (1) single source, (2) multiple sources combining incoherently, and (3) phased arrays combining

coherently. The Phase I analysis considered only acoustical sources operating at the ground surface, but there will be analogous results for subsurface sources.

With a single source, the intensity at any given point in the remediation domain is proportional to the power of the device. A single source is considered viable for field deployment for only volumetrically small remediation sites.

With multiple sources combining incoherently (analogous to the summation of light intensities from a set of light bulbs) the intensity at the center of the remediation domain is considered to be insufficient for AER deployment. In such a configuration, the intensity will scale linearly with the number of acoustical sources, and as the inverse square of the spatial dimension of the array. While multiple sources can cover larger remediation volumes than a single source, it is expected to be very expensive to generate the required acoustical intensities.

With phased arrays, that is multiple source arrays with identical frequencies and phases, constructive interference can be generated at a given region within the remediation domain potentially creating very high acoustical intensities. Phased arrays provide a high degree of flexibility in producing high intensity AEFs because the maximum local intensity is proportional to the power of the individual sources and the square of the number of sources, and inversely proportional to the spatial dimension of the array. Thus, it is more cost-effective, to divide the remediation domain into a larger number of relatively low power sources, rather than using a small number of high power sources.

Applications

The Phase I investigation has shown that AER technology can (1) significantly enhance the remediation of NAPLs in unconsolidated soils and ground water based on laboratory bench scale testing, and (2) be successfully deployed in the field. Phase I demonstrated that NAPL recovery enhancements with acoustic excitation relative to traditional pump and treat in excess of 70% for permeable homogeneous and heterogeneous sands, and markedly increased water flux through low permeability silt and clay. Based on the Phase I results, similar enhancements for removal of NAPL trapped in silt and clay are expected. Thus, the Phase I findings indicate that AER technology is applicable to unconsolidated soil remediation sites throughout the country.

It should be noted that the Phase I testing was conducted under drained conditions such that no significant buildup in pore pressure could be developed in the soil test samples beyond what was controlled by the test soil's hydraulic conductivity. In the field, undrained coniditions will exist, consequently, there will be a much greater tendency to build-up pore pressure in the soil favoring the beneficial effects reported for AER technology.

AER technology appears to be contaminant insensitive in that it can be used to affect the permeability of low permeability sediments, and/or the mobility of contaminants. As such, it can be used to remediate fuel hydrocarbons, chlorinated hydrocarbons, radionuclides, or heavy metals.

AER technology is also considered a "piggy-back" methodology. It can be superimposed on both traditional remediation technologies (e.g., ground water pump and treat and its vadose zone equivalent, soil vapor

extraction), and most advanced remediation technologies (e.g., steam flooding, soil heating, surfactant flushing).

A significant reduction in unconsolidated soil cleanup time and cost is expected with the use of AER technology because (1) increasing the water flux through low permeability soils, the contaminant flux out of these soils is also increased, and (2) the faster the NAPL source term is removed, the faster a contaminated site can be remediated and returned to other uses.

Future Activities

Morgantown Energy Technology Center has accepted the acoustically enhanced remediation project Phase II recommendation. Phase II will focus on identifying the characteristics of a field deployable AER technology system based on (1) two-dimensional tank-scale testing of the phased array approach for vadose zone and ground water conditions contaminated with a chlorinated hydrocarbon DNAPL, and (2) two- and three-dimensional modeling of the fluid flow and contaminant transport behavior under baseline and excited conditions, and of the acoustical responses generated in the soil and ground water. Phase II will also address the sorbed and dissolved phases, and a field site for Phase III testing will be identified. Phase II is excepted to be 10 months in duration.

Acknowledgments

We are thankful for the significant assistance and guidance provided by our former COR, Mr. R. McQuisten of the Laramie Project Office who recently retired, our current COR, Mr. Karl-Heinz Frohne at METC, our Contracting Specialist, Ms. R. Diane Manilla, also at METC, and Dr. Alan Browne of Energetics, the support contractor at METC for the Research Opportunity Announcement (ROA) program. We also thank METC and DOE for making the ROA program possible. The Phase I period of performance was from July 1994 to October 1995.

References Cited

Cohen, R. M. and J. W. Mercer, 1993. DNAPL Site Evaluation, C. K. Smoley, Boca Raton, Florida.

Iovenitti, J. L., T. M. Rynne, J. W. Spencer, Jr., 1994, Acoustically Enhanced Remediation of Contaminated Soils and Ground water, proceedings of Opportunity'95 - Environmental Technology Through Smll Business Conference, Morgantown Energy Technology Center, p. 87-99.

Jones, S. C. and W. O. Roszelle, 1978. Graphical Techniques for Determining Relative Permeability from Displacement Experiments, Journal of Petroleum Technology, vol. 15, pp. 807-817.

Reddi, L., S. Berliner and K. Y. Lee, 1993. Feasibility of Ultrasonic Enhancement of Flow in Clayey Sands, Journal of Environmental Engineering, vol. 119, pp. 746-752.

Reddi, L., A. Hadim, R. N. Prabhushankar and F. Shah, 1994. Vibratory Extraction of Clay Fines From Subsurface, Journal of Environmental Engineering, vol. 120, pp. 1544-1558.

Wilson, J. L., S. H. Conrad, W. R. Mason, W. Peplinski and E. Hagen, 1990. Laboratory Investigation of Residual Liquid Organics, U.S. Environmental Protection Agency, EPA/600/6-90/004.

PII.5 Measuring Fuel Contamination Using High Speed Gas Chromatography and Cone Penetration Techniques

Stephen P. Farrington, P.E. (stephen.farrington@ned.ara.com; 802-763-8348)
Wesley L. Bratton, Ph.D., P.E. (wes.bratton@ned.ara.com; 802-763-8348)
Applied Research Associates, Inc.
Box 120-A Waterman Road
South Royalton, VT 05068

Michael L. Akard, Ph.D. (313-662-3410)
Mark Klemp, Ph.D. (75511.371@compuserve.com; 313-662-3410)
Chromatofast, Inc.
912 North Main Street, Suite 14
Ann Arbor, MI 48104

Introduction

Decision processes during characterization and cleanup of hazardous waste sites are greatly retarded by the turnaround time and expense incurred through the use of conventional sampling and laboratory analyses. Furthermore, conventional soil and groundwater sampling procedures present many opportunities for loss of volatile organic compounds (VOC) by exposing sample media to the atmosphere during transfers between and among sampling devices and containers. While on-site analysis by conventional gas chromatography (GC) can reduce analytical turnaround time, time-consuming sample preparation procedures are still often required, and the potential for loss of VOC is not reduced.

Research sponsored by the U.S. Department of Energy's Morgantown Energy Technology Center, under contract DE-AR21-95MC31186 with Applied Research Associates, Inc., RR1 Box 120-A Waterman Road, South Royalton, VT 05068; telefax : 802-763-8283.

Approach

A High Speed Gas Chromatography (HSGC) and Cone Penetration Testing (CPT) system is being developed which can detect and measure subsurface fuel contamination at DOE sites *in situ* during the cone penetration process. The system is portable and can conduct measurements in the unsaturated and saturated zones. Two modes of operation are supported in the unsaturated zone; a continuous screening mode that will provide uninterrupted screening for fuel contamination in near real time during the penetration process, and an advanced analysis mode that will provide analytical precision to the parts per billion (ppb).

Project Description

The HSGC/CPT system for use in the unsaturated zone consists of a heating sampling CPT probe coupled via a heated sample transfer line to a specialized uphole gas chromatograph located on the CPT rig.

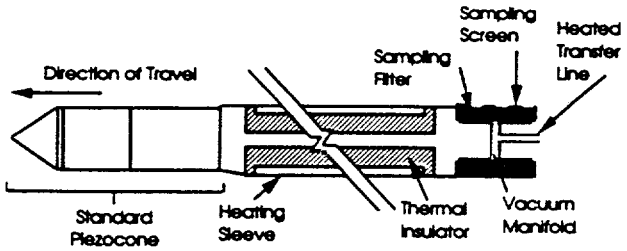

Figure 1. Schematic of Heating Sampling Probe for Use in the Unsaturated Zone

The primary physical features of the heating sampling probe are the heating sleeve and the sampling port. A schematic of the probe is shown in Figure 1. As the probe advances through the ground, the heating sleeve heats the soil matrix ahead of the sampling port to increase the proportion of VOC contamination residing in the vapor phase.

By elevating the temperature of the soil matrix, the equilibrium partitioning distribution changes. This causes an increase in vapor phase (volatilized) concentrations and a decrease in solid phase (adsorbed) and liquid phase (dissolved) concentrations. Soil gas is continuously drawn into the probe through the sampling port and transferred under slight vacuum to the surface for introduction to the HSGC. The transfer lines are heated to prevent sampled vapors from condensing before they reach the HSGC inlet.

The HSGC uses direct vapor phase sample introduction with a Flame Ionization Detector (FID) and a Photoionization Detector (PID). Cryo-focusing inlet technology limits the time over which the sample is introduced to the column to just a few milliseconds. The shortened introduction window in conjunction with mixed stationary phase and/or tandem column separation enhancement techniques facilitates clean separations over a compact column length. Screening mode analyses for BTEX compounds can be performed typically in 20 seconds or less (about every 40 centimeters of probe advancement). In the advanced analysis mode, concentrations can be detected in the ppb range within a one to three minute analysis time.

Principle of Operation - Probe

A nonionic organic compound in the unsaturated zone will partition among four phases: pure phase, solute in water (aqueous phase), soil (adsorbed phase), and air (gas phase). The equilibrium distribution of an organic compound into the four phases depends on system pressure and temperature, thermodynamic properties of the compound, soil chemistry, and the presence of other compounds in the system. If the bulk concentration of the compound present does not exceed the saturated capacity of the matrix, then the pure phase may not be present. The equilibrium distribution is described by the following relations.

For equilibrium between the solute gas phase and dissolved phase of a compound at low concentrations, Henry's law is often applied (1,2):

$$C_w = \frac{P_i}{H} \qquad (1)$$

where C_w is the concentration of the solute in water on a molar basis (mol/m^3), P_i is the partial pressure of the compound in the gas phase (atm), and H is the compound's Henry's law constant (atm-m^3/mol). The Henry's law constant can be calculated using the pure vapor pressure P^0 and solubility C^S of the solute (3,4) in the expression $H = P^0/C^S$. Thus the influence of temperature on vapor pressure and solubility will affect the equilibrium phase distribution between gas and aqueous phases.

To evaluate the effect of heating on the solute/vapor phase equilibrium distribution, consider that the variation of vapor pressure with temperature is described by the Clausius-Clapeyron equation, using the compound's latent heat of vaporization, ΔH^{vap}, and the universal Gas-law Constant, R, as follows:

$$P^0 = P_*^0 e^{\frac{\Delta H^{vap}}{R}\left(\frac{1}{T_*}-\frac{1}{T}\right)} \qquad (2)$$

where the * subscript indicates an arbitrary reference temperature. The Clausius-Clapeyron equation clearly indicates that saturation vapor pressure increases strongly with increasing temperature.

Solubility as a function of temperature has been approximated by a smoothing equation (5) of the form:

$$\ln C^S = A + \frac{B}{T} + C \ln T \qquad (3)$$

which, for positive values of the coefficients B and C, can be shown to result in decreasing solubility with increasing temperature. Considering the temperature dependencies in Equations 2 and 3 with regard to Equation 1, we can anticipate a shift of the equilibrium phase distribution of an organic solute toward greater gas phase concentration and lower aqueous phase concentration when the temperature of the system is increased.

For equilibrium partitioning between the adsorbed and solute phases, if the isotherm is linear, a partitioning distribution coefficient is usually applied (2, 6):

$$q = K_d C_{eq} \qquad (4)$$

where q is the adsorbed phase concentration (mass basis), K_d is the distribution coefficient, and C_{eq} is the liquid phase (solute) equilibrium concentration.

The distribution coefficient is correlated to the fraction of organic carbon f_{oc} in the soil by use of an organic carbon partition coefficient, K_{oc}, and expressed as $K_d = K_{oc} f_{oc}$. Although we may estimate the temperature dependence of the distribution coefficient, K_d, for halogenated organic solutes from solubility-temperature data by direct proportionality (6), we do not know the relationship for BTEX compounds. However, sorbed/gaseous phase partitioning equilibrium should be strongly dependent on temperature in the same manner as the aqueous/gaseous phase distribution due to the influence of temperature on the vapor pressure.

Since phase partitioning relationships are temperature-dependent and exhibit an apparent tendency toward greater gaseous phase concentration with increasing temperature, the heating sampling probe is designed to increase the concentration of fuel-based contaminants in the vapor phase by increasing the temperature of the unsaturated soil matrix. Laboratory experiments are planned to quantify this effect using three fuel types and four soil types. However, no quantitative data are available at this time.

Design Considerations - Probe

The probe was designed such that, for a given penetration rate, soil thermal characteristics, and power supplied to the heating sleeve, the maximum temperature of internal probe components would not reach damaging levels, while supplying as much heat as possible to the soil. These considerations influenced the probe geometry and construction materials.

To achieve maximum heat transfer at the soil/probe interface for a given penetration rate,

the CPT cone was given the longest heating surface possible without sacrificing strength or elevating internal probe temperatures to damaging levels. The long heating surface maximizes contact time with the soil. As the probe advances, the power supplied to the heating sleeve is dissipated by thermal transfer into both the soil matrix and the rest of the probe. Heat transferred into the probe also dissipates axially along the probe and is consequently also transferred into the soil through contact ahead of and behind the heating sleeve. This axial heat conduction provides some cooling of the probe interior within the heating sleeve.

Thermal transfer modeling was conducted, using the finite element code TOPAZ, to predict temperature distributions in the soil and probe under different soil conditions, power levels, and penetration speeds. Both one-dimensional, radially symmetric, static (probe not moving) heating and two-dimensional, dynamic (probe moving) heating were modeled. Results will be compared with laboratory experiments and used in modeling the enhanced volatilization due to soil heating.

The probe sampling port was designed with both sampling performance and survivability in mind. The sampling screen consists of a lengthwise slotted steel sleeve, backed by a sintered steel filter. The slotted sleeve protects the sintered filter from damage due to penetration stresses. The sintered filter keeps fine debris from clogging the gas sampling manifold located behind the filter. The manifold provides unencumbered flow along the whole length of and around the entire circumference of the interior surface of the filter. This arrangement promotes equal pressure distribution across the filter at all sections. The sampling port length was kept relatively long to draw the sample gas at a given flow rate from as close to the probe/soil interface as possible, where the maximum soil temperature, and thus maximum gaseous phase contaminant concentration, is achieved.

Principle of Operation - High Speed Gas Chromatography

Gas chromatography (GC) is frequently used for air monitoring because of its potential for complete speciation of VOCs with relatively high precision, accuracy and powers of detection. For ambient air monitoring, detection limits in the part-per-billion (ppb) and part-per-trillion (ppt) range are often required. Some form of sample enrichment is needed to achieve these concentrations. The sample collection and inlet system must perform three basic functions. These include the sampling of a precise volume of gas, concentration of the VOCs from that volume, and injection of the sample onto the column.

The use of mechanical valves with sample loops is a significant limitation for automated, high work-load GC systems. These valves often are maintenance intensive. In addition, sample loss or alteration, or contamination on valve surfaces can be a significant problem. It is also difficult to change sample size, since the fixed volume of the sample loop must be changed, or several valve cycles must be used. A cryofocusing inlet system for high-speed gas chromatography (HSGC) (7) is used which requires no sample loops or mechanical valves in the sample flow path. The system uses a vacuum pump to pull the sample through the capillary metal cold trap. The pressure at the sample source can be anywhere from just above the vacuum pump pressure (about 20 Torr) to just less than the carrier gas pressure. Thus, direct sample collection from the sample transfer line of the HSGC/CPT system can be achieved.

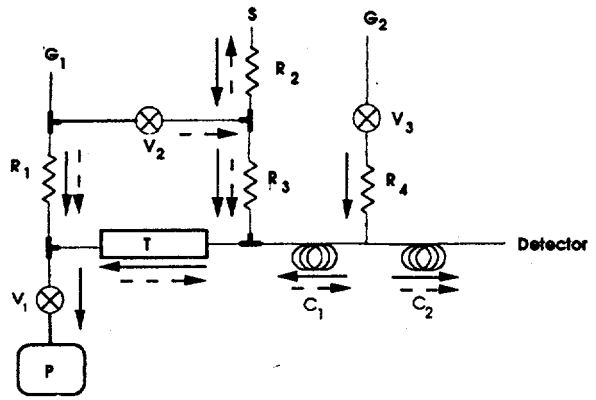

Figure 2. Direct Sample Introduction Air Monitor Concept

Figure 2 shows the concept of the reverse-flow sample collection system planned for the system. Solid lines with arrows show the reverse gas flow directions during sample collection, and broken lines with arrows show the normal flow directions used during the GC analysis. During sample collection a vacuum pump P is used to pull sample from the source S into the metal cold trap tube T. A continuous flow of cold nitrogen gas cools the trap tube to temperatures ranging from -50°C to -100°C. During this operation carrier gas also flows from the gas source G_1 to the vacuum pump, and the separation columns C_1 is backflushed with additional carrier gas from G_2. Restrictors R_2 and R_3 can be adjusted to control the sample gas flow rate during sample collection. After sample collection the normal flow direction is resumed, and carrier gas flows from left to right through the trap tube. A current pulse from a capacitive discharge power supply rapidly heats the metal trap tube (8), and the sample is vaporized and introduced to the first separation column C_1 as a narrow plug. Note that the condensed sample plug in the trap tube is injected into the column from the down-stream end of the trap tube during normal flow operation. This has several advantages relative to previous cryofocusing inlet system designs, including reduced risk of sample decomposition in the hot metal tube and reduced band broadening from the tube dead volume.

To use this system for extended cryointegration from a low-concentration sample source, the analytical column can be divided into two segments, C_1 and C_2. Valve V_3 and carrier gas supply G_2 provide carrier gas to backflush C_1 during sample collection. The forward flow direction through C_2 prevents water formed in the FID from being pulled into the trap tube and freezing. If sample collection is restricted to a few seconds this portion of the instrument can be omitted. However, this configuration is also useful for preventing deterioration of water or air sensitive stationary phases.

A necessary consideration in the development of a HSGC system is the minimization of extra-column band broadening (9). A problem with the cold trap is that the length of the trap tube must be long enough to cryofocus the most volatile component in the sample. Studies have suggested trap lengths greater than 20-cm are necessary for efficient operation (10). By initially placing the sample at the downstream end of the cold trap, the effect of this dead volume is minimized. While the trap length was 25 cm in this study, longer trap lengths might be used without adding dead volume to easily trapped components. Injection band widths from the cold trap were around 6 ms.

Table 1 shows statistical data for cryointegration with relatively low sampling flow rates and a trap diameter of 0.031 mm i.d. With the use of high flow rates and wider bore traps of 0.058 mm i.d., detection limits have been determined at 0.775 ppb for benzene and correlation coefficients ranging from 0.9998 to 0.999998 were observed for normal alkanes.

Table 1. Statistical Data for Cryointegration

Component	Correlation Coefficient	Log-Log Slope	LOD[a] ppb[b] 10[c]	110[c]
Benzene	01993	0.99	26	4.6
n-Heptane	0.997	1.04	37	6.9
Toluene	0.999	1.07	25	4.0
n-Octane	0.995	1.07	47	8.4
p-Xylene	0.999	1.09	29	4.4

[a] Limit of detection is 3 times signal to noise ratio
[b] Parts per billion (vol/vol)
[c] Sampling times

HSGC focuses on obtaining drastic reductions, often two orders of magnitude, in analysis time. Most of this work has involved the use of relatively short capillary columns coupled with efficient inlet systems. The use of short columns, relative to conventional practice, results in a significant loss in resolution and zone capacity. Thus, the use of HSGC has been limited to relatively simple mixtures.

When HSGC is applied to more complex mixtures, greater control of relative peak positions within the chromatograms is essential. Any single stationary phase at a specified temperature will result in a specific selectivity. By the use of mixed stationary phases, a more continuous range of selectivities can be obtained. Several mixed-phase columns are available commercially for specific applications, often involving U.S. regulatory-driven procedures. The phase mixture is formulated to give the best separation of the worst-case (critical) pair of compounds in a specified mixture. Similar results are achieved by varying the length ratio of a tandem (series-coupled) combination of columns using different stationary phases.

Optimization strategies for both the mixed-phase and tandem-column cases usually are based on the construction of a window diagram in which the relative retention (capacity factor ratio) of the poorest separated pair of components (critical pair) is plotted versus the phase-quantity fraction of either phase for a mixed-phase column or the equivalent column-length fraction of either column in a tandem pair. The largest peak in the diagram identifies the best phase or length fraction. HSGC usually involves the use of relatively low capacity factors to reduce analysis time and to increase the rate of theoretical plate production. Capacity factor is defined as the ratio of the amount of component in the stationary phase to the amount of component in the mobile phase. However, the number of plates required for a separation increases rapidly with decreasing capacity factor for small capacity factor values. This increase is the result of inadequate interaction of the solutes with the stationary phase. The use of relative retention does not take this into account and thus can over-estimate the quality of the separation as well as result in the incorrect choice of phase-quantity fraction or column length fraction for the best separation.

An alternative retention function for the construction of window diagrams can be obtained from the Purnell equation for chromatographic resolution.

$$R = \frac{\sqrt{N}}{4}\frac{(D_2 - D_1)}{D_{av}}\frac{k}{(k+1)} \quad (5)$$

where N is the number of plates on the column, D_1, D_2 and D_{av} are the phase distribution ratios for components 1 and 2 and their average value, respectively, and k_{av} is their average capacity factor. Since distribution ratios and capacity factors are proportional, Equation 5 can be recast as Equation 6.

$$R = \frac{\sqrt{N}}{4}\frac{(k_2 - k_1)}{k}\frac{k}{(k+1)} \quad (6)$$

From this, an optimization parameter called relative resolution R_{rel} can be defined.

$$R_{rel} = \frac{(k_2 - k_1)}{(k+1)} \quad (7)$$

$$R = R_{rel}\frac{\sqrt{N}}{4} \quad (8)$$

Relative resolution has been shown to be the best parameter for HSGC (11).

Most HSGC work has been done isothermally. The choice of the column temperature is crucial to the separation. It has been shown that the greatest plate production per time for HSGC occurs when the capacity factor is in the range from 1 to 2 (4, 11). Lower temperatures will increase the capacity factors of earlier eluting components, generally improving their separation and increasing the zone capacity of the separation. Later eluting components will have increased retention which decreases the plate production per time, increases the overall separation time, and reduces powers of detection. Higher temperatures have the opposite effect.

Temperature has a more dramatic effect when tandem columns are used. The capacity factors decrease on both columns as the temperature is increased, but typically change at different rates. The result of this differential change in capacity factor on the different phases with respect to temperature is that selectivity will change with temperature. Window diagrams have been used to predict the selectivity tuning with respect to temperature.

The capacity factor, k, is dependent on the selective interactions of the solute with the stationary phase, and on the saturation vapor pressure P^0 (12).

$$k = \frac{1}{\gamma P^0(T)} \quad (9)$$

As shown in Equation 9, P^0 is a function of the column temperature, T. Selective interaction with the stationary phase can be expressed by the activity coefficient γ. Previous work predicts capacity factors at a given temperature using retention indices. Capacity factors can be calculated directly by Equation 10 using aluminum oxide PLOT columns (13).

$$\log(k) = \frac{m}{T} + b \quad (10)$$

Results

Water vapor in the air sample, can result in ice formation in the trap tube. Other studies have shown that up to about 2 mL of water saturated air can be collected in the trap tube without significant flow changes from ice formation. For the following data the maximum sample size collected was about 0.6 mL and thus no ice formation problem was observed.

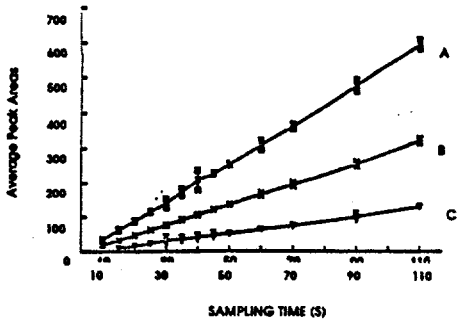

Figure 3. Plots of Peak Area Versus Sampling Time with Mid-Point Backflush.

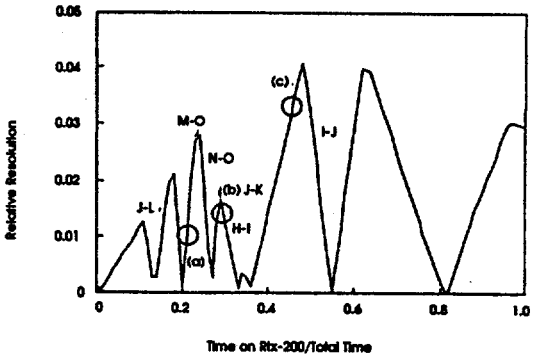

Figure 4. Window Diagram Plotting Relative Resolution of the Critical Pair Versus the Hold-Up Time Fraction of Rtx-200.

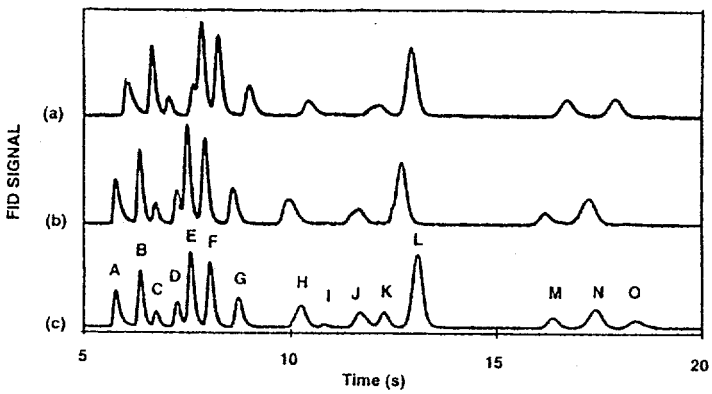

Figure 5. Chromatograms for the Components Listed in Table 2, at a Temperature of 40°C
(The second column is DB-5.)

Figure 3 shows plots of average peak area versus sample collection time for a three-component mixture with make-up gas. Plots labeled A, B, and C are for p-xylene, toluene, and n-octane, respectively. The sample flow rate was 0.0083 ml/s. The trap tube temperature during sample collection was -110°C and +150°C for sample injection. When make-up gas is used, reasonably linear plots of peak area versus sampling time are observed over a range of sample collection times from 10 s to 110 s. Peak area reproducibility is satisfactory with relative standard deviations less than about 2%.

The slope m and intercept b were determined experimentally for a set of components on the four different stationary phases. With the slope and intercept values, the capacity factor can be determined at any temperature and window diagrams can then be produced to determine the best separation. Figure 4 shows a window diagram for the components listed in Table 2. Note that points labeled (a), (b), and (c) correspond to the chromatograms shown in Figure 5. The chromatograms (a), (b), and (c) correspond to hold-up time fractions on Rtx-200 of 0.21, 0.30,

Table 2. Component List for Figures 3 and 4 and the Relevant Log (k) vs. 1/T data on the DB-5 and Rtx-200 Columns

Components	Log (k) vs. 1/T DB-5			Log (k) vs. 1/T Rtx-200		
	slope (m)	intercept (b)	R^2	(m)	(b)	R^2
A Acetaldehyde	2174	-9.814	0.079	2072	-7.767	0.887
B *tert*-Butyl methyl ether	1807	-6.715	0.992	2255	-7.856	0.967
C Chloroform	1392	-5.190	0.993	1498	-5.373	0.975
D Tetrachloromethane	1723	-6.044	0.997	1869	-6.441	0.982
E Benzene	1508	-5.357	0.998	1658	-5.600	0.995
F Fluorobenzene	1685	-5.820	0.999	1752	-5.701	0.997
G 3-Pentanol	1608	-5.517	0.999	1760	5.666	0.999
H 3-Methyl-1-butanol	1862	-5.137	0.999	1912	-5.939	0.999
I 1-Pentanol	1935	-5.245	0.999	1950	-5.959	0.998
J 2-Pentanone	1752	-5.989	0.999	1877	-5.702	0.999
K Tetrachloroethylene	1844	-5.835	1.000	1829	-5.709	0.999
L 1,3-Dichloropropane	1871	-5.988	1.000	1905	-5.700	0.999
M Chlorobenzene	1899	-5.870	1.000	1893	-5.614	1.000
N 1-Chlorohexane	2029	-6.233	1.000	1964	-5.810	1.000
O Cyclopentanone	1870	-5.992	1.000	2035	-5.789	1.000

and 0.45, respectively. A length fraction corresponding to 40% Rtx-200 would therefore successfully separate the given mixture in under 20 seconds.

Benefits

A new method of measuring fuel contamination in the field is being developed which uses High Speed Gas Chromatography and Cone Penetration Techniques. The new method has been shown to be feasible and offers several distinct advantages over conventional sampling and analysis.

First, the new method is fast. HSGC/CPT generates a virtually continuous profile of results in near real time. A screening measurement is made approximately every twenty seconds, or about every 40 centimeters (16 in.) of vertical advancement without retracting the probe from the ground. Traditional drilling approaches to sampling and analysis can only practically generate a measurement about every two feet, and require retracting the auger from the hole for each sample taken. Thus production is faster and coverage is more thorough using the CPT based system.

Second, the new method is sensitive. In addition to more thorough site coverage, HSGC/CPT can detect low concentrations with greater precision than conventional, direct injection soil gas or headspace analyses because the heating probe thermally extracts contaminants from the dissolved and adsorbed phases, elevating the concentration in the soil gas sample above ambient conditions, and

cryointegration allows a large sample volume to be concentrated while limiting the introduction time onto the separation column. If contamination is detected in the screening mode, probe advancement can be temporarily interrupted to perform a more accurate analysis of the specific compounds present by increasing the analysis time to one to three minutes.

Third, the new method is accurate. Loss of VOC is minimized with HSGC/CPT because sample exposure to the atmosphere is eliminated. Soil gas is sampled *in situ* and transferred via closed conduit to the injection port of the gas chromatograph, where analysis begins.

Last, the new method is safe. HSGC/CPT produces no drilling spoils or wastes that can require costly handling and disposal. Thus, the potential for worker exposure to contamination is also greatly reduced.

Future Activities

In the immediate future, laboratory studies will be conducted to obtain experimental soil heating data for comparison to the thermal transfer modeling results. Subsequently, sample recovery enhancement due to heating will be quantified.

This project includes several other development tasks that are in differing stages of completion. A second sampling probe, currently in the design stage, will sample groundwater from the saturated zone and purge the sample downhole, transferring the purge gas to the surface for HSGC analysis. Downhole traps will also be integrated into this probe to provide the option of retaining purged contaminants for later analysis.

The unsaturated and saturated zone probes and HSGC will be field tested in winter 1995-96. The fully integrated system will be demonstrated at Savannah River Site in spring 1996.

Acknowledgments

The authors wish to acknowledge Dr. Richard Sacks of the University of Michigan, Department of Chemistry for his contribution to the HSCG work, and William Congdon of Applied Research Associates, Inc.'s Colorado division for performing the thermal transfer modeling. We also wish to acknowledge the METC Contracting Officer's Representative, Steve Cooke. The period of performance for this contract is February 1995 through July 1996. The subcontractor on this project is Chromatofast, Inc.

References

1 Shoemaker, C.A., T.B. Culver, L.W. Lion, and M.G. Peterson, April 1990. Water Resources Research, Vol 26, No. 4.

2 Fuentes, H.R., E.H. Essington, J.L. Smith, W.L. Polzer, 1990. Hazardous Waste and Hazardous Materials, Vol 7, No. 4.

3 Mackay, D., and S. Peterson, September 1981. Environmental Science and Technology, Vol 15, No. 9.

4 Mackay, D., October 1979. Environmental Science and Technology, Vol 13, No. 10.

5 Lide, D.R., 1994. Handbook of Chemistry and Physics, 74th ed., CRC Press.

6 Curtis, G.P., P.V. Roberts, and M. Reinhard, December, 1986. Water Resources Research, Vol 22, No. 13.

7 Klemp M., M. Akard and R. Sacks, 1993. Anal. Chem. 65, 2516.

8 Annino R., and Leone, J. 1982. Chromatogr. Sci. 20, 19.

9 Graydon J., and K. Grob, 1983. J. Chromatogr. 254, 265.

10 Mouradian R., S. Levine, and R. Sacks, 1990. J. Chromatogr. Sci. 28, 643.

11 Ewels B., and R. Sacks, 1985. Anal. Chem. 57, 2774.

12 Mouradian, R., S. Levine, R. Sacks and M. Spence, 1990. Am. Ind. Hyg. Assoc. J. 51, 90.

13 Gaspar G., P. Arpino, and G.J. Guiochon, 1977. J. Chromatogr. Sci., 15, 256.

PII.8

Fiber Optic/Cone Penetrometer System for Subsurface Heavy Metals Detection

Dr. Steven Saggese (ssaggese @ seasd.com; 619-294-6982)
Dr. Roger Greenwell (greenwel@seasd.com; 619-294-6982)
Science & Engineering Associates, Inc.
2878 Camino del Rio South Suite 315
San Diego, CA 92108

Needs

The characterization, monitoring and remediation of contaminated soils is extremely expensive and time consuming due to the magnitude of the effort and the utilization of laboratory chemical analysis techniques. The present laboratory methods of evaluating environmental samples offer high sensitivity and the ability to evaluate multiple chemicals, but the time and cost associated with such methods often limit their effectiveness. Heavy metal soil contamination is an area of great concern for government and industry. Table 1 shows a

Table 1. Summary of Metals Contamination in Super Fund Sites for (a) Different Industries and (b) the Number of Sites Reporting Specific Metal Contamination[1]

(a)

# of Sites	Industry	Metals Most Often Reported
154	landfill/chemical waste dump	As Pb Cr Cd Ba Zn Mn Ni
43	metal finishing/plating/elect.	Cr Pb Ni Zn Cu Cd Fe As
35	chemical/pharmaceutical	Pb Cr Cd Hg As Cu
28	mining/ore proc./smelting	Pb As Cr Cd Cu Zn Fe Ag
21	federal (DOD, DOE)	Pb Cd Cr Ni Zn Hg As
19	battery recycle	Pb Cd Ni Cu Zn
18	wood treating	Cr Cu As
16	oil and solvent recycle	Pb Zn Cr As
13	nuclear processing/equip.	Ra Th U
5	pesticide	As
5	vehicle and drum cleaning	As
3	paint	Pb Cr Cd Hg
29	other	As Pb Hg Cr

(b)

Metal	# of Sites
Pb	133
Cr	118
As	77
Cd	65
Cu	49
Zn	40
Hg	32
Ni	24
Ba	10
Ag	10

Research sponsored by the U.S. Dept. of Energy's Morgantown Energy Technology Center, under contract DE-AR21-95MC32089 with Science & Engineering Associates, Inc., 6100 Uptown Blvd. NE, Suite 700, Albuquerque NM 87107, telefax: 505-884-2300.

summary of the metals problem in National Priority (Superfund) Sites. Forty-one per cent of the sites report metals problems, with Pb and Cr being most often cited for a wide variety of industries. There exists a requirement for economically feasible, real-time, in-situ, systems for the characterization of the subsurface. Such technologies will enable efficient prioritization of remediation efforts.

Objectives

The objective of this project is to develop an integrated fiber optic sensor/cone penetrometer system to analyze the heavy metals content of the subsurface. This site characterization tool will use an optical fiber cable assembly which delivers high power laser energy to vaporize and excite a sample in-situ and return the emission spectrum from the plasma produced for chemical analysis. The chemical analysis technique, often referred to as laser induced breakdown spectroscopy (LIBS), has recently shown to be an effective method for the quantitative analysis of contaminants in soils. By integrating the fiber optic sensor with the cone penetrometer, we anticipate that the resultant system will enable in-situ, low cost, high resolution, real-time subsurface characterization of numerous heavy metal soil contaminants simultaneously.

There are several challenges associated with the integration of the LIBS sensor and cone penetrometer. One challenge is to design an effective means of optically accessing the soil via the fiber probe in the penetrometer. A second challenge is to develop the fiber probe system such that the resultant emission signal is adequate for quantitative analysis. Laboratory techniques typically use free space delivery of the laser to the sample. The high laser powers used in the laboratory cannot be used with optical fibers, therefore, the effectiveness of the LIBS system at the laser powers acceptable to fiber delivery must be evaluated. The primary objectives for this project are:

- Establish that a fiber optic LIBS technique can be used to detect heavy metals to the required concentration levels.
- Design and fabricate a fiber optic probe for integration with the penetrometer system for the analysis of heavy metals in soil samples.
- Design, fabricate, and test an integrated fiber/penetrometer system.
- Fabricate a rugged, field deployable laser source and detection hardware system.
- Demonstrate the prototype in field deployments.

Approach

In order to conduct subsurface analysis for heavy metals, a LIBS system with a fiber optic probe will be integrated with a cone penetrometer. Figure 1 shows the approach. The optical instrumentation will be located within the penetrometer truck and the optical fibers will bring the signal to the soil via the push rod. A LIBS configuration typically consists of a laser source to produce the plasma, an optical fiber for delivering the laser beam, launch and collection optics, a spectrometer to spectrally resolve the emission spectrum, an array detector for simultaneous measurements of intensities over a range of wavelengths, a trigger to coordinate the laser pulse and the temporal measurement window of the detector, and a computer to conduct equipment control, data acquisition, and data analysis. Figure 2 shows a sample emission spectra for 1000 ppm Pb in soil. In order to conduct quantitative analysis, the system is calibrated to evaluate the peaks of the emission. Each peak can be assigned to an element and

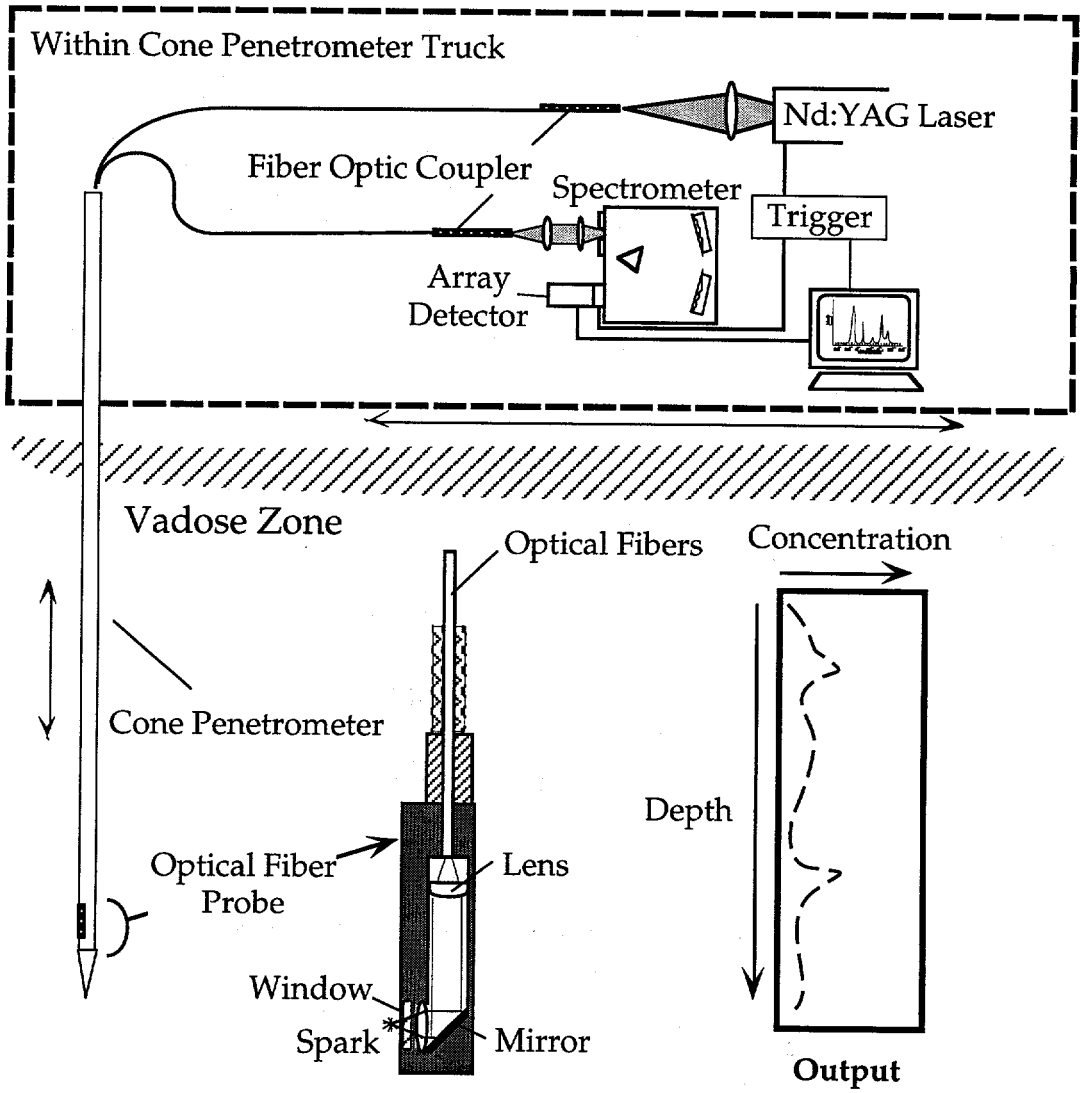

Figure 1. Fiber Optic/Cone Penetrometer System for Subsurface Analysis

the intensity of the peak will be an indication of the concentration. The cone penetrometer will enable a subsurface map to be generated by moving the probe vertically and laterally.

Project Description

This project includes an initial 6 month feasibility evaluation phase and an optional 18 month prototype development phase.

The feasibility evaluation effort has begun and it consists of three primary tasks; 1) determination of the system requirements, 2) design of the optical probe, and 3) the evaluation of the probe for conducting quantitative analysis of heavy metals in soils.

The purpose of the initial task is to establish the requirements of the sensor system, including information on the specific analytes of interest,

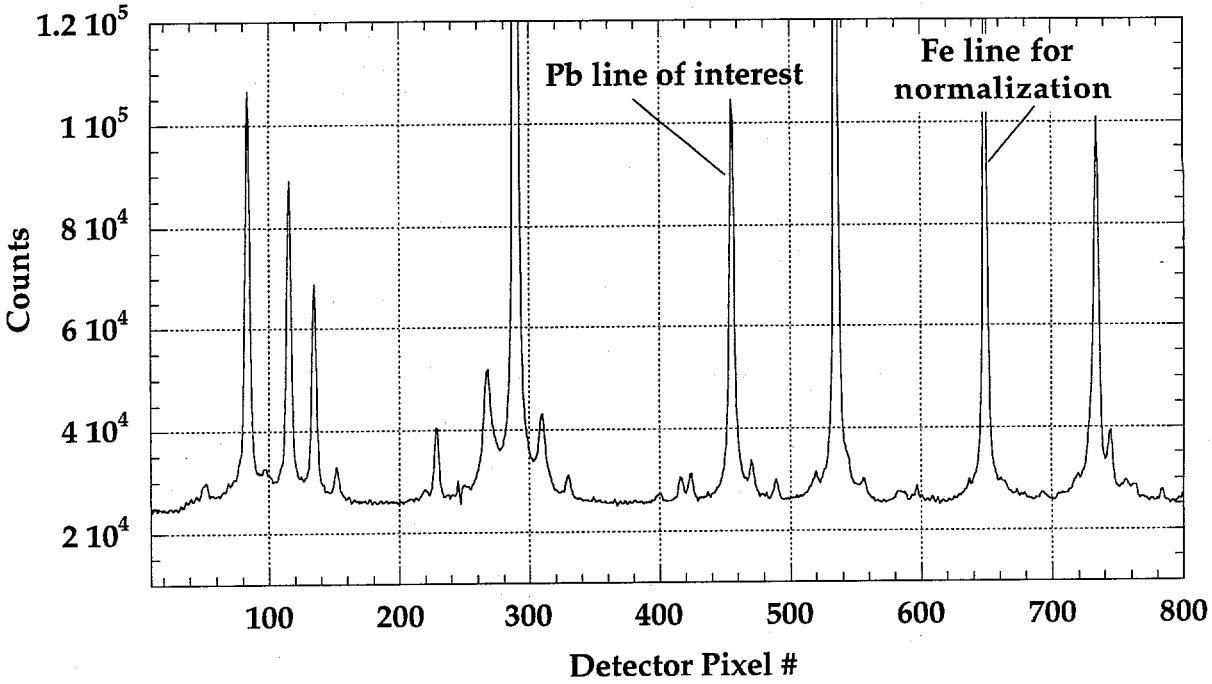

Figure 2. LIBS Emission Spectra for 1000 ppm Pb in Soil

concentration levels, ranges, and the typical depths of subsurface contamination. Regulatory information has been obtained so that the system sensitivity can be evaluated against accepted remediation action levels. This task has also documented the present knowledge for the LIBS analysis relating to soil and fiber optic delivery. In addition, the deployment system characteristics, such as the dimensions of present penetrometer designs, conditions during deployment, and space limitations in the deployment vehicle will be investigated.

The next task is to design and evaluate an optical fiber probe to enable access to the soil from the penetrometer. In order to effectively complete this task, a laboratory LIBS will be used to conduct quantitative analysis on trace metals in soils. The system will be capable of using free space delivery of the laser to the soil to establish a baseline performance of the system by which the fiber system can be compared. This laboratory data will be used to establish the methodology for conducting quantitative analysis. In addition, this task will investigate the various ways to optically access the soil via the cone penetrometer/fiber optic system. Based on this work, fiber optic probe(s) will be designed.

For Task 3, SEA will fabricate the most promising probe(s) to simulate penetrometer deployment and evaluate the probes for the ability to conduct quantitative analysis on soils. The performance will be compared to the laboratory (non-optical fiber) LIBS analysis and laboratory analytical methods. In particular, quantitative analysis of Cr and Pb in various types of soils will be conducted.

Upon successful completion of this Phase I effort, the Phase II project will fabricate a

rugged system that integrates the optical source and detection equipment, optical fiber probes, and cone penetrometer. This phase will consist of laboratory evaluation, optimization, field demonstrations of the entire system using a cone penetrometer vehicle and culminate with site evaluations at a government facility.

Results

The Phase I effort was started in mid-July 1995 and SEA is presently starting the second task described above. A laboratory LIBS set-up has been used to evaluate the effectiveness of a LIBS system for quantitative analysis of Pb in soils. Figure 2 shows the overall spectra from the soil using a free space delivery of the laser and the peaks of interest have been labeled. Figure 3 shows a close view of the Pb line as a function of Pb concentration. To conduct quantitative analysis, it is beneficial to ratio the area of the Pb peak to the emission of another element in the sample - preferably an element that has a nearly constant concentration. The Fe line shown in Figure 2 is often used and this helps minimize the effects due to fluctuations in the shot-to-shot laser power and variations in the sample. Figure 4 shows a calibration curve that was constructed for a range of Pb concentrations. From this data, it was determined that the minimum detection limit for this arrangement was in the 10-40 ppm range. The EPA's Office of Solid Waste and Emergency Response (OSWER) has indicated a soil screening level for Pb at 400 ppm. Pb concentrations exceeding this level would trigger further remediation activities.[2] The LIBS system without fiber delivery is readily sensitive below this 400 ppm Pb level.

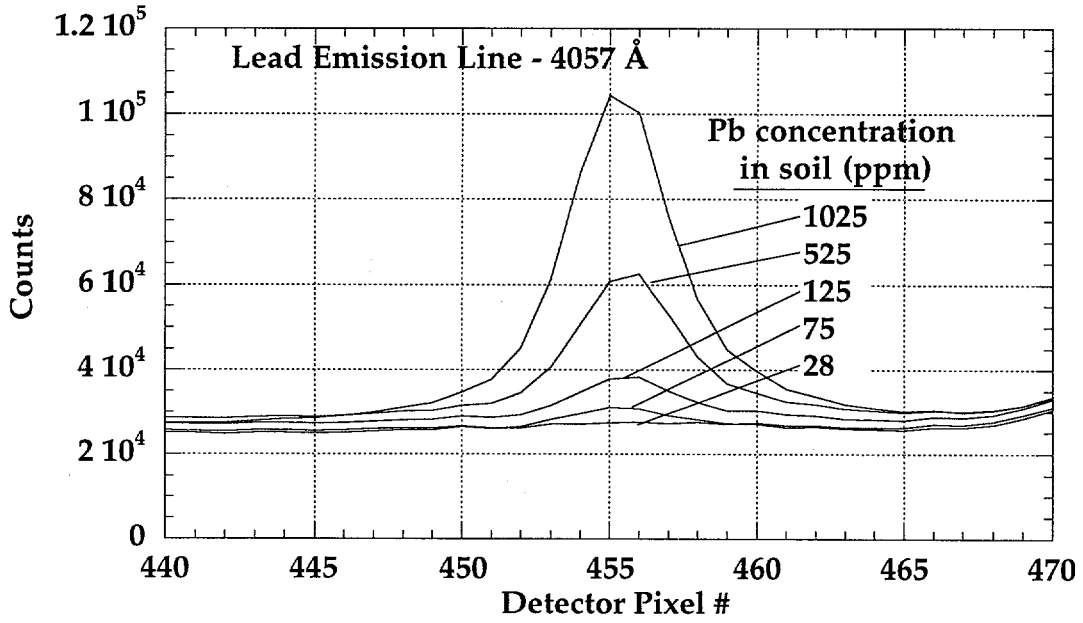

Figure 3. Alteration of the Pb Emission Intensity at 4057Å as a Function of Pb Concentration in Soil

Benefits

The benefits of this system are:

- In-situ evaluation will limit the personnel exposure and public exposure during transportation of samples, and sites will be characterized faster, therefore, remediation can occur sooner.

- The system will provide a more detailed, higher resolution analysis of the site.

- The system will reduce the need for expensive laboratory techniques.

- Since the system is real time, decisions on the remediation can be made faster with more intelligence. The system could be used to monitor the remediation process in-situ, thus enabling this process to be modified for optimum performance.

- The LIBS technique has a broad range of applicability and the addition of optical fibers makes remote applications and industrial applications feasible.

Future Activities

The near future plans are to complete the primary feasibility evaluations. The optical access to the soil from the penetrometer will be evaluated and probes will be fabricated and tested. The Phase II effort will develop a complete integrated system for field deployments.

Acknowledgments

This work is being conducted for the DOE Office of Environmental Restoration and Waste Management with a focus on Characterization, Sensors, and Monitoring. SEA would like to

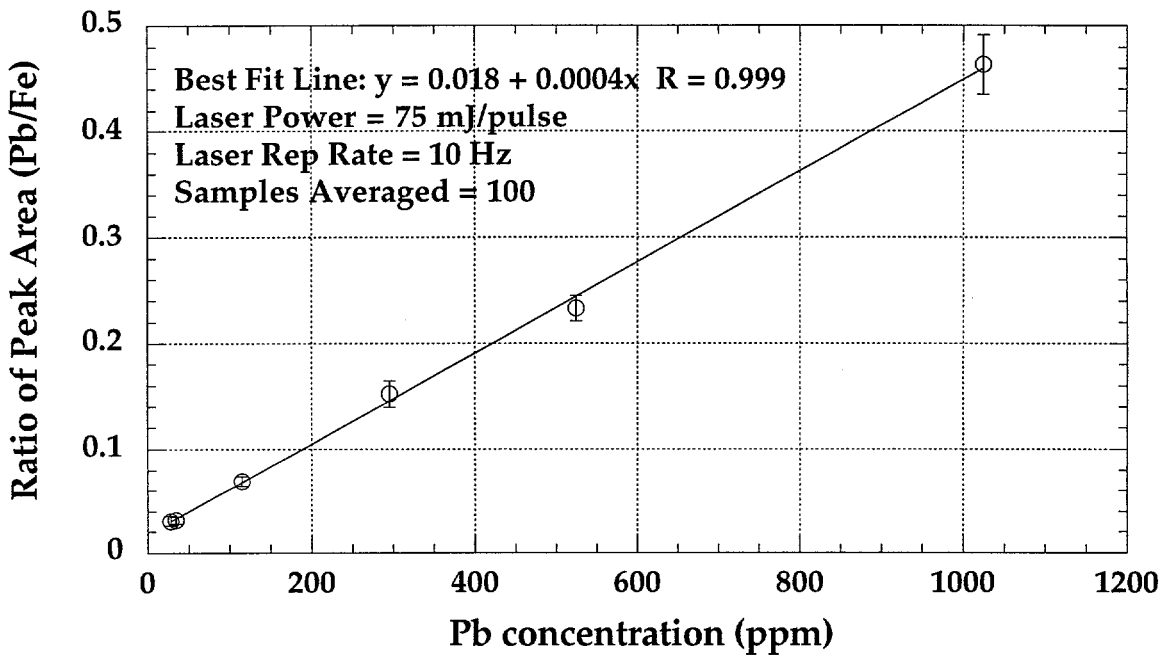

Figure 4. Calibration Curve for Pb in Soil Using Free Space Delivery of the Laser to the Soil

acknowledge the METC COR, Mr. Karl-Heinz Frohne, and subcontractors Applied Research Associates (ARA) and Los Alamos National Labs (LANL). ARA personnel have successfully developed numerous advanced cone penetrometer systems for the chemical and physical evaluation of the subsurface and LANL personnel are recognized experts on the development of LIBS systems for the analysis of soils. This effort, if completely funded, will have a 24 month period of performance.

References

1. Allen, H.E., C.P. Huang, G.W. Bailey, A.R. Bowers, 1995, *Metal Speciation and Contamination of Soil*, Lewis Publishers, Boca Raton.

2. EPA OSWER Directive #9355.4-12, July 14, 1994, *Revised Interim Soil Lead Guidance for CERCLA Sites and RCRA Corrective Action Facilities.*

PII.9

Radioactivity Measurements Using Storage Phosphor Technology

Y.T. Cheng (YJZC51A@PRODIGY.COM; 301-975-6216)
NeuTek
13537 Scottish Autumn Lane
Darnestown, MD 20878-3990

J. Hwang (301-424-0850)
Advanced Technologies and Laboratories International
17 Yearling Court
Rockville, MD 20850

M.R. Hutchinson (301-975-5532)
National Institute of Standards and Technology
Ionizing Radiation Division, Physics Laboratory
Gaithersburg, MD, USA 20899

Introduction

We propose to apply a recently developed charged particle radiation imaging concept in bio-medical research for fast, cost-effective characterization of radionuclides in contaminated sites and environmental samples. This concept utilizes sensors with storage photostimulable phosphor (SPP) technology as radiation detectors. They exhibit high sensitivity for all types of radiation and the response is linear over a wide dynamic range (>10^5), essential for quantitative analysis. These new sensors have an active area of up to 35 cm x 43 cm in size and a spatial resolution as fine as 50 μm. They offer considerable promise as large area detectors for fast characterization of radionuclides with an added ability to locate and identify hot spots.

Research sponsored in part by the U.S. Department of Energy's Morgantown Energy Technology Center, under contract DE-AR21-95MC32090 with NeuTek, 13537 Scottish Autumn Lane, Darnestown, MD 20878-3990; telefax: 301-948-6427.

Tests with SPP sensors have found that a single alpha particle effect can be observed and an alpha field of 100 dpm/100 cm^2 or a beta activity of 0.1 dpm/mm^2 or gamma radiation of few μR/hr can all be measured in minutes. Radioactive isotopes can further be identified by energy discrimination which is accomplished by placing different thicknesses of filter material in front of the sensor plate. For areas with possible neutron contamination, the sensors can be coupled to a neutron to charged particle converter screen, such as dysprosium foil to detect neutrons. Our study has shown that this approach can detect a neutron flux of 1 n/cm^2s or lower, again with only minutes of exposure time. The utilization of these new sensors can significantly reduce the time and cost required for many site characterization and environmental monitoring tasks. The "exposure" time for mapping radioactivity in an environmental sample may be in terms of minutes and offer a positional resolution not obtainable with presently used counting equipment. The resultant digital image will lend itself to ready analysis.

The SPP technology has been investigated for applications to medical x-ray imaging and is well proven in molecular biology and radiopharmaceutical research[1-4]. The concept of the technology involves radiation-caused trapping in a sensor plate and release of the trapped energy as light when the sensor is stimulated under the scanning of a laser beam in a reader unit. A photomultiplier tube detects the light and coordinates the light intensity with the scanned positions, creating a digital image of the radiation field. After scanning, the sensor plate can be quickly cleaned and reused again. The separation of the sensor, a semi-flexible plastic plate coated with a thin layer of a special phosphor material, from the laser reader unit means that multiple sensor plates can be used simultaneously for radiation monitoring, thus increasing the effective detector area. For environmental monitoring, this two-step process involved in the SPP application may prove to be advantageous, in that multiple imaging sensor plates can be used to cover a large area of interest, or to assay a group of samples simultaneously. After a short time of exposure the sensor plates can be collected and taken to a data reading station for reading. The reading station consists of a PC-class computer and a laser readout unit which in its current configuration resembles a medium size printer. The station can be placed in a small vehicle or mounted on a cart. The reading process takes about two minutes per sensor plate. Afterwards sensor plates can be quickly cleaned by exposing to a UV source in an eraser and be reused again.

Experiment and Results

A test was conducted on one type of SPP imaging sensors with $BaFBr:Eu^{2+}$ as the phosphor to determine its potential as an alpha particle detector. Two National Institute of Standards and Technology (NIST) standard alpha sources AA840 and AA370 (^{238}Pu, 12.75 cm x 20.25 cm active area, 3.85×10^2 dps and 2.33×10^3 dps respectively) were used. Figure 1 shows the results of 20 second and an 100 second exposure respectively with the source AA840 being held 0.4 cm away from the SPP imaging sensor plate. The 20 second exposure is shown on the left and the 100 second exposure is shown on the right with background area of the imaging sensor plate in the center. A hot spot in the source was detected in the 100 second image and was also visible in the inverted 20 second exposure image. The table in figure 1 lists the integrated relative radiation strength in the three areas defined by the circles. The result of a two second exposure of the same source is shown on the right in figure 2. The 16-fold enlargement of an area defined by the small square in the two second exposure is shown on the left. It is interesting to see the marks left by individual alpha particles. The energy of a ^{238}Pu alpha particle is about 5.5 MeV and it appears to affect about 10 to 15 pixels which can be readily distinguished from background. When an alpha particle entered the imaging plate at an angle far away from normal, a track was formed much like that in a cloud chamber. The two second exposure represents a counting sensitivity of 0.03 alpha/mm^2 and shows a signal-to-noise ratio (SNR) of 15. Figure 3 shows the integrated SPP sensor response as a function of exposure time for the two NIST alpha sources. There is excellent linearity.

The principle of the SPP technology indicates that it is sensitive to the incident energy of radiation. The sensor system, therefore in addition to possessing the capability of imaging individual alpha particles, has the potential to identify unknown alpha emitters through energy differentiation. To explore the possibility of radionuclide speciation by the SPP technology, transmission measurements were conducted with several alpha and beta sources. Filters of various thicknesses were placed between the sources and a SPP sensor plate to measure the attenuation

effect of the filter material as a function of material thickness. The filter material used was DuPont MYLAR polyester film #15 XM555 with a density of 0.552 mg/cm^2.

Figure 4 shows the results of transmission measurements of a group of five alpha emitters by the SPP technology. For each source the SPP imaging sensor responses were normalized to their measurement responses with no filters. The slopes of the response curves indicate the attenuation property of the filter material with respect to different incident energies and follow a predicted pattern that lower energy alphas were being filtered out faster. Notice that the response of ^{241}Am is very close to ^{238}Pu, both emitting alpha particles with energy around 5.5 MeV. However, ^{241}Am also emits a higher percentage of x- and γ-rays and shows an appreciable residual spectrum compared to ^{238}Pu. ^{243}Cm also shows a residual spectrum from radiation other than alpha particles. Figure 5 shows the same type of test with two ^{238}Pu and one ^{239}Pu source. The two ^{238}Pu sources while differing in strength by a factor of 150 produce similar response curves. The ^{239}Pu source with an alpha energy around 5.1 MeV however shows a slightly steeper response slope.

Figure 6 shows the same type of test with two depleted uranium samples. The two samples exhibit very different response curves marked AA101 and AA102 respectively, indicating they have different matrix compositions. Both samples show considerable residual transmissions after 31 μm of MYLAR filter. The test results with ^{238}Pu and ^{239}Pu in figure 5 demonstrate that after 31 μm of MYLAR filter, practically all alpha particles with energies less than 5.5 MeV will be filtered out. Therefore the residual transmissions shown in AA101 and AA102 were from more penetrating radiations such as beta, gamma or x-rays. If these residuals were subtracted from their respective response curves however, the subtracted curves for the two samples marked AA101-X and AA102-X respectively would behave similarly. The residual subtracted curve would fit in between that of ^{208}Po and ^{148}Gd in figure 4, suggesting that the main alpha activities in both uranium sample were from ^{238}U. The energy differentiation property of the SPP sensor system for alpha particles is summarized in figure 7. The slope of attenuation is defined as $(Ln(A_t)-Ln(A_0))/t$ where A_t denotes the activity of the source measured by the SPP sensor with a MYLAR filter of thickness t. The residuals have been subtracted from the response measurements of ^{243}Cm, ^{241}Am and ^{238}U sources before their slopes of attenuation were calculated.

The energy differentiation capability of the SPP system to beta particles was also tested and the results are presented in figures 8. An extended and more detailed test with ^{147}Pm is shown in figure 9. That extended test, covering over six orders of magnitude in beta activity measurement clearly demonstrates the high sensitivity and excellent linearity of the SPP sensors to beta particles. These tests with alpha and beta emitters suggest that the SPP sensor system can be utilized as a fast, high spatial resolution and economical radionuclide analyzer for waste characterization applications. Unknown waste samples can be quickly screened to determine the types of radiation and then the specific radioactive isotopes involved can be identified. Radioactivity dosage can be accurately measured when the SPP sensor system is calibrated.

Another test was carried out to confirm the sensitivity of the SPP imaging plate to beta particles and to demonstrate how the new sensor can be used for neutron detection[5] as well. A metal foil with high neutron absorption cross-section and other desired nuclear properties such as having a simple decay scheme and a manageable half-life is used as a neutron to

charged-particle converter in conjunction with a SPP sensor system. A dysprosium (Dy) foil was activated in a nuclear reactor cold neutron beam and the decay history of the foil was subsequently traced by placing the foil in close contact with a SPP sensor in a series of timed-exposures. A commercially prepared 125 μm thick Dy foil about 1.5 cm x 1.5 cm in size was exposed to a cold neutron flux of 3 x 10^7 n/cm^{2}s for 30 seconds at the NIST cold neutron research facility. Figure 10 presents the logarithm of the fraction of radioactivity remaining in the dysprosium foil as a function of time. I(t) is the relative radiation strength of the foil at time t after the neutron activation as recorded by a SPP imaging plate. The imaging sensor plate exposure time to the neutron activated foil was set for 5 minutes for measurements conducted when t is less than 30 hours and was set for 20 minutes when t is greater than 30 hours except that for the last measurement at t = 40 hours then the exposure was set for 1 hour. All data were normalized to a 5 minutes imaging plate exposure time for the graphing in figure 10. The thermal/cold neutron activation of Dy produces a relatively short-lived (half-life 1.26 minutes) metastable state of dysprosium-165 (^{165M}Dy) and the dysprosium-165 ground state (^{165}Dy) with a half-life value of 2.35 hours. ^{165}Dy decays mainly by emitting beta particles. The slope of the decay history line in figure 10 is consistent with the known ^{165}Dy half-life and all measurements were within 1% of the predicted decay values except that for t = 36.2 hours and 37.5 hours, which were within 5%. The slightly larger errors probably were caused by the foil not being in good contact with the imaging plate. The overall excellent linearity of the SPP sensor system response exhibited in figure 10 suggests it can be used in precision quantitative analysis of neutron distributions. Figure 11 shows the SNR of the SPP imaging sensor plate as a function of time in the tracking of the same Dy foil decay. The time is expressed in units of ^{165}Dy half-life.

The time of 40 hours represents about 17 half-lives or a decay factor of more than 130,000 for ^{165}Dy. Figure 11 suggests that at 18 half-lives after activation, a decay factor of more that 260,000, the remaining beta activity in the Dy foil could still be measured with a SNR of 5. The Dy foil was activated in a cold neutron flux of 3 x 10^7 n/cm^{2}s for 30 seconds and generated an estimated ^{165}Dy radioactivity of 2 x 10^4 dpm/mm^2. After decaying for 17 half-lives, the remaining ^{165}Dy radioactivity in the foil would be about 0.15 dpm/mm^2 and equivalent to that of a foil at the end of a 30 second activation with a neutron flux of 2 x 10^2 n/cm^{2}s. If left decaying for 18 half-lives, the remaining ^{165}Dy radioactivity would again be half as much at 0.07 dpm/mm^2, similar to a foil activated for the same 30 seconds with a neutron flux of 1 x 10^2 n/cm^{2}s. A foil exposed to a neutron flux of 1 n/cm^{2}s for about one hour will also generate a similar ^{165}Dy radioactivity. This test demonstrates that the SPP sensor system when coupled with a proper neutron to charged-particle converter can function as a very high sensitivity large area neutron detector. Simple metal foils can be placed in a neutron contaminated area. After a short time the foils can be collected and put in contact with SPP sensors to register the neutron effects.

As an example of how the new sensor technology can be useful in environmental monitoring of radionuclides, we sprinkled a small amount of soil sample from Rocky Flats on a SPP imaging sensor plate with a thin MYLAR foil as a barrier. The soil sample was taken from NIST standard reference material SRM 4353. The SRM certificate states that each bottle of SRM typically contains one or two "hot" particles. Figure 12 shows the image of the soil sample captured by a ten hour exposure with a SPP sensor. A "hot" spot was detected and a 16-fold enlargement of the image area is shown on the right. A threshold was set that only pixels of relative high values, or areas of high radioactivity

are shown. The table in the figure lists the relative radioactivity strength in units of intensity value PSL per 1 mm^2 at the four marked positions in the enlarged area. The table indicates that at position No. 1 there are clusters of particles with relatively high radioactivity, but these are not the only particles with high radioactivity. Figure 13 shows the SPP image of another batch of soil sample from the same SRM, also with ten hours exposure time. At first glance of the image shown on the left of figure 13, there does not appear to be any "hot" spots. We selected an area indicated by the square and enlarged it 16 times. Again by setting the threshold level so only pixels with the highest relative values in the defined area would remain. The table in the figure shows the relative radioactivity strength at the five marked positions. The radioactivities at four positions are "hotter" than the "hot" spot found in figure 12, each shows a level 400 times or more above background. It is estimated that an exposure time of 10 minutes or less will be adequate for the detection of these "hot" spots. The above examples demonstrate that quantitative analysis and mapping of environmental samples can be conducted in an efficient manner using the new sensors. A filter system can be designed to distinguish alpha particle response from that of betas or gamma rays. The proposed approach with the new sensors can reduce the cost and complexity of radionuclide characterization while improving throughput.

Merits of the Technology

As demonstrated in our initial evaluation, the SPP technology shows great potential that it can be developed to be a low operating cost, high sensitivity monitor for environmental radioactivity and site radionuclide characterization. It offers the following advantageous characteristics:

- high sensitivity, is capable of imaging single alpha particles, can be used to measure many types of radioactivities, alpha activity of 100 dpm/100 cm^2, beta activity of 0.1 dps/mm^2, low energy neutron flux of 1 n/cm^2s or x-ray level of 20 μR/Hr can be detected in 10 min. or less;

- energy sensitive, can identify radionuclide through energy differentiation;

- high resolution, detector size can be as large as 35 cm x 43 cm with pixel size as fine as 50 μm, is capable of locating concentrations of radioactivity such as "hot" particles;

- wide dynamic range and highly linear, can be used for quantitative analysis and digital output lends itself for ready image and data processing;

- low secondary waste generation, very thin polyester film can be used for contamination barrier when contact measurements of radioactive samples are required, SPP sensor plates are re-usable;

- low operating cost, one reader can support many re-usable SPP plates;

- quick implementation of the technology, once the performance characteristics are calibrated a laboratory system or field transportable unit can be assembled quickly by using mostly off-the-shelf components, also a microprocessor based portable/remote operable unit can be designed using currently available technology;

- potential for in liquid operation, having a protective polyester cover the SPP sensor

plates are moisture resistant and do not require dark room setup.

Future Activities

We will conduct more detailed measurements to further characterize the SPP technology and compare it to other radiation measurement methods. We will examine soil samples from Rocky Flats and from Oak Ridge to verify the sensitivity and analytical capability of the technology for environmental monitoring. After the sucessful laboratory demonstration, we will assemble a transportable unit for field test at suitable DOE sites. It should provide quick turn-around time for on-site quantitative soil radioactivity analysis. Meanwhile, we will also design and fabricate several large area thin alpha reference sources with various strength for field calibration to ensure quality of measurement results by the SPP technology. The reference sources will be made in collaboration with NIST and the DOW Chemical Co. and be traceable to NIST. We will adapt the technology to field condition and DOE requirements by establishing both GIS and CAD interfaces, hardening and reconfiguring system hardware. Experience gained from the field test will be incorporated into the design of a portable or remote operable unit to further broaden the area of applicability.

References

1. Amemiya, Y. and Miyahara, J. Application of imaging plate. Nature 336, 89 (1988).

2. Johnston, R.J., Pickett, S.C. and Barker, D.L. Autoradiography using storage phosphor technology. Electrophoresis 11, 355-360 (1990).

3. Harrington, M.G., Hood, L. and Puckett, S.C. Simultaneous analysis of phosphoproteins and total cellular protein from PC12 cells. Methods: Companion Methods in Enzymology 3, 133-141 (1991).

4. Patterson, Scott D. and Latter, Gerald I. Evaluation of storage phosphor imaging for quantitative analysis of 2-D gels using the Quest II system. Biotechniques 15, No. 6, 1076-1083 (1993).

5. Niimura, Nobuo., Karasawa, Yuuko., Tanaka, Inchiro., Miyahara, Junji., Takahashi, Kenji., Saito, Hiroki., Koizumi, Satoshi and Hidaka, Masanori An imaging plate neutron detector. Nucl. Instrum. and Methods in Physics Research A 349, 521-525 (1994). and the references contained therein.

Acknowledgement

The author (Y. T. Cheng) wish to thank C. Eddie Christy, the DOE METC Contracting Officer's Representative for his help in clarifying the project goals and also for his effort together with Sean M. Goodwin, the Contract Specialist, getting the project off to a smooth start. The period of performance of the base phase of the contract is from August 25, 1995 for six months.

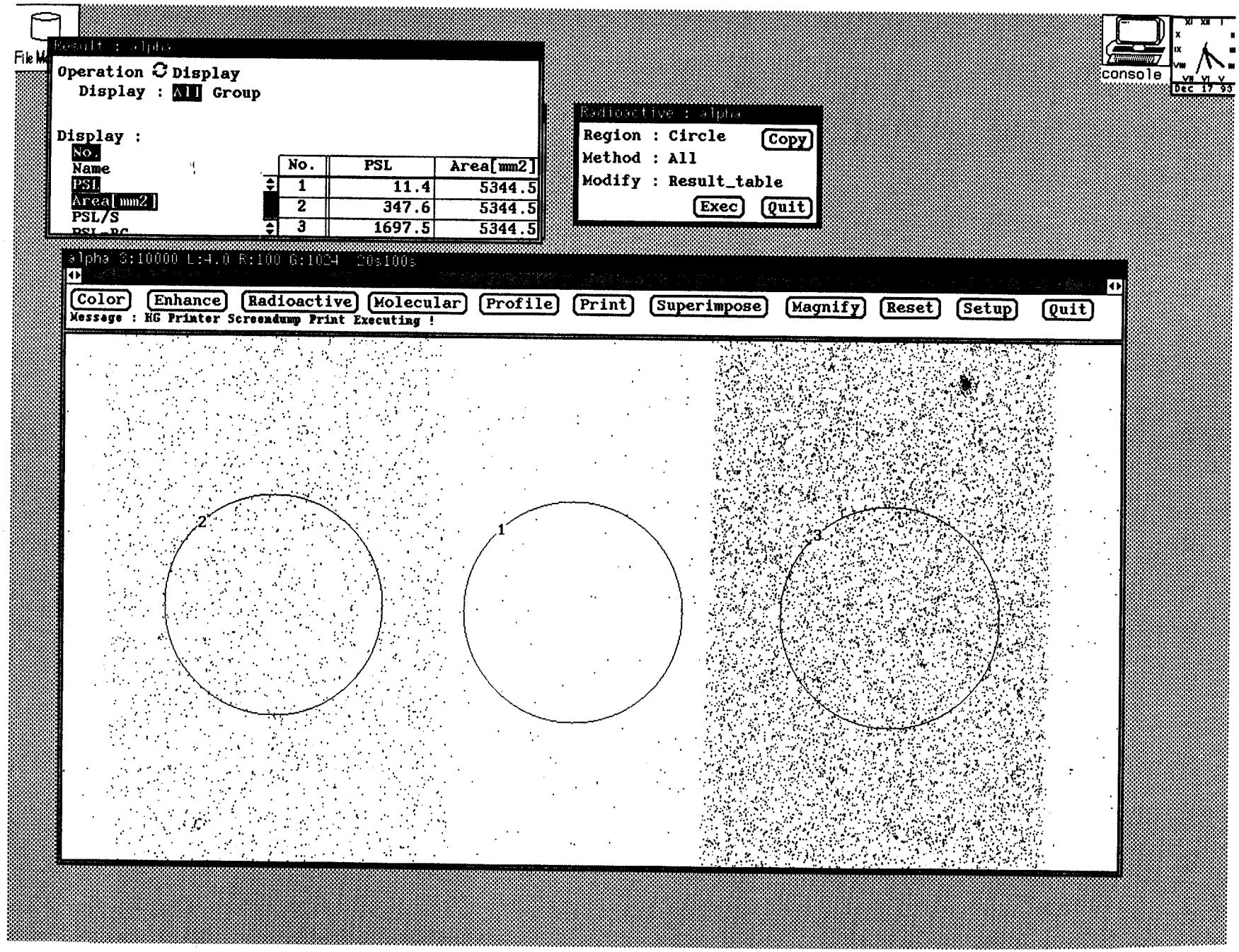

Figure 1. **A 20-second (left, inverted) and an 100-second exposures of a NIST standard large area ^{238}Pu source with a SPP imaging sensor plate.**

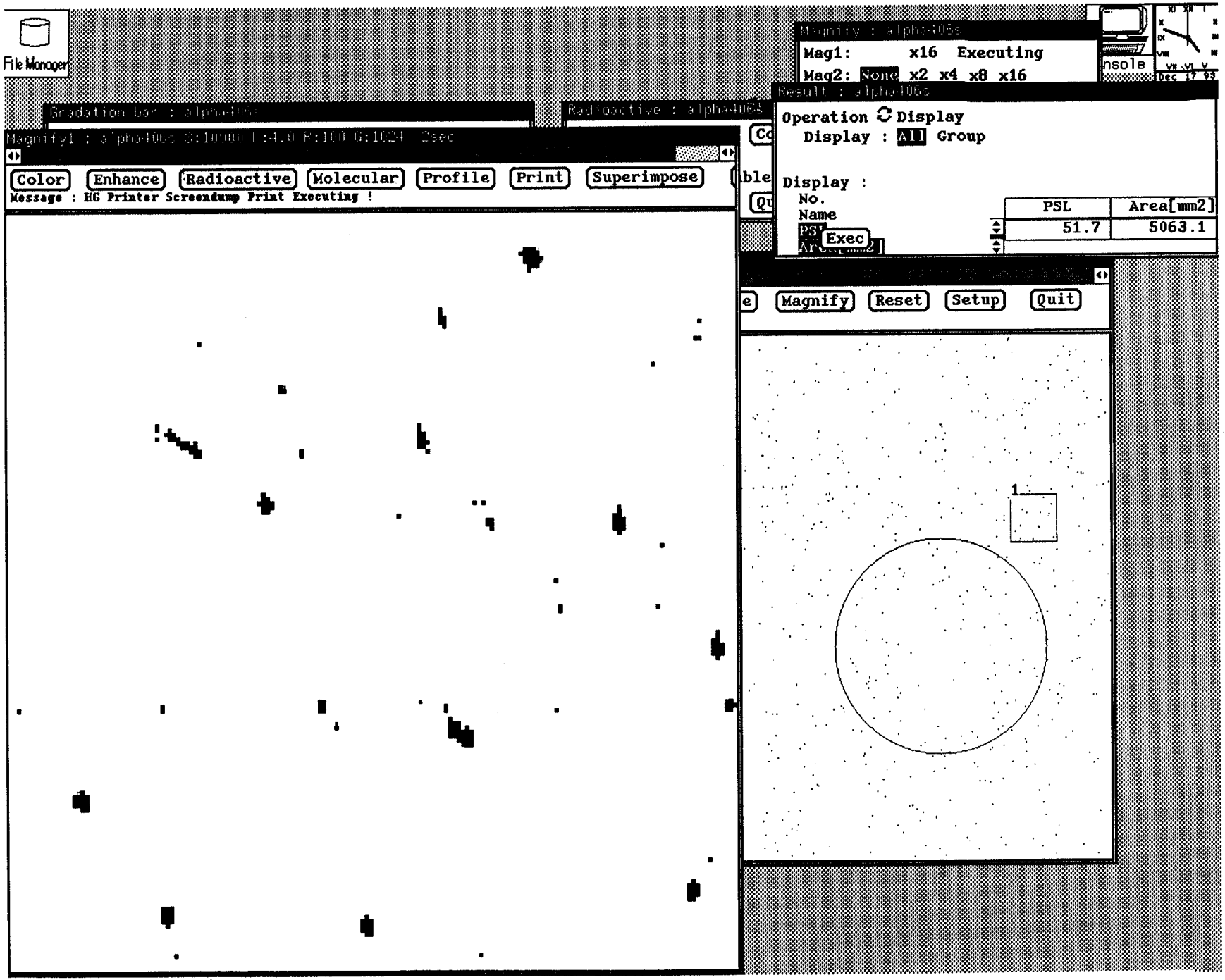

Figure 2. **A two-second exposure (right) and detail enlargement of the same ^{238}Pu source with a SPP imaging sensor plate.**

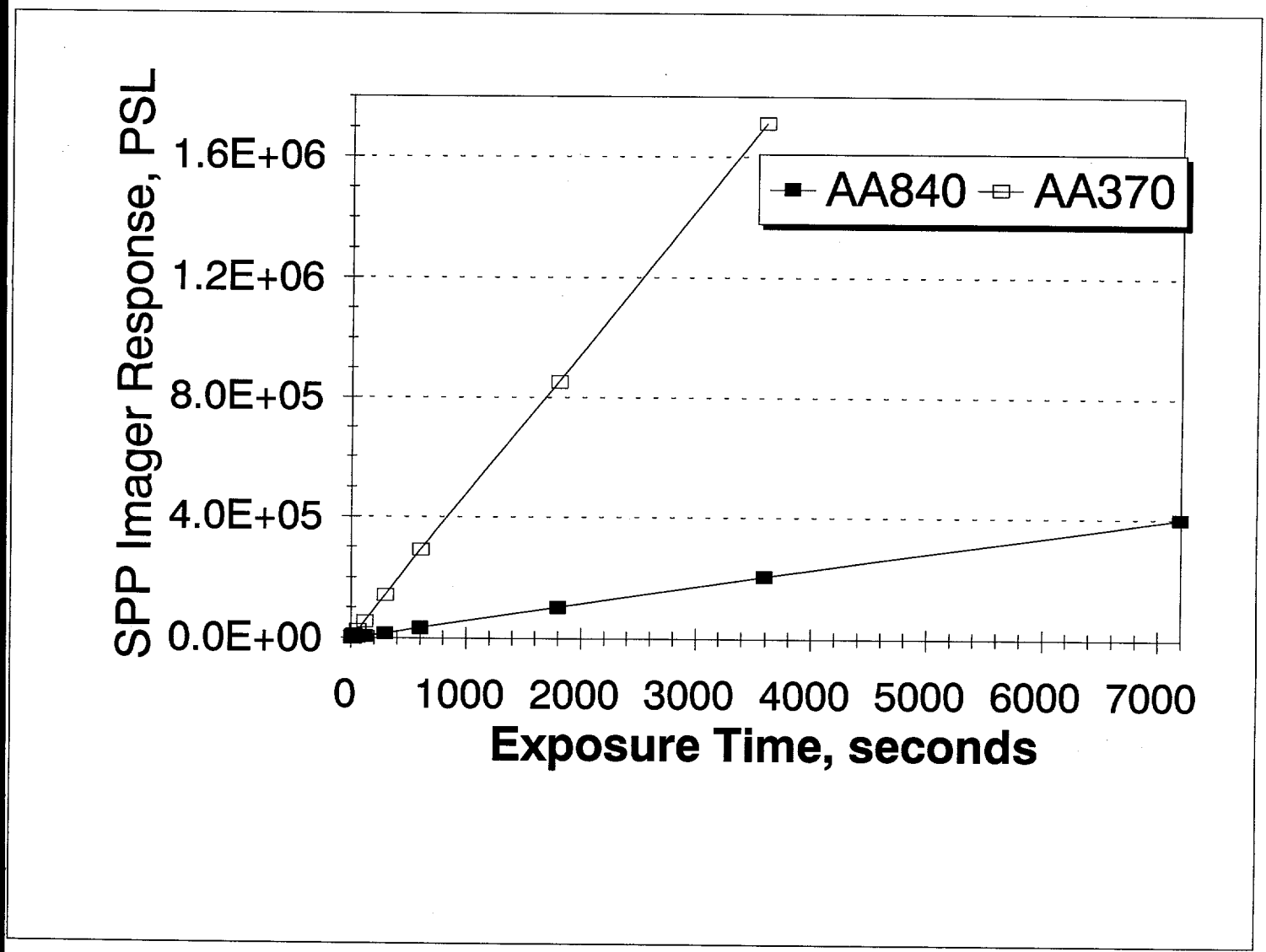

Figure 3. **SPP sensor response as a function of exposure time to NIST large area ^{238}Pu sources AA840 and AA370.**

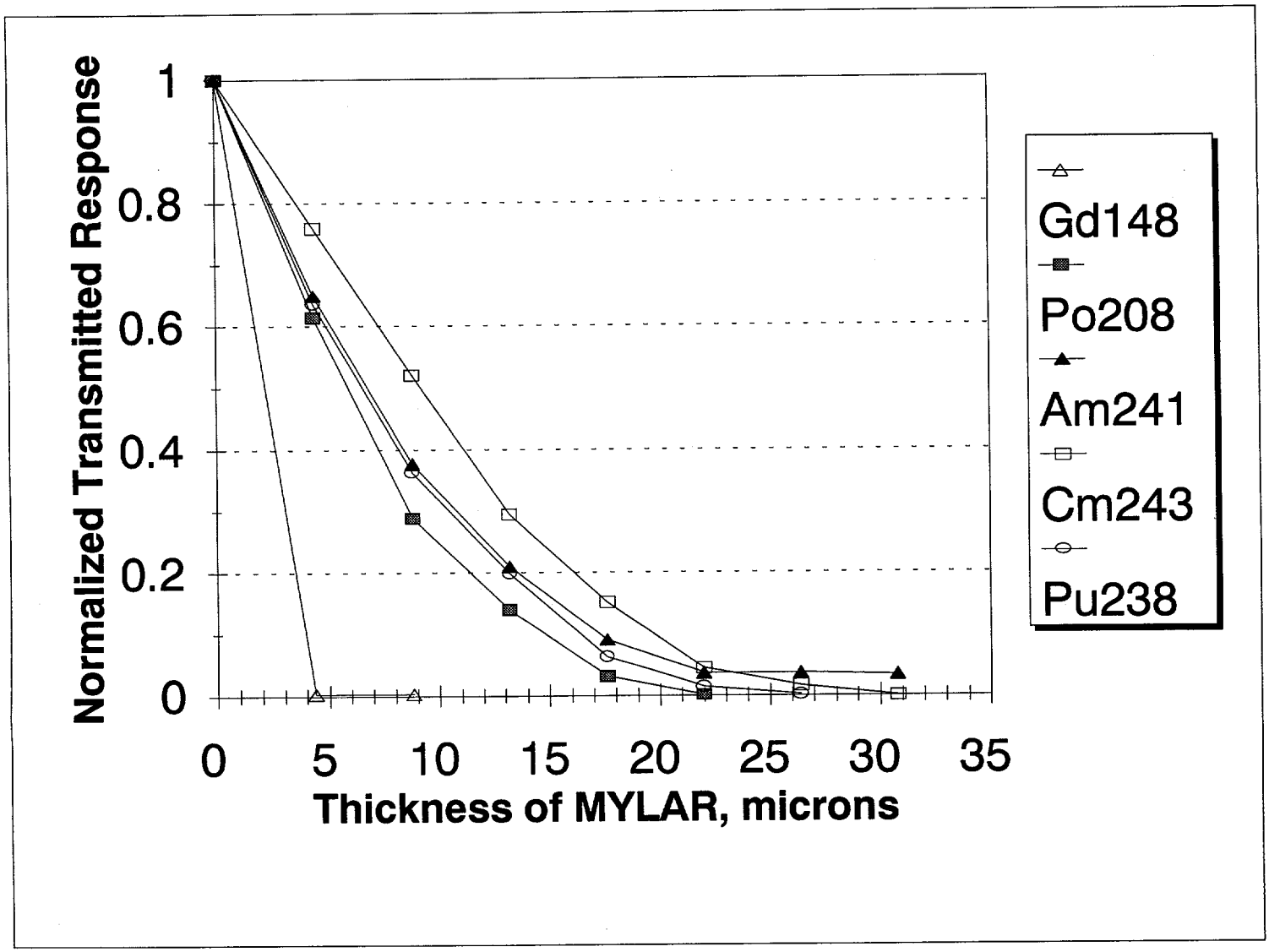

Figure 4. **Radioactivity attenuations of five alpha sources in MYLAR.**

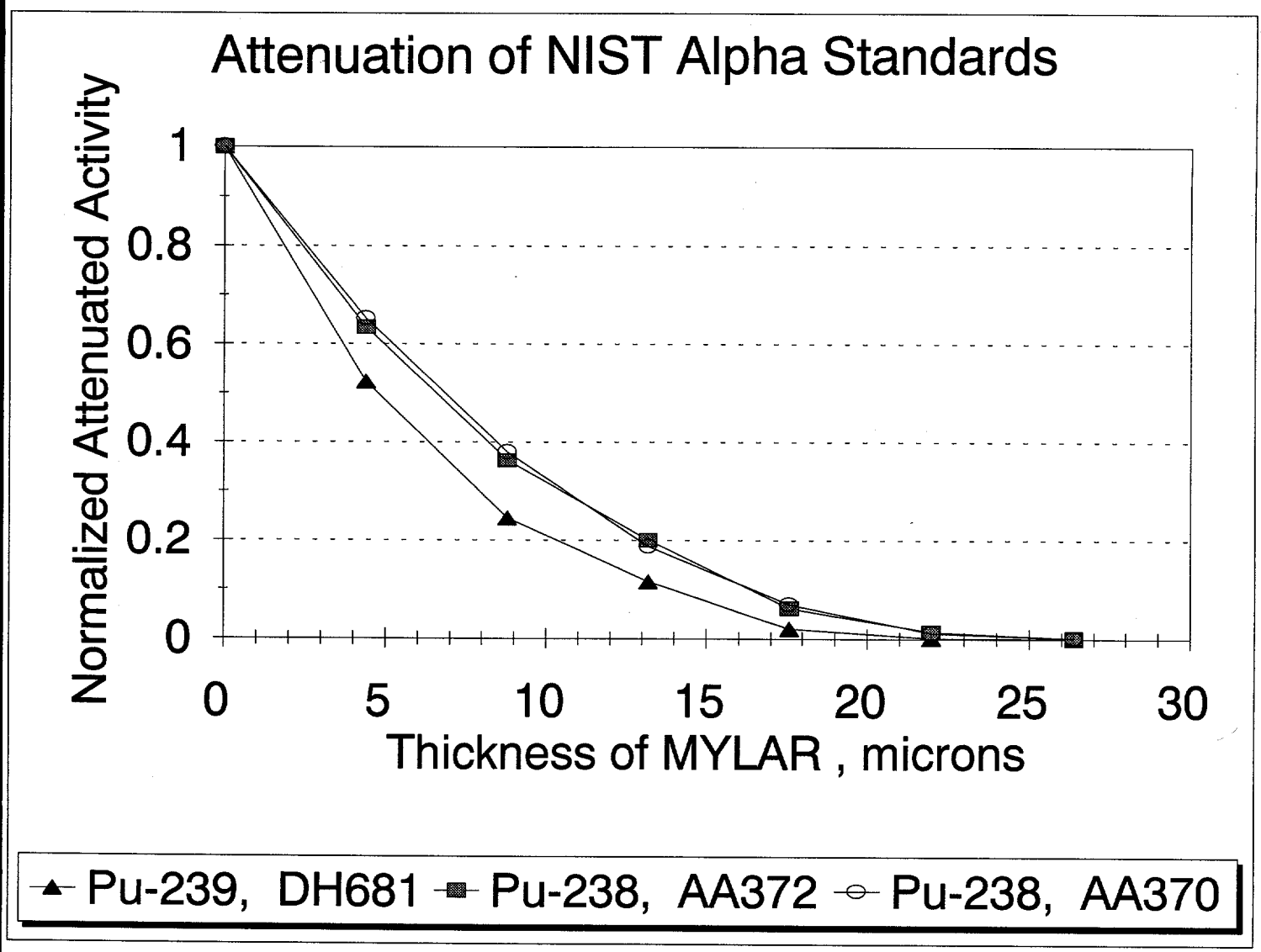

Figure 5. **Comparison of ^{238}Pu radioactivity attenuation in MYLAR to that of ^{239}Pu with a SPP sensor.**

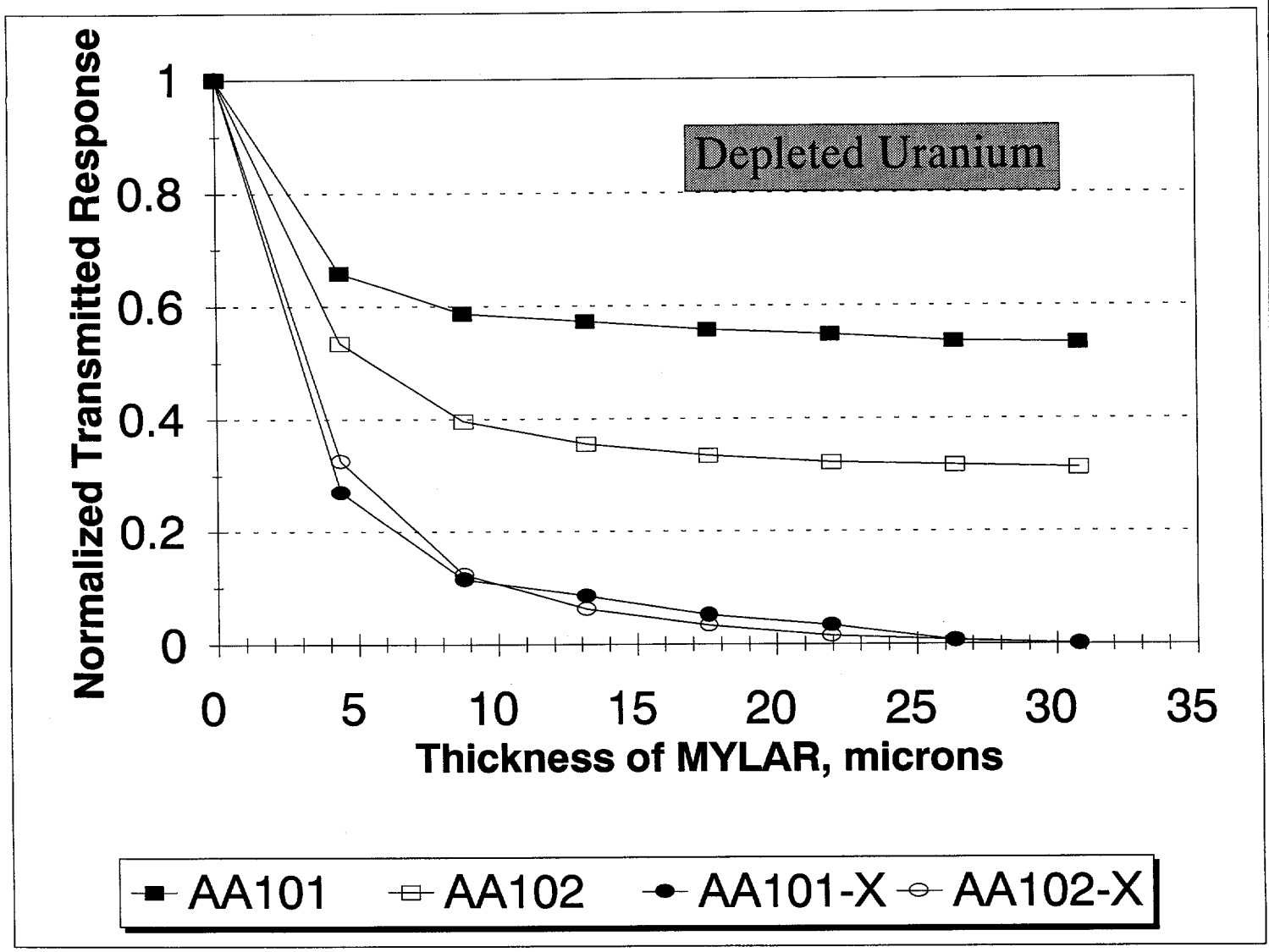

Figure 6. **Radioactivity attenuation of two depleted uranium samples in MYLAR.**

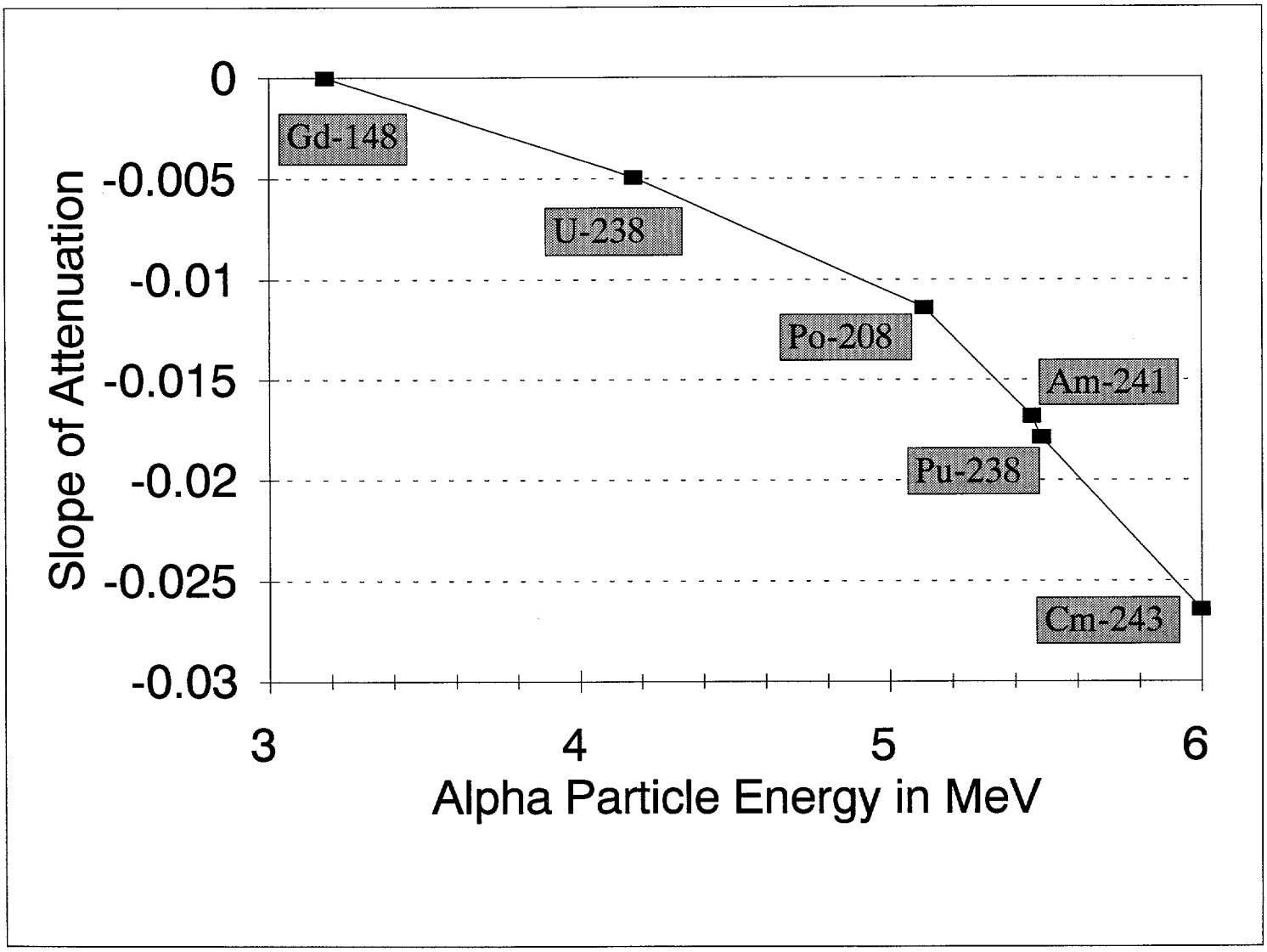

Figure 7. **Slopes of attenuation curves of alpha emitters vs. alpha particle energy measured by the SPP technology.**

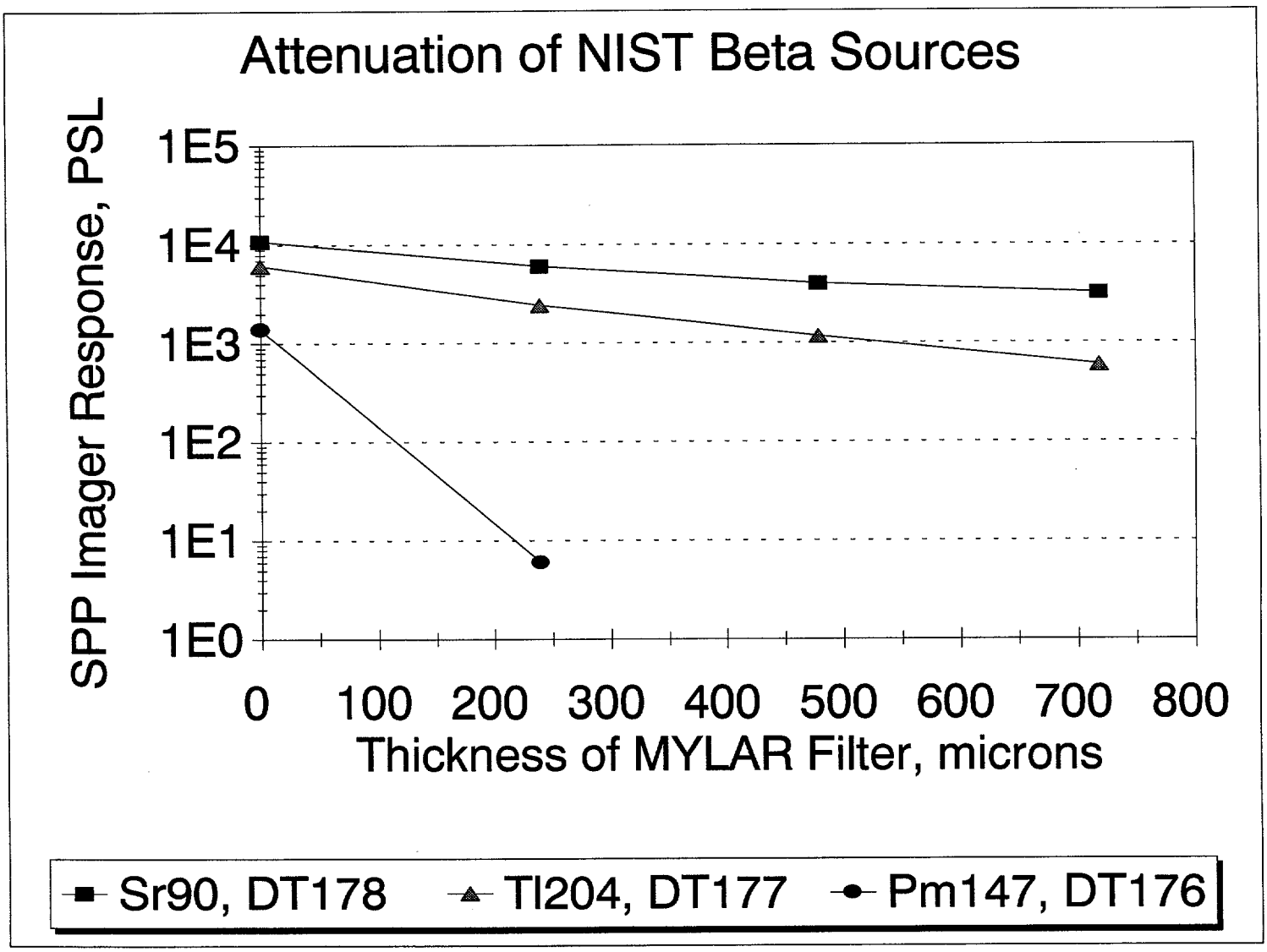

Figure 8. **Attenuation of ^{90}Sr, ^{204}Tl and ^{147}Pm radioactivity in MYLAR.**

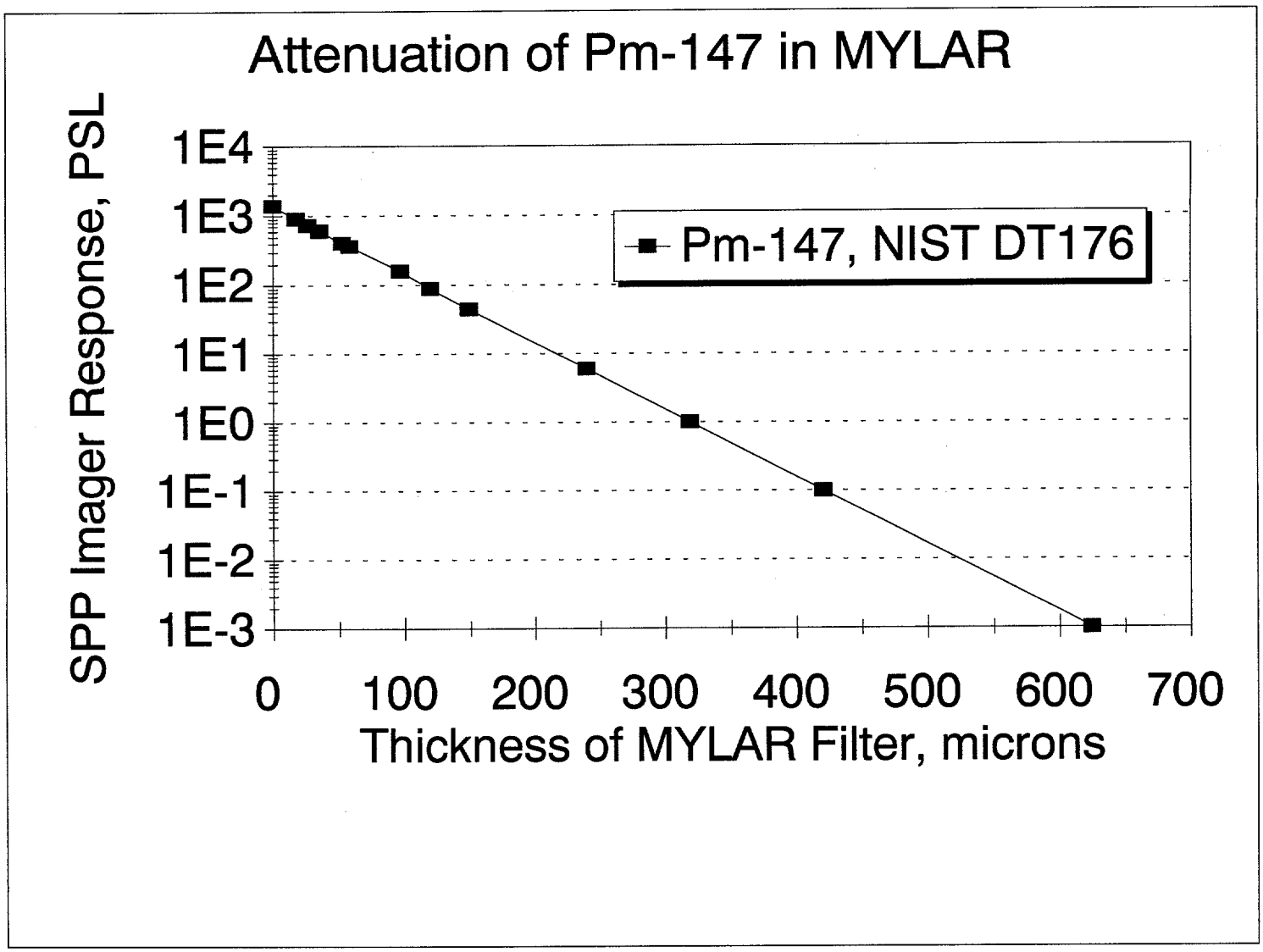

Figure 9. Attenuation of ^{147}Pm radioactivity in MYLAR.

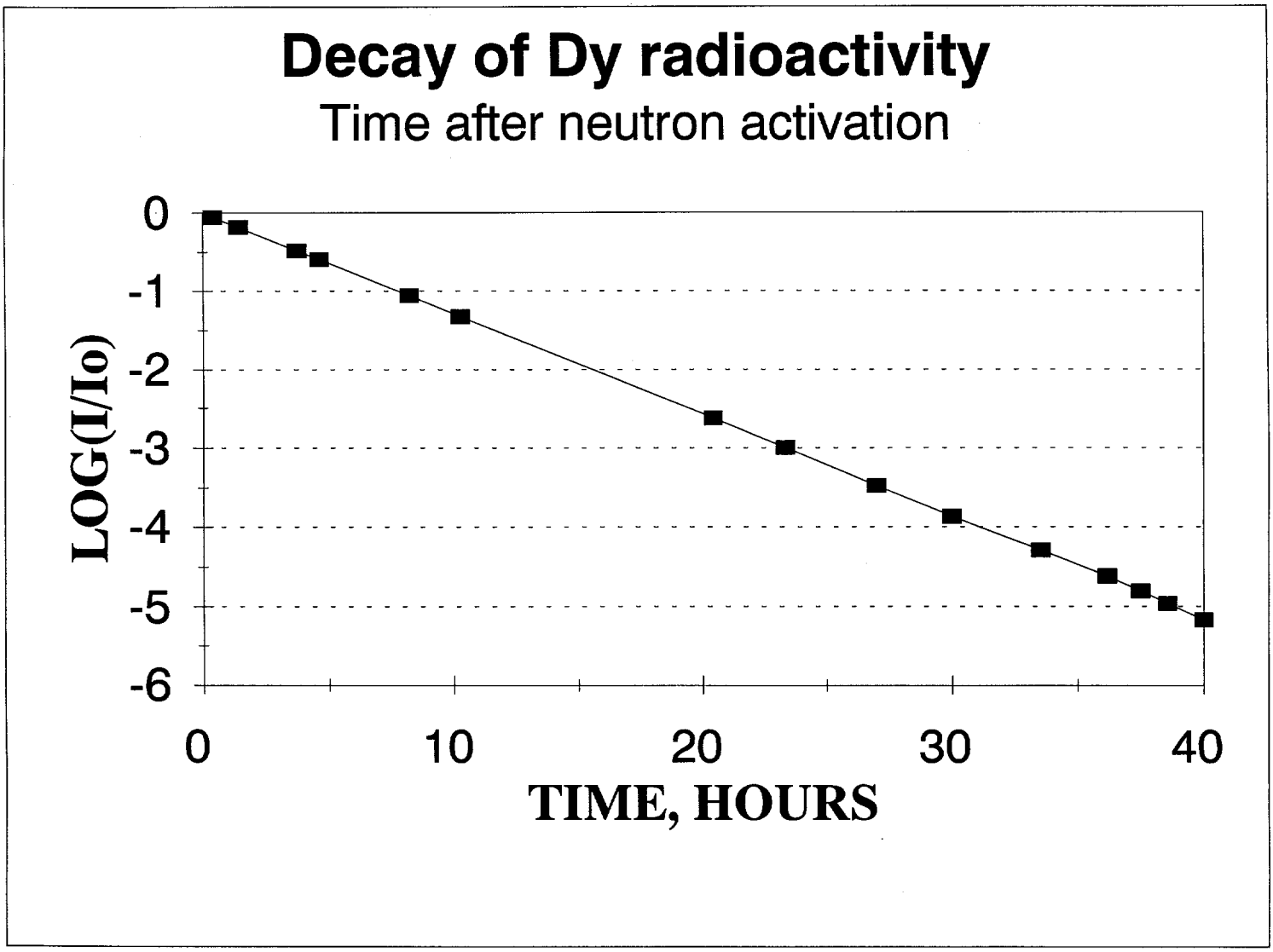

Figure 10. **The decay of a neutron-activated dysprosium foil monitored with a SPP sensor plate.**

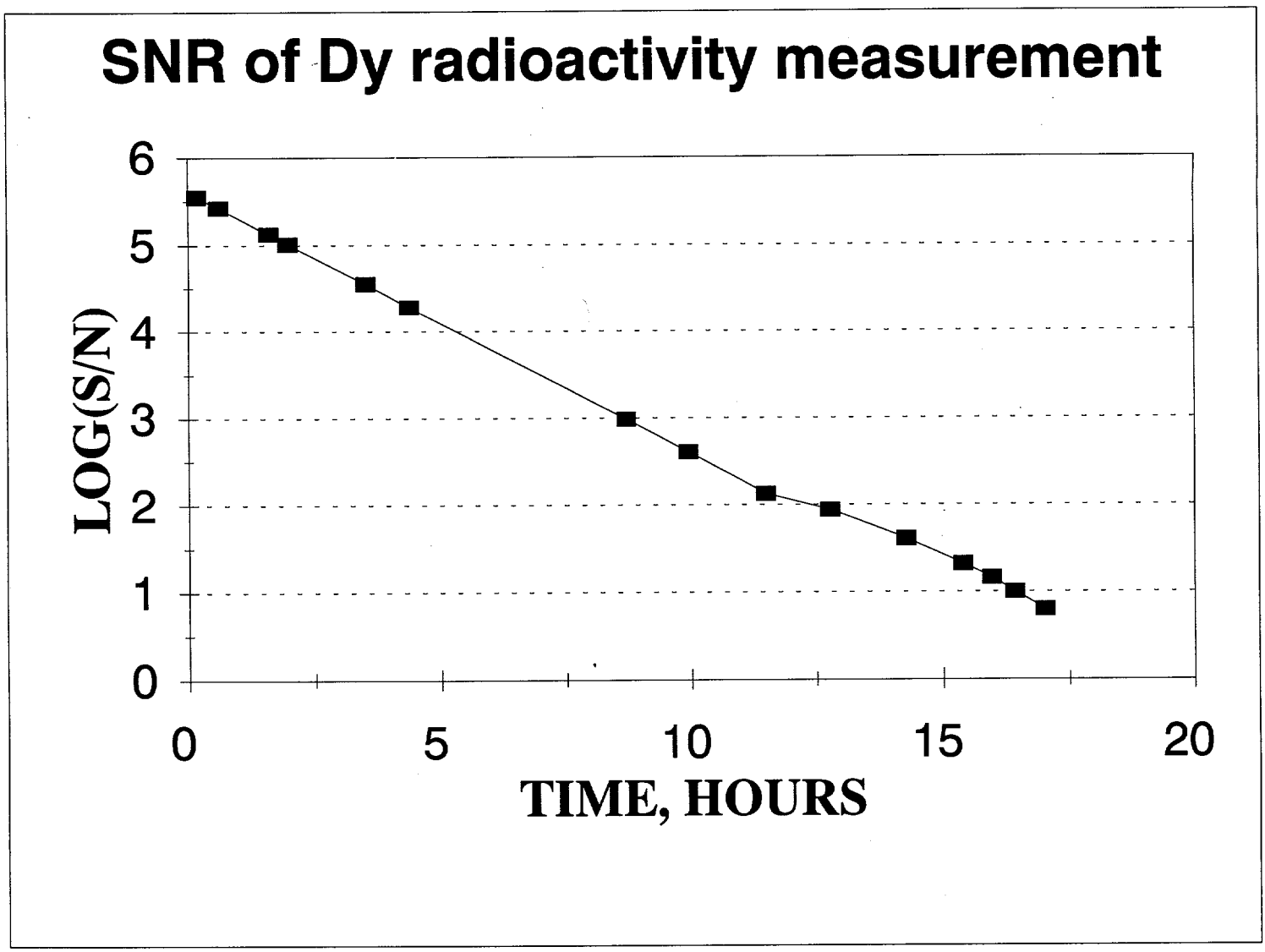

Figure 11. **The radioactivity signal-to-noise ratio as measured with a SPP sensor of a neutron-activated dysprosium foil at different half-lives after activation.**

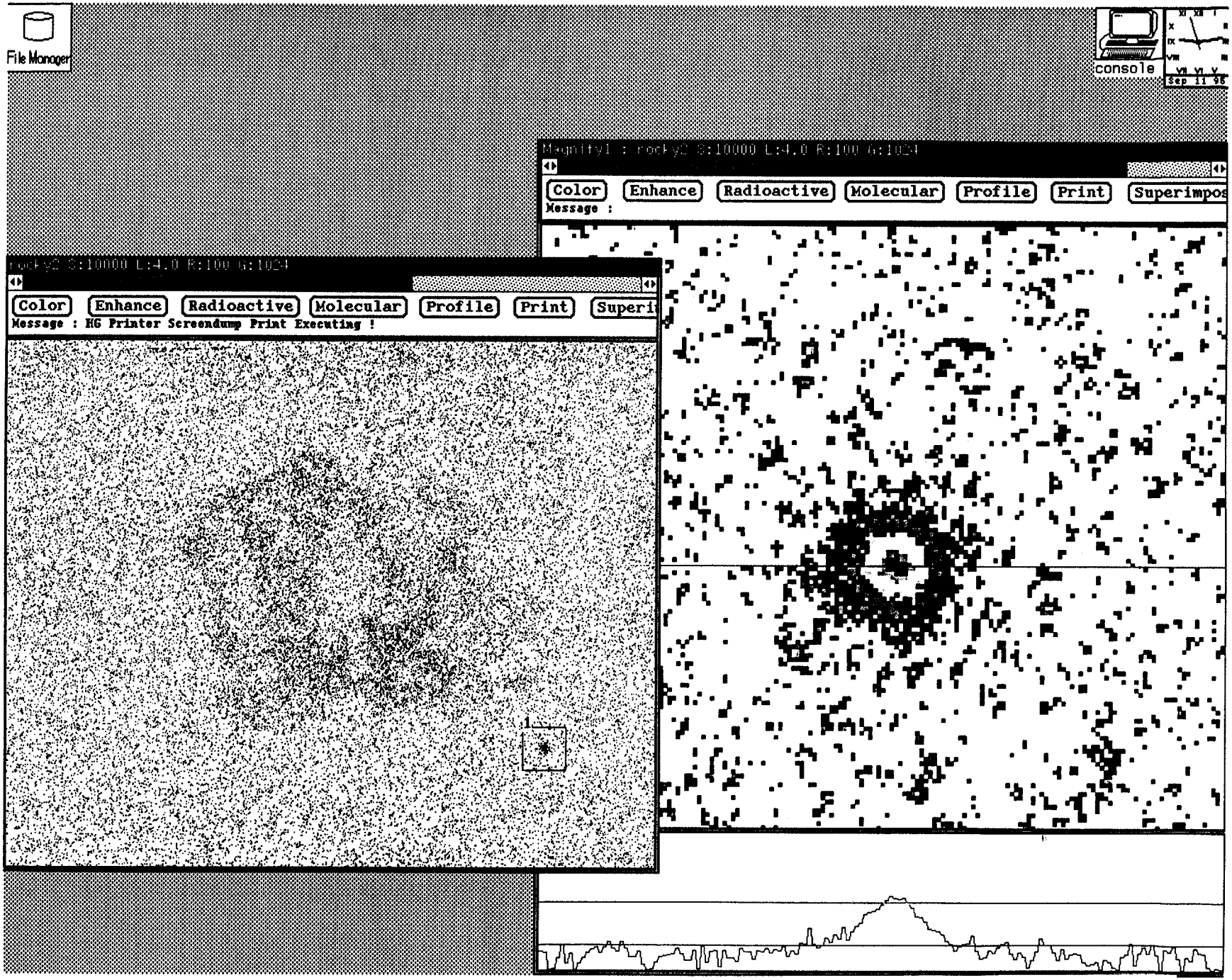

Figure 12. **10-hour exposure image of a sample taken from NIST SRM 4353 on a SPP sensor.**

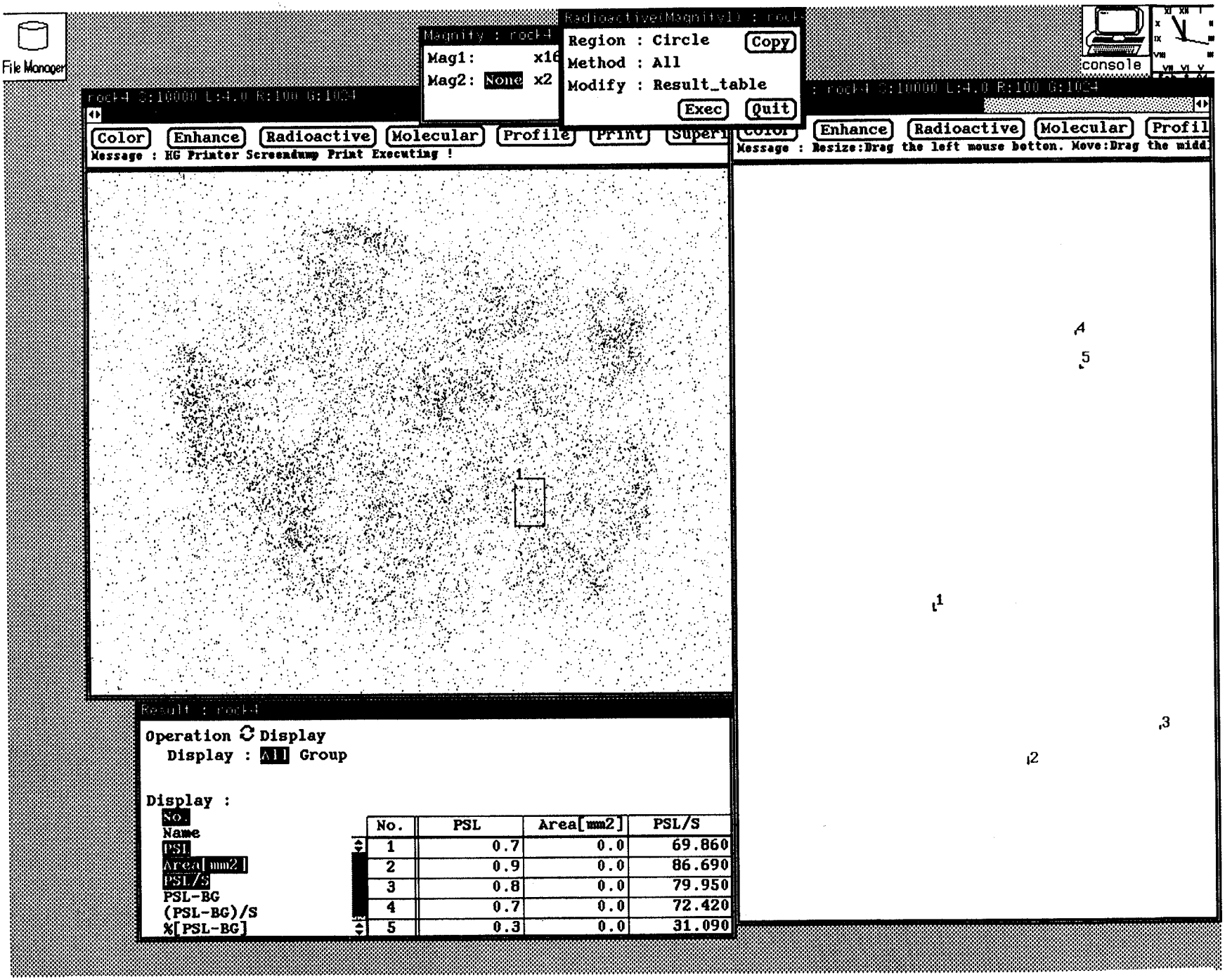

Figure 13. **10-hour exposure image of a second sample taken from NIST SRM 4353 on a SPP sensor.**

PII.10 Surfactant-Modified Zeolites as Permeable Barriers to Organic and Inorganic Groundwater Contaminants

R.S. Bowman (bowman@nmt.edu; 505-835-5992)
E.J. Sullivan (jeri@nmt.edu; 505-835-5466)
Department of Earth and Environmental Science
New Mexico Institute of Mining and Technology
Socorro, NM 87801

Abstract

We have shown in laboratory experiments that natural zeolites treated with hexadecyltrimethylammonium (HDTMA) are effective sorbents for nonpolar organics, inorganic cations, and inorganic anions. Due to their low cost (~$0.75/kg) and granular nature, HDTMA-zeolites appear ideal candidates for reactive, permeable subsurface barriers. The HDTMA-zeolites are stable over a wide range of pH (3-13), ionic strength (1 *M* Cs^+ or Ca^{2+}), and in organic solvents. Surfactant-modified zeolites sorb nonpolar organics (benzene, toluene, xylene, chlorinated aliphatics) via a partitioning mechanism, inorganic cations (Pb^{2+}) via ion exchange and surface complexation, and inorganic anions (CrO_4^{2-}, SeO_4^{2-}, SO_4^{2-}) via surface precipitation.

Introduction

The overall goal of the project is to test and demonstrate the use of surfactant-modified zeolite (SMZ) as a permeable barrier to groundwater contaminants. A permeable barrier allows water pass through while stopping or retarding contaminant migration (Figure 1).

The project is divided into three phases:

- Phase I: SMZ Laboratory Testing and Analysis
- Phase II: Pilot-Scale Testing of Barrier Technology
- Phase III: Field Demonstration

Work on Phase I began in June 1995. This paper summarizes some of our previous work with SMZ and describes our progress under Phase I.

Background

Zeolites are naturally occurring minerals characterized by high surface areas and high cation exchange capacities. Zeolites occur in massive deposits in many areas of the world, and are common in the western United States. We've found that a commercial zeolite from the St. Cloud mine in Winston, New Mexico, is high in the desirable zeolite mineral clinoptilolite and low in smectite clays. Mined zeolite can be ground and sized as desired, thus tailoring its hydraulic properties. The sized zeolite is stable mechanically and hydraulically. After grinding

Research sponsored by the U.S. Department of Energy's Morgantown Energy Technology Center, under contract DE-AR21-95MC32108 with Department of Earth and Environmental Science, New Mexico Institute of Mining and Technology, Socorro, NM 87801; telefax: 505-835-6436.

and sizing, the St. Cloud zeolite (which is about 95% pure clinoptilolite) costs $60-$100 per ton.

Materials and Methods

One-half ton of sized zeolite (14 to 40 mesh, or 1.4 to 0.4 mm size range) was obtained from the St. Cloud mine for Phase I testing Raw zeolite was mixed with a cationic surfactant dissolved in water. Many different surfactants can be used. Our work has concentrated on zeolite modified with hexadecyltrimethylammonium (HDTMA), commonly found in hair conditioners and mouth washes. The surfactant binds to the external exchange sites on the zeolite surface (Figure 2). The surfactant forms an organic coating, greatly enhancing the sorptive properties of the zeolite (Haggerty and Bowman, 1994). Internal exchange sites remain available for sorption of small metal cations such as Pb^{2+} (Figure 2). Previous work has shown that solutions of high or low pH, high salt concentrations, and organic solvents do not remove the surfactant coating, as shown in Table 1 (Bowman et al., 1995).

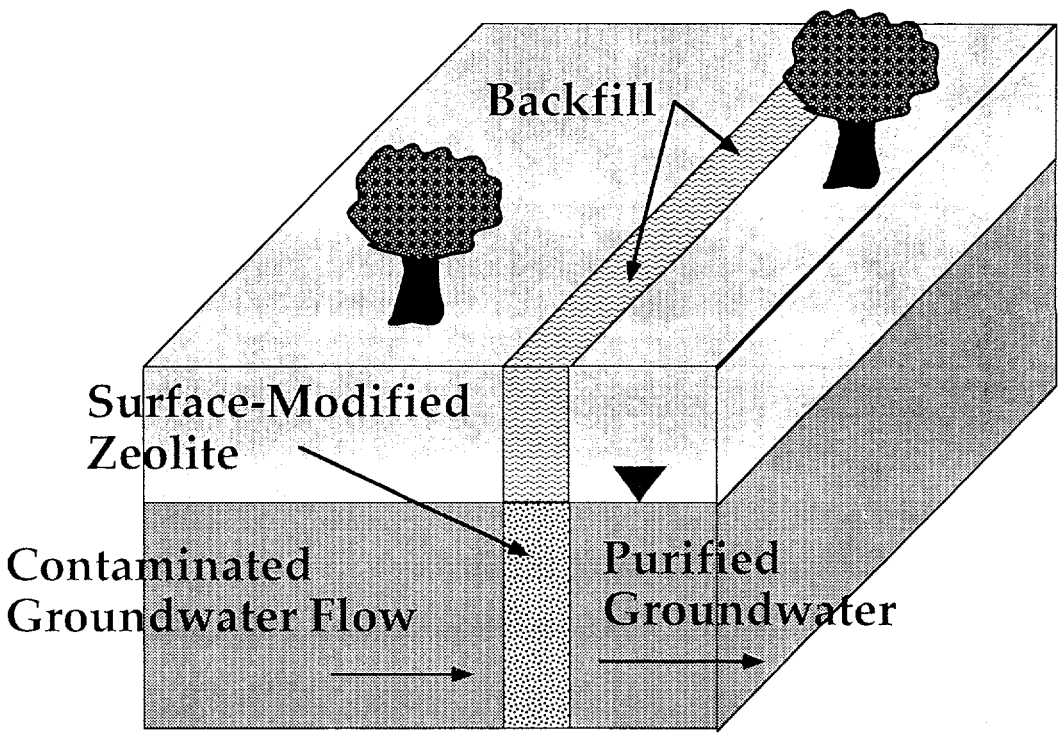

Figure 1. Schematic of surfactant-modified zeolite permeable barrier.

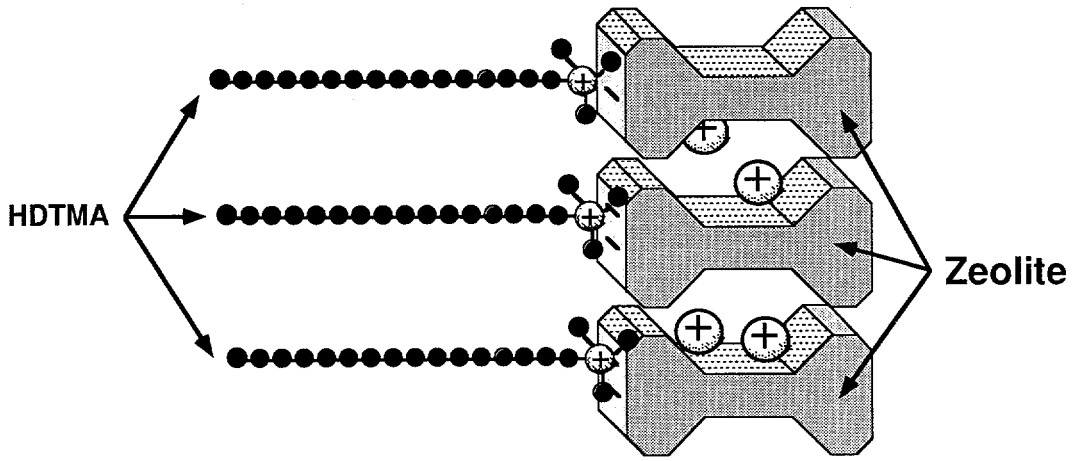

Figure 2. Schematic of surfactant sorption to zeolite surface.

Table 1. Percent of Surfactant Remaining on the Zeolite Surface after 72-Hour Exposure to Various Solutions/Solvents

Solution/Solvent	*%Surfactant Remaining*
distilled water	99.3
0.005 *M* $CaCl_2$	99.1
pH 3	98.3
pH 5	98.3
pH 10	99.0
0.10 *M* CsCl	98.6
1.0 *M* CsCl	97.2
50 mg/L $Cr0_4^{2-}$	99.4
methanol	96.0
benzene	99.6
toluene	99.6

Results and Discussion

The surfactant treatment is complete within 8 hours (Figure 3). The surfactant is retained by the zeolite quantitatively up to a saturation plateau (Figure 4). For the example shown, this amounts to 220 mmol/kg, or about 6% by weight. Surfactant retained at or below the plateau (about 220 mmol/kg) is not removed by successive washings with water (Figure 5).

Based on these results, we estimate the cost of the SMZ, using commercial-grade surfactants, to be in the range of $400 per ton.

Previous work on the properties and applications of SMZ are presented in Bowman et al. (1993, 1995), Haggerty and Bowman (1994), Neel and Bowman (1992), Sullivan et al. (1994), and Teppen et al. (1995).

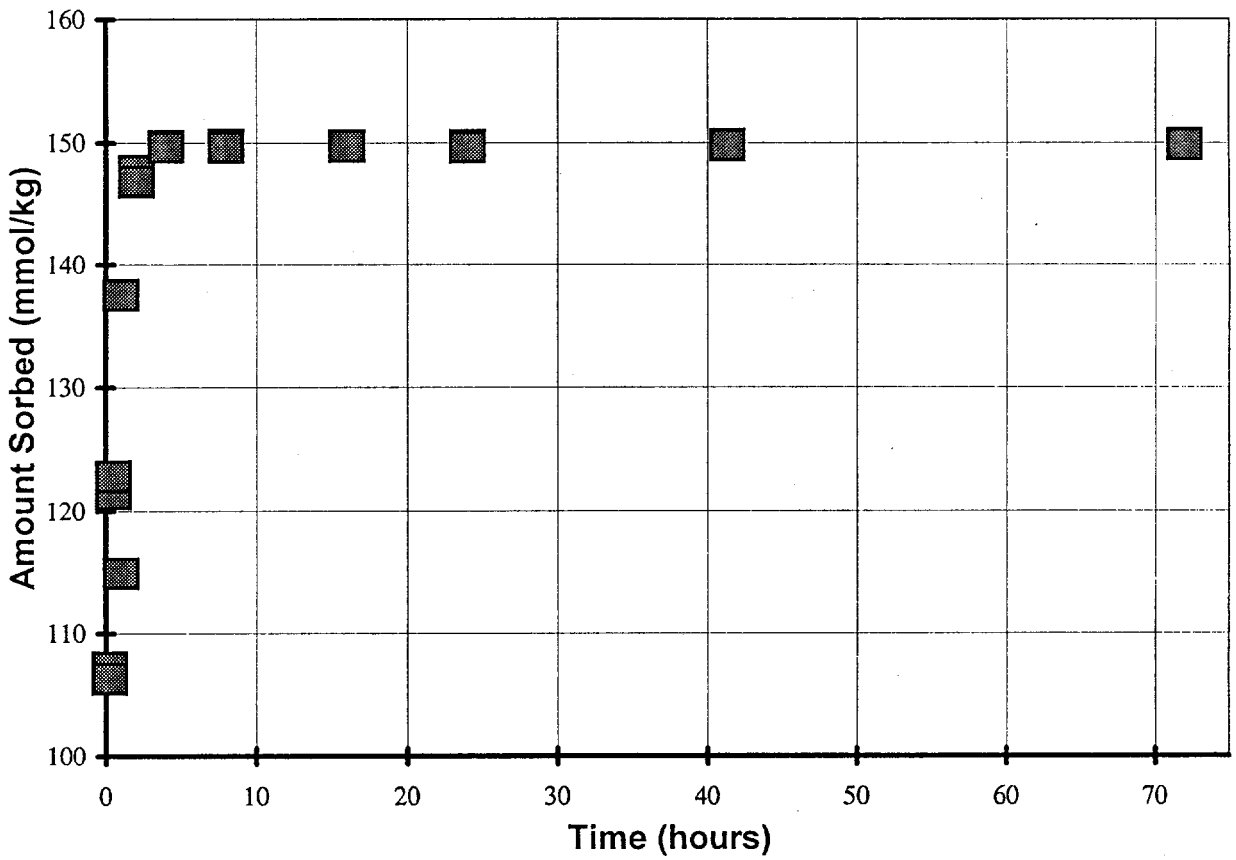

Figure 3. Sorption of HDTMA versus time.

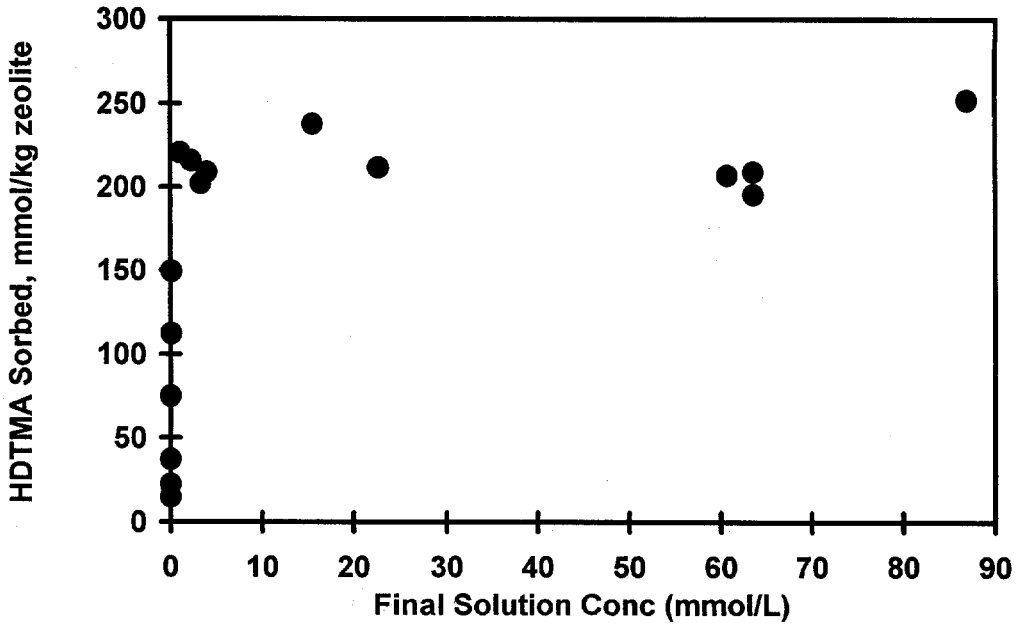

Figure 4. Sorption of HDTMA as a function of solution concentration.

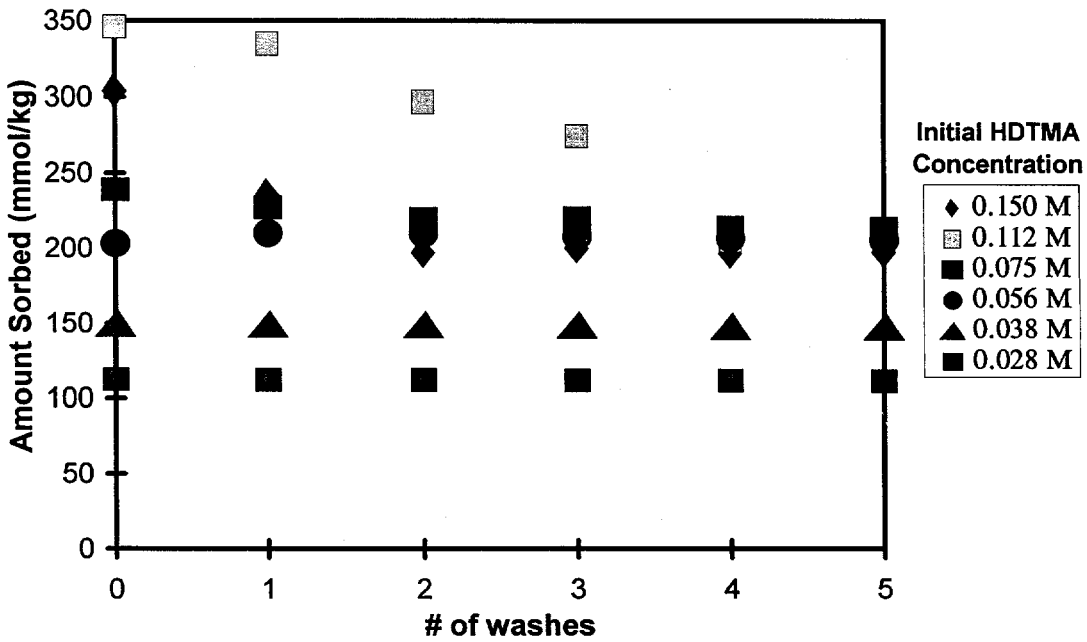

Figure 5. Stability of HDTMA-zeolite as a function of loading.

References

Bowman, R.S., G.M. Haggerty, R.G. Huddleston, D. Neel, and M. Flynn. 1995. Sorption of nonpolar organics, inorganic cations, and inorganic anions by surfactant-modified zeolites. p. 54-64. *In* D.A. Sabatini, R.C. Knox, and J.H. Harwell (eds.). Surfactant-enhanced remediation of subsurface contamination. ACS Symposium Series 594. American Chemical Society, Washington, DC.

Bowman, R.S., M. Flynn, G.M. Haggerty, R.G. Huddleston, and D. Neel. 1993. Organo-zeolites for sorption of nonpolar organics, inorganic cations, and inorganic anions. p. 1103-1109. *In* Proc. Joint CSCE-ASCE National Conference on Environmental Engineering, 12-14 July 1993, Montreal, Quebec, Canada.

Haggerty, G.M., and R.S. Bowman. 1994. Sorption of inorganic anions by organo-zeolites. Environ. Sci. Technol. 28:452-458.

Neel, D., and R.S. Bowman. 1992. Sorption of organics by surface-altered zeolites. p. 57-61. *In* Proc. 36th Annual New Mexico Water Conf., 7-8 November 1991, Las Cruces, NM.

Sullivan, E.J., R.S. Bowman, and G.M. Haggerty. 1994. Sorption of inorganic oxyanions by surfactant-modified zeolites. p. 940-945. *In* Proc. SPECTRUM '94, Nuclear and Hazardous Waste Topical Mtg., 14-18 August 1994, Atlanta, GA.

Teppen, B.J., D.B. Hunter, P.M. Bertsch, E.J. Sullivan, and R.S. Bowman. 1995. Modeling organic modification of a natural zeolite surface. p. 181-184. *In* Preprints of Papers, American Chemical Society Annual Meeting, 20-24 August 1995, Chicago, IL.

Acknowledgements

This work is currently being supported by the U.S. Department of Energy's Morgantown Energy Technology Center, under contract DE-AR21-95MC32108.

Prior support was from the New Mexico Waste-management and Education Research Consortium (WERC) under contract 01-4-23190.

Ioana Anghel, Matthew Flynn, Bruce Gamblin, Grace Haggerty, Roger Huddleston, Daphne Neel, and Julia Whitworth contributed to the results presented in this paper.

PII.11 Barometric Pumping with a Twist: VOC Containment and Remediation Without Boreholes

W. Lowry (sea@roadrunner.com; 505-983-6698)
Sandra Dalvit Dunn (sea@roadrunner.com; 505-983-6698)
Robert Walsh (sea@roadrunner.com; 505-983-6698)
Paul Zakian (sea@roadrunner.com; 505-983-6698)
Science and Engineering Associates, Inc.
1570 Pacheco St., Suite D-1
Santa Fe, NM 87505

1. Abstract

A large national cost is incurred in remediating near-surface contamination such as surface spills, leaking buried pipelines, and underground storage tank sites. Many of these sites can be contained and remediated using enhanced natural venting, capitalizing on barometric pumping.

Barometric pumping is the cyclic movement experienced by soil gas due to oscillations in atmospheric pressure. Daily variations of 5 millibars are typical, while changes of 25 to 50 millibars can occur due to major weather front passage. The fluctuations can cause bulk vertical movement in soil gas ranging from centimeters to meters, depending on the amplitude of the pressure oscillation, soil gas permeability, and depth to an impermeable boundary such as the water table. Since the bulk gas movement is cyclic, under natural conditions no net advective vertical movement occurs over time.

Science and Engineering Associates, Inc., is developing an engineered system to capitalize on the oscillatory flow for soil contaminant remediation and containment. By design, the system allows normal upward movement of soil gas but restricts the downward movement during barometric highs. The earth's surface is modified with a sealant and vent valve such that the soil gas flow is literally "ratcheted" to cause a net upward flow over time. A key feature of the design is that it does not require boreholes, resulting in a very low cost remediation effort and reduced personnel exposure risk.

In the current phase (Phase I) the system's performance is being evaluated. Static and transient analysis results are presented which illustrate the relative magnitude of this advective movement compared to downward contaminant diffusion rates. Calculations also indicate the depth of influence for various surface and soil configurations. The system design will be presented, as well as a cost assessment compared to conventional techniques.

2. Environmental Restoration Technology Need

The majority of the planned remediation sites within the DOE complex are contaminated with volatile organic compounds (VOCs). In many instances the contamination has not reached the

Research sponsored by the U.S. Department of Energy's Morgantown Energy Technology Center, under Contract DE-AR21-95MC32109 with Science and Engineering Associates, Inc., 1570 Pacheco St., Suite D-1, Santa Fe, NM 87505; telefax: 505-983-5868.

reached the water table, does not pose an immediate threat, and is not considered a high priority problem. These sites will ultimately require remediation of some type, either by active vapor extraction, bioremediation, or excavation and ex-situ soil treatment. The cost of remediating these sites can range from $50 K to well more than $150 K, depending on site characteristics, contaminants, and remediation method. Additionally, for many remediated sites, residual contamination exists which could not practically be removed by the applied remediation technology. This contamination must be immobilized, contained, or controlled.

These circumstances result in modest sites with contamination of limited risk, but by regulation they must still be controlled. A remediation solution being developed by Science and Engineering Associates, Inc. (SEA) for the Department of Energy serves as an in-situ containment and extraction methodology for sites where most or all of the contamination resides in the vadose zone soil. The approach capitalizes on the advective soil gas movement resulting from barometric pressure oscillations.

3. Approach

Oscillations in barometric pressure are both diurnal, corresponding to daily heating and cooling of the atmosphere, and of longer time periods, resulting from the passage of weather fronts. Daily variations will average about 5 millibars (one millibar is roughly one thousandth of an atmosphere) while those due to weather front passage can be 25 or more millibars. As the barometric pressure rises, a gradient is imposed on the soil gas which drives fresh surface air into the soil. As it drops, gas vents upward from the soil into the atmosphere. The pressure changes and resulting gradient are depicted in Figure 1, which shows data records in Albuquerque, NM. The total movement of soil gas is dependent primarily on the magnitude of the pressure oscillations, the soil gas permeability, and the depth to an impermeable boundary. This boundary can be the water table, bedrock, or extensive layers of very low permeability , such as caliche or clay. Since the fractional change in atmospheric pressure is small (typically 0.5 percent) the overall soil gas displacement during the daily cycle is also small. Furthermore, the daily oscillations in atmospheric pressure always return to a mean value. Over time, no net soil gas displacement occurs due to advective forces alone.

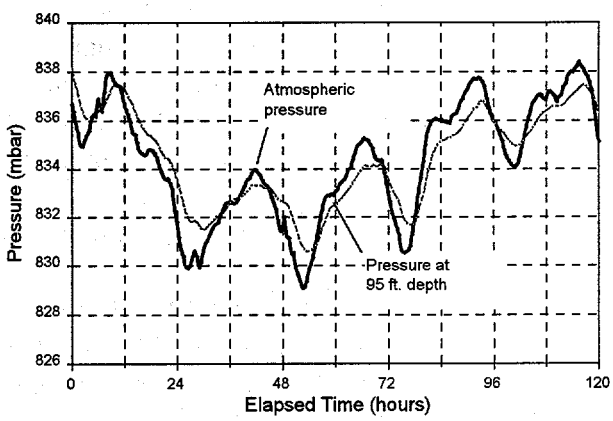

Figure 1. Barometric pressure, and soil gas pressure response at 95 ft. depth, recorded in Albuquerque, NM.

Displacement of soil gas can be controlled using surface features which impede the downward movement of vapors, but allow upward movement. The design incorporates a surface seal, a plenum, and an extraction vent valve. These components are depicted in Figure 2.

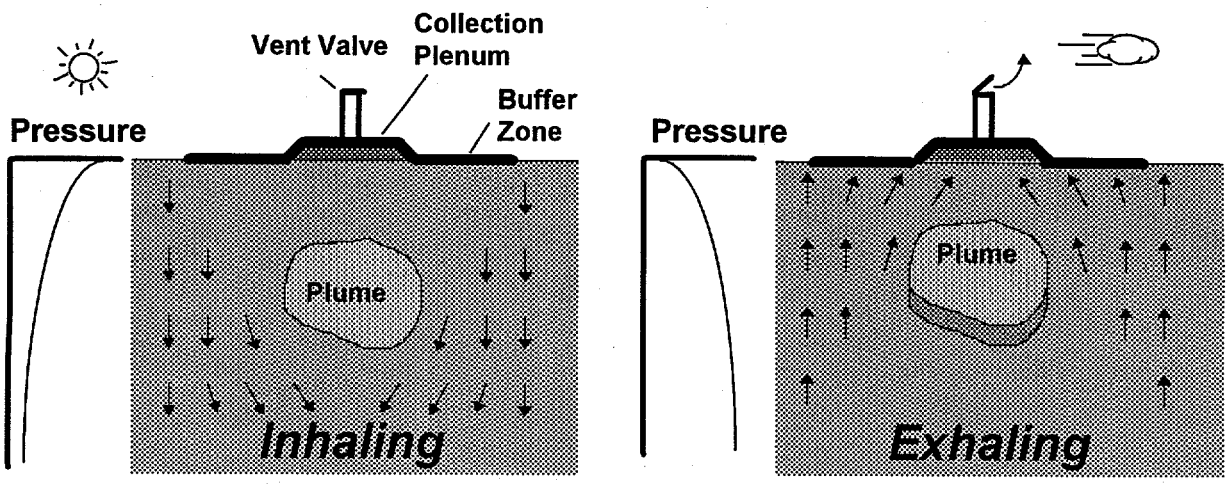

Figure 2. The surface treatment system controls the movement of soil gas due to barometric pressure changes

Directly above the contaminant plume is a layer of highly permeable material, such as pea gravel, which forms a collection plenum for the upward-moving soil gas. A surface seal is placed over and radially outward from the collection plenum directly on the soil surface to form a buffer zone, which controls the radial movement of air flowing into the soil during the high pressure periods. The surface seal is an impermeable, rugged material (such as a geotechnical membrane) which forms a no-flow boundary at the ground surface. The plenum is connected to atmospheric pressure with a high volume vent valve, open only when soil gas is moving upward (during a barometric low pressure cycle).

In operation the system ratchets the upward soil gas air flow by allowing normal upward flow during barometric lows but restricting downward air flow during high pressure cycles. High pressure periods result in restricted downward gas movement because the vent valve is closed and soil gas tends to flow around the plume ("inhaling"). When the atmospheric pressure is lower than the soil gas pressure at depth, soil gas flows upward and the surface seal forces the contaminated gas into the plenum, where the opened vent valve exhausts it to the atmosphere ("exhaling").

4. Project Description

The objective of this project is to evaluate, design, and demonstrate a system which relies upon barometric pressure oscillations to remediate soils contaminated with volatile compounds in the unsaturated zone.

The major challenge associated with the development of this system is to demonstrate that the pressure-driven soil gas flow can be controlled such that its net upward vertical velocity (over time) is sufficient to overcome the downward diffusion of contaminants from the liquid source. If this feature can be demonstrated then the system can reliably protect the water table from diffusively transported contaminants.

Phase I of the project consists of four tasks.

In Task 1 SEA will assemble the information required for the DOE to prepare the appropriate level of NEPA documentation for the project. This will assume a demonstration test planned at a specific site in Phase II.

In Task 2, SEA will predict the flow of soil gas due to barometric processes. This will include the geometric configuration of the surface seal design, with plenum and buffer zone dimensions. The modeling will evaluate the sensitivity of the extraction rate to plenum areal extent, and buffer zone size, particularly in relation to the depth and size of the plume. The analysis will also compare the advective gas flow rate caused by barometric pumping to the estimated diffusion rate of typical contaminants. Thermal effects of the soil surface will be considered.

For Task 3, using the results of parametric evaluations of the previous task, we will develop general design guidelines for the implementation of the barometric pumping system. The guidelines will define the relationship between plenum size, buffer zone configuration, plume depth and geometry, and geologic setting (depth to impermeable zone). Monitoring requirements and general monitoring system design will also be developed. The cost of a prototypical installation will be estimated.

The results of the analysis and design efforts will be summarized in the topical report prepared in Task 4.

5. Accomplishments

Results to date have shown that the system can capitalize upon naturally occurring vertical air flow to sweep contaminated soil gas upward. Static analyses have been conducted to demonstrate that non-trivial displacements can occur. Transient simulations show the integrated effects of local setting and installation geometry.

In a homogeneous medium the movement of soil gas caused by fluctuations in the surface barometric pressure is analogous to the displacement of a piston in a cylinder (Figure 3). As the barometric pressure (P_1) rises, the piston is displaced downward a distance Δx until the barometric pressure (P_1) equilibrates with the soil gas pressure below (P_2). In the absence of diffusion or density-related forces a molecule of soil gas will undergo the same displacement as the piston. In soil, the displacement is:

$$\Delta x = \frac{\Delta p}{P_{amb}}(L - d) \qquad \text{(Eq. 1)}$$

where ΔP is the amplitude of the cyclic variation in barometric pressure, P_{amb} is the average barometric pressure, d is the depth of the gas in the soil, and L is the depth below surface to the impermeable layer. This is a steady state relation, appropriate if the soil gas response is relatively rapid (i.e., L is not too large and the soil permeability is not too small). The measurements in alluvial deposits (Figure 1) showed the response at depth to be almost immediate.

Using Equation 1 it is possible to predict the gross movement near the surface. For example, given a 5 mbar pressure change and depth to the water table of 100 m., soil gas at 5 m will displace:

$$\Delta x = \frac{5\text{mbar}}{1000\text{mbar}} \bullet (100\text{m} - 5\text{m}) = 0.475\text{m}$$

For the same setting a 50 mbar change will result in 4.75 m total displacement. Since the

barometric pressure always returns to its original value, this displacement is oscillatory

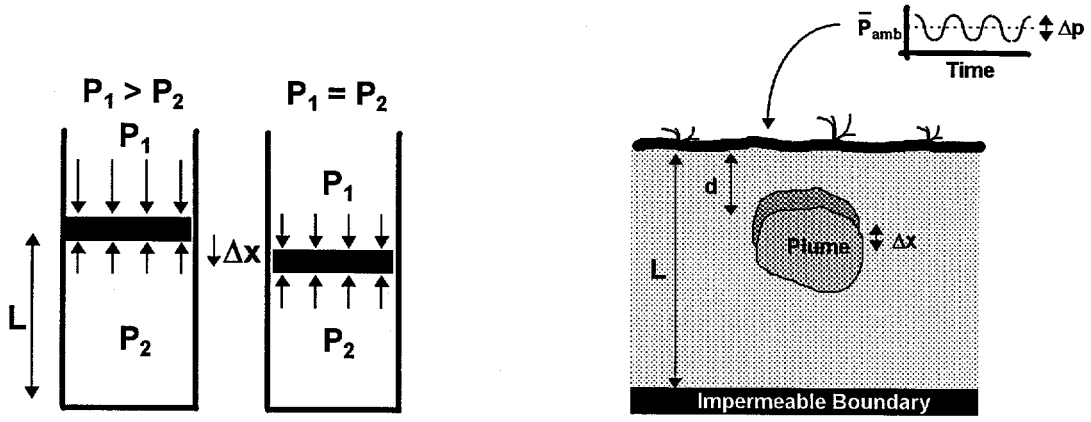

(a) (b)

Figure 3. Piston/cylinder analogy of soil gas movement due to barometric pressure changes (a), and the parameters affecting steady state soil gas displacement due to barometric pressure oscillations (b).

and results in no net vertical movement, except very near the surface where release directly to the atmosphere occurs on each upward cycle. Consequently, to incur bulk upward flow at depth the natural forces need to be harnessed through the use of engineered features to "ratchet" the flow upward.

The transient multidimensional process is being modeled with the Los Alamos National Laboratory FEHM (Finite Element Heat and Mass transfer) code. The oscillatory surface pressure, the surface treatment (plenum and buffer zone), and the one way valve can be modeled to determine the extent of impact of the surface features. This allows parametric variations of the plenum and surface seal geometry, soil gas permeability, and depth to the water table. A typical case includes these conditions:

- Soil gas permeability = 5 Darcies
- Soil gas porosity = 35%
- Plenum radius = 5 m
- Buffer zone extends additional 5 m radially outward from plenum
- Barometric pressure varies a total of 5 mbar with a 24 hour period.
- Depth to the impermeable zone = 100 m

The average vertical soil gas velocity which occurs along the vertical centerline (i.e., directly below the center of the plenum) over 24 hours is shown in Figure 4. Note that for the plotted depth it is always positive (upward). With no surface treatment the average velocity would everywhere be zero. While the numbers appear small, at the soil's surface the velocity results in almost 1 m of vertical displacement in a day.

This will happen every day, as long as the surface treatment is in place.

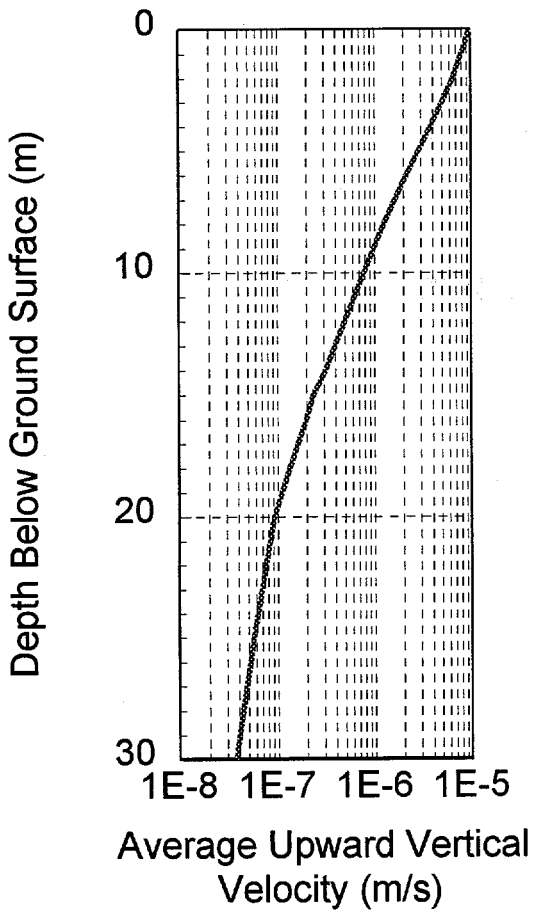

Figure 4. Average upward soil gas velocity over a 24 hour period, for the case cited in the text.

6. Applications and Benefits

The proposed system is applicable to near surface VOC contamination in the vadose zone. In general, this will be an attractive approach if one or several of the following conditions are met:

- The plume is not posing a significant, immediate threat to water contamination.

- The site has already been actively remediated (by vapor extraction, for example) but residual contamination exists. Incorporating this system can assure no residual contamination reaches the water table.

- Usage of the site is not imminent. If the site became a desirable location for a parking lot, for example, the parking lot could perform the role of the surface seal.

- Typical applications may include underground storage tanks, leaking buried pipelines, surface spills, or shallow landfills.

The system serves as an in-situ containment and extraction methodology for contaminated sites where most or all of the contamination resides in the vadose zone soil. The approach capitalizes on the advective soil gas movement resulting from barometric pressure oscillations to result in a system which harnesses this mechanism to assure a net vertical upward soil gas flux in the contaminated soil. Its main benefits include:

- The design prevents soil vapor flow down to the water table by assuring a net upward movement of soil gas.

- No boreholes are required for the remediation/containment process.

- The vented air, since this is a slow process, is of sufficiently low volatile concentration that under most state regulations can be

released to the air where it is naturally degraded by the sun's ultraviolet radiation.

- Fresh surface air is brought into the contaminated zone to replenish the air released at the surface, enhancing natural diffusion and biodegredation.

- The design allows simultaneous use of the area for other purposes.

- The system requires no site power.

- The design is very low cost (probably less than $30 K per installation) since it does not require boreholes or an active off-gas treatment system.

Remediation of VOC-contaminated soils is presently accomplished by excavation of soil and ex-situ treatment or disposal, soil vapor extraction (SVE), enhancement of microbial degradation with bioventing, and SVE processes enhanced with electrical heating. All of these processes require boreholes or soil excavation, resulting in waste generation and high construction costs (ranging from $50 K to well more than $150 K for typical sites).

7. Future Activities

The Phase I predictive analysis will be completed in September 1995. An initial field demonstration is planned to start in November (the tentative start date of Phase II if Phase I is successful). The first effort in Phase II is to select an appropriate demonstration site. The initial test will probably be conducted using a surrogate, inert tracer (such as sulfur hexafluoride) which can be injected into the soil under controlled conditions. The field test will last 12 months. Subsequent tests on contaminated sites will be conducted depending on the success of the initial demonstration.

8. Acknowledgments

The authors wish to acknowledge the support of the METC COR, Mr. Carl Roosmagi, and DOE/METC in general for supporting innovative technology development. The Los Alamos National Laboratory EES-5 Division is also acknowledged for their support of the FEHM simulations.

This contract's period of performance is from March through mid-November 1995 for Phase I. If funded, Phase II will run for 18 months as a demonstration test.

PII.12 Measurement of Radionuclides Using Ion Chromatography and Flow-Cell Scintillation Counting with Pulse Shape Discrimination

T.A. DeVol (tdevol@ese.clemson.edu; 803-656-1014)
R.A. Fjeld (fjeld@ese.clemson.edu; 803-656-5569)
Clemson University
Department of Environmental Systems Engineering
Clemson, SC 29634-0919

Introduction

The use of ion chromatography (IC) for radiochemical separations is a well established technique. IC is commonly used in routine environmental monitoring applications as well as in specialized research applications. Typical usage involves the separation of a single radionuclide from the non-radioactive constituents. During the past decade, a limited amount of research has been conducted using automated IC systems in actinide separation applications (e.g., [1]). More recently, separation procedures for common non-gamma emitting activation and fission products were developed utilizing a high performance liquid chromatography (HPLC) system [2,3] (Figure 1). In addition, a separation procedure for six common actinides has been developed using a HPLC system [4]. These latter systems used on-line flow-cell detectors for quantification of the radioactive constituents of the effluent stream. Figure 2 is an example of the actinide separation and on-line flow-cell detection of convenient activities (20-80 Bq/radionuclide) [5]. In order to apply HPLC with on-line detection to environmental samples, sample reconcentration and lower detection limit are requisite.

Flow-cell scintillation detection systems have been developed over the past 30 years. Although other designs have been evaluated, the most common is a translucent tube in close proximity to two photomultiplier tubes (PMTs) coupled in coincidence. The coincidence counting system is used to reduce the background count rate. Radioactive samples come in contact with the scintillator in the flow-cell and the scintillation photons are measured by the PMTs. The flow-cell

Research sponsored by the U.S. Dept. Of Energy's Morgantown Energy Technology Center, under contract DOE-AR21-95MC32110 with South Carolina Universities Research and Education Foundation, Strom Thurmond Institute Building, Clemson, SC 29634-5701; telefax: 803:656-0958.

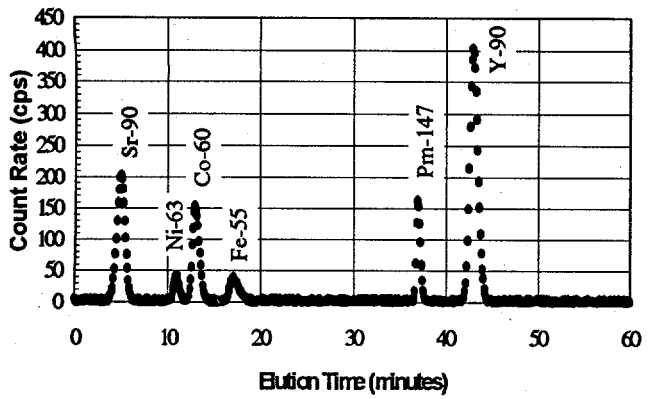

Figure 1. A Typical Chromatogram of Select Beta-emitting Radionuclides using Cationic Elution [3].

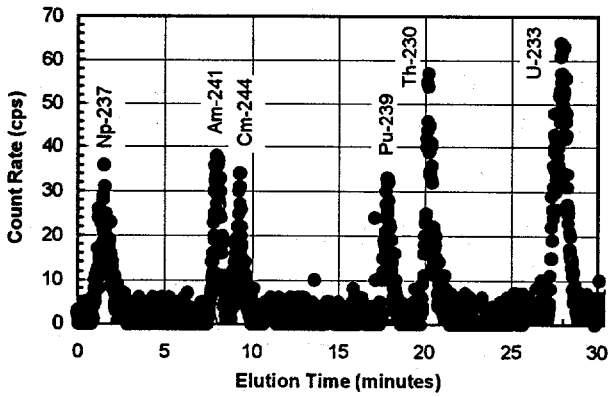

Figure 2. A Typical Chromatogram of Select Actinides using Cationic Elution [5].

can contain either a homogeneous (liquid) scintillator or a heterogeneous (powder) scintillator. In a homogeneous detection system the sample is mixed with the liquid scintillation cocktail upstream of the flow-cell, and the mixture passes through the flow-cell for quantification. The major advantages of a homogeneous flow-cell are high probability of interaction and relatively low background count rate. Disadvantages include variable quench, relatively low luminosity, and increased complexity resulting from the additional pump and mixing apparatus. The heterogeneous flow-cell typically consists of an inert inorganic scintillator that is crushed and sieved into small (50-100 μm) particles. Advantages of a heterogeneous flow-cell are ease of use and relatively high luminosity. Disadvantages are higher background count rates and a high probability of self-absorption resulting in an overall detection efficiency that is lower than for a homogeneous flow-cell, particularly for low energy beta emitters.

Objectives

A project has just been initiated at Clemson University to develop a HPLC/flow-cell system for the analysis of non-gamma emitting radionuclides in environmental samples. An important component of this project is development of a low background, flow-cell detector that counts alpha particles and beta particles separately through pulse shape discrimination (PSD). The objective of the work presented here is to provide preliminary results of an evaluation of the following scintillators: CaF_2:Eu, scintillating glass, and BaF_2. Both CaF_2:Eu and scintillating glass are common heterogeneous flow-cell detector materials. The advantage of CaF_2:Eu is the higher luminosity while the advantage of the glass is its inertness. BaF_2 was chosen as a new material for investigation, with potential advantages during later parts of the project.

Project Description

Flow-Cell Detectors

CaF_2:Eu and glass scintillators (GS-20: cerium activated lithium glass) were purchased from Bicron; BaF_2 was purchased from Optovac, Inc. CaF_2:Eu and BaF_2 were purchased as rough crystals that were subsequently crushed and sieved to a 63 to 90 μm particle size range. GS-20 scintillator was purchased as 63 to 90 μm particles. The scintillators were individually packed into 3.0 mm OD X 1.5 mm ID polytetrafluoroethylene tubing and coiled to 1.5 turns to yield an approximate active volume of 0.2 ml.

Radioactive Sources

Slightly acidic aqueous solutions of an alpha emitter, ^{233}U ($E_\alpha = 4.8$ MeV), and a pure beta emitter, ^{45}Ca (E_{max} = 0.257 MeV), were used to evaluate the flow-cell. $^{233}UO_2(NO_3)_2$ solution at pH 5.5 and concentration of 475 Bq/ml was used. $^{45}CaCl_2$ was dissolved in deionized water at pH 5.5 at a concentration of 670 Bq/ml.

Electronic Circuit

A schematic diagram of the electronic circuit used to acquire the data is presented in Figure 3. The electronic modules were all standard Nuclear Instrument Module electronics. The flow-cell detector resides in a bath of silicon oil positioned between two Hamamatsu R292 PMTs that were separated by 1 cm. The anodes of the PMTs were grounded through a 50 Ω resistor and used for timing. The timing signal, generated by the Ortec 935 constant fraction discriminator, was fed into an Ortec 567 time-to-amplitude converter (TAC). The TAC range was set to 50 ns, and the output gated the pulse height and pulse shape inputs to the analog-to-digital converter (ADC, Aptec MCA card). The pulse height signal was acquired from dynode 11 and had a 1 MΩ load resistor. The pulse height outputs from the PMTs were connected to Ortec 113 scintillation preamplifiers which were connected to Canberra 2021 amplifiers with 3 μs shaping times. The unipolar outputs from the amplifiers were connected to an Ortec 533 sum amplifier which is output to the pulse height ADC and the data stored on a personal computer.

Minimum Detectable Activity

In radiation detection applications, the traditional approach for quantifying detector sensitivity is through the lower limit of detection (LLD). LLD is defined, on the basis of statistical hypothesis testing, as the smallest amount of

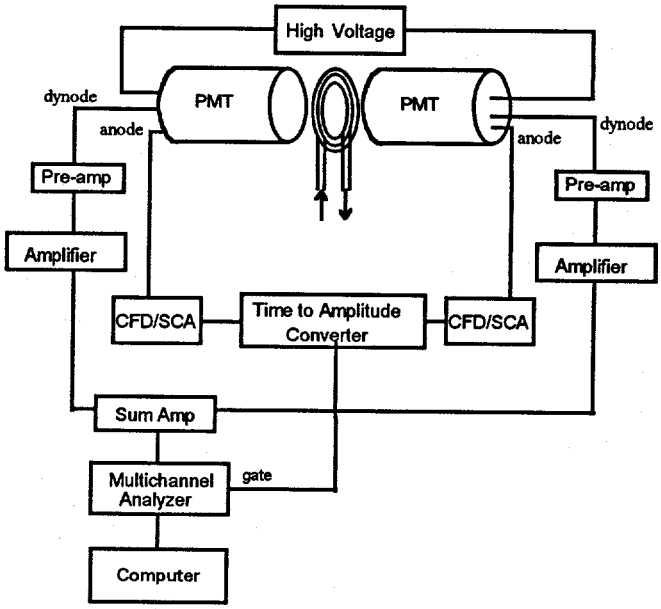

Figure 3. Experimental Schematic of the Pulse Shape Discriminating Flow-Cell Detection System.

activity that will yield a net count for which there is a confidence at a predetermined level that activity is present [6]. For 5% risks of false detection and false non-detection, LLD is given as:

$$\text{LLD} = 2.71 + 4.65\sqrt{C_B t}, \quad (2)$$

where C_B is the background count rate and t is the residence time of the sample in the detector.

Minimum detectable activity (MDA) is a function of the theoretical LLD, count time, and detection efficiency:

$$\text{MDA} = \frac{\text{LLD}}{\varepsilon\, t}, \quad (3)$$

where ε denotes detection efficiency. To lower the MDA, t and/or ε could be increased, and/or C_B could be reduced. For applications involving HPLC, t is limited by the resolution of the chromatographic peaks. A 30 second residence time is typical while 60 seconds would be an upper

limit. For a heterogeneous flow-cell, ε is limited by the particle size of the scintillator. The range of the ^{233}U alpha particles in water is 43 μm. This range is on the order of the interstitial spacing in the flow-cell. A smaller particle size would yield smaller interstitial spacing and hence higher efficiencies resulting from less self-absorption, but is limited by increased back pressure. The remaining variable parameter affecting the MDA is C_B. For this paper, coincidence detection techniques are used to reduce the background events that are attributed to thermonic emissions of electrons from the photocathode of a PMT.

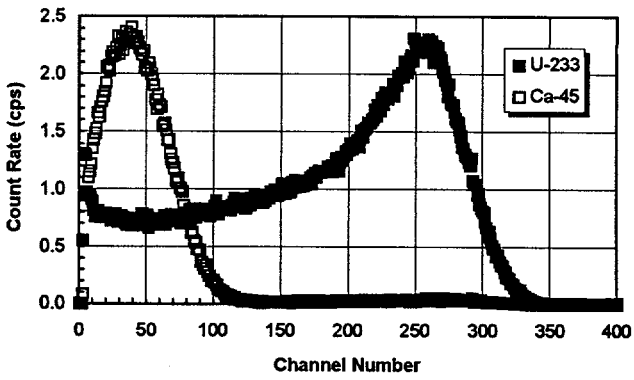

Figure 4. Pulse Height Distribution of the CaF_2:Eu Flow-Cell.

Coincidence Detection

The count rate of a coincidence detection system is related to the background rate in each detector in the following manner:

$$R_{coin} = 2\tau R_1 R_2, \tag{4}$$

where

R_{coin} = the coincidence count rate,
R_1, R_2 = the single detector count rates, and
τ = resolving time of the detection system.

As stated earlier, τ was set to 50 ns. With the typical background count rate for a PMT at 500 counts per second (cps), the expected count rate of the coincidence detection system is 0.025 cps. The theoretical lower limit will be obtained only in the case when there are no electrical or magnetic interactions between the PMTs, when no optical cross-talk occurs, when the scintillator is not inherently radioactive, and when the shielding from external radiation is sufficient.

Results

A typical pulse height distribution for a flow-cell detector is displayed in Figure 4, shown here for the CaF_2:Eu flow-cell. Tailing of the ^{233}U alpha full-energy peak is due to self-absorption effects. In the cases of GS-20 and BaF_2 the amplifier gains were adjusted to X3 and X2, respectively, the setting used for CaF_2:Eu. Increasing the gain compensated for the reduced luminosity of the latter scintillators thus keeping the alpha peak channel approximately the same.

The concept of using coincidence detection as a means to reduce the background count rate appears to have potential, but care must be taken in selecting a scintillator with a low intrinsic background. Table 1 summarizes the background count results for the CaF_2:Eu flow-cell. Note that the measured background count rate is considerably above the theoretical background count rate (typical for the other scintillators as well), thus giving an indication of the margin for improvement. The elevated background count rates of CaF_2:Eu and BaF_2 were attributed to the insufficient inertness of the materials resulting in adsorption of the radionuclide onto the scintillator. Elevated background count rates of BaF_2 and also GS-20 were attributed to intrinsic radioactivity of the scintillation material. By gamma-ray spectroscopy it was determined that the intrinsic background in BaF_2 was due, at least in part, to radium contamination. The elevated background of GS-20

Table 1. Results of the Single Detector Versus the Coincidence Detection System for a Typical Background.

Scintillator	R_1 (cps)	R_2 (cps)	[1]R_{coin} (cps)	[2]R_{bkg} (cps)
CaF_2:Eu	180.2	274.6	.005	0.405
GS-20				0.550
BaF_2				0.378

[1]Theoretical coincidence rate as calculated with equation 4
[2]Experimentally determined background count rate

Table 2. Properties of Scintillators and Detection Limits.

Scintillator	ε_β	MDA_β(Bq) t=30s	ε_α	MDA_α(Bq) t=30s
CaF_2:Eu	0.66*	0.96	0.49	1.29
GS-20	0.38	1.89	0.52	1.38
BaF_2	0.66	0.93	0.45*	1.36

*Value could not be measured directly because of radionuclide interaction with the scintillator so the value shown was estimated based on other scintillators.

was attributed to thorium, which is a common contaminant of glass.

Flow-cell detector volumes were determined by a conductivity measurement using a NaCl solution that filled the detector. The detector volumes were all determined to be nominally 0.2 ml. Acidic ^{233}U solution ($^{233}UO_2(NO_3)_2$, pH 1) at a concentration of 130 Bq/ml was used to determine the efficiency of the flow-cells. An acidic solution was necessary to ensure minimal adsorption of the radionuclide onto the scintillator. The CaF_2:Eu and GS-20 flow-cells had a detection efficiency of 0.54 for ^{233}U. The GS-20 and BaF_2 flow-cells had detection efficiencies of 0.38 and 0.66, respectively, for ^{45}Ca. But since the uranium in the aqueous solution interacted with the BaF_2 and the ^{45}Ca interacted with the CaF_2:Eu, the efficiency could not be directly measured. Table 2 summarizes these results. The MDA was calculated using the experimentally determined background count rate (Table 1) and detection efficiency, and a 30 second count time.

Application

Based on the results obtained in this study, coincidence detection should be used to reduce the electronic noise associated with the photomultiplier tubes. The reduction in the background count rate was several orders of magnitude (from a single PMT rate of ~200 cps to a background count rate of ~1 cps). Despite the relatively high background count rates, the minimum detectable activities calculated for these flow-cells were ~1 Bq for CaF_2:Eu and BaF_2, and ~1-2 Bq for GS-20.

Future Activities

Presented here were preliminary results of the first task of the project. Additional work on this task includes the evaluation of additional scintillators and the addition of pulse shape discrimination, active shielding, and passive shielding to the detection system. Other tasks include the identification of sample interferences in the chromatographic portion of the apparatus, the development of sample processing protocols, and laboratory testing of the entire system using surrogate environmental and waste samples.

Acknowledgments

The authors wish to thank David D. Brown for his assistance in preparing the radioactive solutions as well as measuring the detector volumes, Dr. John D. Leyba for assisting in the intrinsic radioactivity analysis of the scintillators, and Jagdish L. Malhotra, METC Contracting Officer's Representative. Period of Performance: 6/15/95 - 2/15/98.

References

[1] S. Usuda, "Rapid ion-exchange separations of actinides," *J. Radioanal. Nucl. Chem.*, Vol. 123, No. 2, pp 619-631, 1988.

[2] S. H. Reboul and R. A. Fjeld, "A rapid method for determination of beta-emitting radionuclides in aqueous samples," *Radioactivity and Radiochemistry*, Vol. 5, No. 3, 1994.

[3] D. Bradbury, G. R. Elder and M. J. Dunn, "Rapid analysis of non-gamma radionuclides using the "ANABET" system," Waste Management, Tucson, Arizona, 1990, pp 327-329.

[4] S. H. Reboul and R. A. Fjeld, "Separation of actinides by ion chromatography," submitted for publication in *Radiochimica Acta*, 1995.

[5] S. H. Reboul and R. A. Fjeld, "Potential effects of surface water components on actinide determinations conducted by ion chromatography," *Health Physics Journal*, Vol. 68, No. 4, pp 585-589, 1995.

[6] L. A. Currie, "Limits for qualitative detection and quantitative determination: application to radiochemistry," Anal. Chem., Vol. 40, No. 3, pp 586-593, 1968.

PII.13 Development of HUMASORB™, A Lignite Derived Humic Acid for Removal of Metals and Organic Contaminants from Groundwater

H.G. Sanjay (archtech@cais.com; 703-222-0280)
Kailash C. Srivastava (arctech@cais.com; 703-222-0280)
Daman S. Walia (arctech@cais.com; 703-222-0280)
ARCTECH, Inc.
14100 Park Meadow Drive, Suite 210
Chantilly, VA 22021

Introduction[1]

Heavy metal and organic contamination of surface and groundwater systems is a major environmental concern. The contamination is primarily due to improperly disposed industrial wastes. The presence of toxic heavy metal ions, volatile organic compounds (VOCs) and pesticides in water is of great concern and could affect the safety of drinking water. Decontamination of surface and groundwater can be achieved using a broad spectrum of treatment options such as precipitation, ion-exchange, microbial digestion, membrane separation, activated carbon adsorption, etc. The state of the art technologies for treatment of contaminated water however, can in one pass remediate only one class of contaminants, i.e., either VOCs (activated carbon) or heavy metals (ion exchange). This would require the use of at a minimum, two different stepwise processes to remediate a site. The groundwater contamination at different Department of Energy (DOE) sites (e.g., Hanford) is due to the presence of both VOCs and heavy metals. The two-step approach increases the cost of remediation. To overcome the sequential treatment of contaminated streams to remove both organics and metals, a novel material having properties to remove both classes of contaminants in one step is being developed as part of this project.

Objective

The objective of this project is to develop a lignite derived adsorbent, **Humasorb™**, to remove heavy metal and organic contaminants from groundwater and surface water streams in one processing step. As part of this project, **Humasorb™** will be characterized and evaluated for its ion-exchange and adsorption capabilities.

Approach

Humic acid is a natural material with many properties which can be exploited for several cost effective applications. Humic substances are complex mixtures of naturally occurring organic materials. These substances are formed from the decay of plant and animal

[1] Research sponsored by the U.S. Department of Energy's Morgantown Energy Technology Center, under Contract DE-AR21-95MC32114 with ARCTECH, Inc. 14100 Park Meadow Drive, Chantilly, VA 22021; telefax: 703-222-0299.

residues in the environment. Humic acid constitutes a significant portion of the acid radicals found in humic substances.

Humic acid is dark brown to black in color and is considered a complex aromatic macromolecule with various linkages between the aromatic groups. The different compounds involved in linkages include, amino acids, amino sugars, peptides, aliphatic acids and other aliphatic compounds. The various functional groups in humic acid include, carboxylic groups (COOH), phenolic, aliphatic and enolic - hydroxyl and carbonyl (C=O) structures of various types. Humic acid is an association of molecules forming aggregates of elongated bundles of fibers at low pHs and open flexible structures perforated by voids at high pHs. The voids can trap and adsorb both organic and inorganic particles if the charges are complementary.

A major source of humic acid is coal- the most abundant and predominant product of plant residue coalification. All ranks of coal contain humic acid but lignite represents the most easily available and concentrated form of humic acid. Humic acid concentration of lignite varies from 30-90 % depending on location. Peat, humates and sewage sludge also contain significant quantities of humic acid.

Chelation of metals

Metals are bound to the carbon skeleton of humic substances through heteroatoms such as nitrogen, oxygen or sulfur. The most common metal binding occurs via carboxylic and phenolic oxygen, but nitrogen and sulfur also have a positive effect on metal binding. The cation exchange capacity (CEC) of humic acid derived from leonardite is 200-500 meq/100 grams, whereas the CEC of leonardite is only 50 meq/100 grams.

Musani et al. (1) studied the chelation of radionuclides such as ^{65}Zn, ^{109}Cd and ^{210}Pb by humic acid isolated from marine sediments. The chelation of metals by humic acid was observed to be significant. The binding mechanism was found to be different depending on the physical state of the humic acid. Binding was stronger with precipitated humic acid than with dissolved humic acid. The chelation effect was stronger for the metals in the absence of calcium and magnesium. The order of binding was determined to be Pb>Zn>Cd (1).

Pahlman and Khalafalia (2) used humic acid to remove heavy metals from process waste streams. The efficiency of heavy metal removal by humic acids derived from lignite, a sub-bituminous coal and peat were evaluated. The effect of pH on metal removal was determined. Humic acid was very effective in removal of toxic metal ions. The pH range of 6.5 to 9.5 was determined to be the optimal range for complete removal of heavy metal ions by humic acids derived from lignite and subbituminous coal. The efficiency of heavy metal removal by humic acid was higher compared to the conventional lime treatment even at lower concentrations of metals. Humic acids were very effective in the removal of the most toxic metals such as cadmium, mercury and lead. The removal of these toxic metals by lime is incomplete, particularly at near neutral pH.

Adsorption of organics

The adsorption of organic chemicals onto humic substances such as humic acid have been studied extensively. The reported investigations on adsorption of organic compounds by humic acid include studies on:

- non-ionic organics such as benzene, halogen substituted benzene, and chlorinated

hydrocarbons such as 1,1,1-trichloroethane (TCA),
- nitrogen compounds such as urea and anilines,
- polychlorinated biphenyls (PCB),
- fumigants such as telone and insecticides such as DDT,
- herbicides such as paraquat, diquat, triazines,
- organophosphorous compounds such as parathion.

It is believed that humic acid combines with herbicides by electro-static bonding, hydrogen bonding and ligand exchange. In addition, the high concentrations of stable free-radicals in humic acid are capable of binding herbicides that can ionize or protonate to the cation form. The mechanisms that have been postulated for the adsorption of organic compounds include (3):

- Van der Waals attractions
- hydrophobic bonding
- hydrogen bonding
- charge transfer
- ion-exchange
- ligand exchange.

The adsorption of benzene, halogen substituted benzenes, and chlorinated hydrocarbons such as TCA, and similar nonionic organic compounds on soil containing different amounts of soil organic matter has been reported by Chiou (4). The adsorption on soil organic matter of various nonionic organic compounds from water was attributed primarily to solute partitioning into the organic adsorbent. The partitioning theory was supported by experimental observations of linear adsorption isotherms up to concentrations approaching saturation. In addition, the absence of competitive effects between solutes support the partition approach. The presumed partition was also analyzed in relation to the equilibrium properties of organic compounds in solvent-water mixtures (4).

Humic acid has been shown to adsorb considerable amounts of nitrogen compounds such as urea, anilines, etc. The stable free radicals in humic acid are believed to play a significant role in urea-humic acid interaction (5). In addition, it has been postulated that urea forms an addition complex with humic acid through the carboxyl and phenolic hydroxyl group (6). It has been further determined that the complex formed is very stable and that the decomposition of urea is inhibited in the presence of humic acid. The adsorption of aniline on soil organic matter is directly related to the concentration of the humic acid. The adsorption of aniline on humic acid has been shown to follow both the Freundlich and Langmuir relations (6).

Adsorption of PCBs from aqueous streams has been reported by Haque and Schmedding (7). The adsorption on humic acid increased with the increase in the number of chlorine atoms in the PCB. Adsorption isotherms of PCBs on humic acid followed the Freundlich equation and the constant K (measure of adsorptive capacity) increased from di- to hexa-chloro PCB. The high K value on humic acid was attributed to a combination of high surface area and the number of functional groups present in humic acid.

The brief discussion in this section and a review of the literature clearly indicate the unique properties of humic acid to chelate metals and adsorb organics. The humic acid complex however, will dissolve in water above pH 2 and in the presence of ions such as sodium and potassium. The aim of this project is to develop a humic acid polymer that will be insoluble in water under the conditions

encountered during remediation of contaminated streams. The various steps involved in the development of Humasorb™ are discussed in the following section.

Project Description

The starting material for the development of Humasorb™ is **actosol**[R], a humic acid based soil amendment product manufactured by ARCTECH, Inc. The various phases in the development of this unique material include:

- isolation and purification of humic acid
- construction of metal-sorption and organic adsorption isotherms
- characterize and quantify metal-sorption and adsorption capacity
- cross-link humic acid to make it insoluble at higher pH
- evaluate cross-linked humic acid polymer for metal-sorption and adsorption capacity.

Isolation and purification of humic acid

Humic acid was isolated and purified from **actosol**[R] by acidification using concentrated hydrochloric acid (HCl) to lower the pH (below 2). The precipitated solids were purified by repeated washing with distilled water and acidification. A pressure filter (60 psig) was used to separate the precipitated humic acid from the other humic substances dissolved in water. The amount of humic acid recovered ranged from 11.79 % to 14.79 % of **actosol**[R] by weight. Approximately 300 grams of humic acid was isolated and purified to conduct the various experimental tasks in the project.

Metal sorption

The effect of pH on the sorption of metals by **actosol**[R] humic acid was evaluated by adjusting the pH with sodium hydroxide (NaOH, 1 N) or concentrated hydrochloric acid (HCl, 10 N). In polypropylene centrifuge bottles, **actosol**[R] humic acid was contacted with spiked water solution containing known concentration of metals. The spiked solutions were prepared by dissolving the metal salts in water. The centrifuge bottles were shaken at 300 rpm and 25°C for the desired contact time. After the desired contact time, alum (10% solution) was added to the centrifuge bottles to coagulate humic acid. The bottles were then centrifuged at 2000 rpm for 30 minutes to separate the solid and liquid phases. The supernatant in the bottles was analyzed for the target metal.

The adsorption capacity of purified humic acid was evaluated by developing metal sorption isotherms. The spiked water solution was contacted with different amounts of humic acid in centrifuge bottles. The pH was not adjusted in these tests. The centrifuge bottles were shaken at 300 rpm and 25°C for two hours. After the desired contact time, the bottles were centrifuged at 2000 rpm for 30 minutes to separate the solid and liquid phases. The ability of humic acid to reduce toxic metals such as chromium (VI), present as anions ($Cr_2O_7^{-2}$), to less toxic Cr(III) was also evaluated in a similar manner.

Organic adsorption

Isotherms for adsorption of chlorinated and petroleum hydrocarbons were developed using purified humic acid. Initial experiments were conducted using **actosol**[R] humic acid. The chlorinated hydrocarbons used were trichloroethylene (TCE) and tetrachloroethylene

(PCE); benzene was the representative petroleum hydrocarbon used in this study.

Isotherms were developed by contacting spiked water samples with different amounts of humic acid in a 20 ml serum vial. Humic acid was ground to less than 350 mesh for use in the experiments. The spiked water solution and the humic acid were contacted in the crimp-sealed vials at 350 rpm and 25°C for the desired time. The vials were centrifuged at 2000 rpm for 30 minutes after the contact time to separate the liquid and solid phases. The liquid phase was analyzed by using purge and trap GC-MS.

Results

Metal sorption

The effect of pH on uranium removal using **actosol**^{R} humic acid is shown in Figure 1. Clearly, the results indicate that humic acid is very effective in removing uranium from water under acidic conditions. Uranium is soluble in water under acidic conditions and increasing the pH to 4 using NaOH results in only 6 % removal of uranium. Uranium is completely removed from the solution at pHs greater than 6. However, at pH 4, the addition of humic acid removed all the uranium from solution and was recovered as a solid bound to humic acid. The recovery of uranium decreased at higher pH in the presence of humic acid. The observed decrease in uranium recovery at higher pH in the presence of humic acid is expected as humic acid dissolves in water at higher pH levels. The comparison of uranium recovery both in the absence and presence of humic acid indicates that uranium is bound to humic acid over the pH range 2-12 and remains in solution under basic conditions in the presence of humic acid. The addition of a coagulant such as alum did not have a significant effect at higher pH. However, at near neutral pH (6-8), the addition of alum increased the amount of uranium recovery from water. The effect of pH on the removal of different metals using **actosol**^{R} humic acid is shown in Figure 2.

The sorption of copper and nickel by purified humic acid was represented well by both the Freundlich and Langmuir models (Figures 3 & 4). The Langmuir model for nickel however, gave negative values for the constants. However, the sorption of cadmium did not follow either the Freundlich or the Langmuir model indicating a complex multilayer sorption.

The metal sorption data was also analyzed using the method developed by Scatchard (8). The presence of more than one inflection point on a plot based on Scatchard analysis usually indicates the presence of more than one type of binding site. The Scatchard plot for the sorption of different metals by humic acid is shown in Figure 5. The plot clearly indicates the presence of more than one type of binding site for copper and nickel sorption. The plot was however, linear for cadmium indicating that possibly only one type of binding site was active for cadmium sorption.

Humic acid can act as a reducing agent and influence oxidation-reduction of metal species. An unchelatable toxic oxo-anion such as chromium present as dichromate ($Cr_2O_7^{-2}$), is reduced to relatively non-toxic Cr(III). The reduced chromiun is then stabilized through chelation by humic acid. The reduction of different metal species such as mercury, vanadium, iron and plutonium by humic acid has been reported by a number of investigators (9-12). The purified humic acid used in this study was able to reduce Cr(VI) completely as shown in Figure 6.

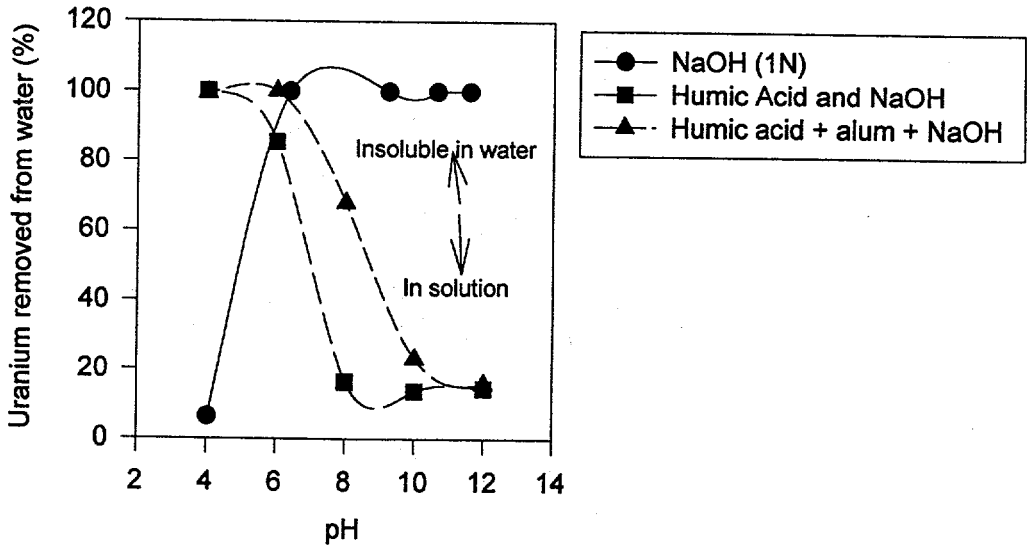

Figure 1. Effect of pH on Uranium Removal Using actosol® Humic Acid

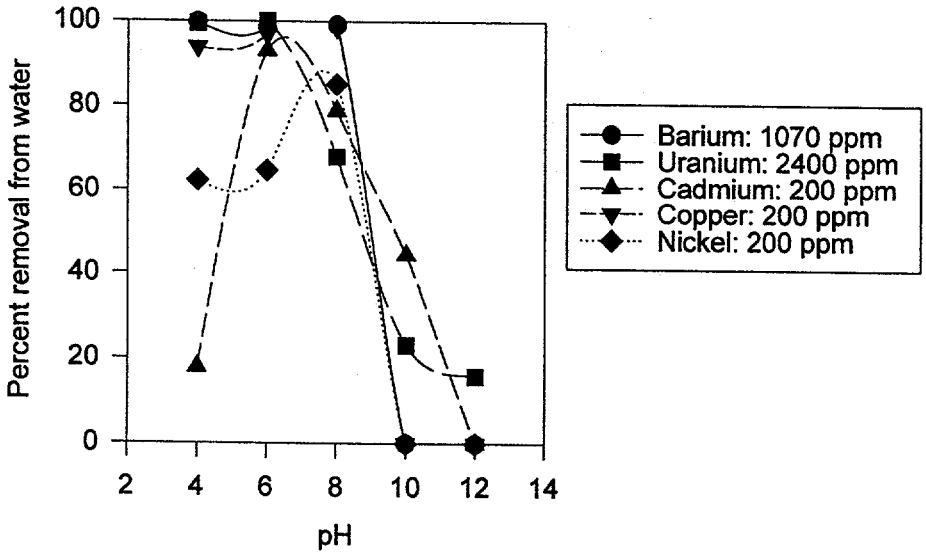

Figure 2. Effect of pH on Metal Removal Using actosol® Humic Acid

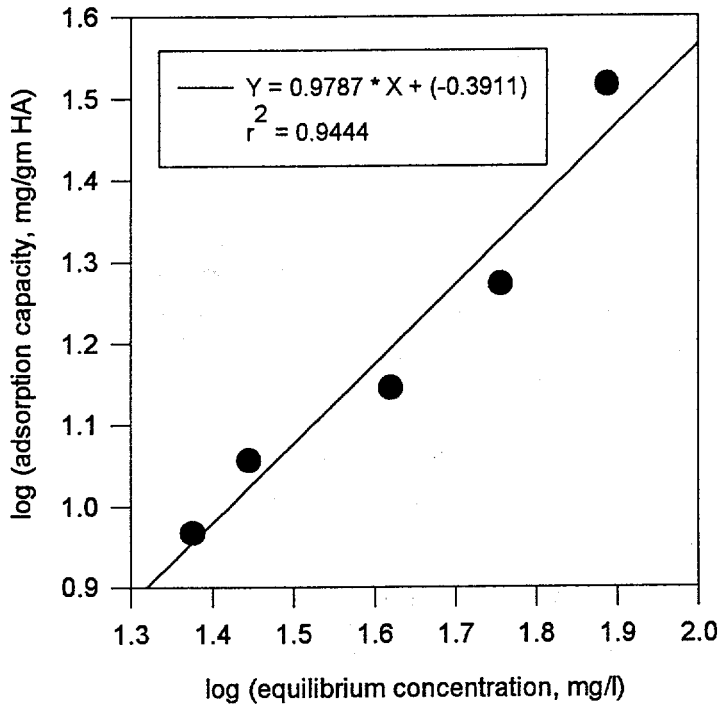

(A) Copper

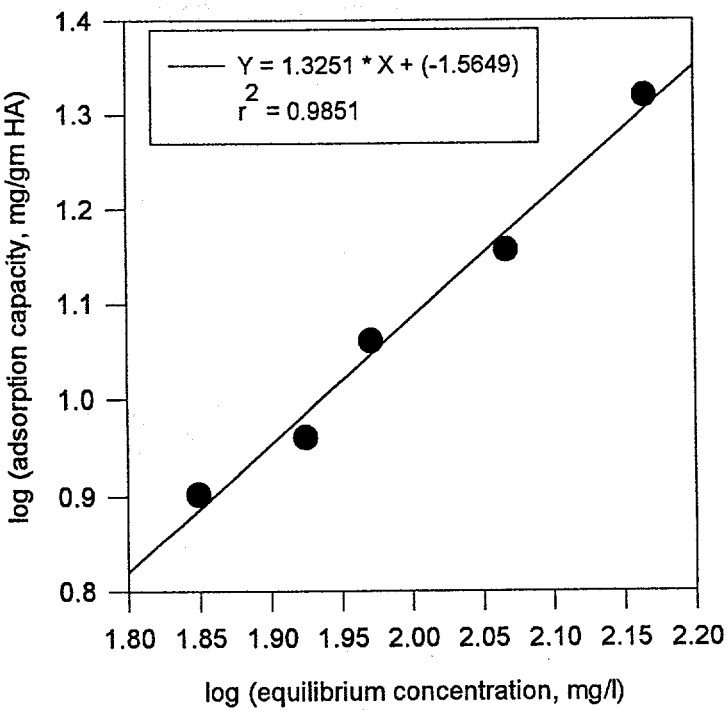

(B) Nickel

Figure 3. Freundlich Plot for Metal Sorption by Humic Acid

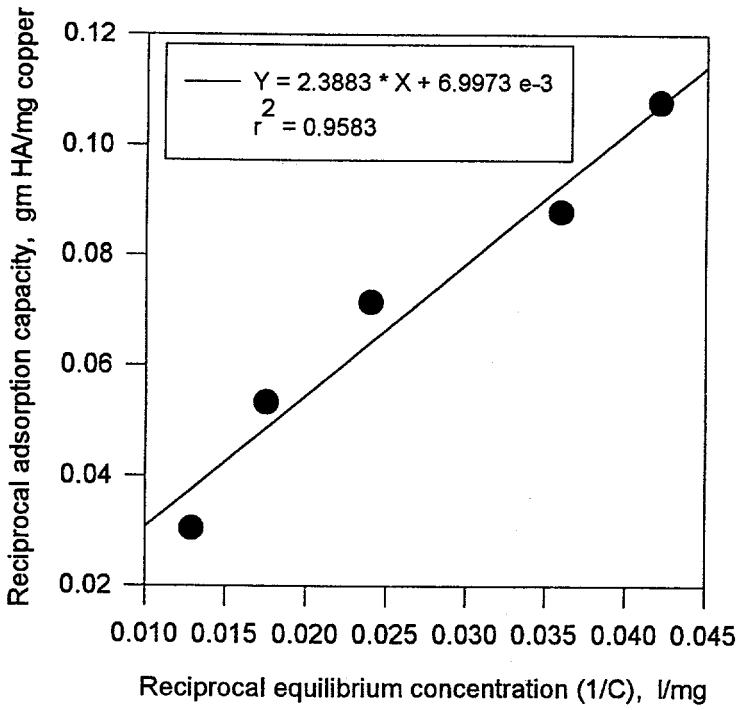

(A) Copper

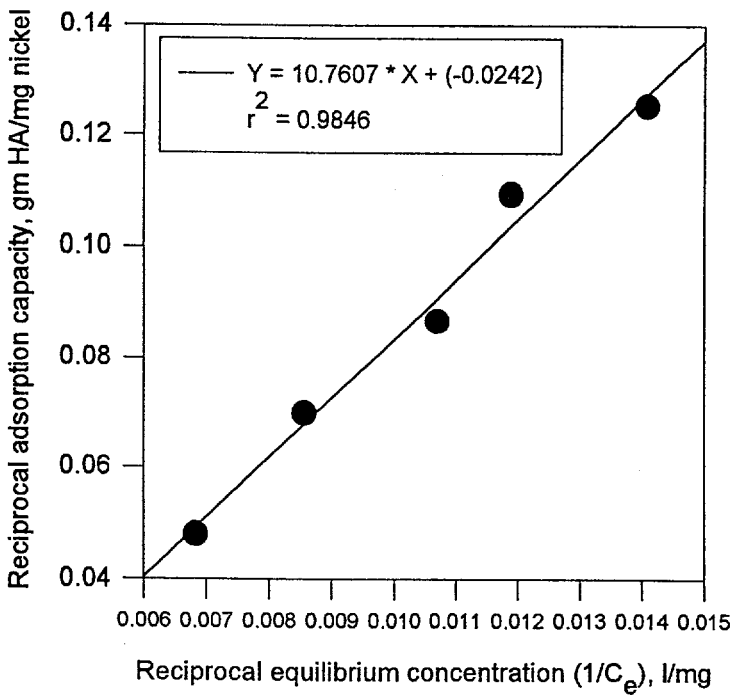

(B) Nickel

Figure 4. Langmuir Plot for Metal Sorption by Humic Acid

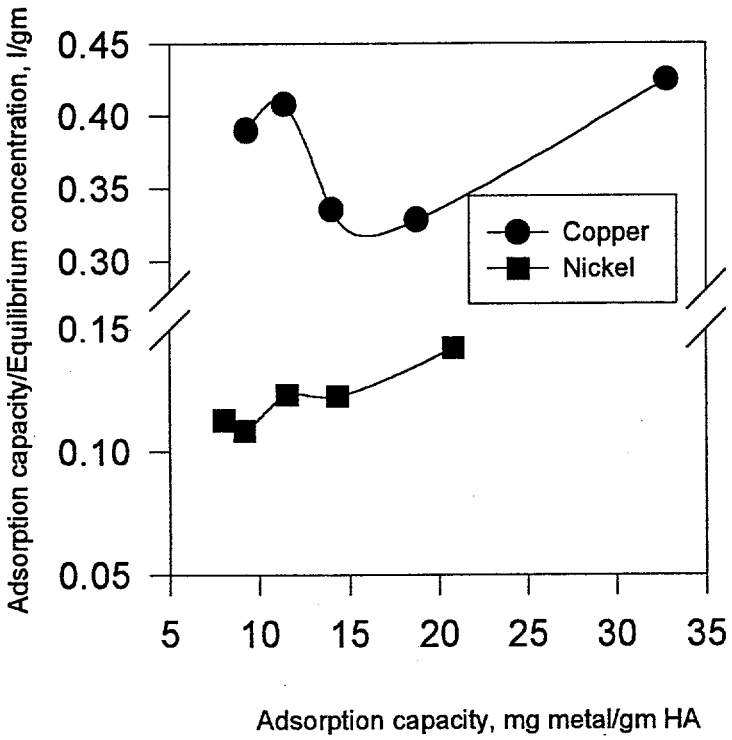

Figure 5. Scatchard Plot for Metal Sorption on Humic Acid (HA)

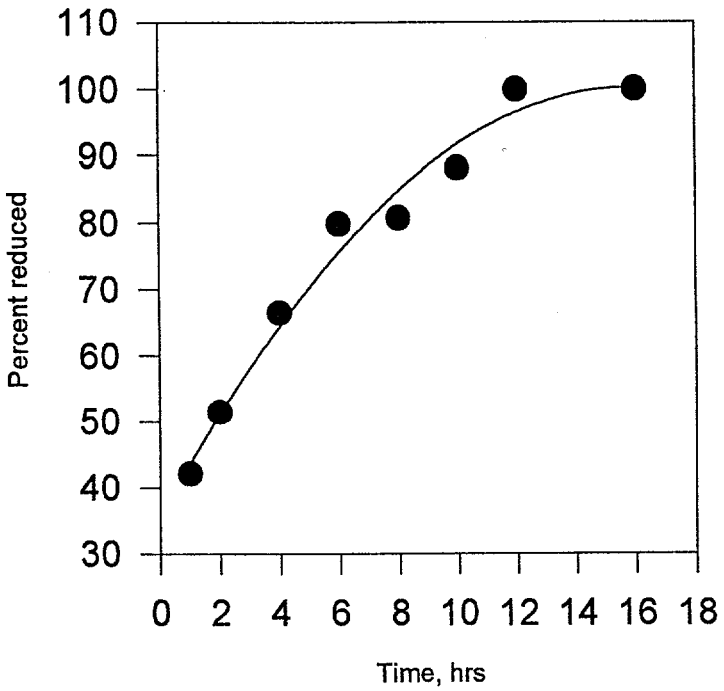

Figure 6. Reduction of Chromium (VI) by Humic Acid

Organic adsorption

Freundlich and Langmuir adsorption models were used to represent the data obtained for organic adsorption. The data for TCE adsorption was not represented by either model (Figure 7). The isotherms show two distinctive phases with adsorption capacity increasing only slightly with concentrations up to 210 ppm and increasing rapidly above 210 ppm. The shape of the isotherm indicates the possibility of multi-layer adsorption, with adsorption capacity increasing rapidly at higher concentration.

The adsorption of PCE on humic acid was also represented well by both Freundlich and Langmuir models as shown in Figure 8. However, the Langmuir model gave negative values for the constants. The Freundlich and Langmuir model parameters determined from the isotherms for some of the contaminants evaluated in this study are shown in Table 1.

Benzene adsorption on humic acid was represented very well by both the models at the relatively higher equilibrium concentrations obtained in this study. The removal of PCE from spiked water was higher compared to the removal of both TCE and benzene under the conditions used for the development of the adsorption isotherms. However, the removal of both TCE and benzene increased significantly with the increase in the amount of humic acid as shown in Figure 9.

Future work

The purified humic acid isolated in this project, though insoluble in water, can dissolve at higher pH in the presence of certain metal ions such as sodium and potassium. The purified humic acid will be rendered insoluble in water by cross-linking and forming a water-insoluble polymer in a number of screening trials. The cross-linked humic acid polymer will be further evaluated for its contaminant removal capabilities. Initial cross-linking studies in our lab have been successful in producing a material that is only sparingly water-soluble at near neutral pH even in the presence of ions such as sodium. Efforts are underway at present to characterize the cross-linked material. The future work in this project includes the following tasks:

- cross-link the purified humic acid to form a water-insoluble polymer,
- evaluate of cation exchange and organic adsorption capacity of cross-linked humic acid polymer,
- bench scale column studies with **Humasorb™**
- conceptual design and economic analysis.

Applications

The remediation of contaminated streams and groundwater has been traditionally approached with at least a two-step process including some combination of activated carbon and ion-exchange process.

The removal of heavy metals from contaminated water has been accomplished by techniques such as the addition of a precipitating agent, ion-exchange or reverse osmosis. These techniques require considerable capital investment and in addition would require pretreatment in some cases to remove oil and suspended solids.

The removal of organic compounds by activated carbon, though very effective, is associated with high capital and operating costs,

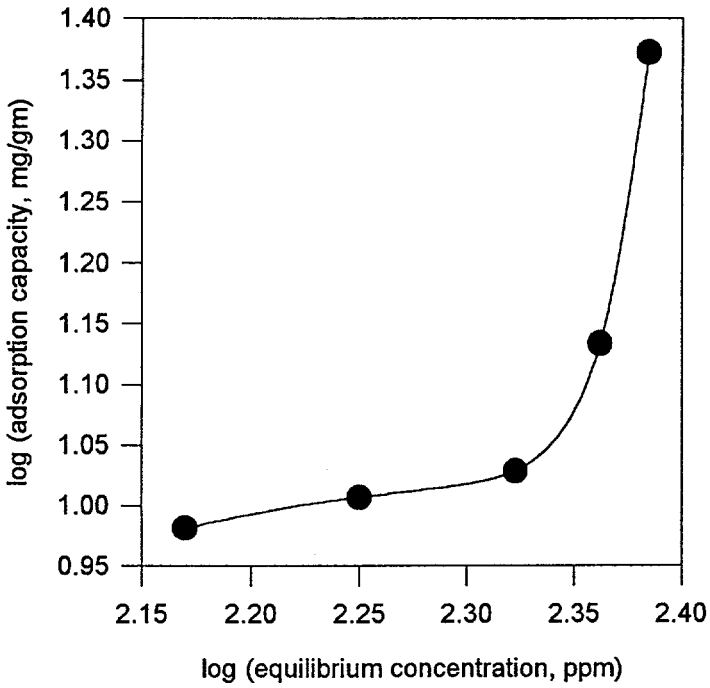

(A) Freundlich

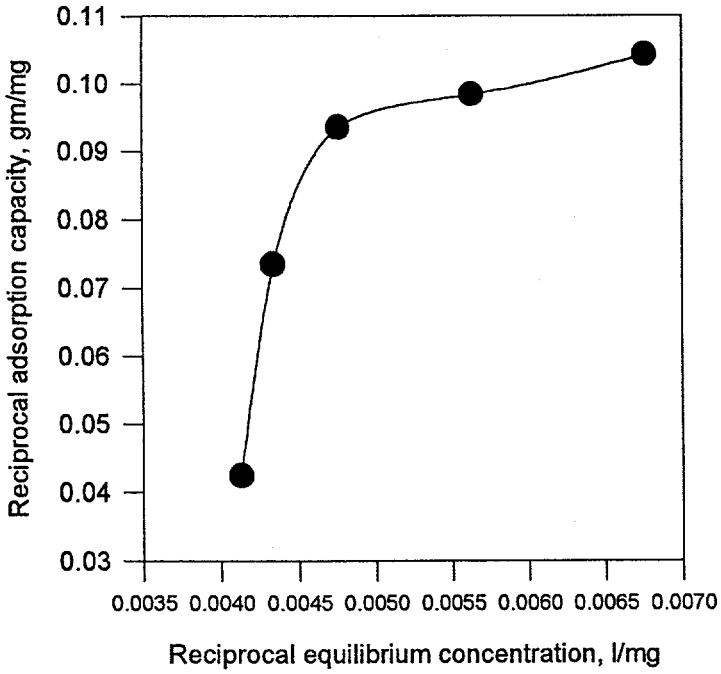

(B) Langmuir

Figure 7. Isotherm for TCE Adsorption on Humic Acid

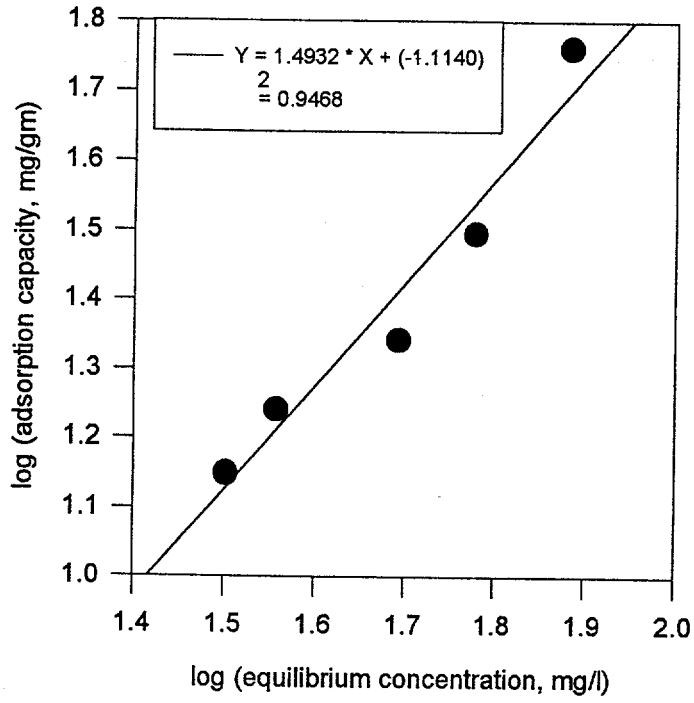

(A) Freundlich

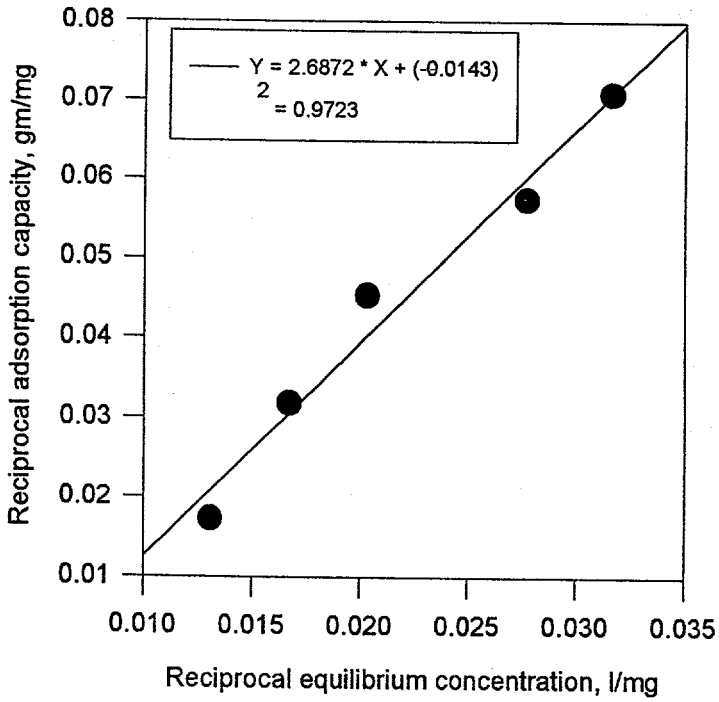

(B) Langmuir

Figure 8. Isotherm for PCE Adsorption on Humic Acid

Table 1.

Freundlich and Langmuir Model Parameters

Contaminant	Freundlich	Langmuir
Copper	K = 0.4064 mg/gm n = 1.0218	K = 142.91 mg/gm b = 0.0029 l/mg
Nickel	K = 0.0300 mg/gm n = 0.7500	Negative values
PCE	K = 0.07691 mg/gm n = 0.6697	Negative values

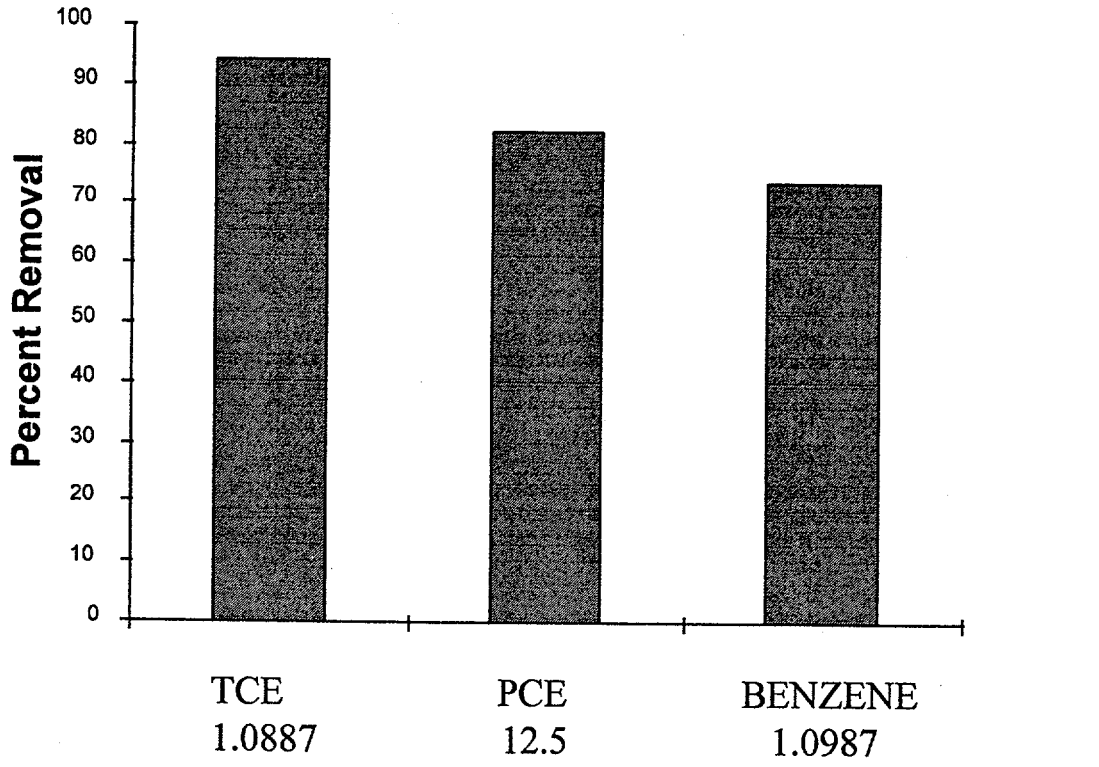

Figure 9. Organic Contaminant Removal using Humic Acid

especially when regeneration is carried out by the most effective process-thermal reactivation. Also, this technique is very sensitive to the presence of suspended solids, oil and grease requiring pretreatment for effective performance.

Humasorb™, derived from a naturally occurring material has the potential to alleviate some of these limitations by combining remediation efforts into a single step process. **Humasorb™** can be used for groundwater cleanup both in the *in-situ* mode and in a pump and treat process. The examples of potential applications for the remediation of DOE contaminated sites include the following:

- Hanford: chromium, uranium and chlorinated compounds
- Fernald: uranium and chlorinated compounds
- Oakridge: mercury and chlorinated compounds.

References

1. Musani, Lj., et al. On the chelation of toxic trace metals by humic acid of marine origin, Estuarine and Coastal Marine Science, II, 639-649, 1980.
2. Pahlman, J.E., and Khalafalia, S.E. Use of lignochemicals and humic acids to remove heavy metals from process waste streams, Bureau of Mines report of investigations, 9200, 1988
3. Choudhary, G.G. Humic substances: Sorptive interactions with environmental chemicals. Toxicological and Environmental Chemistry, 6, 1983.
4. Chiou, C.T. Roles of organic matter, minerals, and moisture in sorption of nonionic compounds and pesticides by soil. In Humic substances in soil and crop sciences: selected readings. Eds: MacCarthy, P. et al., American Society of Agronomy, Inc. Madison, Wisconsin, USA.
5. Pal, P.K., and Banerjee, B.K. Interaction of ammonia and soil humic acid in presence of ammonium sulfate, Technology (Sindri), 3, 87, 1966.
6. Haque, R., and Schmedding, D. Studies on the adsorption of selected polychlorinated biphenyl isomers on several surfaces. Journal of Environmental Science and Health, B (2), 129, 1976.
7. Singhal, J.P., and Kumar, D. Environmental influence on adsorption of 1,3-dichloropropene by "AKLI" bentonite, J. Indian Chem. Soc., 55, 68, 1978.
8. Scatchard, G. The attraction of proteins for small molecules and ions, Ann. New York Acad. Sci., 51, 660-672, 1949.

PII.14 Field Raman Spectrograph for Environmental Analysis

John W. Haas III (617-769-9450)
Robert W. Forney (617-769-9450)
Michael M. Carrabba (617-769-9450)
R. David Rauh (617-769-9450)
EIC Laboratories, Inc.
111 Downey St.
Norwood, MA 02062

Introduction

The enormous cost for chemical analysis at DOE facilities predicates that cost-saving measures be implemented. Many approaches, ranging from increasing laboratory sample throughput by reducing preparation time to the development of field instrumentation, are being explored to meet this need. Because of the presence of radioactive materials at many DOE sites, there is also a need for methods that are safer for site personnel and analysts.

Objectives and Approach

For nearly a decade, our objective has been to pursue the development of fiberoptic spectroscopic instruments for *in situ* chemical analysis. Ultimately, this approach can provide the highest quality, most timely, and least expensive analytical data at a site. By making measurements remote from the analyst, this approach also virtually eliminates the risk of exposure to hazardous chemicals.

Research sponsored by the U.S. Department of Energy's Morgantown Energy Technology Center, under contract DE-AC21-92MC29108 with EIC Laboratories, Inc., 111 Downey St., Norwood, MA, 02062; telefax: 617-551-0283.

Technology Description

This project entails the development of a compact Raman spectrograph for field screening and monitoring of a wide variety of wastes, pollutants, and corrosion products in storage tanks, soils, and ground and surface waters. Analytical advantages of the Raman technique include its ability to produce a unique, spectral "fingerprint" for each contaminant and its ability to analyze both solids and liquids directly, without the need for isolation or cleanup.

Technical Accomplishments

Spectrograph

We have assembled a Raman spectrograph that is unique in its optical configuration and, with no moving parts, is well suited for field work. The optical layout of the system is shown in Figure 1. Key components in the spectrograph are two prisms and an echelle grating which disperse the Raman spectrum from a sample in two-dimensions onto a CCD detector array. This allows a full Raman spectrum to be collected without repositioning the grating and with high resolution (better than 1 cm^{-1}). No other spectrograph provides this powerful combination of high resolution and wide spectral range. Furthermore, with no moving parts, frequent wavelength calibration

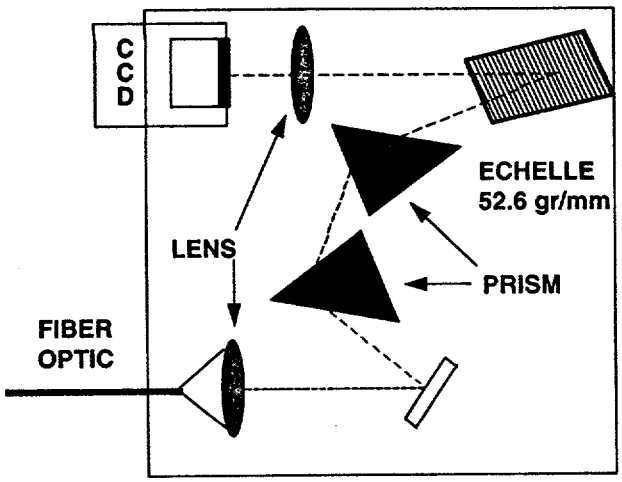

Figure 1. Optical Layout of the Near-IR Echelle Raman Spectrograph.

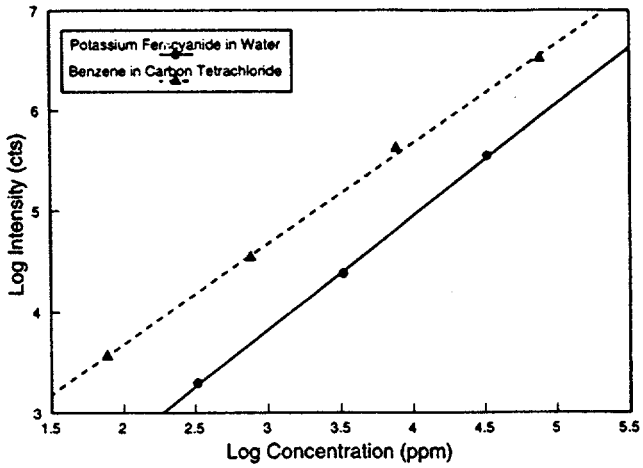

Figure 2. Raman Response vs. Concentration for Two Waste Tank Components.

required with other spectrographs is not necessary with the echelle spectrograph. Using Raman shifts established by ASTM for naphthalene, the echelle spectrograph's calibration was measured to be accurate within 1 cm^{-1} over the whole Raman range and no change in wavelength calibration was observed over several months of operation.

The echelle spectrograph is also an optically efficient instrument, providing rapid detectability from ppm to percentage level concentrations. Figure 2 shows Raman response vs. concentration plots for potassium ferricyanide in water (a Hanford waste tank problem) and benzene in carbon tetrachloride (an Oak Ridge waste tank problem). Lower detection limits for most analytes are in the range 50-500 ppm. This level of sensitivity compares favorably with conventional laboratory Raman instruments and is suitable for *in situ* identification and monitoring of major components in waste mixtures found in tanks or drums or NonAqueous Phase Liquids (NAPLs) underground. Some of the throughput-enhancing (time-reducing) features of the instrument include direct fiber optic coupling (replacing slits), low f-number transmission (f/3), and extensive use of antireflection coatings.

Physically, the echelle spectrograph is compact, 16 in (W) x 24 in (L) x 8 in (H) which allows it to be easily transported and operated in small trucks, vans, or automobiles. At approximately 60 lbs, the spectrograph is light enough for a person to carry for short distances.

Lasers

Another important component of a Raman system is the laser source. The echelle spectrograph assembled in this project is designed to be used with near-IR laser sources such as solid-state or ion lasers. The advantage of this approach is that for many samples interference from fluorescence is reduced in the near-IR. As part of this program, new high-power lasers are being evaluated for field use. To date, pulsed alexandrite and external cavity diode lasers providing 500mW or more optical power have been determined to be most useful for field Raman analysis.

Fiber Optic Probes

A significant part of this program has been directed to the development of fiber optic probes for use with the Raman spectrograph in specific field applications. These probes are much smaller than commercially available probes and utilize microfilters to provide "clean" spectra over long fiber lengths. One of these devices is a "side-viewing" probe that has been configured for deployment in a cone penetrometer to identify NAPLs in soil and groundwater. A schematic representation of the device is shown in Figure 3. The small, 0.5 in diameter of the EIC Raman probe is critical for this application because of the limited space available in the cone. Other commercial Raman probes do not come close to fitting in even the largest penetrometer cones. A slightly modified, lighter weight version of the cone penetrometer Raman probe is the "punch-probe" designed for Raman analysis in waste tanks and drums.

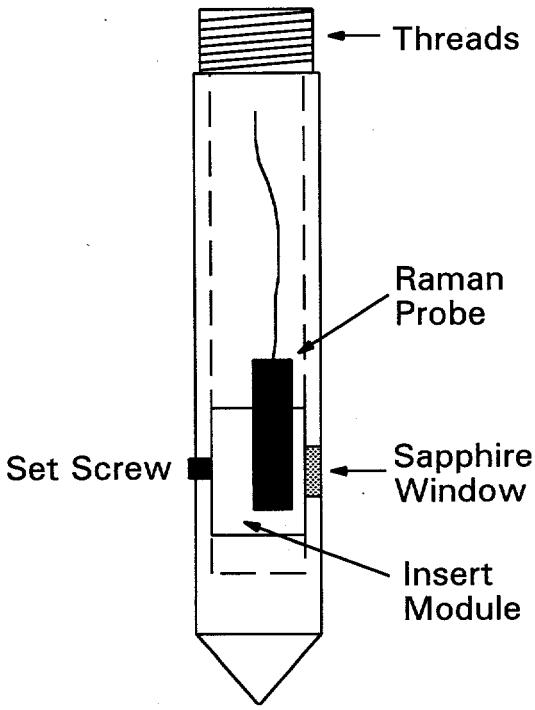

Figure 3. Cone Penetrometer Raman Probe.

A second, "end-viewing" probe designed to be pointed through the side of a bottle in order to identify the bottle's contents has also been assembled. Additional probes designed to profile the contents of Hanford's waste tanks and for other applications are currently under development.

Spectral Library

Qualitative Raman identification of sample components can be achieved by spectral interpretation, but this process is slow and prone to error, particularly when complex sample mixtures are analyzed. Many analysis techniques (e.g., GC/MS and FTIR) now use libraries of standard compounds with sophisticated search and peak matching routines to facilitate analyte identification. We have begun to create a Raman spectral library that includes chemicals of interest to the DOE. To date, a catalog of intensity corrected, wavelength calibrated Raman spectra for over 70 compounds found at DOE sites has been compiled. The bulk of the catalog consists of spectra for chlorinated and light aromatic hydrocarbon solvents found throughout the DOE complex, and inorganic salts found in Hanford's waste tanks.

DOE Applications

Waste Storage Tank Profiling. In order to test the capabilities of the echelle Raman spectrograph for rapidly profiling the contents of waste storage tanks, three simulants representing different tanks and/or chemical processes were obtained from Hanford and analyzed. Strong Raman signals were collected from inorganic species including nitrates, nitrites, sulfates, and cyanides in all three samples in just a few seconds, as shown in Figure 4. It is notable that the spectra are markedly different, clearly demonstrating the ability to detect compositional differences with the Raman technique. In the

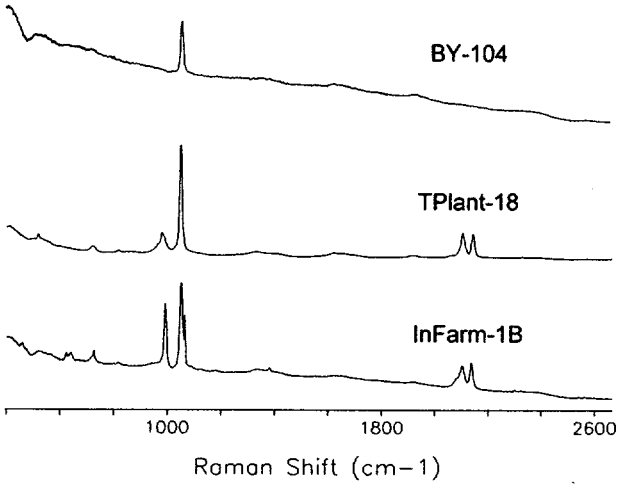

Figure 4. Raman Spectra of Hanford Waste Tank Simulants.

course of analyzing the samples, it also became evident that the high resolution capability of the echelle spectrograph is essential for this application because small spectral shifts were observed for closely related species (e.g., ferricyanides with different cations) or single species at different levels of hydration.

Searching for NAPLs. At many sites the most important goal of initial characterization is to locate and identify a high concentration NAPL pollution source so that immediate action can be taken. The most common NAPLs are Dense NAPLs (DNAPLs) such as trichloroethylene (TCE) and perchloroethylene (PCE) and Light NAPLs (LNAPLs) such as gasoline. Both types are projected to be present, for example, in locations at the Savannah River site (SRS). Figure 5 shows how even similar chlorinated hydrocarbon solvents can be differentiated and identified based on their Raman spectral "fingerprints."

We are exploring the use of the cone pentrometer Raman probe described earlier to identify NAPLs in soil and groundwater (i.e., "floating" on or below the water table). To test feasibility for detecting NAPLs in soil (the more challenging matrix), soils were collected from

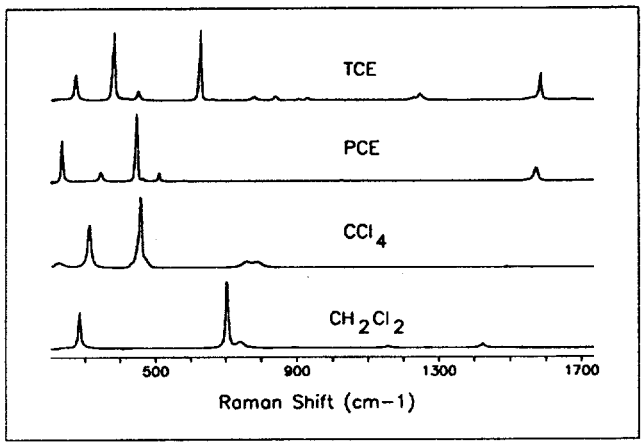

Figure 5. Raman Spectra of Four Common Solvents can be Differentiated Easily.

SRS at depths where PCE DNAPL might be expected to be found and analyzed with the cone penetrometer Raman probe. The samples collected were "clean," but when spiked to saturation, the PCE was detected readily. The spectrum for a 105.2 ft sample is shown in Figure 6.

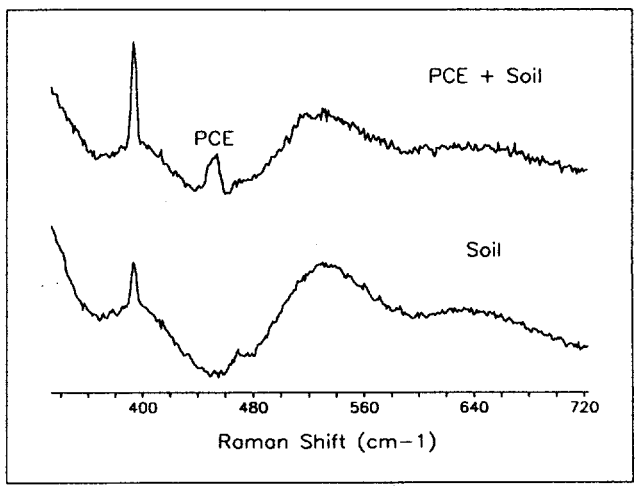

Figure 6. DNAPLs are Detectable in SRS Soil.

Based on the demonstrated feasibility for Raman detection of NAPLs, field testing with a cone penetrometer at SRS is scheduled for the next phase of the project.

PII.15

An Advanced Open-Path Atmospheric Pollution Monitor for Large Areas

L. Taylor (taylor@cis.pgh.wec.com; 412-256-1650)
Westinghouse Science & Technology Center
1310 Beulah Road
Pittsburgh, PA 15235-5098

Need

Large amounts of toxic waste materials, generated in manufacturing fuel for nuclear reactors, are stored in tanks buried over large areas at DOE sites. Flammable and hazardous gases are continually generated by chemical reactions in the waste materials. To prevent explosive concentrations of these gases, the gases are automatically vented to the atmosphere when the pressure exceeds a preset value. Real-time monitoring of the atmosphere above the tanks with automatic alarming is needed to prevent exposing workers to unsafe conditions when venting occurs.

Objectives

This project is to design, develop, and test an atmospheric pollution monitor which can measure concentrations of DOE-specified and EPA-specified hazardous gases over ranges as long as 4 km. A tentative list of the 14 most dangerous DOE analytes is given in Table 1 with their required detection limits. This list was provided in 1994 by the Hanford Research Laboratory and is updated periodically.

Research sponsored by the U. S. Department of Energy's Morgantown Energy Technology Center, under contract DE-AR21-95MC32087 with the Westinghouse STC, 1310 Beulah Rd., Pittsburgh, PA 15235-5098; Telefax: 412-256-1661.

Table 1. Analytes of Concern

Chemical	Detection Limit ppm
Acetone	25.00
Ammonia	2.50
n-Butanol	50.00
Butyronitril	0.80
Dodecane	10.00
Hexanone	0.10
Methylene Chloride	0.05
Nitrogen Dioxide	0.10
Nitrogen Oxide	0.10
Nitrogen Trioxide	0.10
Toluene	5.00
Tributyl Phosphate	0.40
Vinyl Acetate	0.40
Vinylidene Chloride	0.40

Approach

A CO_2 laser (1) to measure absorption spectra in the 9-11 μm region and (2) to determine the distance over which the measurements are made, is combined with an acousto-optic tunable filter (AOTF) to measure thermal emission spectra in the 2-14 μm region.

More explicitly, for long open-path remote sensing and quantitative measurements of atmospheric concentrations of trace vapors, differential-absorption lidar (DIAL) is the best

technique in which the laser is tuned to the absorption peak of a pollutant gas and then to a nearby wavelength at which the pollutant does not absorb. Furthermore, *infrared* DIAL systems are preferred because they are highly sensitive to the laser energy, are relatively "eye safe", and, most importantly, can cover the spectral range where most molecule-specific absorption lines occur, that is, the infrared "fingerprint region" of 8-12 μm.[1] These systems can also measure the distance over which the measurements are made -- without the use of retroreflectors.

However, all laser systems have limited wavelength coverage. Thus, a DIAL system must be complemented with a system which covers a broader range of wavelengths. An AOTF is a good choice for the complementary system because it (1) is easily integrated into a DIAL system, (2) covers a broad wavelength region of 2-14 μm, (3) monitors emission spectra passively, (4) can be quickly tuned to any desired wavelength, (5) has high sensitivity to narrow lines via derivative spectroscopy, (6) does not have moving mechanical parts, and (7) provides complete images which can be used with focal plane array detectors.

Project Description

System Description

The remote monitor, shown in Figure 1, is comprised of seven key elements: a CO_2 laser, a harmonic generator crystal, optics, an AOTF, detectors, a computer, and a gas calibration cell (not shown).[2] The pulsed commercial CO_2 laser has ~60 lines which, due to the laser lines being very narrow, provides high spectral selectivity in the 9.2-10.9 μm region. The laser operates at 10 pulses/s with 1 to 250 mJ/pulse and a 100 ns pulse width.

An optional harmonic generator (not included in the contract) doubles the laser frequency and provides 1 to 15 mJ/pulse for detecting molecules with absorption spectra in the 4.6-5.4 μm region. The harmonic generator would be fabricated from internally grown thallium arsenic selenide (TAS) crystals which have produced the highest efficiency[3] (57%) and the highest laser power[4] (6 W) in the mid-infrared at 4.6 μm . Figure 2 shows a TAS harmonic generator.

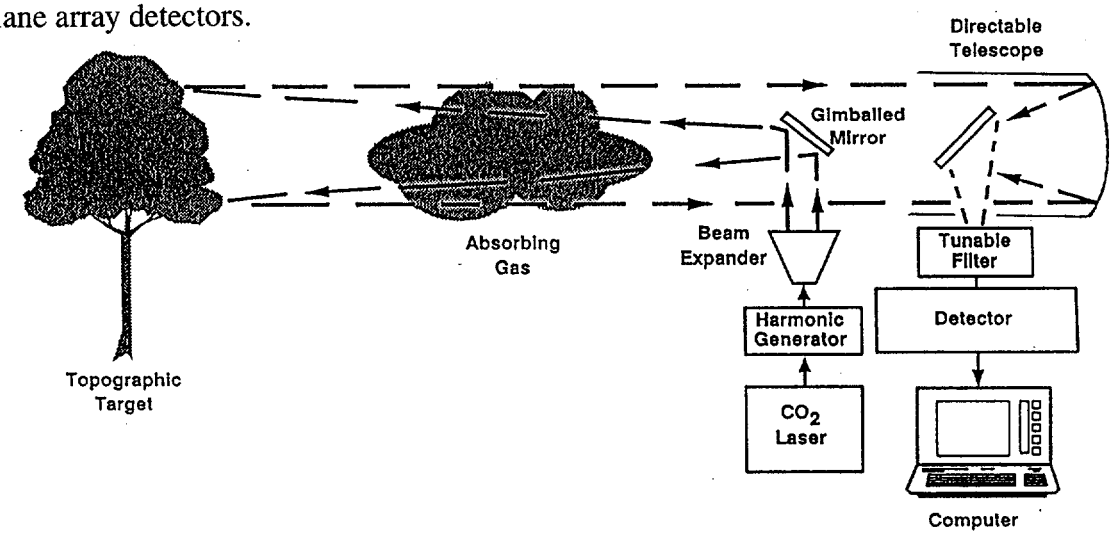

Figure 1 - Basic Configuration of Remote Monitor

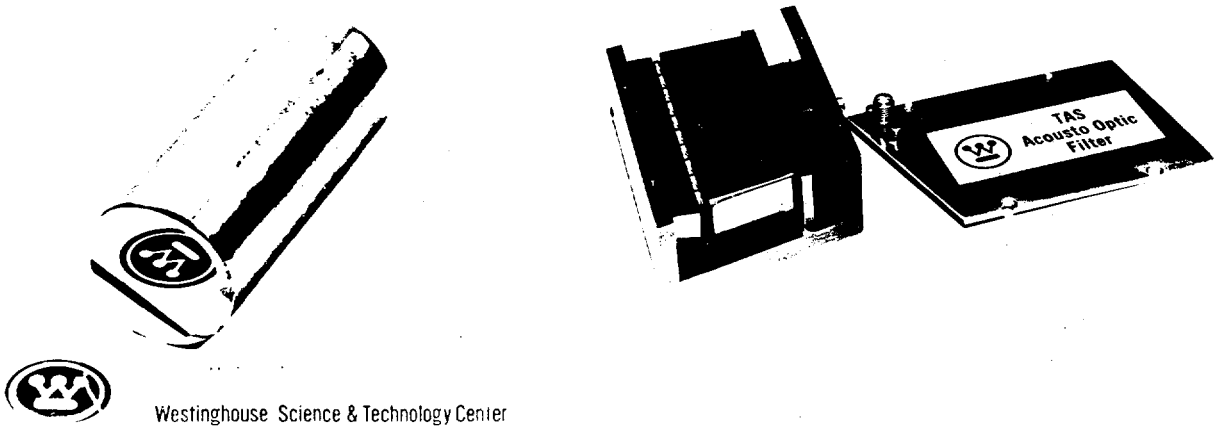

Figure 2 - Harmonic Generator and AOTF are Small Solid-State Components

The 250 mJ/pulse laser energy is sufficiently high that topological objects such as trees or buildings can be used as a back-reflectors, but the laser intensity is sufficiently low, due to the 20 cm diameter output beam diameter, that the laser beam is eye-safe. The use of topological objects is a major convenience in operation and allows fugitive releases to be monitored anywhere within the monitor's operational radius.

The reflected laser beam is collected with a 40 cm diameter mirror. The large mirror diameter reduces the effects of laser speckle. The laser power is pulsed to allow a convenient time-of-flight measurement of the distance to any topological back-reflector. This distance is needed to determine the average concentration of any gas along the optical path.

The received laser beam or thermal emission radiation is focused through the AOTF onto the detectors. The AOTF is fabricated from a TAS crystal, as shown in Figure 2, and operates as shown in Figure 3. The received beam, linearly polarized as indicated by the arrows, enters the crystal and interacts with a periodically varying spatial distribution of indices of refraction set up by an acoustic beam inserted via the transducer. Only a narrow spectral band, ~10 cm^{-1}, will be phase matched to the acoustic beam and diffracted out of the main beam, with its plane of polarization rotated 90° since TAS is a birefringent crystal. The center wavelength of the diffracted beam is uniquely determined by the frequency of the acoustic beam.

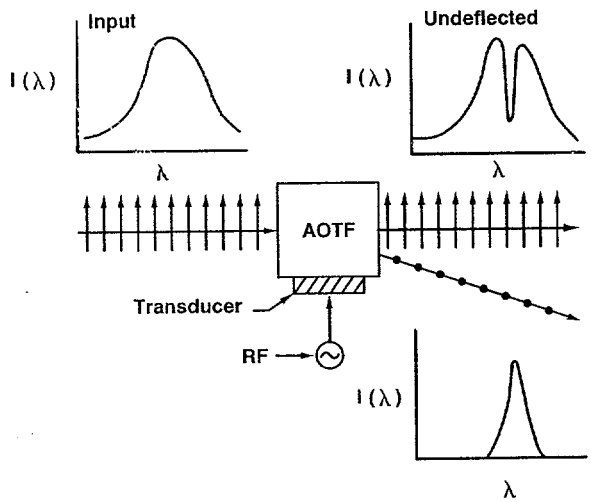

Figure 3 - AOTFs are Electronically Tuned

Two point detectors are used for improved sensitivity. One detector operates from 2 to 6 μm and one operates from 6 to 14 μm. The AOTF directs the received radiation to the two detectors by using one transducer for the 2-6 μm and a second transducer for the 6-14 μm portion. The transducers are placed on different faces of the crystal and diffract the two portions of the beam into two different directions. The detector signals are then analyzed by the computer to obtain path-averaged concentrations from the emission intensity and laser-determined range.

System Operation

The CO_2 laser wavelengths are switched in a predetermined pattern, typically staying on each wavelength for one second. An electronically controlled gimbaled telescope directs the beam to any target in real time. Thus, large areas can be quickly monitored via several beam paths.

The AOTF is computer controlled through the rf drive, thereby allowing the integration time and wavelength selection to be adjusted for optimum detection, either on a continual basis or whenever the need arises. The AOTF has two functions. During absorption measurements the AOTF increases the signal-to-background ratio by restricting radiation from the atmosphere to a narrow spectral range around the laser line. During emission measurements, the AOTF is operated from 2 to 14 μm. By careful selection of the acoustic frequency, the wavelength of the diffracted beam can centered on key emission lines of specific gases, such as shown in Figure 4. These key emission lines can be monitored when absorption measurements are not being taken, and if preset thresholds are exceeded the laser can be activated for more detailed measurements. Alternatively, the entire

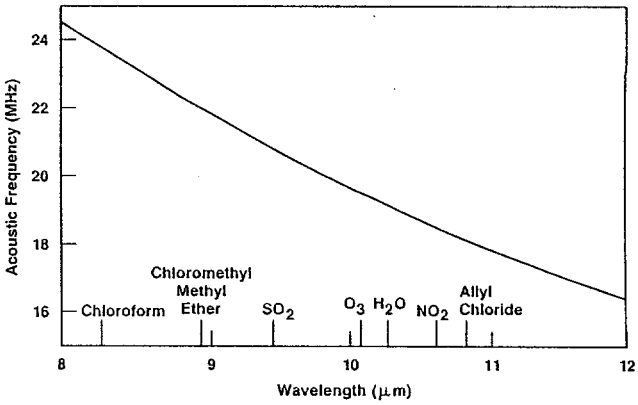

Figure 4 - AOTF Wavelength is Centered on Line by the Acoustic Frequency

wavelength region can be scanned to obtain spectra such as the one for benzene shown in Figure 5.

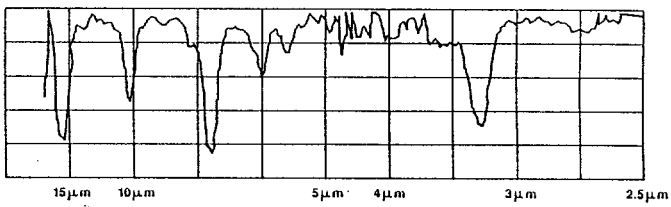

Figure 5 - Benzene Spectrum Generated by Scanning an AOTF

The detectability of sharp emission lines is enhanced by dithering the acoustic frequency at a fixed modulation frequency, ~1 kHz, as shown in Figure 6. This modulation sinusoidally shifts the AOTF passband. The modulation does not affect the radiation from sources which have relatively constant intensities over the AOTF passband, but modulates the intensity from emission lines narrower than the AOTF passband. A lock-in amplifier tuned to the modulation frequency gives the first derivative of the spectra within the AOTF passband. The second derivative is obtained in a similar manner.[5]

The computer calculates concentrations and the range to the reflecting target. It sounds

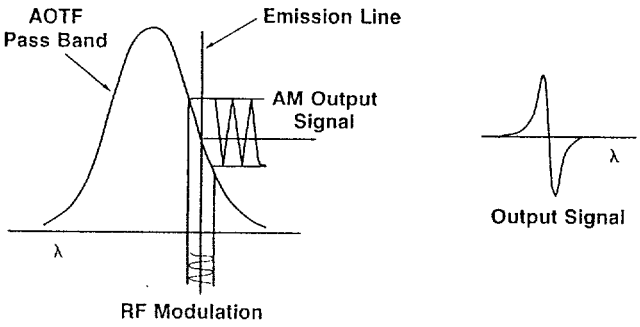

Figure 6 - AOTF Derivative Detection is Very Sensitive to Narrow-Lines

an alarm whenever any preset concentration level of a hazardous gas is exceeded anywhere within a radius of 4 km. It also stores the results, displays the results, controls the operation of the monitor, and periodically inserts, by optical means, the gas calibration cell into the optical path to calibrate both the absorption and emission measurements.

Results

The laser power is sufficiently large that signal-to-noise ratios over 8 km path lengths is not a problem. In this mode of operation the monitor is essentially the same as other CO_2 DIAL systems and has the same sensitivities. In the 9.2-10.9 μm region, computed detection limits vary from 1 ppb for Freon 12 to 60 ppb for ethyl-mercaptan to 340 ppb for sulfur dioxide. In the 4.6-5.4 μm region, computed detection limits vary from 0.3 ppb for carbonyl sulfide to 21 ppb for nitrous oxide to 187 ppb for carbon monoxide.

In measuring emission spectra the large wavelength coverage allows the monitoring of literally hundreds of gases. However, the sensitivity is lower because the emitting gas is at or near the same temperature as the atmosphere which is emitting as a blackbody. Fortunately, many atmospheric vapors have narrow line widths which allows modulation of the AOTF to increase the sensitivity by obtaining first and second derivatives of the spectra. An example of this enhancement is shown in Figure 7 for a laser line with 1% of the spectral radiance of a glow bar in the background. The laser line cannot be seen in direct detection but when the first derivative is taken the laser line is clearly seen.

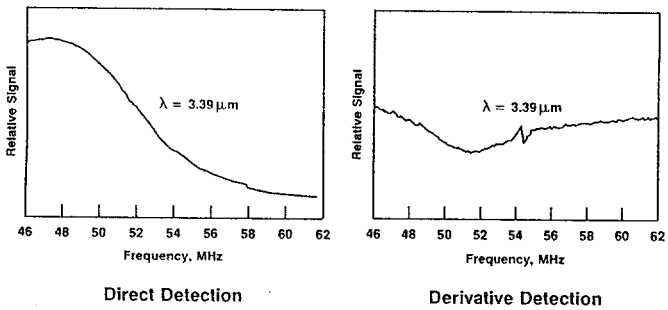

Figure 7 - Measurements of HeNe Laser Line with 1% the Radiance of a Glow Bar

The theoretical sensitivity of the spectral derivative technique can be in the ppb range but is wavelength dependent because of the atmospheric blackbody wavelength dependence. The signal (emission line) to background (atmospheric radiation) ratio is increased, by taking the first derivative, by a factor of 9 at 10.6 μm, by 36 at 5.3 μm, and by 75 at 3.7 μm. The second derivative increases are 68 at 10.6 μm, 1100 at 5.3 μm, and 4700 at 3.7 μm. However, the signal-to-noise ratio decreases with each higher derivative.[5]

Of the fourteen Analytes of Concern in Table 1, the system performance can be estimated for the nine Analytes for which we have spectra. Table 2 contains those estimates for dry air which are presented in the form of ranges between 0.2 km and 20 km over which the Analyte concentration can be measured at the detection limit given in Table 1.

Table 2. Ranges in km over which detection limits in Table 1 can be measured.

Analyte	Absorption		Emission
	Min.	Max.	Min.
Acetone	Cannot Measure		1
Ammonia	2.6	8.7	5
n-Butanol	Too Absorbing		1
Methylene Chlo.	Cannot Measure		80
Nitric Oxide	Interference		2073
Nitrogen Dioxide	7.0	20.	9608
Toulene	0.2	20.	3
Vinyl Acetate	0.2	20	855
Vinylidene Chlo.	0.2	20.	724

The laser absorption mode can measure concentrations for five of the nine Analytes. It cannot measure nitric oxide due to interference from normal atmospheric gases. It could however measure n-Butanol at much lower concentrations but at 50 ppm it completely absorbs the laser beam. Methylene Chloride and Acetone do not have spectra which overlap with any of the laser lines. These results are for a minimum measurable power difference at the detector of 5% and a topological reflector with a reflectivity of 6%.

For the thermal emission performance estimates in Table 2 it is assumed that the atmosphere is at 23 C and the background object is a concrete building at 25 C with an emissivity of 0.92. All nine Analytes can be detected but the shortest detection range, assuming a minimum detectable difference of 3% between the building and the atmosphere, varies widely. However, these results are for a single measurement at a medium temperature difference between the atmosphere and background. Monitor performance would be improved by averaging several measurements and/or by applying derivative spectroscopy.

The example results in Table 2 illustrate how the absorption and emission spectra complement each other. Laser absorption is useful at any time of day or night but is limited in the number of pollutants it can measure. In contrast, thermal emission is useful for all pollutants but it does not measure range and cannot be used at all times or for all ranges; there will always be times or geometries when the background radiance matches that of the intervening atmosphere, thereby rendering measurements impossible.

Benefits

The open-path atmospheric pollution monitor will:

- reduce personnel exposure to harmful gases
- monitor inaccessible or dangerous regions
- reduce monitoring costs for large areas
- be easily setup in any location
- be easily pointed in any direction
- be manually or automatically operated
- be self-calibrating via a calibration gas cell
- be self-contained, except for electrical power

Future Activities

The program is divided into a Base Program plus two options. The 13 month Base Program is to design, build, and bench test the complete pollution monitor within the Westinghouse laboratory. Furthermore, the list of Analytes of Concern will be updated and

absorption spectra will be measured for those Analytes which do not have digitized absorption spectra. The five month Option I is to support independent testing, under carefully controlled conditions, of the monitor at METC to determine the full range of its performance capabilities. The six month Option II is to support open-path atmospheric testing at the Hanford National Laboratory to determine atmospheric effects on system performance. Commercialization activities for this monitor will proceed in parallel with the options.

Acknowledgments

The METC COR is Darren Mollot for this two-year EM-50 contract.

References

1. D. K. Killinger and N. Menyuk, "Remote Probing of the Atmosphere Using a CO_2 DIAL System," IEEE J. Quantum Electron. QE-17: 1917-1929 (1981).

2. L. H. Taylor, "A New Concept for Open Path Air Pollution Monitoring," Proc. Measurement of Toxic & Related Air Pollutants, 563-568 (1993).

3. D. R. Suhre, "Efficient Second Harmonic Generation in Tl_3AsSe_3 Using Focussed CO_2 Laser Radiation," J. Appl. Phys. B52: 367-370 (1991).

4. D. R. Suhre and L. H. Taylor (unpublished results).

5. M. Gottlieb, "Acousto-Optic Tunable Filters," Chap. 5, 197-284, Design and Fabrication of Acousto-Optic Devices, A. P Goutzoulis and D. R. Pape, Eds., Marcel-Dekker, New York (1994).

PII.16

Nitrate to Ammonia Ceramic (NAC) Bench Scale Stabilization Study

W. Jon Caime (803-646-2413)
Steve L. Hoeffner (803-646-2413)
RUST - Clemson Technical Center
Clemson Research Park
100 Technology Drive
Anderson, SC 29625

Introduction

Department of Energy (DOE) sites such as the Hanford site, Idaho National Engineering Laboratory (INEL), Savannah River site, Oak Ridge National Laboratory (ORNL) have large quantities of sodium-nitrate based liquid wastes. At INEL alone there are 800,000 gallons. The largest quantity of these wastes is the 149 single shell tanks (SSTs) tanks at Hanford which can hold 1 million gallons each.

Problem

Stabilization of this waste is difficult because nitrates are very mobile. Additionally vitrification of these wastes produces large quantities of hard to manage NO_X emissions.

A process called the Nitrate to Ammonia Ceramic (NAC) has been developed at ORNL, by A.J. Mattus, to remove a majority of the nitrate content from wastes such as these. In the NAC process solid aluminum at low temperatures (50-80°C) and low energy, reduces nitrate to ammonia, and a solid aluminum oxide material is formed. The process destroys the nitrates.

In the initial development of the NAC process the aluminum reduces the nitrates to ammonia. A raw product is formed which is then calcined at 600-800°C. This product is then uniaxially pressed at 10,000 psi and sintered in the range of 1300-1400°C to form a ceramic like product.

To take the raw product to the ceramic stage requires significant energy to heat the waste to a high temperature. At these high temperatures, volatile radionuclides may be released, creating additional containment problems. In addition a large scale ceramic process capable of handling the large quantity of raw product is currently not available.

Solution

Because of these concerns and issues, alternative ways to form a solid non-leachable product are desired. As detailed below, RUST-Clemson Technical Center, is investigating other stabilization options for the raw sludge produced from the NAC process. Results will indicate which of the stabilization hosts can be used to stabilize the raw NAC material.

Research sponsored by the U.S. Department of Energy's Morgantown Energy Technology Center, under contract DE-AR21-95MC32113 with RUST-Clemson Technical Center, Clemson Research Park, 100 Technology Drive, Anderson, SC; telefax: 803-646-5311.

Technology Description

The NAC solid product will be produced using a nitrate solution spiked with 8 RCRA metals (As, Ba, Cd, Cr, Pb, Hg, Se, & Ag) and 3 semi-volatile organics (2,4-Dinitrotoluene, 2,4,6-Trichlorophenol, and Nitrobenzene). Rather than taking this product to the ceramic stage, four low temperature stabilization hosts will be examined. Each of the stabilization hosts selected have been previously considered and/or used for stabilization of radioactive and/or hazardous wastes.

The process layout for this treatability study is shown in **Figure 1**. A waste product (NAC sludge) was produced by adding powdered aluminum into the RCRA contaminated nitrate solution. Reaction temperature was maintained at 50-80°C. The raw product produced was filtered and then dried to a powdery consistency. This raw product will be stabilized as detailed in the following paragraphs.

A waste loading of 55-75% will be investigated for portland cement/flyash stabilization. This well established stabilization technology chemically fixates RCRA constituents.

The second stabilization host, sulfur polymer cement (SPC) is an encapsulation process. The waste loading to be investigated will be 35-90%.

Vinyl ester styrene is also an encapsulation process. Waste loadings for this host will be 35-90%.

The fourth stabilization host is high alumina cement. $Ca(OH)_2$ will be combined with the NAC slurry (which is high in alumina) at approximately 70% waste loading, to create a stabilized waste form. If problems occur with flash set, a retarder may be utilized. Other options may have to be pursued to overcome flash set problems.

Initial screening tests will be conducted to determine the waste loadings for each stabilization host. Screening formulations will be evaluated based on visual observations of mixing ability, 24 hour load bearing strength and evaluation of stabilization performance using a quick leach with leachate screened for RCRA constituents.

Once the waste loadings have been determined, performance comparisons for each stabilization host will be based on leachability and compressive strength. Each waste form will be subjected to a TCLP analysis of 8 RCRA metals and three semi-volatile organics. Leachability of sodium from the stabilized products will be tested by ANSI 16.1 method (abbreviated test). The unconfined compressive strength will also be determined for each host.

Application

The NAC process can utilize the large existing inventory of scrap aluminum at DOE facilities. Some of this aluminum has been irradiated and the NAC process offers a economical disposal option for this waste. This process can be used to treat the large amount of tank wastes at DOE facilities.

Utilizing the NAC process, a problematic waste stream constituent (sodium nitrate) can be decomposed to an innocuous gas (ammonia). The residual product can then be incorporated into a stabilized waste form for disposal.

Future Activities

The treatability study utilizing the four stabilization hosts is currently being conducted. Further studies in this area may be warranted.

Acknowledgements

The Clemson Technical Center acknowledges the work Al Mattus inventor of the NAC process and consultant on this work. We also acknowledge the work of the METC Contracting Officer's Representative (COR), Jim Poston, period of contract performance 5/23/95-3/23/96.

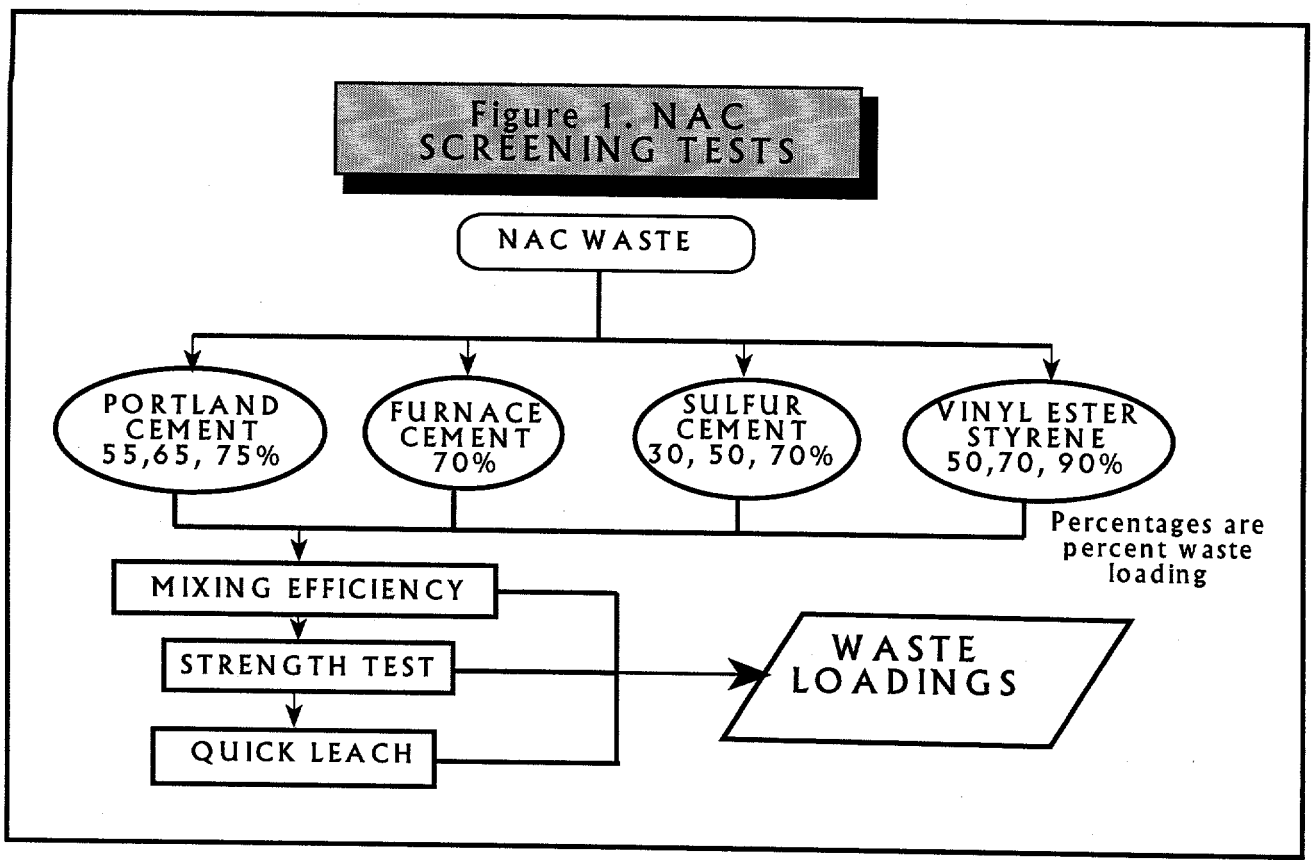

Session 4

Contamination Plume Containment and Remediation, and Landfill Stabilization Focus Areas

4.1 Field Portable Detection of VOCs Using a SAW/GC System

Edward J. Staples, 805-495-9388; FAX 805-495-1550
Amerasia Technology, Inc.
2301 Townsgate Road
Westlake Village, CA 91361

Introduction

This paper describes research on a fast GC vapor analysis system which uses a new type of Surface Acoustic Wave detector technology to characterize organic contamination in soil and groundwater. The project was sponsored by the Department of Energy, Morgantown Energy Technology Center.

Project Objectives

The research objectives were to demonstrate detectability and specificity of a Surface Acoustic Wave Gas Chromatograph (SAW/GC) to a representative number of VOC materials followed by field demonstrations of the new technology at a DOE site. Field testing of the SAW/GC was performed at the DOE Savannah River Site. The performance of the SAW/GC analyzer was validated by comparing results taken with an on-site HP chromatograph. Tests were performed with water, soil and gas samples. By these tests, the SAW based analyzer's ability to identify and quantify the presence of VOCs was to be demonstrated.

Technology Description

The basic structure of a SAW/GC is shown in Figure 1. The system utilizes a two position, 6 port GC valve to switch between sampling and injection modes. In the sample position environmental air is passed through an inlet preconcentrator or water trap and then through a sample loop trap. The function of the loop trap is to concentrate VOC materials when into the sample position. During sampling helium carrier gas

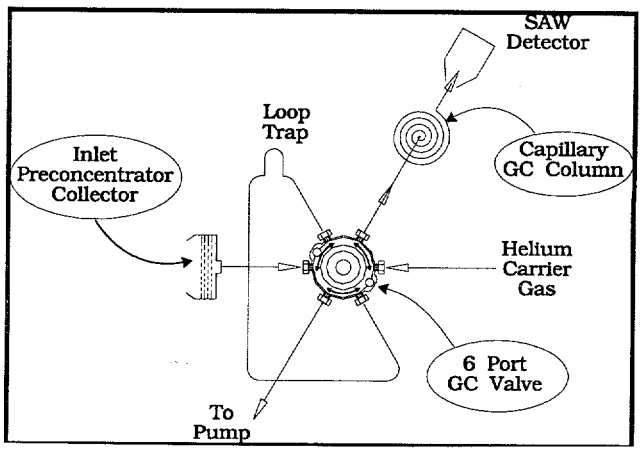

Figure 1. SAW/GC System Description

flows down a capillary column and impinges onto the surface of a temperature controlled SAW resonator crystal[1] as shown in Figure 2.

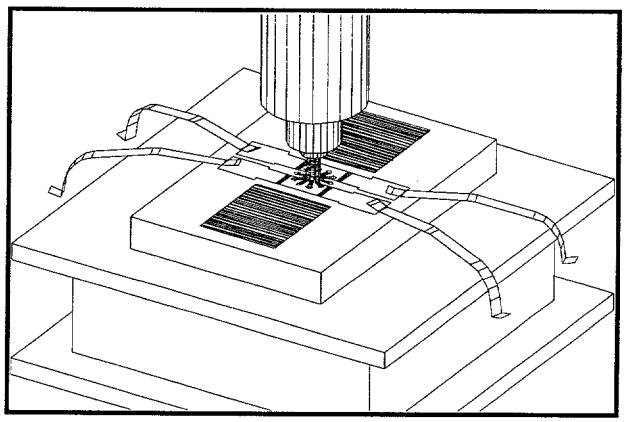

Figure 2. Surface Acoustic Wave GC Detector

[1] United States Patent No. 5,289,715, Vapor Detection Apparatus and Method Using an Acoustic Interferometer.

Research sponsored by the U.S. Dept. of Energy's Morgantown Energy Technology Center, under contract DE-AR21-94MC31177 with Amerasia Technology, Inc., 2301 Townsgate Rd., Westlake Village, CA 91361; telefax: 805-495-1550.

Switching the valve to the inject position causes helium carrier gas to flow backwards through the loop trap and onto the column. After the valve is switched into the inject position the loop trap is rapidly heated to 200°C causing the trapped VOC materials to be released into the GC column. The temperature of the GC column is linearly raised to approximately 125°C over a 5-10 second time and this causes the VOC materials to travel down the column and exit at a time characteristic of the VOC material.

The SAW resonator is a unique type of GC detector. VOC materials as they exit the GC column are trapped on the surface of the resonator and causes a change in the characteristic frequency of the crystal. The adsorption efficiency of each VOC material is a function of the crystal temperature and by operating the crystal at different temperatures the crystal can be made specific to materials based upon the materials vapor pressure. Also, since the crystal acts as a micro-balance it integrates the total amount of material present and to obtain a conventional chromatogram plot of retention time, the derivative of frequency Vs time is calculated. This is in contrast to a conventional GC detector which detects the flux and peak integral calculations are required to obtain the amount of each material present.

Results and Accomplishments

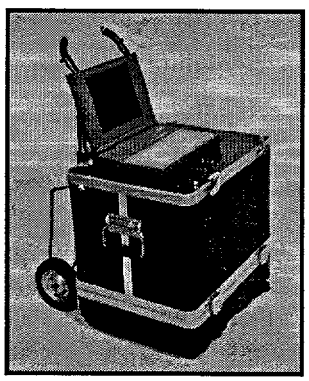

Figure 3. Portable Laboratory SAW/GC

To demonstrate the technology a portable laboratory scale instrument shown in Figure 3 was constructed and tested with the representative VOC materials listed in Table 1.

Table 1. VOC Materials Tested

Material Name	Formula
Trichloroethylene	C_2HCl_3
Tetrachloroethylene	C_2Cl_4
Carbon Tetrachloride	CCl_4
Chloroform	$ChCl_3$
Dichloromethane	CH_2Cl_2
1,2-Dichloroethane	$C_2H_4Cl_2$
1,1,1-Trichloroethane	CH_3CCl_3
1,1-Dichloroethylene	C_2H2Cl_2
1,1,2,2-Tetrachloroethane	$C_2H_2Cl_4$
Trichlorofluoromethane	CCl_3F
Benzene	C_6H_6
Toluene	C_7H_8
Gasoline	--
Diesel Fuel	--

Each material was tested with a calibrated vapor source either purchased as bottled gas or created by injection into a known volume (tedlar bag). Calibration results based upon a 10 second sample are listed in Table 2. In general the sensitivity of the instrument for all materials

Table 2. Representative Calibration Results

VOC Material	Test Concentration (ppm)	Detected Amplitude (Hz)	Detection Limit (ppm)	Scale Factor (Hz/ppm/cc)
Dichloromethane	133	678	5.88	0.45
Chloroform	37	63	17.62	0.15
1,2-Dichloroethane	45	144	9.38	0.28
Trichloroethylene	10	383	0.78	3.4
Toluene	2.4	272	0.26	10.1
Tetrachloroethylene	1.6	517	0.09	28.7

was 1 ppm or better. For materials with lower vapor pressure, such as toluene and tetrachloroethylene, sensitivity extends well into the ppb range. To achieve ppt sensitivity it is only necessary to extended sample time. However, the advantage of a short sample times is near real time operation.

Field Test Results

To field test the laboratory prototype the instrument was transported to Savannah River where it was used to obtain real time measurements of well head gases. Although the instrument was capable of battery operation for limited periods of time, uninterrupted power was most reliably obtained from the automobile which was used to transport the system to each well head as shown in Figure 5.

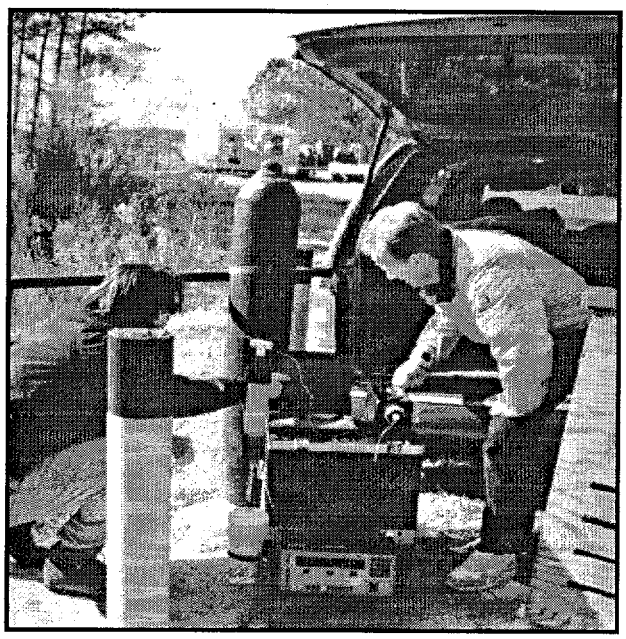

Figure 5. Field Testing SAW/GC at DOE Savannah River Site

To verify the accuracy of the instrument, calibrated tedlar bag samples were used to calibrate the SAW/GC. A typical output screen for one such bag containing approximately 100 ppm TCE and PCE is shown in Figure 4. The user interface shows two chromatograms, one is the derivative of SAW frequency and the other is SAW frequency vs time. The duration of the chromatogram is 10 seconds and retention times for TCE and PCE is 3.54 and 5.54 respectively. The operator can display quatitative information as ppm/ppb, in mass units of picograms or nanograms, or alternately in SAW units of frequency.

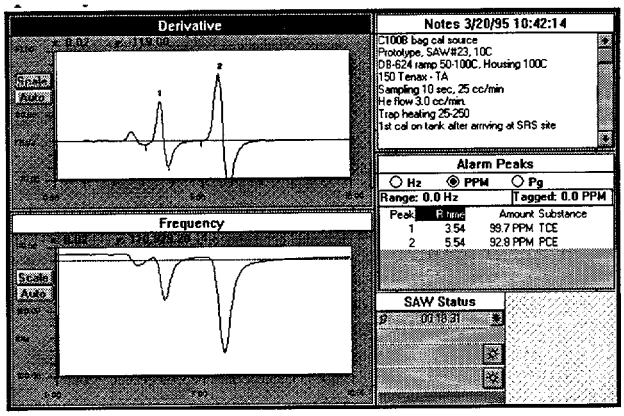

Figure 4. Typical Screen Display Showing PCE (92.8 ppm) and TCE (99.7 ppm) Tedlar Bag Calibration Results

Many different measurements were taken and compared with an on-site HP GC as shown in Figure 6. The results of this relative comparison indicate that the SAW/GC and the HP GC agree within approximately 20%. Much of the variation is attributed to variations in sampling and preconcentration within each instrument.

Application or Benefits

There are many related applications for SAW/GC technology. While at Savannah River the instrument was also used to measure catalytic converter performance, DNAPL probe experiments, and to characterize VOC break through in carbon scrubbers.

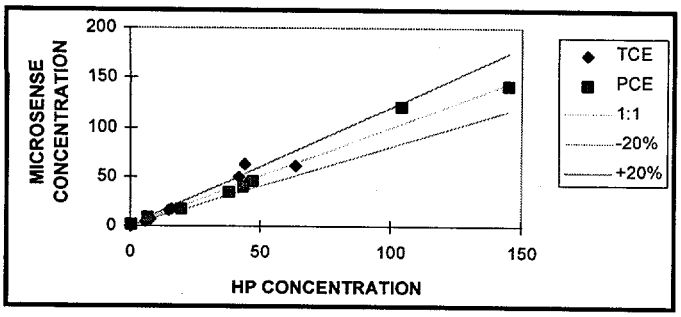

Figure 6. Cross Check of System Accuracy Using HP Laboratory Style GC

The advantages of the SAW/GC are portability, accuracy, and speed. The new SAW sensor demonstrated sufficient specificity and sensitivity to be used as a fast trace analyzer or screening tool at DOE remediation sites. Using the SAW/GC analyzer as a field screening tool, cost savings over current techniques, which require expensive laboratory testing, are estimated to be more than $50,000 per month. We conclude that the cost of the SAW/GC screening instrument will be recovered within less than one month of operation.

Future Plans

Based upon the current results the goals are to begin development of SAW/GC screening instruments for use at DOE remediation sites. The commercialization effort is being carried out by Electronic Sensor Technology, Inc., a limited partnership company managed by Amerasia Technology and tasked with the development of SAW/GC instruments.

The commercialization effort is being aided by a partnership between Amerasia Technology, Inc., and the Morgantown Energy Technology Center. This new program will involve continued field testing at DOE sites, EPA certification and verification, and the development of new SAW/GC instruments to detect and quantify Dioxins, Furans, and PCBs at DOE sites.

Acknowledgements

We wish to thank Mr. Eddie Christy, our METC Contracting Officer, for excellent support and supervision. Work in this project was supported by the U.S. Department of Energy's Morgantown Energy Technology Center, under contract DE-AR21-94MC31177, which covered the period June 1994 to March 1995.

Also we wish to express our appreciation to Dr. Joe Rosabbi, Westinghouse Savannah River Co., for his support and encouragement during field testing at the Savannah River Site.

4.2

Field-Usable Portable Analyzer for Chlorinated Organic Compounds

William J. Buttner (wbuttner@interaccess.com; 708-357-0004)
William R. Penrose (wpenrose@interaccess.com; 708-357-0004)
Joseph R. Stetter (jstetter@interaccess.com; 708-357-0004)
Transducer Research, Inc.
999 Chicago Avenue
Naperville, Illinois 60540

INTRODUCTION

Transducer Research, Inc. (TRI) has been working with the DOE Morgantown Energy Technology Center to develop a new chemical monitor based on a unique sensor which responds selectively to vapors of chlorinated solvents. We are also developing field applications for the monitor in actual DOE cleanup operations. During the initial phase, prototype instruments were built and field tested. Because of the high degree of selectivity that is obtained, no response was observed with common hydrocarbon organic compounds such as BTX (benzene, toluene, xylene) or POLs (petroleum, oil, lubricants), and in fact, no non-halogen-containing chemical has been identified which induces a measurable response. By the end of the Phase I effort, a finished instrument system was developed and test marketed. This instrument, called the RCL MONITOR (Figure 1), was designed to analyze individual samples or monitor an area with automated repetitive analyses. Vapor levels between 0 and 500 ppm can be determined in 90 s with a lower detection limit of 0.2 ppm using the hand-portable instrument. In addition to the development of the RCL MONITOR, advanced sampler systems are being developed to: (1) extend the dynamic range of the instrument through autodilution of the vapor and (2) allow chemical analyses to be performed on aqueous samples. When interfaced to the samplers, the RCL MONITOR is capable of measuring chlorinated solvent contamination in the vapor phase up to 5000 ppm and in water and other condensed media from 10 to over 10,000 ppb(wt)--without hydrocarbon and other organic interferences.

OBJECTIVES

Chlorinated solvents, such as carbon tetrachloride or trichloroethylene, were extensively used as degreasing agents in industrial operations. Because of past handling, storage, and disposal procedures, environmental contamination occurred at many of these sites. Chlorinated solvent contamination of soil and ground water is recognized as a major hazardous waste problem at numerous government and private installations (OTA, 1991). There are extensive

Support provided by the Environmental Management Office of Technology Development through Morgantown Energy Technology Center under DOE Contract: DE-AC21-92MC29118 with Transducer Research, Incorporate, 999 Chicago Avenue, Naperville, Illinois 60540 (telefax: 708/357-1055)

ongoing environmental restoration programs for the removal of subsurface RCL contamination. During the remediation process, from site characterization to closure, chemical monitoring is necessary to assure worker safety, locate contaminants, verify environmental compliance of emissions, and track the actual cleanup process. Until recently, the only available technology to selectively analyze for chlorinated organics was a gas chromatograph (GC) equipped with electron capture detector or mass spectrometer detector. In addition to being expensive, gas chromatography requires grab samples and does not provide real-time answers. The shortcomings of laboratory methods have been recognized for certain applications that demand quick response or analyses on large numbers of samples. Field analytical methods (FAMs) are being developed as attractive and cost-effective alternatives (Carpenter et al., 1994). The first step in the development of FAMs is the availability of field-usable instrumentation and the heart of any field instrument is the detector.

APPROACH

A solid state chemical sensor has been developed which exhibits a high degree of chemical selectivity in detecting vapors of chlorinated organic solvents. While the sensor does exhibit a small response to brominated organic compounds, and an even smaller response to iodine and fluorine compounds, it responds quickly, reversibly, and with high sensitivity to vapors of chlorine compounds (Stetter and Cao, 1993). To date, no non-halogen-containing chemical has been identified which induces a measurable response on this device. Using the organic chemist's shorthand notation "R-Cl" for an unspecified chlorine-containing organic molecule, this sensor was named the "RCL" sensor. To exploit its analytical potential, an advanced chemical monitor was designed, built, and field tested using the RCL sensor as the detector system. A two-phase program was developed with support from METC. In the initial phase, an instrument system (the RCL MONITOR and specialized samplers) was developed and field tested. Specifications for the RCL MONITOR are presented in Table I. Independent cost analysis demonstrated that significant cost saving can be achieved with the RCL MONITOR for many applications (Energetics, 1993). At the conclusion of the Phase I effort, specific applications were identified which would benefit from the RCL technology:

- Environmental Compliance
- Health and Safety
- Process Monitor (Vacuum Extraction)
- Environmental Modeling
- Site Characterization

Case studies using the RCL MONITOR are currently underway as part of the Phase II effort. Details on the Phase I development and performance of the RCL MONITOR were presented elsewhere (Buttner et al., 1995).

PROJECT DESCRIPTION

The general theme for the current activity is technology deployment and method development. To accomplish this, several EM40 operations were identified that would benefit from the selective detection and quantitation afforded by the RCL MONITOR. Case studies are currently underway at DOE Hanford, Savannah River Laboratory (SRL) and the Idaho National Engineering Laboratory (INEL), and represent specific Phase II tasks. The selected operations are representative of activities

throughout DOE. Specifically, in the Phase II program, the RCL MONITOR was deployed and evaluated in the following EM40 activity:

- Routine Quarterly Monitoring (INEL)
- Health and Safety Applications (Hanford)
- Vapor Extraction System (Hanford)
- Environmental Modeling Studies (Hanford)
- Environmental Technology Demonstration (SRL)

The deployment plan includes use of the RCL MONITOR for the specific operation, interaction with the cognizant regulator (including Project Manager, State Environmental Officers, and local DOE Officers), and assessment of benefits. To facilitate deployment, TRI has developed a formal training class on operation of the RCL MONITOR

RESULTS

Routine Quarterly Monitoring (INEL)

The Routine Quarterly Monitoring (RQM) consists of quarterly groundwater and vapor sampling and analysis for chlorinated organic contamination in wells surrounding the Radioactive Waste Management Complex within the INEL site, and is an ideal example of the discrete sampling protocol. Samples are obtained from vapor ports and analyzed using a remote on-site gas chromatograph to determine the total concentration of chlorinated organic constituents. Groundwater samples are collected and sent off-site to an analytical laboratory. The RQM requires the collection and analyses of 66 vapors samples from 21 wells and six water samples from six wells. The wells are sampled to characterize the distribution of organic contaminants in the saturated and vadose zones. Original protocols required the collection, transport, and remote analyses of all samples by gas chromatography. Approximately two man-weeks of effort were required for the vapor analyses, and an additional one to two man-weeks for the water samples. Being performed four times annually, this was a labor-intensive exercise which ties up trained personnel. The RCL MONITOR was deployed as an auxiliary analytical tool for the vapor portion of the RQM in June of 1994. Excellent agreement was obtained between the two methods. Because of this agreement, the RCL MONITOR is now being used as the baseline technology for the vapor portion of the RQM. Since samples no longer need to be transported to a remote laboratory for analysis, a significant time and cost saving is achieved with using the RCL MONITOR. The vapor analyses can completed in less than 2.5 days, compared to the 2 man-weeks normally required. A cost analysis, presented in Table II, summarizes the expected savings.

The condensed phase sampler was used on the water samples collected from the six wells, but no contamination was detected. Independent analyses indicate that the total chlorinated solvent contamination is low, typically less than 5 ppb_{wt}. This concentration is below the LDL of the sampler/RCL MONITOR instrument system. Methods to improve the condensed phase sampler, as well as alternative methods of water analysis (W. Buttner, 1995) are currently underway.

Health and Safety (Hanford)

Assurance of Health and Safety for site workers is probably the most important application for vapor monitoring technology and illustrates the need for real-time measurements better than any other application. Two basic applications are being developed--continuous breathing zone monitoring and discrete survey measurements (spot checks). During a four

month period, nearly 100 H&S related spot-check analyses were performed with the RCL MONITOR. Table III summarizes some these measurements. These measurements provided invaluable support to ongoing Hanford clean-up activity.

It is recognized that spot checks will not satisfy those applications requiring real-time monitoring. In many circumstances, continuous monitoring is necessary, and such capability does exist for the RCL MONITOR. Figure 2 depicts measurements performed over a one week period at the PURUS[1] facility. Analyses were performed at 15 min. intervals. This deployment supported the evaluation of a developing remediation technology being tested in an enclosed quonset tent within the 200W area of Hanford over a four month period. Vapor levels were found to range from 0 to nearly 20 ppm, with the higher levels occurring overnight during unattended operation. There was not a single failure during the four month deployment.

Vapor Extraction System (Hanford)

Between 363,000 and 580,000 L of carbon tetrachloride were discharged in three locations within DOE Hanford. As part of the Accelerated Cleanup Activities (the Carbon Tetrachloride Site Expedited Response Activity), vacuum extraction systems have been installed in the 200W area to remove the volatile chlorinated solvents. With the vacuum extraction systems, vapors are extracted from subsurface through a high-powered vacuum system. To prevent atmospheric pollution, it is necessary that exhaust be filtered through an array of three chemical filter stacks containing granulated activated carbon (GACs) in series. Most vapor is scrubbed by the first GAC, while the second and third provide backup. The RCL MONITOR was installed to monitor the air stream passing through the primary GAC. In this configuration, likely vapor levels would range between 5 and 2000 ppm. Although outside the range of the RCL MONITOR, a custom interface system was built and deployed which extended the range of the instrument; details on this sampling system were presented earlier (Penrose et al., 1995). Although a separate interface system was built, its operation could, in principle, be performed by the RCL MONITOR. Data was collected over a 5 month period. During this time, the RCL MONITOR was operated for a week between downloading the data and validating performance. Representative results are provided in Figure 3. During the deployment of the RCL MONITOR, vapor excursions could be directly correlated to event on the VES, such as GAC breakthrough, system shut downs, and diurnal variations. Overall, we had a success rate of only 65%, where a failure is defined as loss of part or a weekly data set, but for the last half of operation, the success rate increased to over 80%. The major modes of failure were due to the sensor and to external causes (e.g., power shut down, lightning strikes). In a final assessment, we discontinued this activity at Hanford because it is unlikely that the RCL MONITOR would be adopted for this application at this site. Nevertheless, we demonstrated that the RCL MONITOR can operate as a Process Monitor or Process Controller.

Environmental Modelling Studies (Hanford)

Geological and geophysical modelling studies are ongoing at Hanford and other DOE sites to support the active cleanup technologies, such as the VES. One promising technology is the passive venting of VOCs, in which vapor

[1]The PURUS system vacuum extract soil vapor and condenses it to the liquid state.

excursions are induced by transient barometric pressure changes. Pressure changes drive air in and out of soils, and that this is facilitated by wells. During periods of decreasing pressure, the vapor levels in outgassing of wells increase dramatically. What is not known is the overall efficiency of the process; this requires measurement of both vapor levels and flow rates over long time periods. While passive venting may not replace active cleanup methodologies, it is viewed as a potential cost-effective complement (Rohay et al, 1994). With METC support, TRI provided RCL MONITORS to Hanford geologists to track vapor excursions. These experiments are ongoing, and expected to continue through to the end of the Phase II effort. Data for a one month period is illustrated in Figure 4. Current activity is ongoing to evaluate method to enhance this process, notably the use of one-way valves to prevent air uptake by the soil.

Environmental Technology Demonstration (SRL)

The Environmental Technology Demonstration (ETD) program was set up to support DOE clean up operations by providing assessments, demonstrations, and training sessions on new and emerging technologies. TRI provided an RCL MONITOR and gas samplers/diluters for use in this demonstration. A second monitor was provided to support necessary H&S activity around wells. Numerous technologies were evaluated, including vapor analyzers (the TRI RCL MONITOR, Quantum FTIR, and the B&K 1302) along with other hardware (e.g., drilling rigs, penetrometers, and sensors). During the assessment, a "Sniff-Off" was performed to compare technologies. These are listed in Table IV. The RCL MONITOR provide true portable analytical capability, and provided quick measurements. Initially, all technologies provided comparable results, but it must be reported that the sensor failed during the evaluation and the instrument would no longer validate.

BENEFITS

The RCL MONITOR provides cost-effective analytical capability not found in any other truly portable instrument system. It is a powerful tool for the on-site determination of chlorinated solvent vapors. A range of 0 to 500 ppm was achieved (5000 ppm with the fixed external 10:1 diluter) and a LDL of 0.2 ppm was achieved. Direct analysis of water samples was possible with the condensed phase sampler. Performance of the instrument for vapor and condensed phase analyses compared favorably with CLP methods now in use. Independent cost analysis demonstrated that significant cost saving can be achieved with the RCL MONITOR for many applications.

The instrumentation is simple to use. Field personnel can be trained in less than five minutes to operate the instrument (a full training sessions requires about 2 hours). Real time data collection, heretofore not possible, on the temporal and spacial characteristics of chlorinated vapor emissions has been obtained. The application of this instrumentation and the development of validated methods should provide for improved field operations, better worker safety, and significant cost savings in hazardous waste management operations.

FUTURE ACTIVITIES

The RCL MONITOR has been formally accepted for at least one application, namely the Routine Quarterly Monitoring, and has been informally adopted by some groups for H&S and

research applications. Continuous monitoring activity was achieved with the instrument, with some reservations about reliability of the sensor over very long-term measurements. An extensive effort is underway to improve sensor performance.

ACKNOWLEDGEMENTS

The assistance and support provided by the Office of Technology Development of EM50; Curtis Nakaishi, the project Contracting Officer Representative (COR) from September 1992 to September 1994; C. Edward Christy, the COR from October 1994 to June 1995; and Rodney Geisbrecht the present COR is acknowledged. The authors also acknowledge the assistance and support provided by our colleagues and collaborators working on EM40 operations at the laboratories including Dr. Kirk Dooley and Scott Barrie of the Lockheed Idaho Technologies Company (LITCO) at the Idaho National Engineering Laboratory; Joseph Rossabi of the Westinghouse Savannah River Company; Virginia Rohay, Jon Fancher, Bruce Tuttle, Randy Coffman, and John Fisler of DOE Hanford. A special thanks is given to Cary Martin and Torry Webb, Nuclear Fuel Systems, Richland, WA.

REFERENCES

Buttner, W.J. "In-Situ Sampling of Aqueous-Phase Contamination by Chlorinated Solvents", Lockheed Idaho Technology Company (LITCO) Contract #: C95-175582.

Buttner, W.J. and Williams, R.D. "Field-Usable Portable Analyzer for Chlorinated Organic Compounds" Phase I Topical Report, Morgantown Energy Technology Center, in press (1995).

Carpenter, S.; Doskey, P.; Erickson, M.; and Lindahl, P. (1994) "Performance Specifications for Technology Development: Application for Characterization of Volatile Organic Compounds in the Environment" Argonne National Laboratory (DOE) Report ANL/ER/TM-3 (1994).

Energetics, Inc. and Morgantown Energy Technology Center (1993) "Evaluation of the Cost and Benefit of the Rare Earth Semiconductor Technology for Field Detection of Chlorinated Hydrocarbons" prepared through DOE Contract No. DE-AC-21-92MC29231, in press.

U.S. Congress, Office of Technology Assessment (1991), "Complex Cleanup: The environmental Legacy of Nuclear Weapons Production", OTD- 404 (Washington, DC: U.S. Government Printing Office, February).

Penrose, W.R.; Buttner, W.J.; Vickers, W.C.; Rohay, V.J.; Fancher, J.D.; and Martin, C. "Continuous Monitoring of Carbon Tetra-chloride During Passive and Active Vapor Extraction of Contaminated Areas", to published in the Proceedings of the ER'95 Conference on Environmental Restoration, DOE, Denver, CO (April 1995).

Rohay, V.J.; Rossabi, J; Looney, B.; Cameron, R.; and Peters, B., (1993) "Well Venting and Application of Passive Soil Vapor Extraction at Hanford and Savannah River", to be published in the Proceedings of the ER'93 Conference on Environmental Restoration, DOE, Augusta GA (Oct. 24-28).

Stetter, J.R and Cao, Z. (1993) "Halogenated Compounds Sensor" U.S. Patent 5,226,309 (July 13).

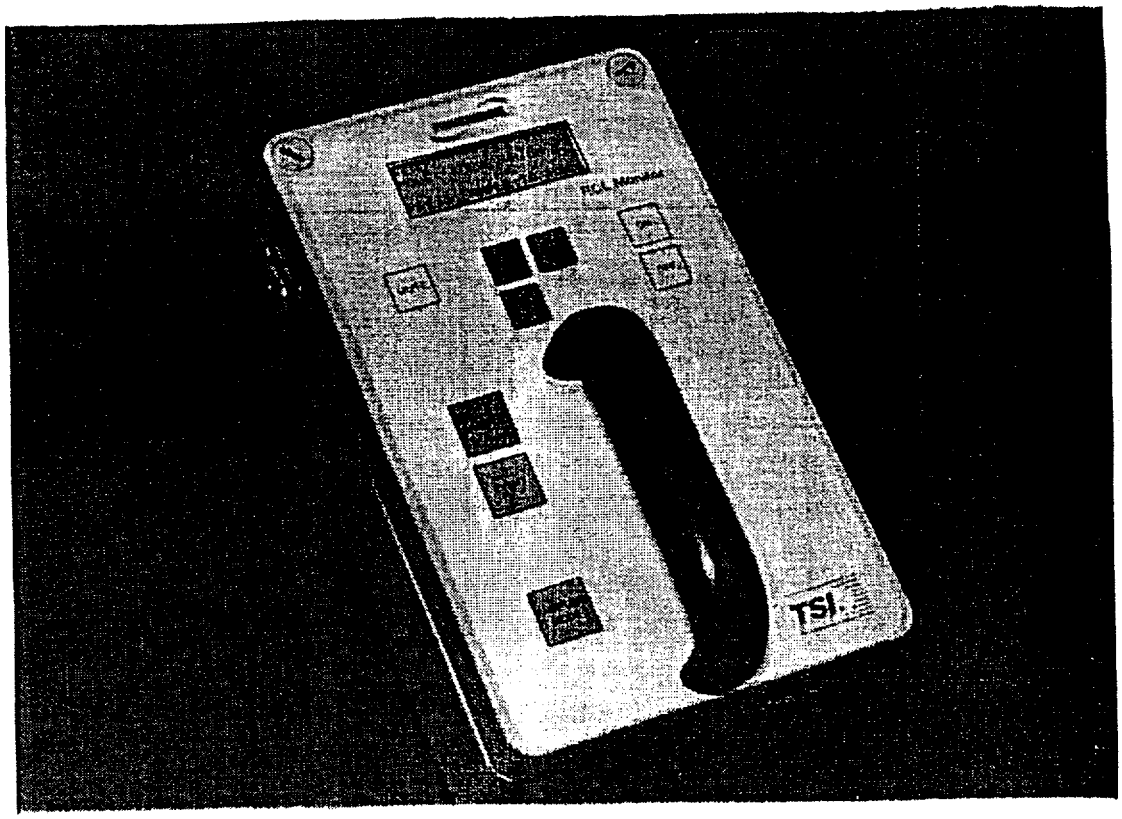

Figure 1: The RCL MONITOR

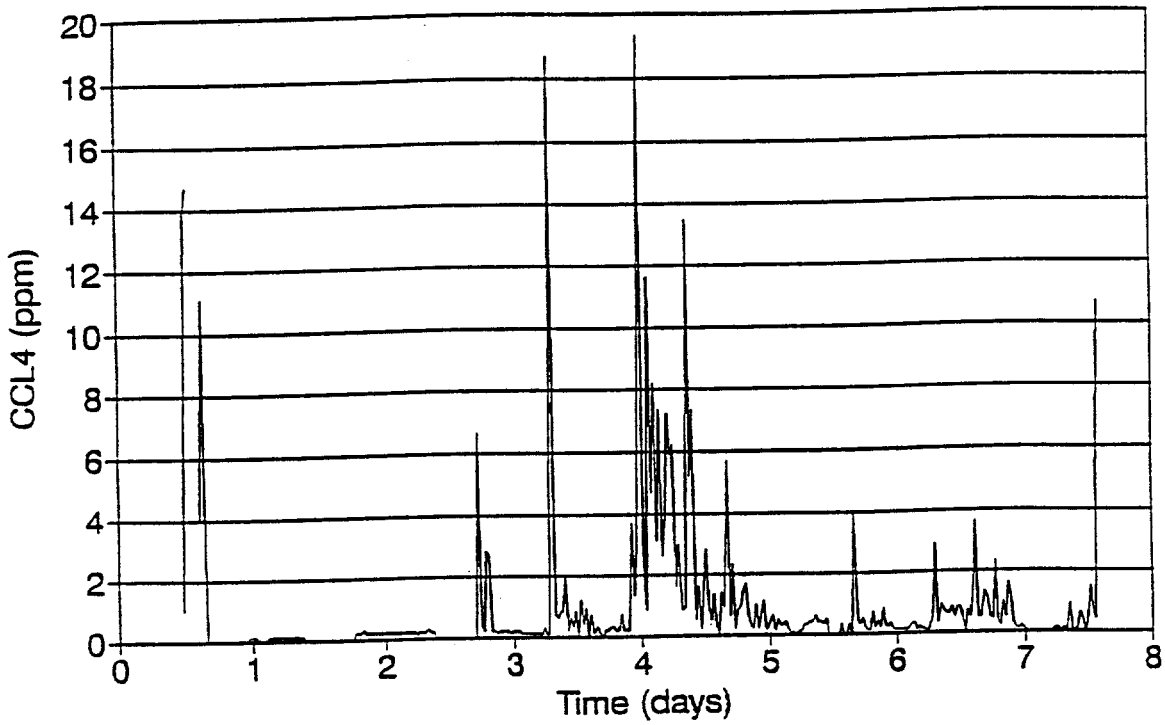

Figure 2: Representative data obtained from the RCL MONITOR during continuous monitoring of the work space air during testing of the PURUS system

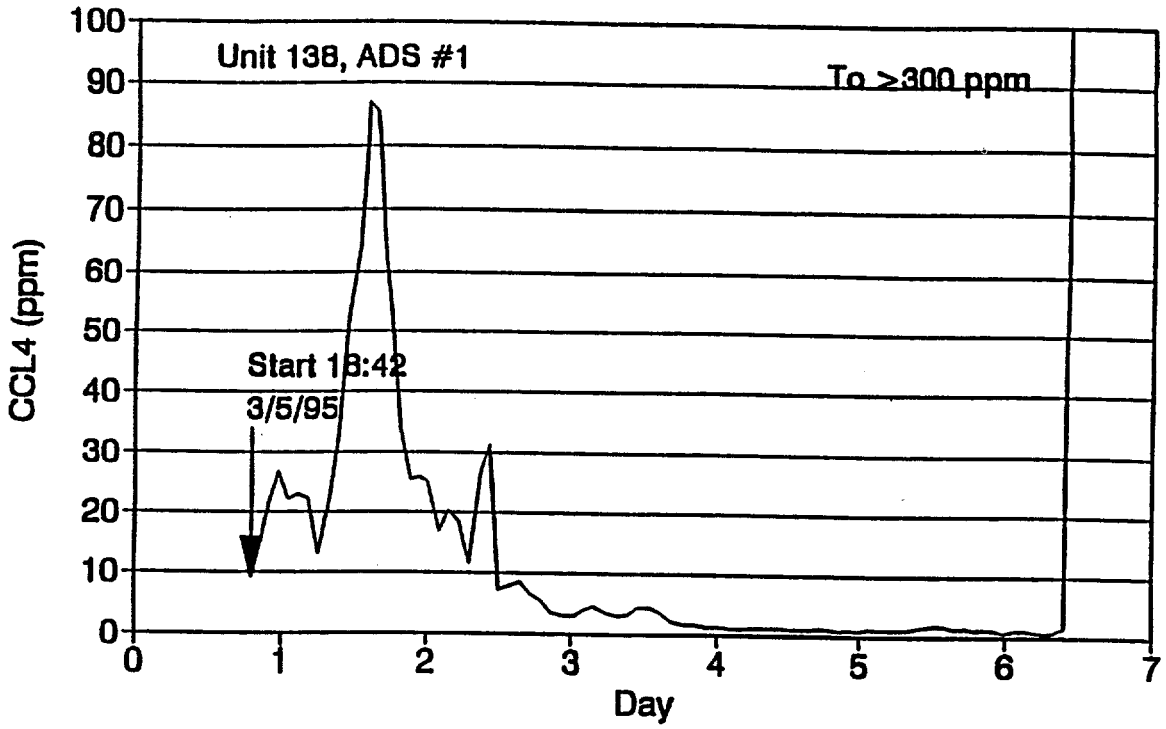

Figure 3: Representative data obtained from the RCL MONITOR during continuous monitoring of the post-primary GAC exhaust. Vapor spikes correlated to VES activity, including saturation of GAC, GAC changes, changeovers, etc.

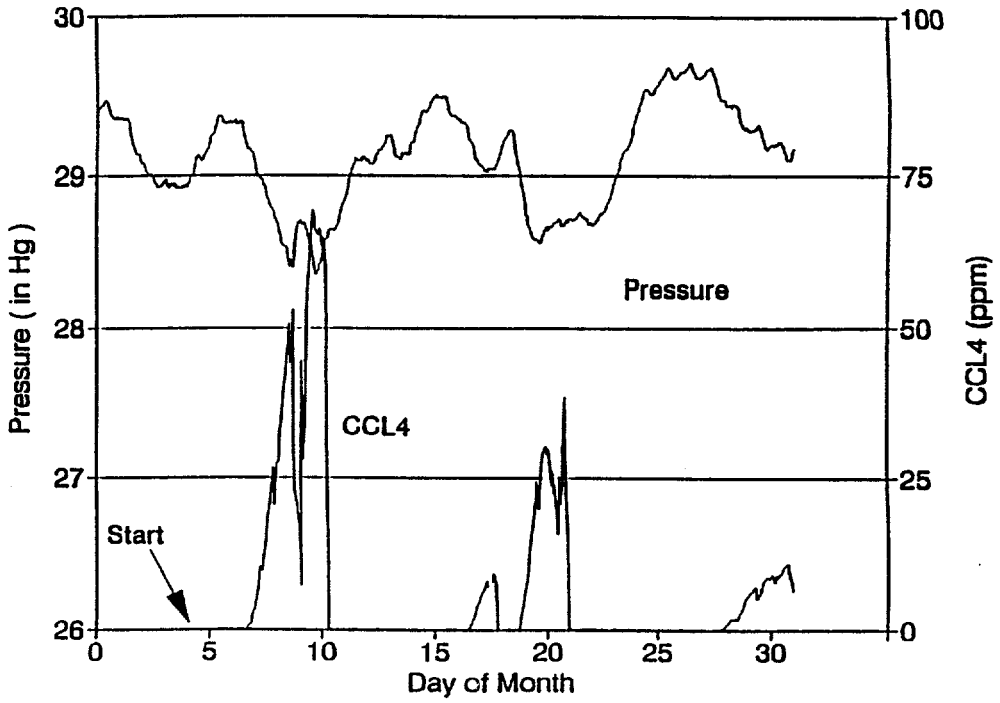

Figure 4: Monthly logging of passive venting of vapors as measured by the RCL MONITOR and barometric pressure.

Table I: Features of the RCL MONITOR vapor monitor.

Design Feature	Description
Measurement	Direct readout 90 s after start of analysis, presented in ppm with a range of 0 to 500 ppm and a LDL of 0.2 ppm. The results are presented on display and stored in memory
Modes of Operation	- SURVEY-LOW (a fast manual mode of analysis, 0.2 to 25 ppm). - SURVEY-HIGH (a fast manual mode of analysis, 2 to 500 ppm) - MONITOR (an automated mode of operation, with HIGH and LOW ranges)
Physical Design Package Weight Power	 All components in one unit (5" x 6" x 12") 5 kg (12 pounds) Internal battery (over 6 hours operation at 25°C) or AC operation

Table II: Cost Benefit Analysis for using the RCL MONITOR instead of a gas chromatograph for the RQM

VAPOR SAMPLES	GC			RCL MONITOR		
SINGLE TIME EXPENSE						
Capital Equipment:			$30,000			$17,500
Capital Equipment (samplers):			1,000			5,000
TOTAL:			$31,000			$22,500
MANPOWER Requirements	man-hrs (RQM)	cost (RQM)	cost annual	man-hrs (RQM)	cost (RQM)	cost annual
LABOR ($62.50/hr)	80	$ 5,000	$20,000	25	$ 1,563	$ 6,250
EQUIPMENT COST						
Annual Maintenance Cost:			2,000			
Supplies:		100	400		200	800
Equipment Preparation Cost:		500	2,000		100	400
Bags:		500	500		250	1,000
Vehicle Expense						
daily fee ($50.00/day)		400	1,600		100	400
Mileage (120 miles/day)		288	1,152		72	288
TOTAL:		$ 6,788	$ 29,152		$ 2,285	$9,138

Table III: Specific H&S Spot-Check Measurements Performed with the RCL MONITOR at HANFORD. All are breathing zone measurements.

Application	Comments
Well Perforation	0-2 ppm (OVM read 200 ppm--therefore nonchlorinated)
Well drilling operations	0-2 ppm
Examine Well cuttings	0-1 ppm
Investigate CCl_4 in enclosure	11-39 ppm
Outside air checks at 200W	(0.1-0.2 ppm)

Table IV: Technologies for chlorinated hydrocarbon analysis evaluated during the March Demonstration of the ETC program at SRL

Technology	Cost
RCL MONITOR	$ 8,500
Quantum FTIR	$50,000
B&K 1302	$30,000

4.3 Development of The Integrated *In Situ* Lasagna Process

S. Ho (svho@ccmail.monsanto.com; 314-694-5179)
C. Athmer (cjathm@ccmail.monsanto.com; 314-694-1670)
P. Sheridan (pwsher@ccmail.monsanto.com; 304-694-1470)
B. Hughes (bmhugh@ccmail.monsanto.com; 314-694-1466)
P. Brodsky (phbrod@ccmail.monsanto.com; 314-694-3235)
Monsanto Company
800 N. Lindbergh Boulevard
St. Louis, Missouri 63167

Introduction

Contamination in deep, low permeability soils poses a significant technical challenge to in-situ remediation efforts. Poor accessibility to the contaminants and difficulty in uniform delivery of treatment reagents have rendered existing in-situ methods such as bioremediation, vapor extraction, and pump and treat rather ineffective when applied to low permeability soils present at many contaminated sites.

Recently the use of electrokinetics as an *in situ* method for soil remediation has received increasing attention due to its unique applicability to low-permeability soils (2-11). Electrokinetics includes the transport of water (electroosmosis) as well as ions (electromigration) as a result of an applied electric field. Electroosmosis in particular has been used since the 1930s for dewatering clays, silts, and fine sands (1). For remedial applications, water is typically introduced into the soil at the anode to replenish the water flowing towards the cathode due to electroosmosis. The water flow is utilized to flush organic contaminants from the subsurface soil to the ground surface at the cathode region for further treatment or disposal.

Advantages with electroosmosis include uniform water flow through heterogeneous soil, high degree of control of the flow direction, and very low power consumption. As currently

Research sponsored by the U. S. Department of Energy's Morgantown Energy Technology Center, under contract DE-AR21-94MC31185 with Monsanto Company, 800 N. Lindbergh Boulevard, St. Louis, Missouri 63167. FAX: (314) 694-1531.

practiced, however, the technology suffers several limitations on large-scale operations. These include low speed (liquid flow induced by electroosmosis typically moves about 1 inch per day for clay soils), additional aboveground treatment and unstable long-term operation resulting from soil drying and cracking, steep pH gradient in the soil bed, and precipitation of metals and minerals near the cathode. Recent efforts to mitigate the pH problem primarily involve conditioning the anode and cathode solutions through external recirculating loops (9,10).

There is a need for a low-cost, in-situ technology that can effectively treat a wide range of contaminants in low-permeability soils or soils containing low-permeability zones. In this paper, we describe an integrated approach that minimizes the drawbacks associated with the use of electrokinetics alone, and present the experimental results of the initial field test.

Technical Approach

Monsanto's new approach is an integrated in-situ treatment in which established geotechnical methods are used to install degradation zones directly in the contaminated soil and electrokinetics is utilized to move the contaminants through those zones until the treatment is completed.

One possible configuration of the process has the following components:

a) create permeable zones in close proximity sectioned through the contaminated soil region, and turn them into treatment zones by introducing appropriate materials (sorbents, catalytic agents, microbes, oxidants, buffers, etc.). Hydraulic fracturing and related technologies may provide an effective and low-cost means for creating such zones horizontally in the subsurface soil. The treatment zones can also be vertical, which can be constructed using sheet piling, trench, slurry wall, etc. Instead of being discrete, the treatment zones can be continuous using *in situ* soil mixing devices.

b) utilize electrokinetics for transporting contaminants from the soil into the treatment zones. Since these zones are deliberately located close to one another, the time taken for the contaminants to move from one zone to the adjacent one can be short. In the horizontal configuration, the zones above and below the contaminated soil area can be injected with graphite particles during the hydrofracturing process to form in-place electrodes.

c) liquid flow can be periodically reversed, if needed, simply by switching the electrical polarity. This mode would enable multiple passes of the contaminants through the treatment zones for complete sorption/destruction. The polarity reversal also serves to minimize complications associated with long-term operation of uni-directional electrokinetic processes as discussed above. Optionally, the cathode effluent (high pH) can be recycled directly back to the anode side (low pH), which provides a convenient means for pH neutralization as well as simplifies water management.

Electrodes and treatment zones can be of any orientation depending upon the emplacement technology used and the site/contaminant characteristics. Schematic diagrams of two typical configurations, horizontal and vertical, are shown in Figure 1. The process has been called Lasagna™ (12) due to the layered configuration of electrodes and treatment zones. Conceptually, the technology could treat organic and inorganic contamination as well as mixed wastes.

Project Description

A consortium was formed in 1994 consisting of Monsanto, E. I. du Pont de Nemours & Co., Inc. (DuPont) and General Electric (GE). With participation from the Environmental Protection Agency (EPA) Office of Research and Development and the Department of Energy (DOE), the consortium combined resources to accelerate the development of the Lasagna technology. The consortium's activities have been facilitated by Clean Sites, Inc., under a Cooperative Agreement with EPA's Technology Innovation Office.

The initial Lasagna technology development is referred to as Phase I in which trichloroethylene (TCE), a major contaminant at many DOE and industrial sites, was selected as the target contaminant . Phase I consisted of three major efforts: 1) developing key technical components of the Lasagna process, 2) conducting field experiments to evaluate the coupling of individual components, and 3) evaluating the overall performance including cost of remediation. For the field test, the Paducah Gaseous Diffusion Plant (PGDP) site was chosen from a list of Department of Energy sites based on the two major criteria of low-permeability soils and TCE as the single contaminant. DOE contributed by providing the contaminated site in Paducah for the test, soil sampling and analysis support (through Martin Marietta), and funds through a Research and Opportunity Announcement (ROA) grant. CDM-Federal, Inc., was hired by the consortium to construct and manage the field experiment.

The purpose of the field test was to experiment with the coupling of electroosmotic removal of TCE from the contaminated soil with in-situ adsorption by activated carbon in treatment zones in the vertical configuration. This was the initial phase of the Lasagna project, to be followed by a subsequent one incorporating in-situ degradation of TCE, either catalytically or biologically.

The major technical objectives for conducting the field test included studying the scaled-up characteristics of key operating parameters and the effectiveness of TCE removal. Important operating issues involved

- design of treatment zones and electrodes, emplacement methods and cost of installation
- electrical effects: voltage, current, power, soil conductivity, heating, etc.
- electrokinetic effects: electroosmotic flow, pH profile, solution conductivity
- responses to polarity & flow reversal

Issues related to TCE removal included extent of soil cleanup, effectiveness of carbon adsorption in an electroosmotic environment, and overall mass balance. Field data were also needed for the development of a mathematical model and for refining an economic model estimating the cost of treatment using the Lasagna process.

Results of the Field Experiment

The field test covered a soil section 15 feet long by 10 feet wide and approximately 15 feet deep. Each electrode zone consisted of 8 steel panels. There were a total of 4 treatment zones installed, each consisting of 11 or 12 individual wickdrains filled with activated carbon. The treatment zones were installed with 21 inches of soil between each zone. Figure 2 shows the layout of the field unit. A 4 ft by 4 ft by 15 ft deep control zone was installed at the west end of the unit and isolated hydraulically from the test site with interlocking sheetpiles. The control zone contained one carbon wickdrain.

The field unit was constructed during November and December 1995. The experiment was started (power on) on January 3, 1995 and lasted for four months. The voltage was then reversed for about one week, primarily to collect voltage and current data, before the power was turned off. Key operating characteristics of the test are reported below.

Electrokinetic Effects

Voltage and Current: The initial voltage was set at 138 volts and the corresponding current was about 41 amps. With the current held constant at 40 amps, the voltage slowly decreased with time and stabilized at about 105 volts after one month of operation. The lower voltage was due to the soil heating up (discussed below), which increased the electrical conductivity of the soil . The voltage gradient ranged from 0.45 to 0.35 volts/cm. The voltage drop across the unit was fairly linear and did not change over the course of the experiment. Total voltage and current trends are shown in Figure 3.

Electrokinetic Effects: During the first month, an electroosmotic flow rate of about 2 L/hr was measured, which was less than one half of the predicted value based on the bench-scale's measurements. This turned out to be due to pluggage in the cathode siphon tubes, causing water to "overflow" the cathode wicks. Once this problem was fixed, the flow rate averaged about 4 to 5 L/hr, corresponding to an electroosmotic permeability of 1.2×10^{-5} cm^2/V-s. This value, as well as the water flow rates, agreed very well with the lab data. With the first month's flow rate corrected to a value of 4 L/hr, the unit moved three pore volumes of water (between adjacent treatment zones) over the 4 month operating period. Figure 4 shows the flow rate and the corresponding pore volumes during the field test.

Conductivity and pH: The pH of the anode fluid dropped from near neutral at the beginning to between 5 and 6 for most of the test. This mild pH behavior for an electroosmosis experiment, which had also been observed in laboratory units, was a direct consequence of iron corrosion rather than water electrolysis as and the predominant anodic reaction. During the last month of the test, however, the anode fluid pH dipped rather unexplainably down to 2-3. The pH of the cathode fluid rose rapidly to about 12 and stayed there for the whole experiment. This is normal for electroosmosis due to the electrolysis of water generating OH^- at the cathode.

The conductivity of the anode solution ranged between 1000 to 3000 μS/cm for most of the test, except near the end when it fluctuated widely with occasional spikes up to 25,000 μS/cm with the prime ion species being iron and chloride. This behavior was probably related to

the low pH noted above during this period. The cathode solution conductivity was fairly constant at about 10,000 μS/cm with the primary ion species being sodium. These values were consistent with the laboratory data. A plot of pH and conductivity values over time are shown in Figure 5.

Temperature Effects: The initial temperature of the soil at the 10-foot depth was 15°C. The temperature rise at various locations due to the electrical power is shown in Figure 6. The core temperature (hottest spot) reached a maximum of 45.2°C at the end of the test. Notice the control zone temperature raises also. A possible reason for the increase in temperature in the control zone is that stray current could flow through it, causing heating. It could also be due to thermal conduction since the control zone was less than one foot from the anode.

To predict temperature rises in field experiment, a mathematical model was developed by General Electric using FIDAP®, a commercial computational fluid dynamics program. The governing equations included energy transport by conduction, electroosmotic convection, and heat generation from Joule heating. Temperature dependencies of electrical conductivity and electroosmotic permeability were accounted for. Specific examples simulating possible scenarios for the Lasagna pilot test in Paducah, KY were studied. With the appropriate values for thermal conductivity and heat capacity of the soil , the model predictions correspond very well with the field data as shown in Figure 7.

Polarity Reversal: Polarity of the DC power to the unit was reversed for 1 week at the end of the test to study the system response. The unit ran stably at a reverse voltage of 90 volts and a current of 39 amps. There was an increase in electrical conductivity of the soil when the polarity was reversed and the pH at the electrodes was shifting from high to low at the new anode and from low to high at the new cathode. These results were expected and similar to laboratory data. Thus, polarity reversal can be readily utilized in the field, if needed for reversing flow or neutralizing pH and/or osmotic gradients.

Overall, the field unit behaved very much like the laboratory and pilot experiments. The unit scale-up was excellent. The electroosmotic conductivity, pH and conductivity trends, power requirements, temperature trends and operational stability all were consistent with laboratory data.

TCE Removal and Mass Balance

Pre-Test Soil Samples: Prior to the installation of the Lasagna field unit, soil samples were taken and analyzed by Oak Ridge National Laboratories (ORNL) personnel. A total of 12 bore holes were made with samples taken every 1 foot to a depth of 15 feet below ground surface. Nine bore holes were completed within the boundary of the Lasagna unit, two in the control area and one to the outside west of the unit. The locations of the bore holes with respect to the wicks are shown in Figure 2. The results show TCE concentrations in the soil ranged from 1 mg/kg to over 500 mg/kg with an overall average of 83.3 mg/kg for the 12 bore holes from 4 to 15 foot depths (Table 2). The average concentration of TCE within the test site (15' x 15' x 10') is almost the same, 83.2 mg/kg, resulting in a total amount of TCE of about 9.25 kg.

Intermediate Carbon Samples: In order to assess the progress of the test, the carbon cassette from wick C4-7 was removed for analysis after 2 pore volumes of water exchange were obtained. Carbon samples were taken every foot from 3 to 15 feet. TCE levels on the carbon were found to be quite high, ranging from several thousand to over 10,000 mg TCE/kg carbon (Figure 8). This indicates that TCE was being effectively flushed from the soil and trapped on the carbon. Also shown in the figure are the additional amounts of TCE trapped on the fresh carbon inserted into cassette of wick C4-7 for the remainder of the test (1 additional pore volume). The data show that, except at the very low depths, not much additional TCE was trapped by the carbon, an indication that the soil was probably clean of TCE.

Post-Test Soil and Carbon Samples: At the completion of the test (3 pore volumes total), all the carbon sampling cassettes were removed and analyzed in the same manner as the intermediate samples. Soil samples were also taken. Twelve bore holes were dug near the original pre-test bore holes to a depth of 15 feet and slightly lower. Results in Table 2 show very high as well as uniform removal of TCE from the treated soil. The final soil concentrations were mostly below 1 mg/kg, with an average of 1.1 mg/kg for the 9 bore holes within the test boundary. TCE removal ranged from 92.4 to 99.8%, with an overall average of 98.4%. The soil samples taken either outside or deeper than the test zone (below 15 feet) still showed substantial amounts of TCE present. TCE removals outside the test boundary were 26% and 51% from the two spots in the control zone, and 68% from the west of the Lasagna unit. The removal in the control zone was probably due to diffusion into the carbon wick (see modeling below). The removal in the area to the west was probably due to both migration and diffusion from the anode area and/or sampling inaccuracies. Despite significant degrees of removal from the control areas, the definite contrast between TCE levels in the soils within the treatment area and without (outside or deeper) is quite remarkable and shows conclusively the effectiveness of the process for cleanup of the contaminated soil.

Several of the pre-test soil samples showed TCE concentrations greater than 225 mg/kg, corresponding to an equilibrium pore water concentration of 1100 mg/l, thus indicated a residual DNAPL situation (12 through 15 foot samples of borehole L-08). In these likely DNAPLs locations, TCE levels were reduced to less than 1 mg/kg, except for the 15 foot deep sample which was reduced to 17.4 mg/kg. These results show that the process could be effective for removing residual DNAPL TCE from the soil.

TCE Mass Balance: Attempts were made to determine the mass balance for TCE taking into account the amounts in the soil before and after the test and the amount trapped on the carbon. This is a complex task due to the following reasons:

a) TCE levels in soil varied in all directions, so an averaging process was needed.
b) Not all the soil samples were taken directly in front of the corresponding carbon cassettes, so another estimating procedure was required.
c) The carbon cassettes were installed at the site about a month before the experiment actually started. So some TCE from the soil was lost due to passive diffusion to

the carbon cassette in the back row opposite the direction of electroosmotic flow. Based on diffusion modeling (Table 3 below), the loss could be about 5%.

d) Volatilization of TCE from the soil into the atmosphere did occur to some extent. Estimates calculated from measurements of the air samples, however, indicated that the volatilization loss was less than 5% of the total.

e) possible TCE degradation

Because of the above complications, the mass balance results ought not to be viewed as more than a gross indication of the fate of TCE.

Contour maps of TCE levels in the treated area were obtained using the kriging method. Table 4 shows the mass balances obtained for various locations, each from 4 to 15 foot depth. As can be seen, the mass balance ranges from about 20 to 78%, with an overall average of about 50%. These numbers are judged to be very good considering the uncertainties mentioned above.

Role of Diffusion: Due to the significant removal of TCE in the control area, the effect of diffusion on the removal of TCE from the contaminated soil was modeled. The results obtained are shown in Table 3. The model assumes

- slab configuration of 22 in. thick bracketed with infinite sinks (zero TCE concentration in the carbon wick drain), which is essentially correct since the activated carbon used has very high capacity for TCE (5000 mg/g carbon) compared to the amount of TCE in soil (equivalent to less than 15 mg TCE/g carbon).
- no retardation from soil interaction, a good assumption due to the very low adsorption of TCE (maximum amount adsorbed = 4.5 mg TCE/kg soil)

As can be seen, TCE removal by diffusion after four months is 22.4% at 15°C, 26.5% at 25°C, and 33% at 40°C. These levels are way below the removal levels obtained in the field test. It is interesting that even after 10 years passive diffusion only removes about 70% at 15°C. Larger treatment zone spacings will drastically reduce the amount of TCE removal from passive diffusion. As shown in the table, after 10 years the TCE removal by diffusion alone for a 9 foot spacing is less than 20%.

In summary, the field experiment was conducted for 4 months, covering a region of 15 ft by 10 ft by 15 ft deep. Both electrical and electrokinetic parameters were found to scale up very well. Soil analyses showed very high and uniform removal of TCE, averaging about 98% with most samples exhibiting 99+% removal from the soil. In addition, good TCE material balance was achieved.

Applications/Benefits

Lasagna has the potential of a very broad and effective in-situ technology for soil remediation. It treats the difficult case of contamination in low-permeability or heterogeneous soils. It requires very little maintenance, has built-in flexibility for handling diverse site situations, is practically non-intrusive to the environment and cost competitive. Based on the initial field results, the treatment cost for a typical 1-2 acre site with contamination to a depth of 40-50 feet would be about \$50 / yd^3. This compares well with other technologies such

as soil mixing (an ex-situ method), soil vapor extraction/bioventing (in-situ method but not effective for clay soils), and excavation/incineration (ex-situ and very high cost). Once developed, the Lasagna technology will have great benefits over existing ones in many aspects including environmental impacts, cost effectiveness, waste generation, treatment flexibility, and breadth of applications.

Future Activities

Phase II development activities are being planned to provide the technical and performance data necessary to advance the technology to the point where it can be commercially utilized as a full scale remediation technique. Phase II will consist of IIa, a commercial-scale development demonstration, and IIb, a full-scale first application demonstration at the approximately 1/2 acre contaminated site at the DOE Gaseous Diffusion Plant in Paducah. Phase II will utilize iron filings as the reagent in the treatment zones for degrading TCE to innocuous products.

Various treatment processes are also being investigated to handle other types of contaminants, DNAPLs situation, heavy metals and mixed wastes. For highly non-polar contaminants, surfactants could be introduced into the circulating water or incorporated into the treatment zones to solubilize the organics. For mixture of organics and metals, the treatment zones can contain sorbents for binding/immobilizing the metals, and microbes or catalysts for degrading the organics.

Acknowledgements

This research addresses the Plumes Focus Area. METC's COR is Mr. Kelly Pearce and the period of contract performance is September 26, 1994 - November 25, 1995. DOE's Office of Technology Development, Office of Environmental Restoration at PGDP, Battelle Pacific Northwest Laboratories, Oak Ridge National Laboratory/Grand Junction, EPA Remediation Technology Development Forum, DuPont, General Electric, CDM Federal Programs, API Contractors, Nilex Corporation, Stanford University, and Clean Sites Inc. provided critical resources and inputs for the successful completion of these studies.

References

1. Casagrande, L. *J. BSCE*, **1952**, 39, 51-83.
2. Hamnett, R. M.Sc Thesis, University of Manchester, Manchester, England, 1980.
3. Shapiro, A.P.; Renaud, P.; Probstein, R. *"Preliminary Studies on the Removal of Chemical Species from Saturated Porous Media by Electro-osmosis"* In *Physicochemical Hydrodynamics*, **1989**, Vol. 11, No. 5/6, 785-802.
4. Hamed, J.; Acar, Y.B.; Gale, R.J. *ASCE*, February **1991**, Vol. 112, 241-271.
5. Bruell, C. J.; Segall, B. A. *J. Environ. Eng.*, Jan/Feb **1992**, Vol. 118, No. 1, 68-83.
6. Segall, B. A.; Bruell, C. J. *J. Environ. Eng.*, Jan/Feb **1992**, Vol. 118, No. 1, 84-100,.
7. Acar, Y.B.; Li, H.; Gale, R.J. *ASCE*, November **1992**, Vol. 118, No. 11, 1837-1852.
8. Shapiro, A.P.; Probstein, R.F. *Environ. Sci. Technol.* **1993**, 27, 283-291.
9. Lageman, R. *Environ. Sci. Technol.* **1993**, Vol. 27, No. 13, 2648-50.

10. Acar, Y. B.; Alshawabkeh, A. N. *Environ. Sci. Technol.* **1993**, Vol. 27, No. 13, 2638-47.
11. Probstein, R.F.; Hicks, R.E. *Science* **1993**, Vol 260, 498-503.
12. P.H. Brodsky and S.V. Ho, U.S. Patent No. 5,398,756 entitled *In Situ Remediation of Contaminated Soils*, March 1995. The term Lasagna™ has also been trademarked by Monsanto.

Figure 1. Integrated In-Situ Remediation Process

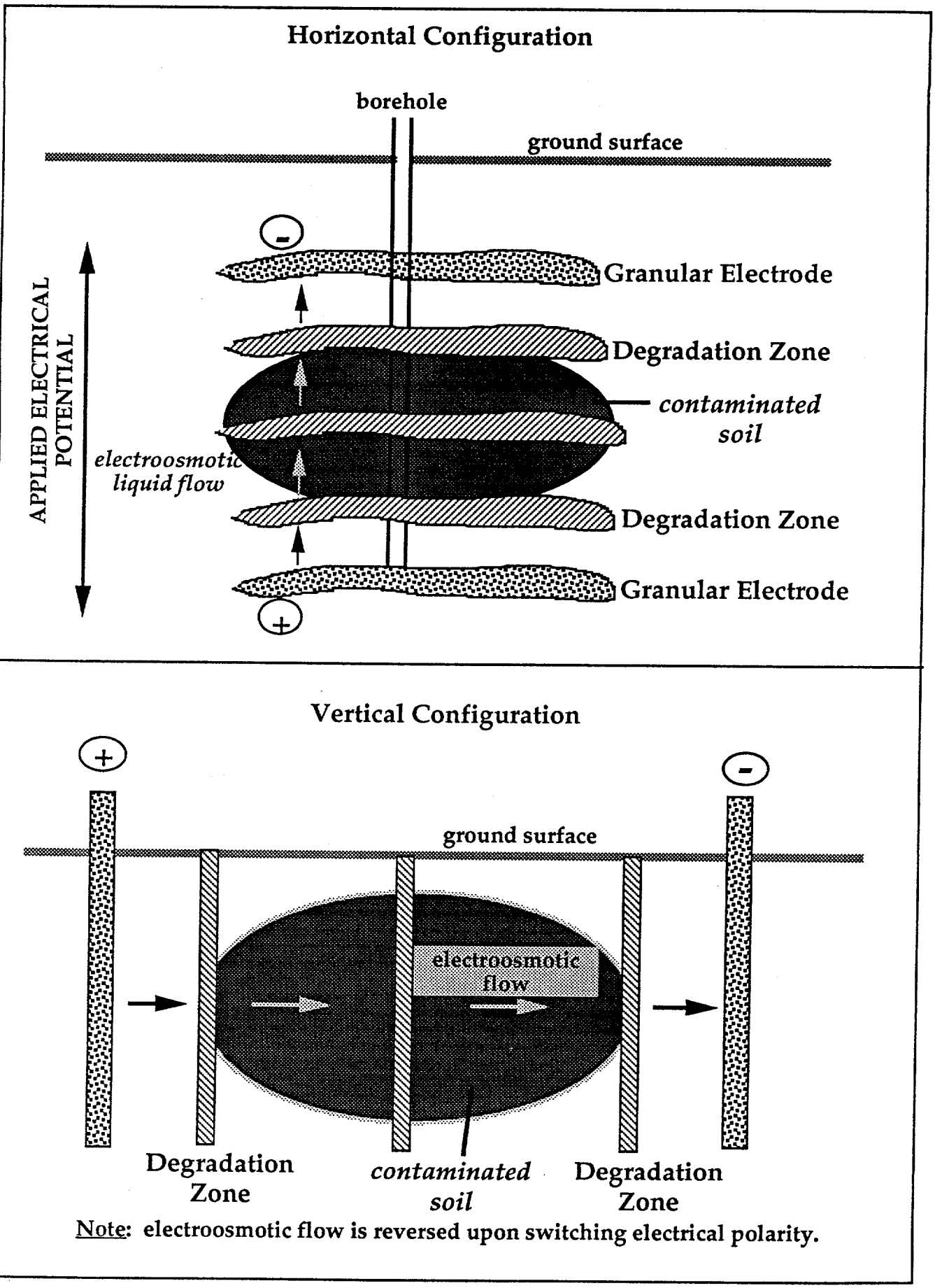

Note: electroosmotic flow is reversed upon switching electrical polarity.

Figure 2. Electrodes and Treatment Zones Installation Scheme
Phase I Field Test

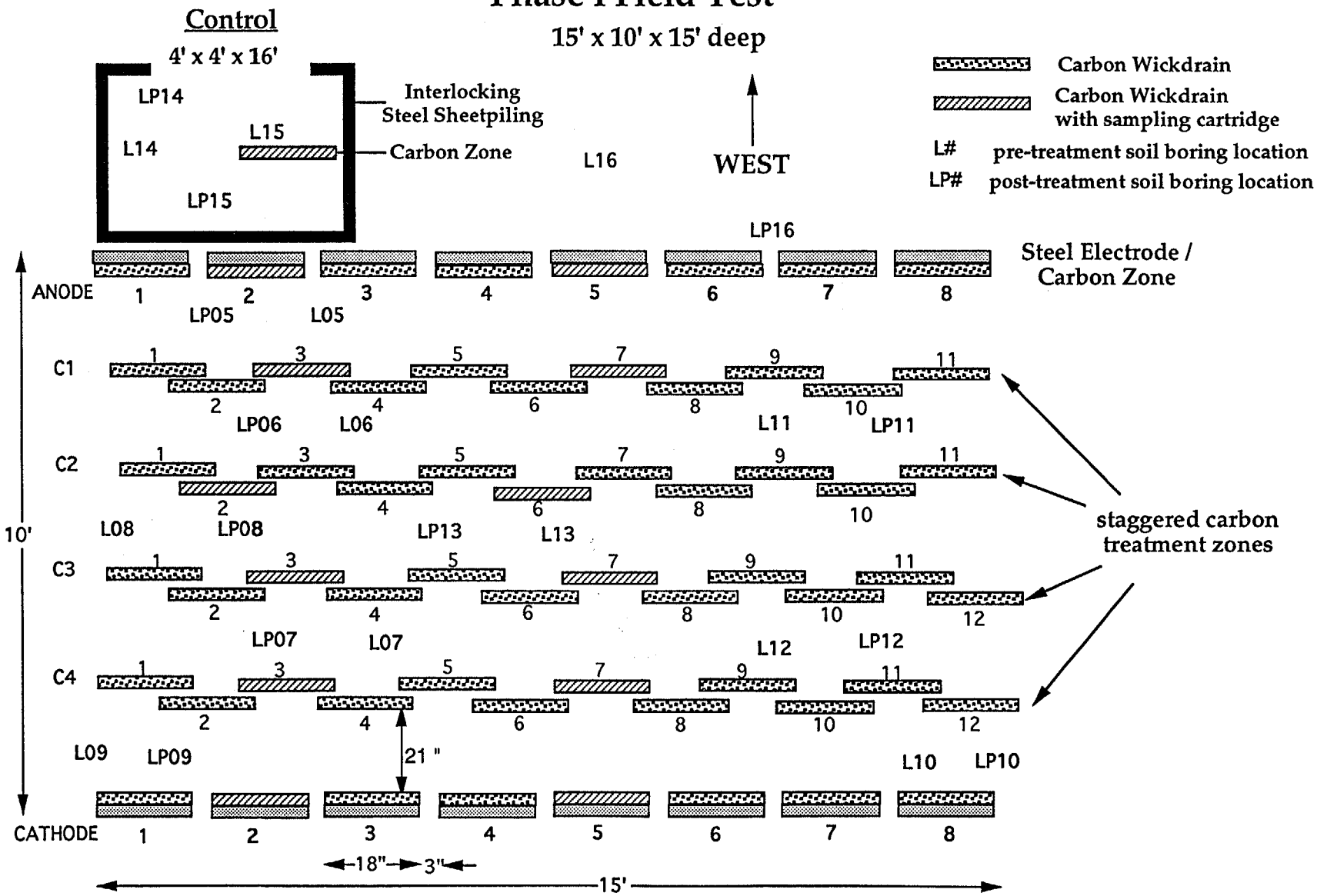

Figure 3. Voltage and Current Trends for Lasagna Field Experiment

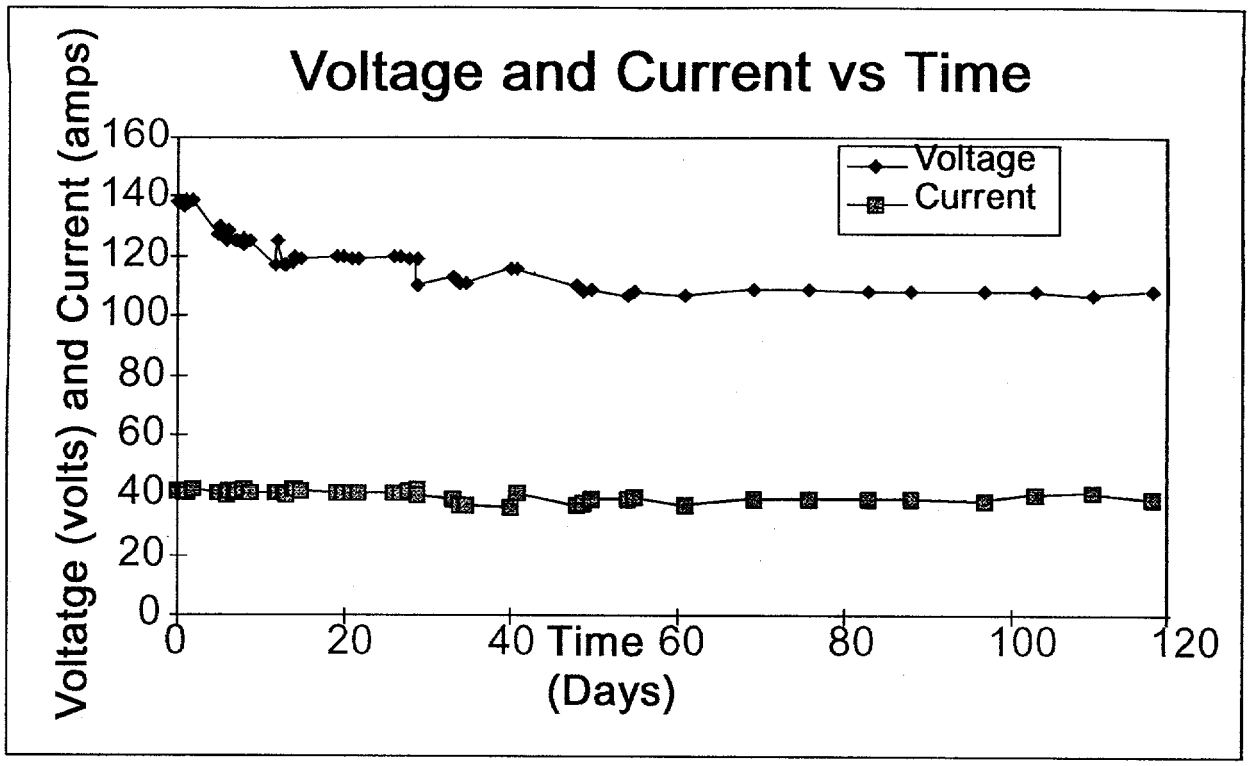

Figure 4. Flow Rate Measurements andAccumulated Pore Volumes

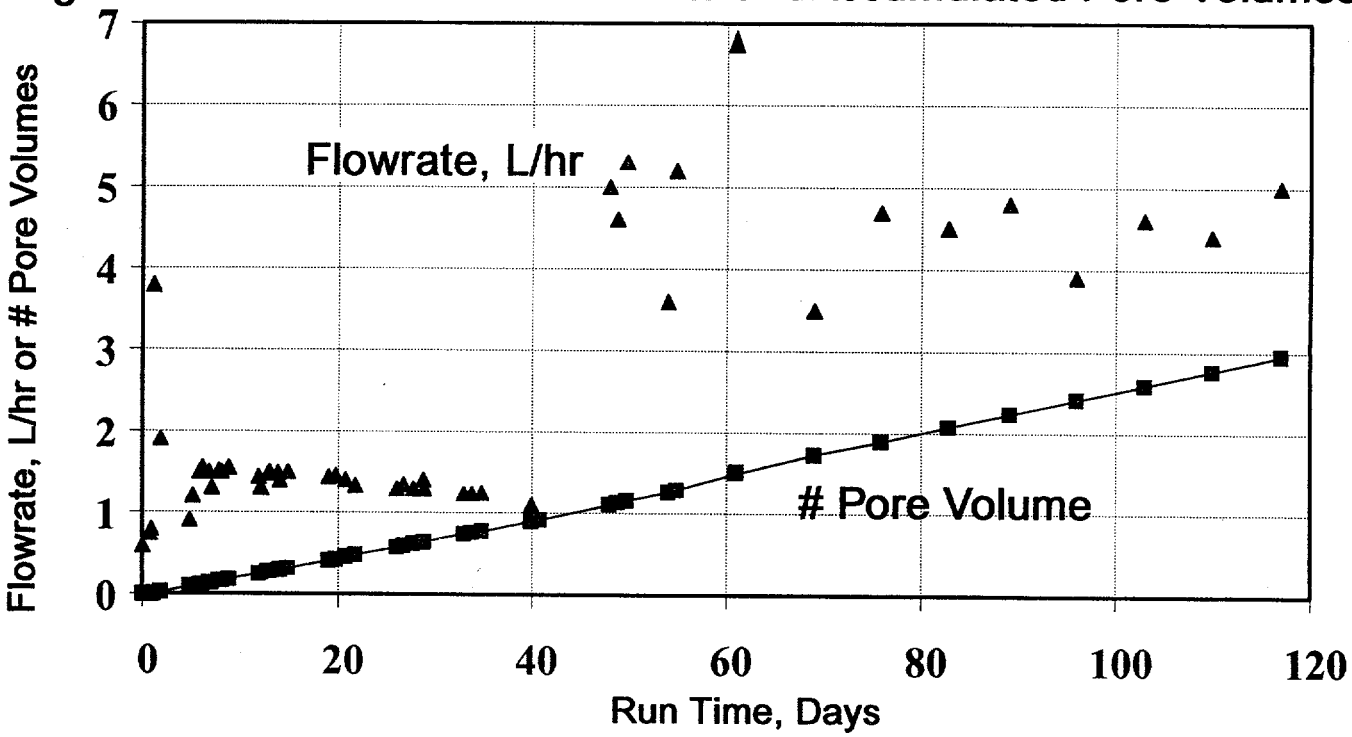

from Intact Core: (ke = 1.2 x 10-5 cm2/v-s)

Est. F = 3.6 L/hr @ 20°C, 0.40 V/cm
F = 5.0 L/hr @ 40°C, 0.37 V/cm

Figure 5. Conductivity and pH of Anode and Cathode Liquid

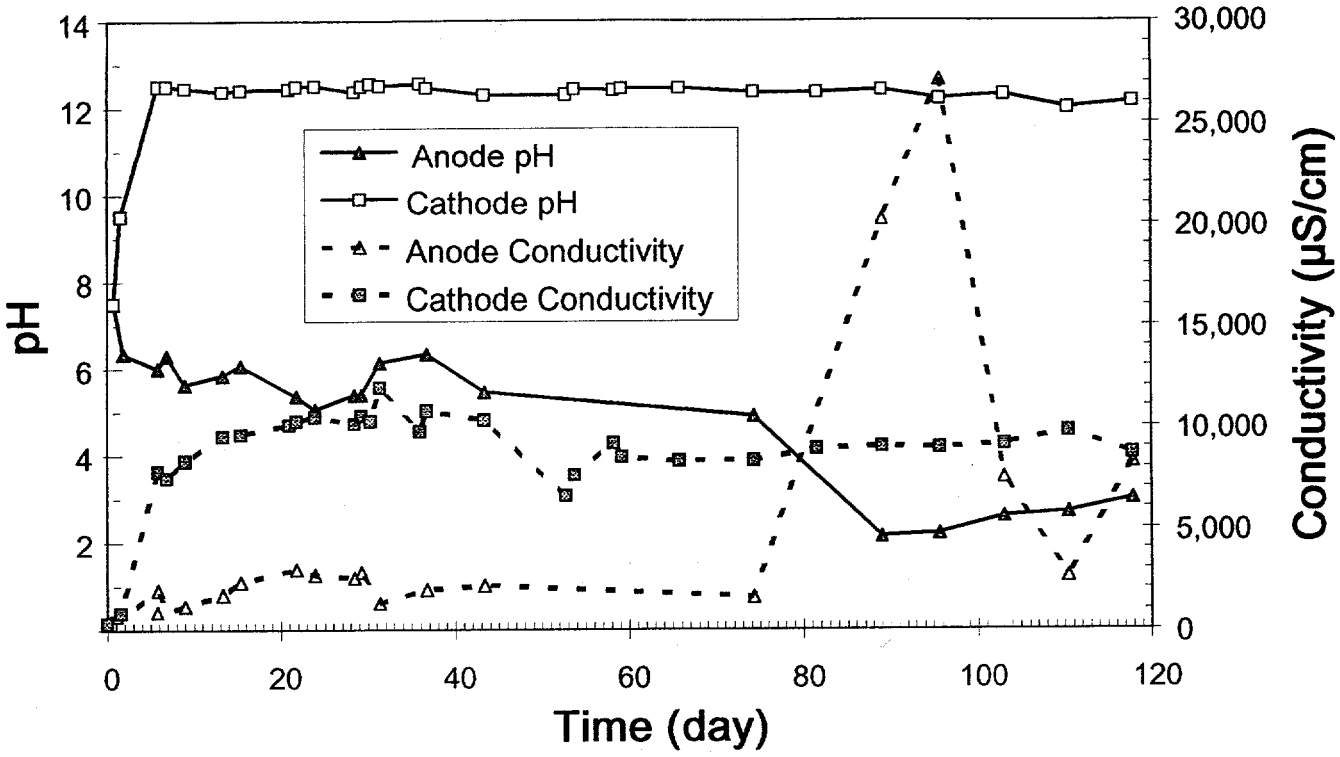

Figure 6. Temperature Trends for Various Locations

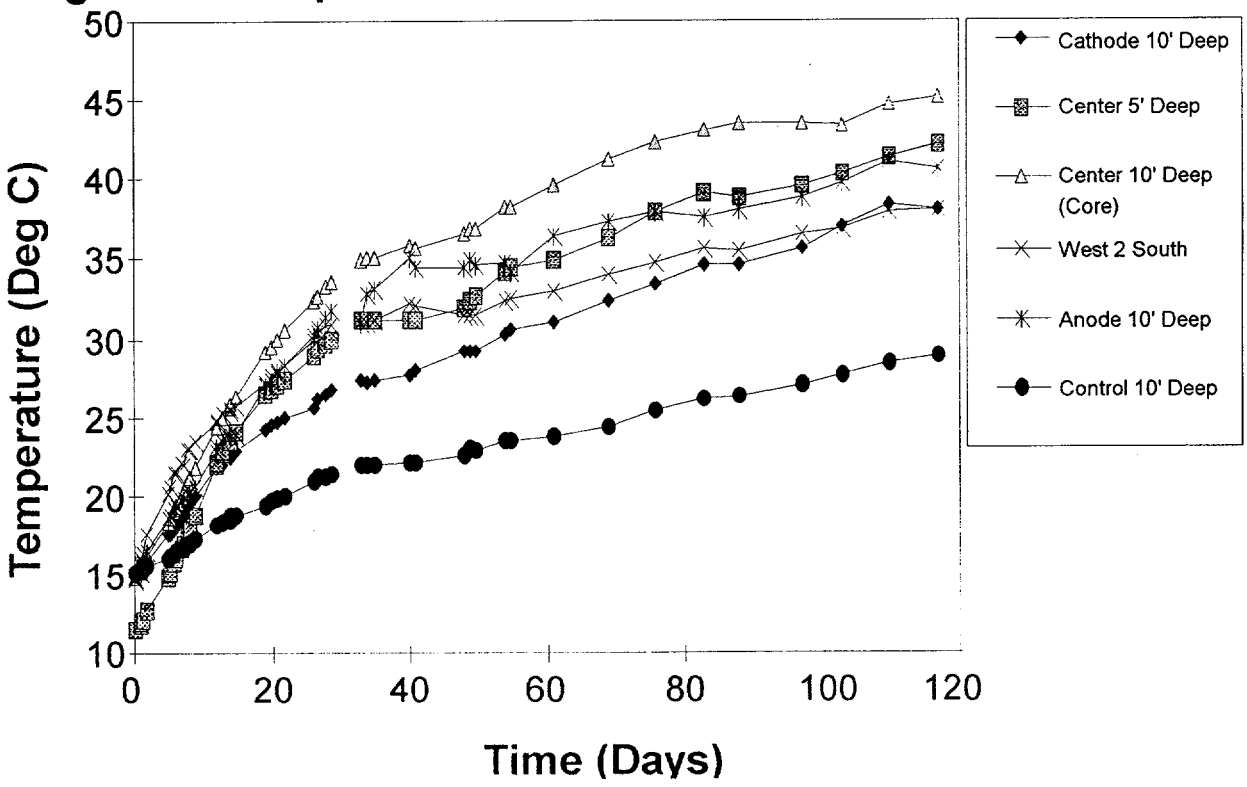

Figure 7. Comparison of Model and Actual Temperatures

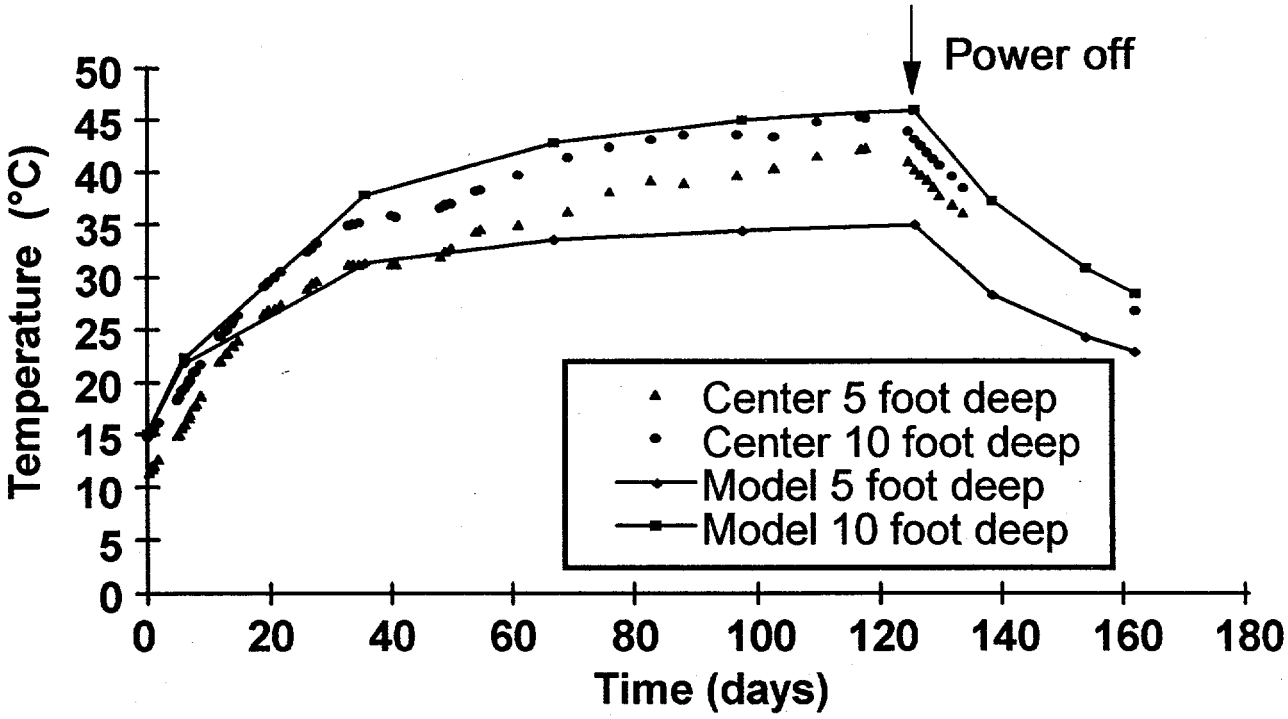

Figure 8. Intermediate Carbon Cassette Sampling

{C4-7} Carbon Cassette

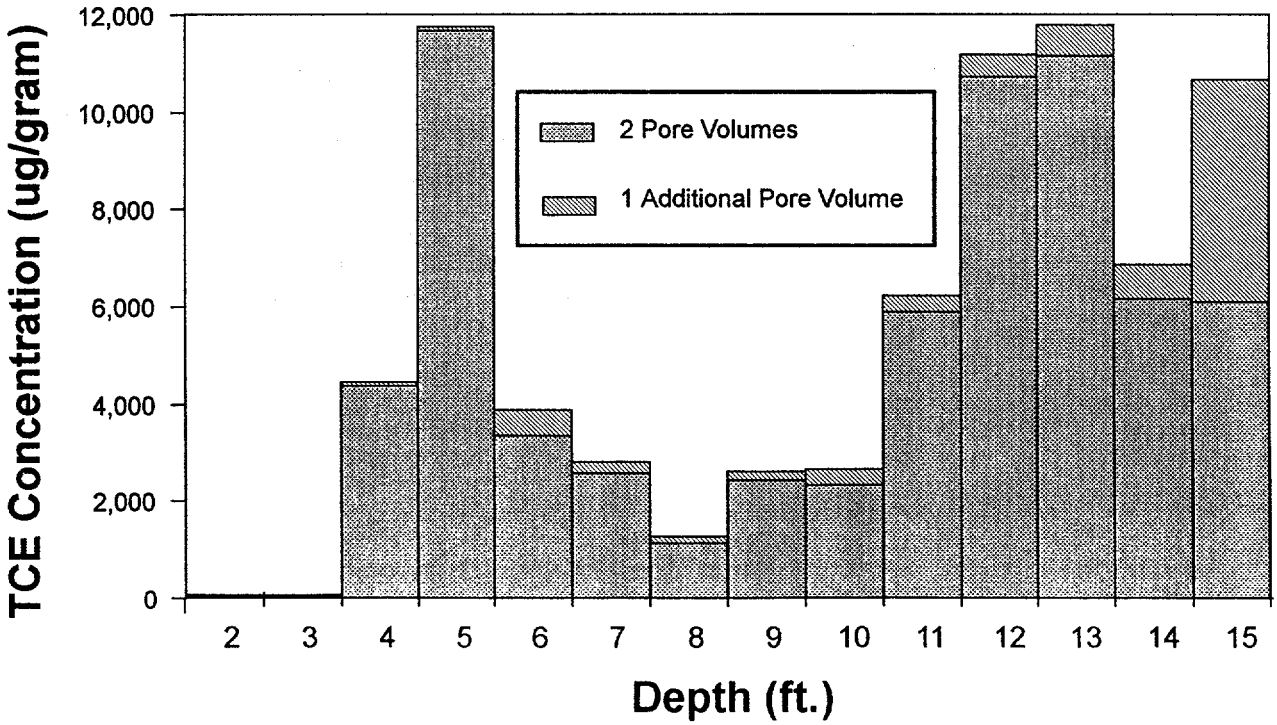

Table 1. TCELevels in Soil Before Experiment

Paducah Drop Test Site (Samples from 12 locations)

Depth	TCE, mg/Kg Soil Minimum	Maximum	Mean	Estimated TCE in Water, mg/l Maximum
4	8.60	61.6	22.8	308.0
5	1.00	63.1	34.5	315.5
6	1.00	79.4	38.3	397.0
7	2.60	114.5	45.1	572.5
8	2.30	79.4	44.4	397.0
9	5.90	129.0	60.3	645.0
10	7.80	138.9	79.5	694.5
11	6.90	165.1	109.7	825.5
12	2.60	292.0	140.6	1460.0
13	4.70	402.5	150.2	2012.5
14	2.10	507.3	151.4	2536.5
15	3.20	237.3	123.2	1186.5
Average	4.06	189.2	83.3	

TCE Solubility in Water @ 25°C =1100 mg/L

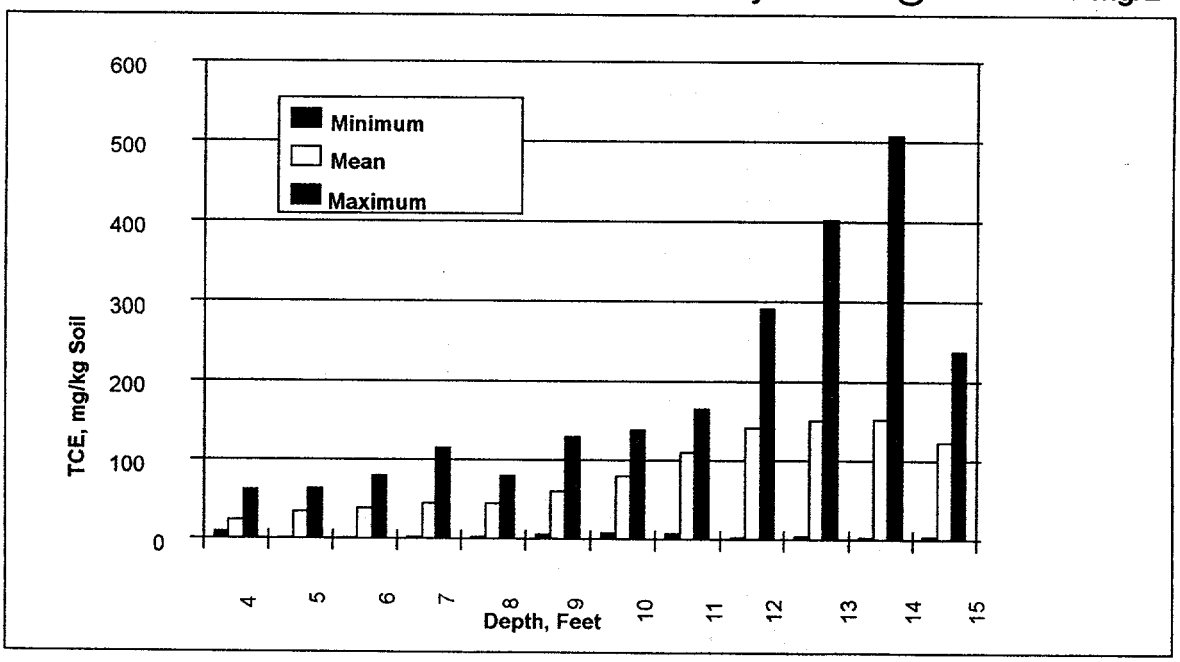

Table 2. TCE Removal Summary Based on Soil Cores

Borehole Number	Bore Holes Within Test Boundary									Avg. in unit	Bore Holes Outside unit		
	L-05	L-06	L-07	L-08	L-09	L-10	L-11	L-12	L-13		L-14	L-15	L-16
Pre-Test Concentration													
High *mg/kg*	169.4	167.3	176.7	368.6	113.1	7.6	144.3	76.9	140.2		178.2	196.8	114.2
Low *mg/kg*	20.3	4.9	37.2	3.0	13.7	1.0	4.1	12.0	38.3		10.4	43.7	10.6
Average *mg/kg*	73.0	82.0	101.6	110.4	66.6	4.0	72.2	44.8	99.1	72.6	108.2	118.6	63.0
Post-Test Concentration													
High *mg/kg*	0.29	1.22	8.62	17.40	15.20	0.47	1.84	5.23	2.29		101.7	109.5	50.8
Low *mg/kg*	0.004	0.21	0.055	0.018	0.002	0.042	0.40	0.002	0.038		24.6	6.7	2.6
Average *mg/kg*	0.14	0.50	1.06	2.07	3.73	0.30	0.89	0.89	0.64	1.14	80.0	58.0	20.1
TCE Removal %	**99.8**	**99.4**	**99.0**	**98.1**	**94.4**	**92.4**	**98.8**	**98.0**	**99.4**	**98.4**	26.1	51.1	68.1

Table 3. Model of TCE Removal by Diffusion in Paducah Soil

Model assumptions & parameters:

- diffusion in slab
- carbon treatment zones as infinite sinks
- no retardation of TCE due to interaction with the soil matrix
- $\varepsilon = 0.4$ (soil porosity); $\tau = 3$ (soil tortuosity)
- $D_{TCE} = 1.03 \times 10^{-5}$ cm2/s at 25°C

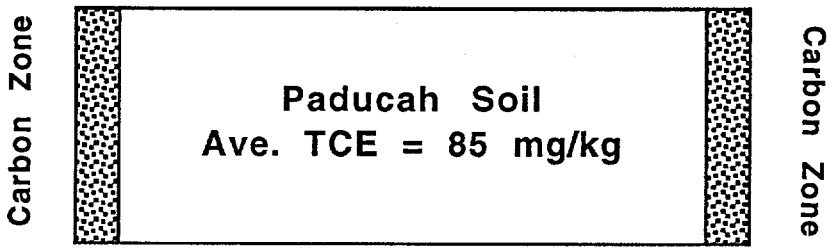

Carbon Zones Spacing = 22"

3. a	Percent TCE Removal at Indicated Soil Temperature			
Exposure Time	**15°C**	**25°C**	**40°C**	**90°C**
1 week	7.1	7.3	7.7	9.3
4 months	13.3	15.4	19.0	31.5
1 yr	22.4	26.5	33.0	54.8
5 yrs	49,9	59.0	71.7	95.7
10 yrs	69.2	79.3	90.1	99.8

3.b	%TCE Removal at 25°C	
Exposure Time	**3-ft carbon zone spacing**	**9-ft carbon zone spacing**
1 week	6.9	6.7
4 months	10.4	7.1
1 yr	16.4	8.0
5 yrs	36.3	12.6
10 yrs	51.2	17.2

Table 4. TCE Mass Balance

Carbon Wick Number	Wick TCE Concentration (mg/kg)	Wick TCE Mass (grams)	Pre-test Soil TCE Concentration (mg/kg)	Pre-test Soil TCE Mass (grams)	Post-test Soil TCE Concentration (mg/kg)	Post-test Soil TCE Mass (grams)	TCE Mass Removed From Soil (grams)	TCE Material Balance (%)
C1-3	1694	10.0	95.5	52.1	0.14	0.074	52.0	19.4%
C1-7	1861	11.0	90.3	49.2	0.14	0.074	49.1	22.5%
C2-2	4273	25.2	121.1	66.0	0.50	0.27	65.7	38.6%
C2-6	4239	25.0	91.2	49.7	0.89	0.49	49.2	51.3%
C3-3	4757	28.1	106.8	58.2	2.10	1.1	57.1	50.2%
C3-7	6788	40.1	95.8	52.2	0.64	0.35	51.9	77.5%
C4-3	2239	13.2	106.6	58.1	1.10	0.58	57.5	23.7%
C4-7	5862	34.6	87.8	47.9	0.89	0.48	47.4	73.3%
Cathode-2	5652	33.4	99.4	54.2	3.70	2.0	52.2	65.3%
Cathode-5	6005	35.4	84.3	46.0	0.30	0.16	45.8	77.4%
Overall Average	**4337**	**25.6**	**97.9**	**53.4**	**1.04**	**0.558**	**52.8**	**49.0%**

TCE soil mass (grams) is figured using 6 inch wide by 21 inch long by 11 feet deep zone of soil in front (up-stream) of the 6 inch wide sampling cassette and the average TCE concentration based on the pre-test soil core kriged data.

4.4 Steerable/Distance Enhanced Penetrometer Delivery System

Ali Amini (703-339-0800)
Joram Shenhar (703-339-0800)
Kenneth D. Lum (703-339-0800)
UTD, Incorporated
8560 Cinderbed Road
Suite 1300
Newington, VA 22122

Introduction

The first steps toward contaminant plume containment and remediation are detection and mapping of the plume. Penetrometers can be used to map the plume efficiently and also provide the means for in-situ sampling and remediation. In traditional penetrometer applications, the instrumentation package located at the tip measures soil resistance. However, for environmental monitoring purposes, an array of environmental sensors is packed inside the penetrometer rods for in-situ sampling and analysis, or for collection of laboratory samples.

At present, penetrometer applications are limited primarily to vertical pushes and because of their heavy weight, the use of penetrometer trucks over shallow buried storage tanks is restricted. To close the technology gap in the use of penetrometers for environmental purposes, UTD took the initiative by developing a new position location device referred to as POLO (short for POsition LOcator), which provides real-time position location without blocking downhole access for environmental sensors. The next step taken was the initiation of work to make penetrometers steerable and capable of greater penetration capabilities. The product of this work will be a relatively lightweight vibratory steerable penetrometer that can provide greater penetration capability than traditional penetrometers of the same weight, permitting applications over shallow buried storage tanks.

The initial development of POLO was carried out through internal funds at UTD. Recognizing the benefits of this new technology, DOE Morgantown Energy Technology Center (METC) funded the development of a prototype system under a PRDA contract. At the completion of the PRDA contract in September, 1994, for the first time the penetrometer operator had the capability of knowing the position of his sampling locations. Encouraged by this capability, DOE awarded UTD a new contract to develop a steerable distance enhanced penetrometer delivery system. In addition, in order to bring POLO into the commercial market in a timely fashion, the new contract was modified (in-scope modification) and new tasks were added to integrate a commercial POLO into a Site Characterization and Analysis Penetrometer System (SCAPS) truck. The new contract including its in-scope modification was awarded under a Research Opportunity Announcement (ROA) program and

Research sponsored by the U.S. Department of Energy's Morgantown Energy Technology Center, under Contract DE-AR21-94MC31178 with UTD, Incorporated, 8560 Cinderbed Road, Suite 1300, Newington, VA 22122-8560; telefax: 703-339-0800.

is comprised of a base program (Phase 1) and two optional phases ({Phase 2 and Phase 3).

Objectives and Approach

An objective of this research effort is to complete the development of steering and vibratory thrusting capabilities for penetrometer delivery systems. Steering permits controlled directional use of the penetrometer, and vibratory thrusting can provide greater depth penetration and improve the ability to penetrate harder materials. Another objective of the research effort is to integrate a commercial POLO into a SCAPS truck.

The project consists of three phases. Phase 1 included analysis, design, and laboratory experiments covering the individual sub-systems required to perform vibratory thrusting and steering of penetrometers. In addition, the work in Phase 1 included the design, assembly and integration of a commercial POLO system into a SCAPS truck.

Phase 2 work includes the integration of all steerable, navigational, and vibratory thrusting components and Phase 3 work includes field testing and demonstration of the full-scale integrated steerable/vibratory system.

Project Description and Results

In order to accomplish the project objectives, a commercial POLO system was manufactured and tested for compatibility with a SCAPS truck. In addition, several sub-systems of a steerable vibratory penetrometer system were analyzed, designed and manufactured. Later, the performance of the various sub-systems was verified through laboratory and field tests. The main sub-systems of a steerable vibratory penetrometer system described in this paper include the steerable tip, and penetrometer rod joints.

Commercial POLO System

Capabilities of the prototype POLO system were demonstrated under a DOE sponsored PRDA contract in July, 1994[1]. The optimum way to make commercial POLO systems available to DOE contractors was to develop a commercial system integrated into a SCAPS truck. This effort involved the design and manufacturing of a commercial POLO module, its initializer, and the integration of a user friendly data acquisition package as shown in Figure 1.

The POLO rod module, the main component of the system, measures bending strains imposed on it as it is pushed into the ground. The strain signals are processed by UTD's down-hole data acquisition package and sent to the surface computer through a two-wire umbilical. The POLO initializer is used to measure the initial orientation of the penetrometer rod as it begins to penetrate the soil surface.

The POLO surface computer is a portable "lunch box" computer connected to an up-hole processor box which receives the strain signals. The computer is also connected to two clinometers of the initializer. The POLO tracking program installed on the surface computer utilizes the strain signals and initializer readouts to compute the path of the penetrometer tip. The tracking data are updated at the end of 1 meter shoves. Figure 2 shows a sample of the tracking data. The data shows the X and Y coordinates of the tip on a reference circle and the Z coordinate along a depth bar. The origin of the reference coordinate system is at the point of insertion of penetrometer rods into the ground. X and Y are orthogonal axes on a horizontal

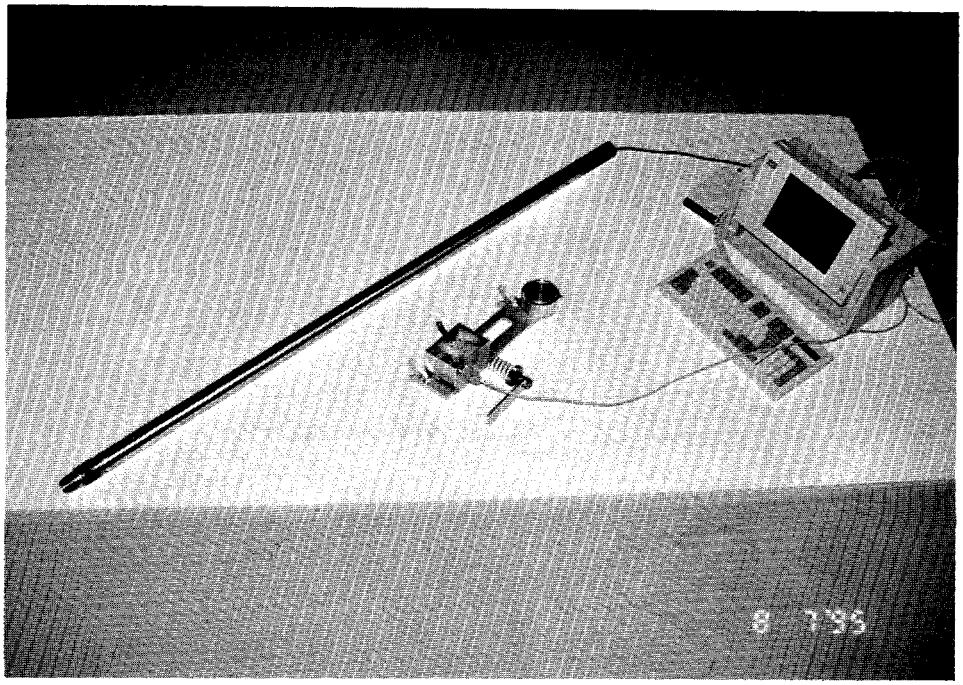

Figure 1. POLO system components.

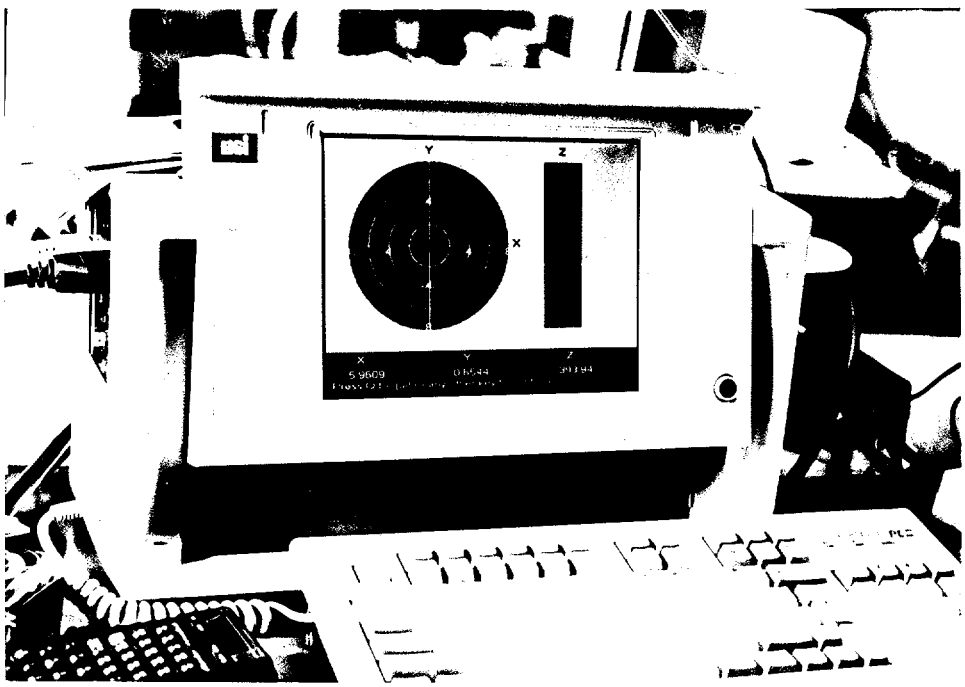

Figure 2. Sample tracking program output.

plane and the Z axis is a vertical axis passing through the point of insertion.

Field tests were performed in order to test POLO within the confines of a SCAPS truck and to familiarize the SCAPS operator with the use of POLO. Figure 3 shows the POLO computer inside the operator compartment of the SCAPS truck and Figure 4 shows POLO initialization in progress.

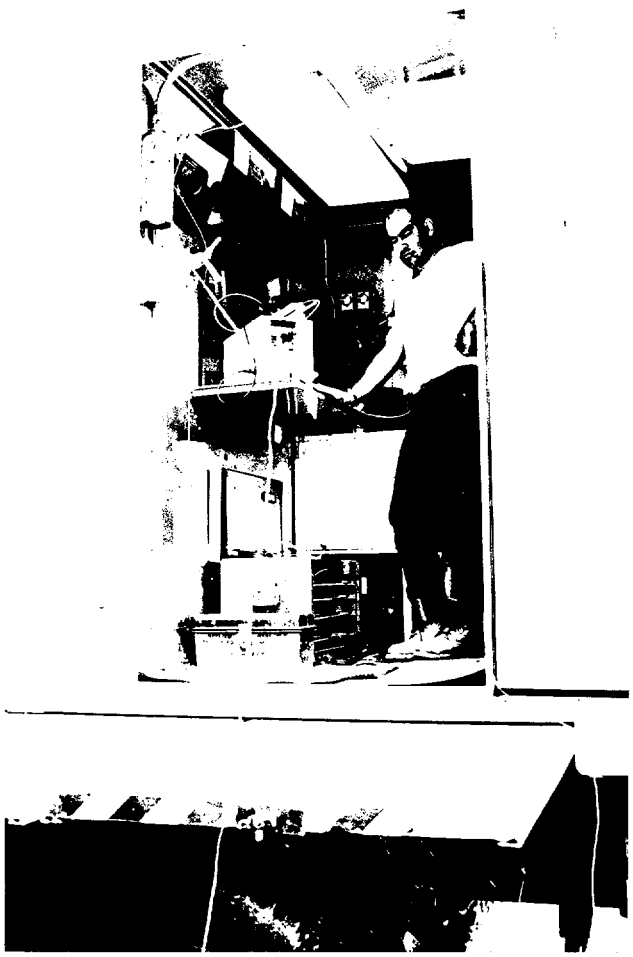

Figure 3. POLO computer inside SCAPS truck.

The results of SCAPS field tests indicated that POLO fits within the confines of the penetrometer truck and does not hinder the normal operations of the truck. At present, commercial POLO systems are available for sale to DOE contractors and commercial penetrometer truck manufacturers and operators.

Steering Tip Analysis and Prototype Manufacture

Analysis and Laboratory Test Currently, penetrometer rods are passive devices used to deliver a set of sensors to a desired underground destination but with no ability of on-line trajectory alteration to correct for course alteration due to unforeseen obstacles. Upon successful completion of this contract, future penetrometer systems will include a steering mechanism, permitting maneuvering of the penetrometer tip. Prior to the development of such a system for commercial applications, a laboratory study was performed to identify system parameters, tool configuration, and operational procedures. The primary purpose of the study was to show that tip maneuver is possible, and to determine procedural guidelines and operational boundaries. In the following paragraphs, a description of the steering methodology is provided. The description includes penetrometer rod and tip modeling, simulation of the penetration process in terms of tip trajectory, and sizing of the force-couple system associated with the penetration process. Laboratory test results validate the theoretical model, test data are compared to simulation results and the prototype steering tip capabilities are demonstrated.

Steerability of a penetrometer may be defined as the ability to change the curvature of the rod and the orientation of its bending plane in real-time in order to achieve a prescribed penetration path. Steering can be achieved by the application of a transverse force to the front end of the rod. Generation of such a force may be

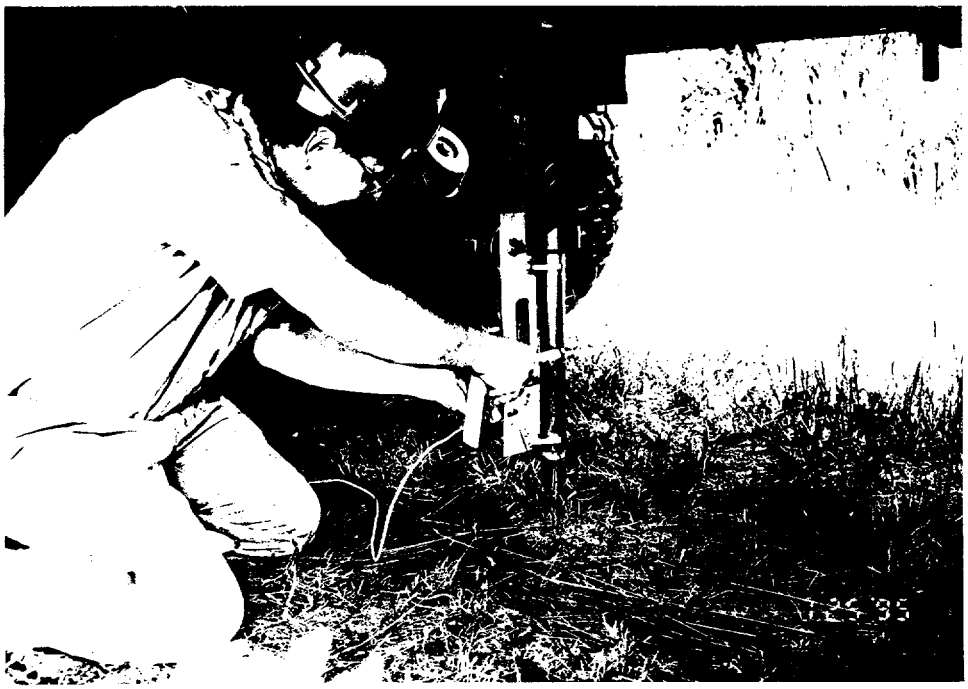

Figure 4. POLO initialization in progress.

accomplished by a directional actuator in the form of a wedge or an oblique conical tip. The intensity of the force depends on the system parameters associated with the penetration process. Some of these parameters are related to the soil properties such as density, angle of internal friction, angle of friction between the soil and steel (skin friction), and point bearing capacity of the soil. Other system parameters are related to the rod material and diameters, the tip geometrical configuration, and penetration process dynamics. An analytical model was employed for a preliminary study and simulation of the rod steering mechanism. For simplicity enhancement, the mathematical model used in this simulation represented a two-dimensional domain and was based on incremental insertion of a planar penetrometer rod equipped with a planar directional wedged tip.

The lateral deflection of each element was modeled as a beam in accordance with the "simple beam theory". The simulation generated the penetrometer rod trajectory and also computed the related force-couple history at the insertion point. A cantilever beam, shown in Figure 5, was selected as the fundamental element of the trajectory calculations and the deflection and rotation of its free end were calculated as a function of soil properties, rigidity of penetrometer rods and the tilt angle of the penetrometer tip.

In Figure 5, α is the wedge slope angle at the tip, δ is the friction angle between the soil and the beam material, Q_p is the tip point force, and q_p and q_0 are the passive and at-rest distributed skin forces per unit length, respectively [2]. The modeled trajectory is an evolution of sequential additions of one beam to another in a tail-to-head fashion as depicted in Figure 5.

Applying soil mechanics principles, the distributed normal and skin friction forces were

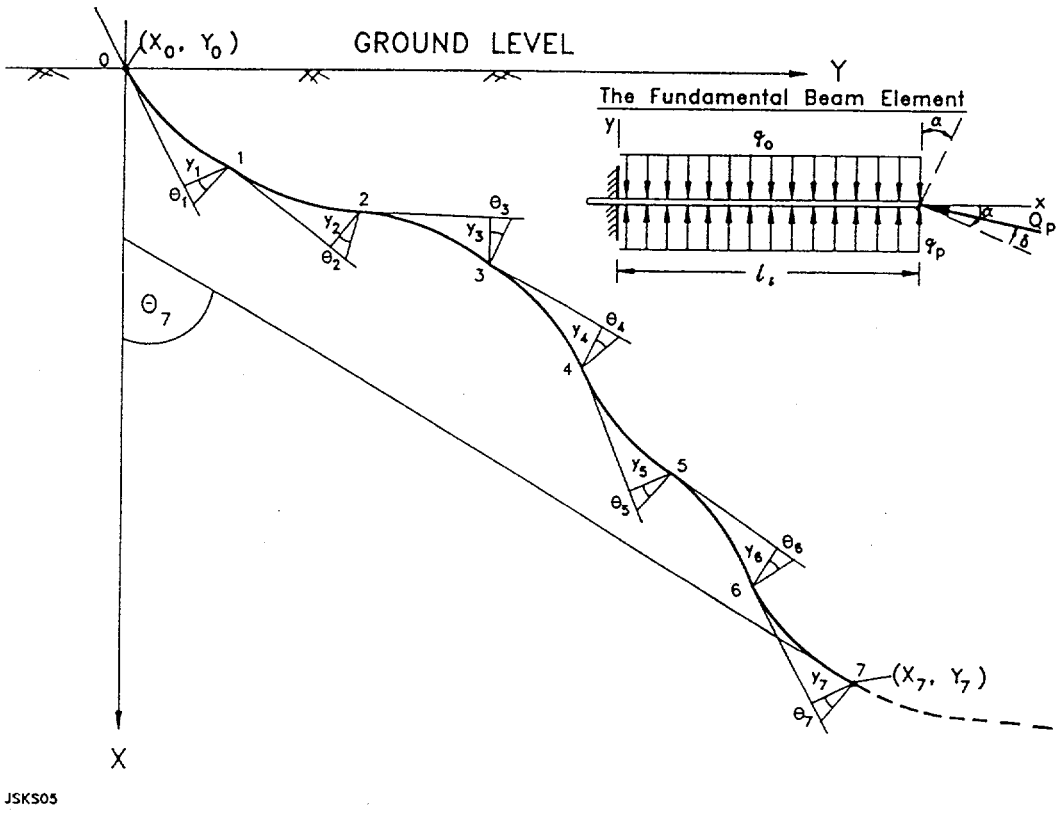

Figure 5. Penetrometer trajectory simulation model.

calculated along the penetrometer rod as well as the point force at the rod tip [2], [3]. The following parameters were selected for simulation

Soil Parameters:

soil density	120 lb/ft^3
angle of soil internal friction	35°
angle of soil-steel surface friction	23°

Penetrometer rod parameters:

outer diameter	1.75 in
inner diameter	1.00 in
modulus of elasticity	28*10^6 psi

The two-dimensional trajectory was generated by the deflected tip force. In this study, the selected tip angle α was fixed in magnitude for a particular trajectory but its polarity could be changed from $+\alpha$ to $-\alpha$ due to a tip command. In addition to trajectory generation, the simulation also computed the force-couple system at the insertion point, (the system origin). Components of the force-couple are the reaction shear force perpendicular to the rod axis, the normal "push" force along the rod axis of symmetry , and the reaction couple. The force-couple calculation for the entire insertion process provides the instantaneous reaction components as a function of the penetration depth that must be supported by the penetrometer insertion equipment.

A set of laboratory experiments was performed to test steerability capabilities of directional tips and also to validate the simulation model. Such validation will enhance confidence in the model and methods used, permitting the

extrapolation of test and simulation results to real-time field work. Two phases of experiments were conducted. In the first, the test bed was constructed as a two-dimensional space to fit a two-dimensional rod and tip configuration. This reduced complexity arrangement allows comparison of test data to simulation results, as well as a preliminary validation of the steerability concept and capabilities. In the second phase of the experiment, the test bed was constructed as a three-dimensional space where a test rod simulating a penetrometer rod was tested for steerability. In both cases, the stiffness of the rod specimen was reduced so as to permit development of observable lateral displacements in the limited space of the laboratory environment.

Figure 6 depicts test results, where a rod with a 5° wedge angle was pushed into wet sand under a constant tip command. Comparison between simulation results and test data, shown in Figure 6, reveals good agreement. The departure of the test data from the simulation output toward the tip of the rod, shown in Figure 6, is mainly due to the proximity of the tip to the sandbox boundaries.

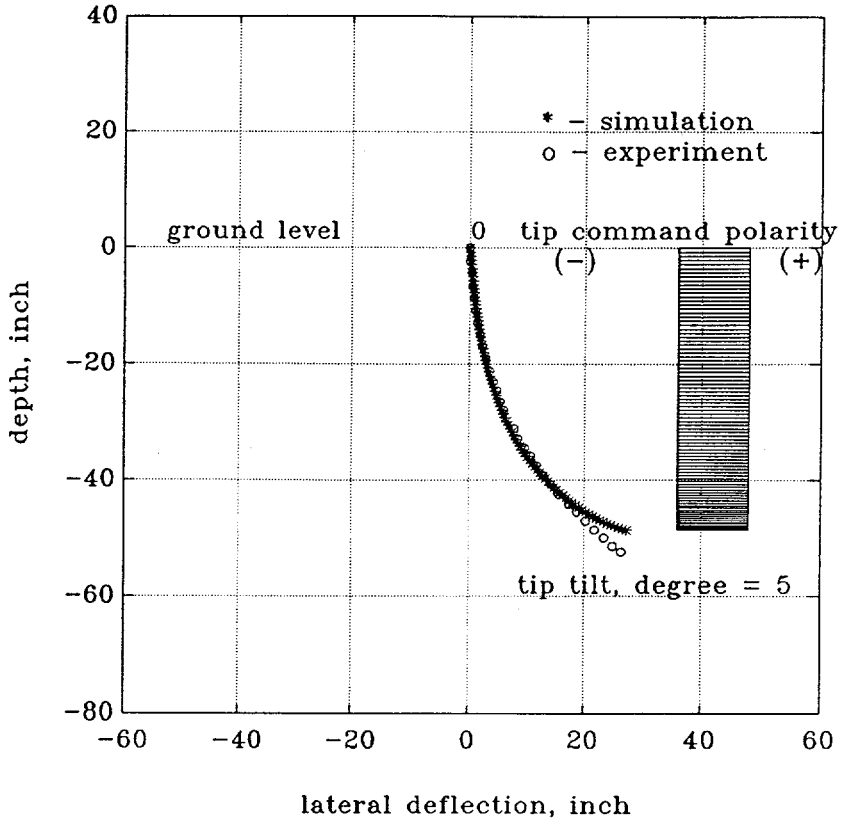

Figure 6. **5° wedge angle with constant tip command: trajectory -- comparison between simulation results and test data.**

In another case, shown in Figure 7, the rod with a 5° wedge angle was pushed into wet sand under a variable tip command. At about 18 inches deep, the rod was carefully pulled out all the way and then returned reversed, to reflect a change in tip command polarity from +5° to -5°. Also for this case, comparison between simulation results and test data, shown in Figure 7, reveals good agreement. Again, the departure of the test data from the simulation output toward the tip of the rod, shown in Figure 7, is mainly due to the proximity of the tip to the sandbox boundaries.

Upon completion of the 2D tests, the sandbox was extended and tests were carried out in three dimensions using a cylindrical specimen with a 5° oblique cone as shown in Figure 8. Experimentally observed deflections are compared with simulation results in Figure 9. In Figure 10 the normal forces measured during the experiment are compared with those predicted by the simulation model.

The simulation study and laboratory test results provide an insight into the directional penetrometer technique and a preliminary parameter evaluation methodology. Test data collected at the sandbox experimental facility were used to establish initial guidelines for directional penetration. The results of the laboratory steering tests led to two important conclusions. First, it was shown that it is possible to reverse the direction of travel of the penetrometer rod by changing the tilt angle of the tip. Second, the simulation model predicted deflections and force levels accurately. As a result, a very useful tool is now available for designing of the prototype and full-scale steering tips.

Prototype Steering Tip Manufacture

Steerability is defined as the ability to change the curvature of a penetrometer rod and the orientation of its bending plane in real-time. Two main factors affect the ability to steer a penetrometer rod toward a prescribed target. One is the ability to generate a transverse bending force of a desirable magnitude at the penetrometer tip; the other is the ability to change its orientation with respect to the rod body so as to achieve tip spatial maneuverability. To this end, several design options were considered, some of which were of the passive tip configuration while others were associated with active tip mechanisms. All options considered for transverse force generation involved tips formed as a simple wedge or an oblique cone.

Using the passive tip approach, a fixed tip configuration is installed. Pushing of the penetrometer rod with such a tip generates rod deflection constantly. In order to reach a specified target, on-line tip position detection coupled with continuous reorientation of its transverse bending force is essential. Obviously, these activities must be commanded from the ground surface. This requires the application of an increasing continuous axial torque to the entire penetrometer rod system. In long pushes, the constant reorientation of the tip from the surface can slow down the penetration process considerably.

The active tip approach involves a mechanical tip installed at the rod front end that can be actuated to turn or change its position through signals sent from the surface. A tip for this purpose will have many mechanical parts and will require an umbilical for the actuation signals. Because of the vibratory nature of the penetration process, a mechanical tip with many parts is susceptible to breakdown and fatigue failure of components and connections. In addition, the actuation signal umbilical occupies a fairly large volume inside the penetrometer

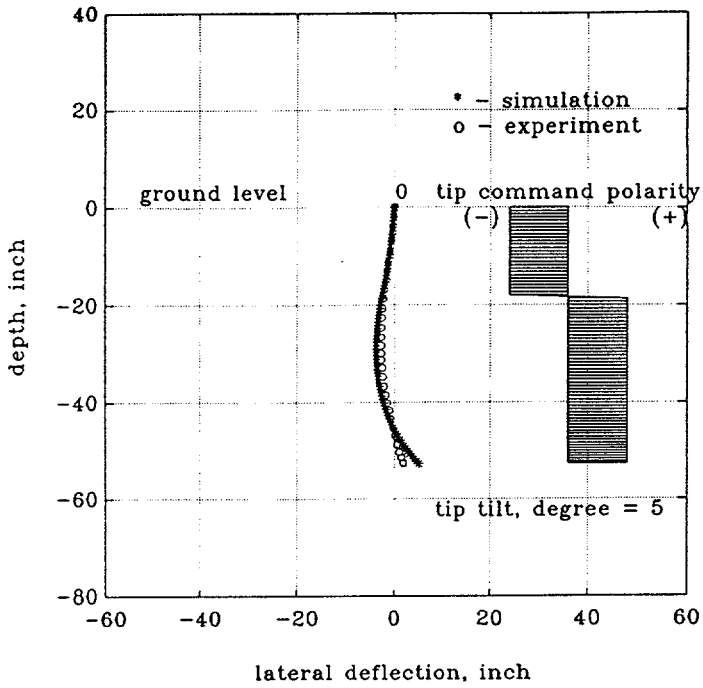

Figure 7. **5° wedge angle with variable tip command: trajectory -- comparison between simulation results and test data.**

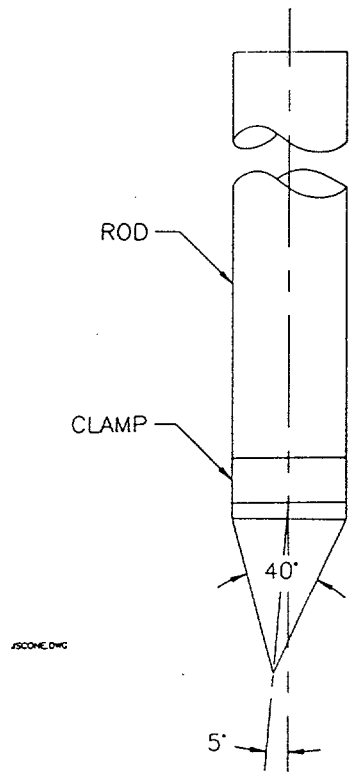

Figure 8. Cylindrical specimen with 5° oblique cone.

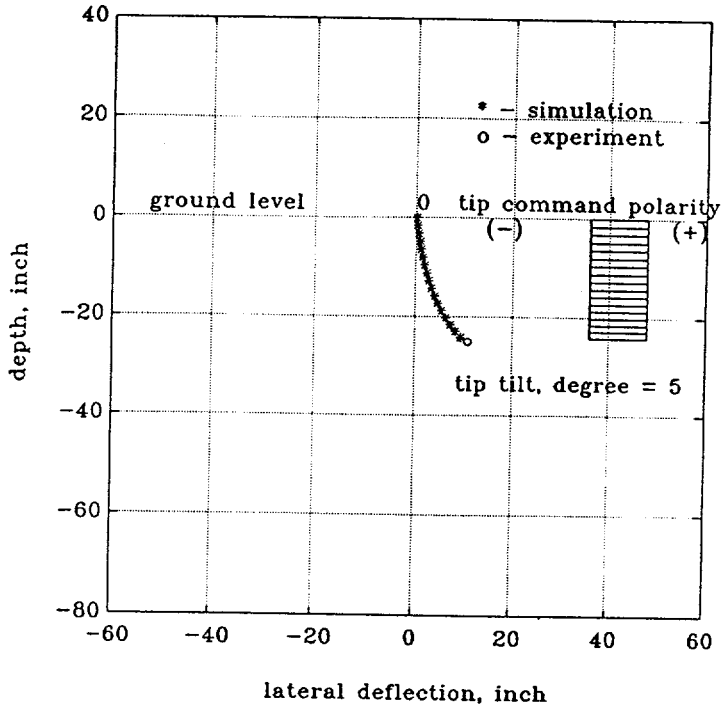

Figure 9. 5° cone angle: trajectory comparison between simulation results and test data.

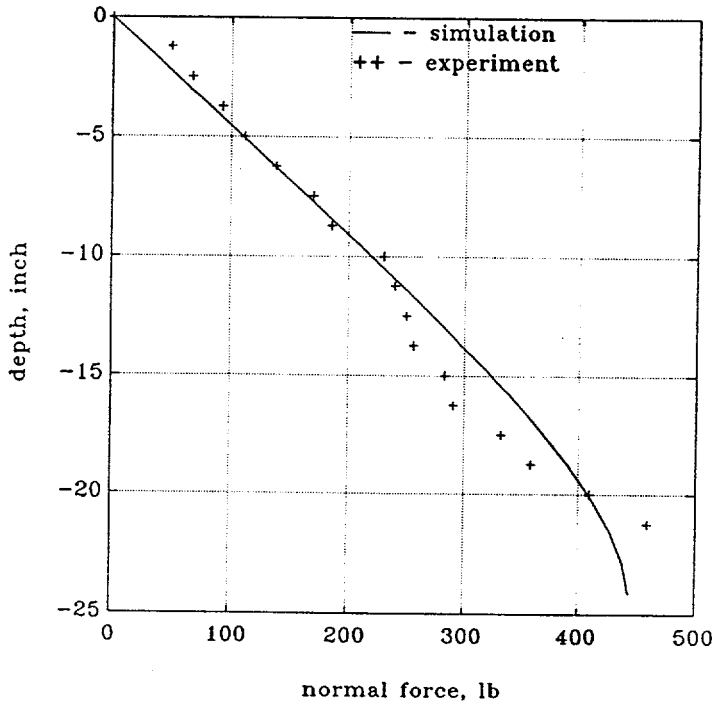

Figure 10. 5° cone angle: normal force comparison between simulation results and test data.

rods, leaving little or no space for the umbilicals of the environmental sensing instruments.

Realizing the limitations of the fully passive or fully active steering tips, it was decided to use a semi-passive tip developed and patented by Foster-Miller Incorporated for ground piercing applications. The semi-passive tip shown in Figure 11 can be pushed into the ground either in a symmetrical configuration, as shown, or in an asymmetrical fashion as shown in Figure 12. The change from symmetrical to asymmetrical configuration is achieved through rotation of the penetrometer rod by 180°. The stabilizer fins at the tip keep its position locked until another 180° rotation is performed from the surface. The advantages of the semi-passive tip lie in its mechanical simplicity and the limited need for re-orientation from the surface, making it easy to use and control in the field. If an unexpected barrier is encountered, the penetrometer tip can be drawn back and redirected to maneuver around the barrier.

The simulation model described earlier was used to determine the tip cone geometry and its angle of attack that would limit the rod bending below the failure margin. A prototype steerable tip was then manufactured and tested in the field. Two sets of tests were performed in two different soils. The tests were carried out at two sites, Ft. Belvoir (1), and Fredericksburg (2), Virginia, using a field POLO module and the META-DRILL vibratory penetrometer system purchased for this project. This equipment is shown in Figure 13. The soil at site 1 consisted of very stiff clay, whereas the soil at site 2 consisted of medium dense sand. The first objective of these tests was to verify that tip configuration changes from symmetric to asymmetric upon a 180° rotation of the rods from the surface. The second objective was to determine the radius of curvature of the bends generated by the steerable tip in different soils.

The tests were begun by setting up the META-DRILL rig at each site and connecting the POLO unit equipped with the steerable tip to the vibratory head. Initially the steerable tip was positioned in a symmetric position (for straight pushes). After about six inches of penetration the drilling operation was stopped and the POLO unit was turned 180° counterclockwise, activating the tip to its asymmetric configuration for a curved push. The POLO tracking program was then turned on and penetrometer operation resumed. The tests were completed after 74 inches of penetration in stiff clay and 173 inches in medium dense sand.

Table 1 shows the radius of curvature of penetrometer rods due to steering in each of the two sites. The radius of curvature for each test was obtained by using the POLO predicted coordinates of the tip. According to Table 1 the radius of curvature obtained in stiff clay was 114 ft, whereas that obtained in sand was 90 ft. It is worth noting that the initial inclination of POLO was vertical and all the tip displacements were due to bending of the rods by the steerable tip.

Penetrometer Rod Joints

Penetrometer joints commercially used today are designed for penetrometer rods inserted in straight trajectories. A typical penetrometer joint is shown in Figure 14. Under straight insertion conditions, the axially applied compression load is transmitted through the shoulders of the mating rod sections. If the joint is subjected to bending due to steering of the penetrometer tip or due to encounter with geologic anomalies, several weaknesses in the joint design may cause failure or permanent damage in the joint.

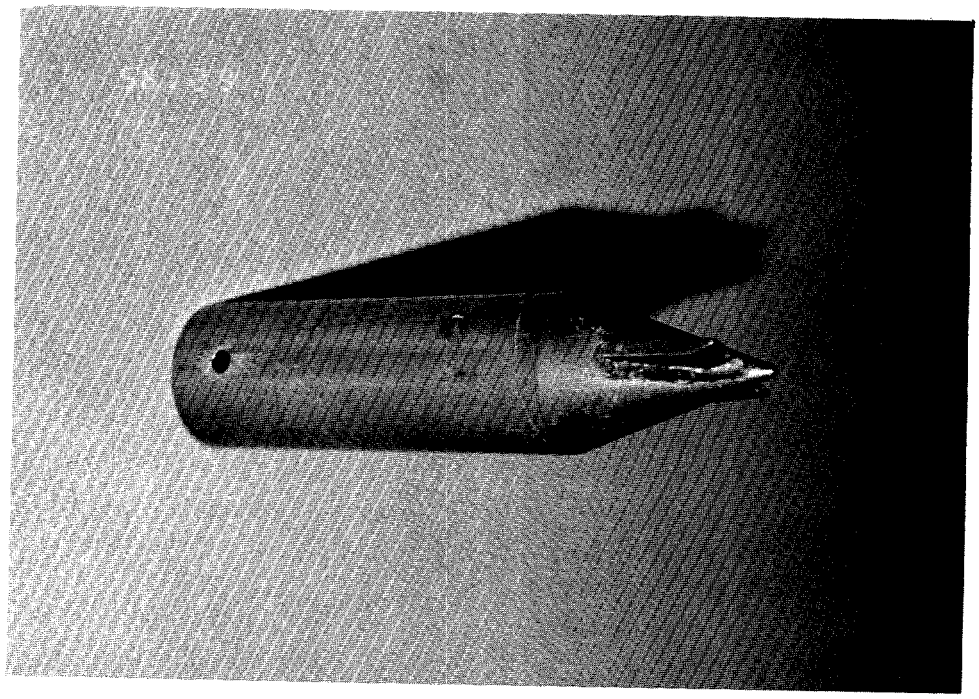

Figure 11. Semi-passive steering tip in a symmetrical configuration.

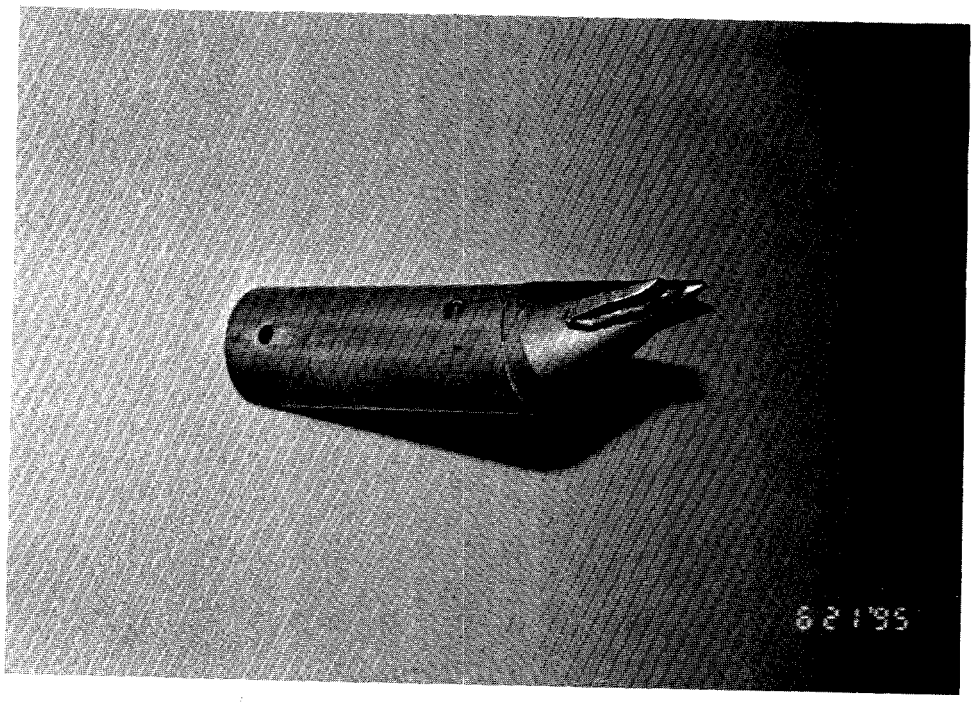

Figure 12. Semi-passive steering tip in an asymmetrical configuration.

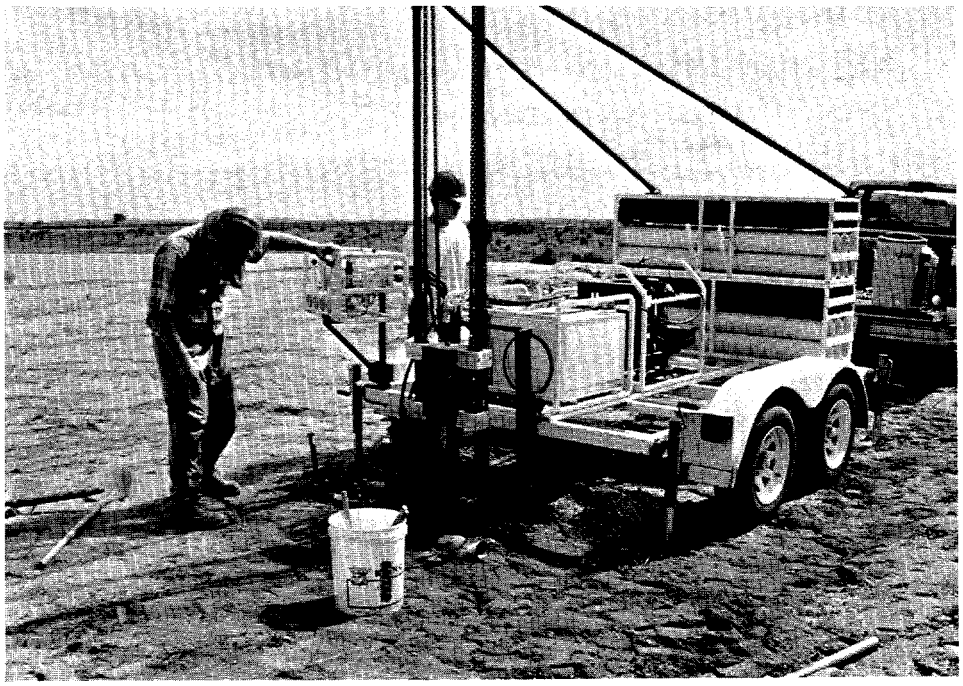

Figure 13. Field testing with the META-DRILL.

Table 1. Steerable tip field test result.

Site	Soil Formation	Radius of Curvature
Ft. Belvoir	Stiff Clay	114 ft
Fredericksburg	Medium Dense Sand	90 ft

One of the weaknesses of a typical joint in bending is the shoulder contact. As shown in Figure 14, thread stresses are intensified in one region of the bend. In addition, the shoulder bearing load is decreased in the tensile region of the bend, and at small axial compressive loads this part of the shoulder may actually separate, resulting in a reduced section modulus. On the other hand, the opposite part of the shoulder will be subjected to increased bearing stresses which can permanently damage the joint.

Another problem with the use of commercial penetrometer joints in a steerable system is loosening of the joints under counterclockwise steering torques. This can happen when the rods are turned from the surface to steer the tip and the steering torque is applied in the opposite direction to that for tightening the joint. To overcome the problems associated with standard joints, a locking joint concept developed earlier by UTD was adapted for the steerable vibratory penetrometer system.

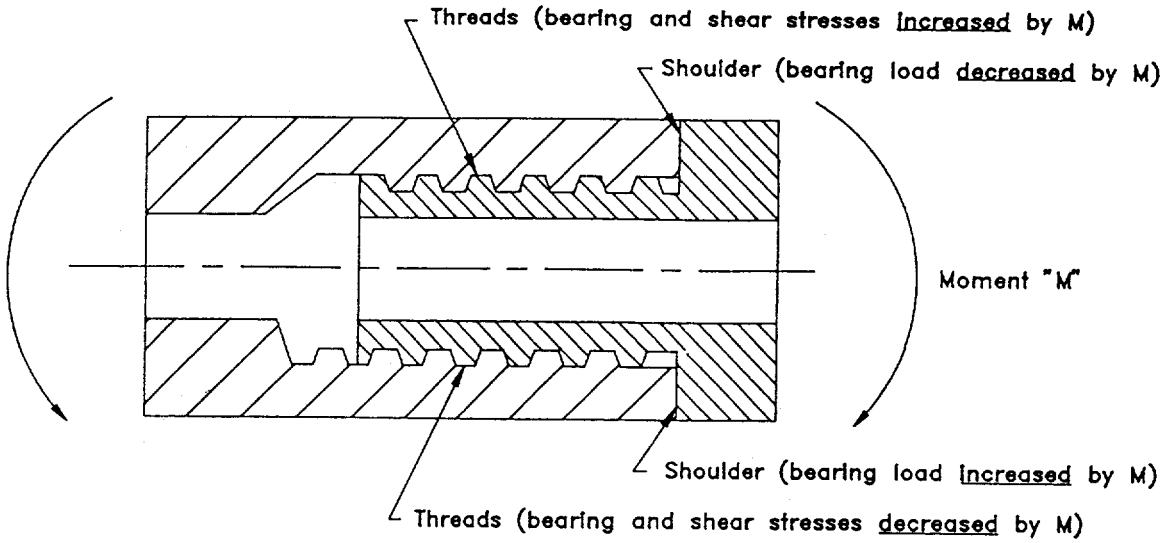

Figure 14. Off-the-shelf commercial penetrometer joint.

To verify the performance of the joint for steerable penetrometers, a set of new joints was machined and tested in a test frame built especially for this purpose. The test frame shown in Figure 15 applies bending moment and axial load simultaneously to a 28 inch long simply supported rod. The joint loadings can be varied independently.

Figure 16 is a summary of test results performed on four different rods made of the same material. In order to establish a baseline, one of the rods tested was jointless. The other three specimens were jointed rods, one using a commercial penetrometer joint, another using the new steerable joint, and the third using the new steerable joint combined with its joint locking mechanism. According to Figure 11, the jointless rod started yielding at a deflection of 0.21" which corresponds to a radius of curvature of 29'.

The curve for the commercial joint had an initial dogleg at 0.07" deflection or 85' radius of curvature. In practice it is common to keep the radius of curvature of commercial rods above 100' to avoid damage to the joints. Another observation related to the shouldered joint is the general yielding of the metal which starts at 0.17" of deflection or 35' radius of curvature. The curve for the steerable joint is very similar to that of the jointless rod except that the joint starts yielding at 0.19" of deflection or 31.5' radius of curvature. In contrast with the commercial joint, the steerable joint does not go through a dogleg phase. Bending test results on the steerable joint equipped with a locking mechanism (Figure 16) indicated that for all practical purposes its performance approached that of the jointless rod.

In addition to bending tests, laboratory torque and field performance tests were performed on the locking joints. The design torque for the locking joint had been selected at 9,000 in-lbs. The torque test was performed at 9,130 in-lbs without any observable damage to the locking joint mechanism.

The field test carried out on the locking joint consisted of vibratory testing using the META-DRILL. The purpose of this test was to

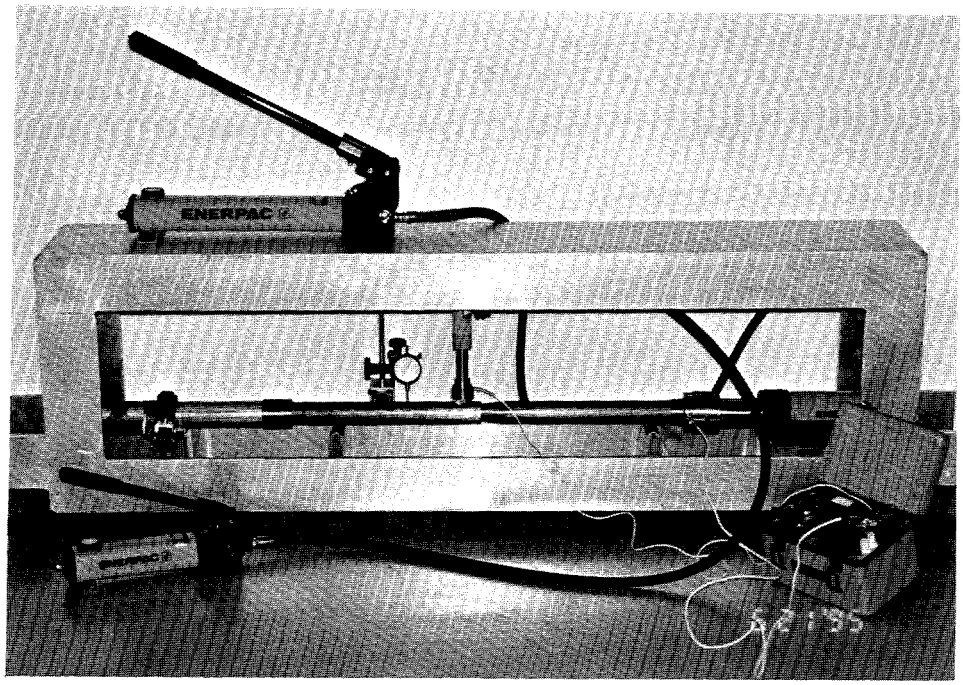

Figure 15. Test frame for laboratory testing of joints.

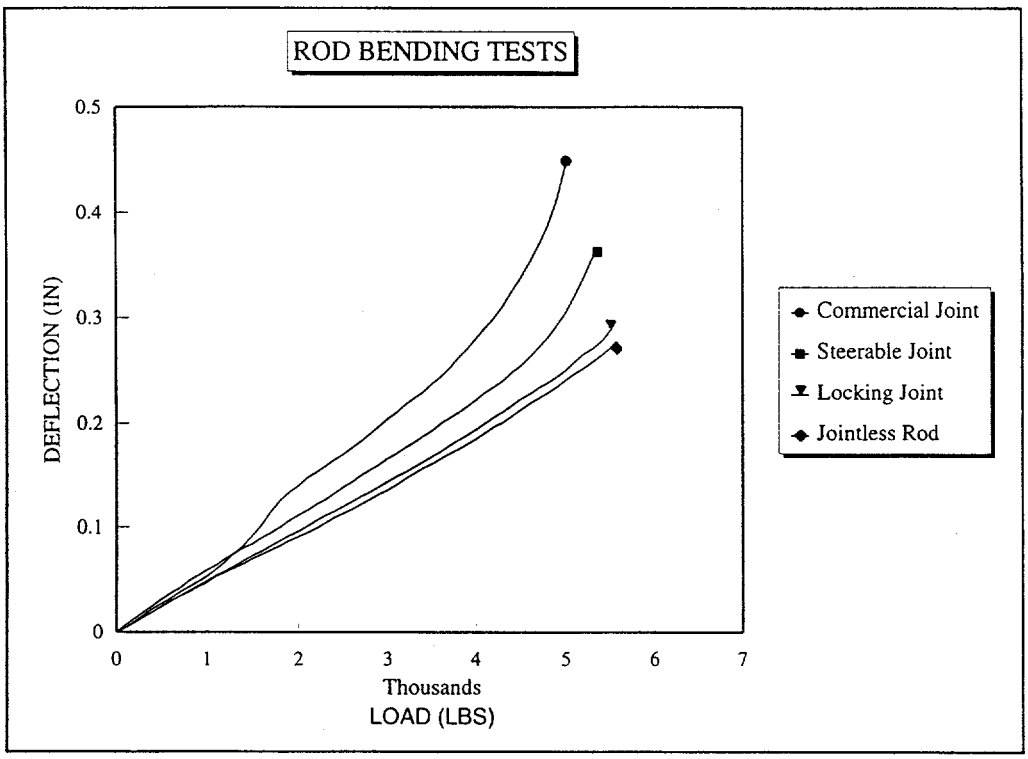

Figure 16. Results of laboratory tests on four rods.

push the locking joint into the ground and to examine its performance under the harsh vibratory environment. After several minutes of vibrations into the ground the locking joint was brought to the surface and examined. The examination indicated that with the exception of a minor component that had come loose, the entire assembly had remained intact and had performed as expected.

Tests For Effects Of Vibrations On Resisting Forces

In normal penetrometer applications the resisting forces exerted by the soil on penetrometer rods depend on the geometry of the rods, and the type of soil. However, under vibratory loading the constant motion between penetrometer rods and the soil reduces the magnitude of the resisting forces because a dynamic rather than a static coefficient of friction applies, which in turn increases depth of penetration for comparable thrust levels. To test this hypothesis, two sets of field tests were carried out with the META-DRILL rig at the aforementioned sites 1 and 2, where site 1 consisted of very stiff clay and site 2 of medium dense sand.

In these tests, first the hydraulic thrusters of the META-DRILL rig alone were used to thrust penetrometer rods into the ground. The vibratory drive was off during this stage of the test. The length of rods pushed into the ground was 32.5" in clay and 24" in sand under a thrust of 1500 lbs. After the rods stopped under the 1500 lbs of thrust, the vibratory drive was turned on, which made it possible to push additional length of rod into the ground equal to 53" in clay and 276" in sand.

The frequency of vibrations in clay was approximately 100 Hz which translates to 1875 lbs of dynamic load. In sand the frequency of vibrations was about 140 Hz which translates to 3,675 lbs of dynamic load. A review of the test results indicated that when the vibrations were turned on, the total thrust force was increased by 125% in clay, but the length of rods pushed increased by 163%. This is an indication that the dynamic nature of the load affected the soil-rod interaction. In sand the effects of vibrations were more pronounced, because by increasing the total force from 1,500 lbs to 5,175 lbs (1,500 lbs static + 3,675 lbs dynamic), namely, an increase of 245%, the length of rods pushed into the ground was increased by 1,150%.

The effects of vibrations were quantified in more detail by applying principles of soil mechanics. In this approach, physical properties of the soils were back calculated from the lengths of rod pushed into the ground by hydraulic thrusting alone. Then the resisting forces for the entire penetration length in clay and sand were calculated and compared with the actual forces, static and dynamic, exerted in the field. The results are shown in Table 2. According to this table the resisting forces under vibratory loading were reduced by 15% in the very stiff clay soil and 48% in medium dense sand.

Application

A steerable, vibratory penetrometer system has many applications in the environmental clean up area. The system can be used in conjunction with POLO to characterize and remediate contaminant plumes at specific locations under buildings and buried storage tanks. It is insensitive to the presence of magnetic or gravitational influences. Because of its light weight the system can also be used over shallow buried storage tanks. These applications will reduce the cost of clean up because of more focused characterization and remediation. They

Table 2. Reduction of resisting forces due to vibrations.

Soil Formation	Penetration Length (ft)	Required Thrust (Static Conditions)	Applied Thrust (Static + Dynamic)	% Reduction
Very stiff clay	7.2	3,942 lbs	3,375 lbs	15%
Med-Dense Sand	25.0	10,052 lbs	5,175 lbs	48%

also provide for in-situ remediation in locations that are not reachable with the current penetrometer technology.

Ongoing and Future Activities

At present, the Phase 2 work, which consists of integrated design of the full-scale steerable vibratory penetrometer system is underway. This work is expected to be completed in the winter of 1996. Upon completion of the Phase 2 work, and award of the Phase 3 option, the full-scale system will be manufactured and field tests will be performed to demonstrate the capabilities of the system. The field tests are expected to occur in the fall of 1996.

References

[1] Hutzel, W.J., and A. Amini, Innovative Directional and Position Specific Sampling Technique, Proceedings of Opportunity '95 - Environmental Technology Through Small Business, November 1994.

[2] Das, B.M., PRINCIPLES OF FOUNDATION ENGINEERING, 2nd edition, PWS-KENT Publishing Company, Boston, 1990.

[3] Bowles, J.E., FOUNDATION ANALYSIS AND DESIGN, 2nd edition, McGraw-Hill Inc., 1977.

Acknowledgments

The work presented in this report was sponsored by the Department Of Energy (DOE), Morgantown Energy Technology Center (METC), Office of Technology Development (OTD). Mr. Carl Roosmagi of DOE, METC, Laramie office was the contract monitor. Mr. Roosmagi's continued support is greatly appreciated. Mr. John Hall of the Ditch Witch of Georgia played a key role in successful field tests performed at his site in Atlanta, Georgia. Mr. David Timian and Mr. Wayne Russell of Applied Research Associates, Inc. provided access to the DOE SCAPS truck and assisted in the POLO field tests. In addition to authors, the technical team working on this project included Dr. Eugene Foster, Mr. Shervin Hojati, Mr. Gregory Boyd, and Mr. Jim Laporte. The administrative staff at UTD who was instrumental in keeping track of contractual obligations, finances of the project, and production of timely reports included Mrs. Carol Horowitz, Mrs. Pam Burrows, Mrs. Jane Whitten, and Ms. Maxine Emory.

4.5 Road Transportable Analytical Laboratory (RTAL) System

Stanley M. Finger (eco@annap.imfi.net; 410-757-3245)
Engineering Computer Optecnomics, Inc.
1356 Cape St. Claire Road
Annapolis, MD 21401

ABSTRACT

U.S. Department of Energy (DOE) facilities around the country have, over the years, become contaminated with radionuclides and a range of organic and inorganic wastes. Many of the DOE sites encompass large land areas and were originally sited in relatively unpopulated regions of the country to minimize risk to surrounding populations. In addition, wastes were sometimes stored underground at the sites in 55-gallon drums, wood boxes or other containers until final disposal methods could be determined. Over the years, these containers have deteriorated, releasing contaminants into the surrounding environment. This contamination has spread, in some cases polluting extensive areas.

Remediation of these sites requires extensive sampling to determine the extent of the contamination, to monitor clean-up and remediation progress, and for post-closure monitoring of facilities. The DOE would benefit greatly if it had reliable, road transportable, fully independent laboratory systems that could perform on-site the full range of analyses required. Such systems would accelerate and thereby reduce the cost of clean-up and remediation efforts by (1) providing critical analytical data more rapidly, and (2) eliminating the handling, shipping and manpower associated with sample shipments.

The goal of the Road Transportable Analytical Laboratory (RTAL) Project is the development and demonstration of a system to meet the unique needs of the DOE for rapid, accurate analysis of a wide variety of hazardous and radioactive contaminants in soil, groundwater, and surface waters. This laboratory system has been designed to provide the field and laboratory analytical equipment necessary to detect and quantify radionuclides, organics, heavy metals and other inorganic compounds. The laboratory system consists of a set of individual laboratory modules deployable independently or as an interconnected group to meet each DOE site's specific needs.

After evaluating the needs of the DOE field activities and investigating alternative system designs, the modules included in the RTAL system are:

- Radioanalytical Laboratory
- Organic Chemical Analysis Laboratory
- Inorganic Chemical Analysis Laboratory
- Aquatic Biomonitoring Laboratory
- Field Analytical Laboratory
- Robotics Base Station
- Decontamination/Sample Screening Module
- Operations Control Center

Each module provides full protection for operators and equipment against radioactive particulates and conventional environmental

Research sponsored by the U.S. Department of Energy's Morgantown Energy Technology Center, under Contract DE-AC21-92MC29109 with Engineering Computer Optecnomics (ECO), Inc., 1356 Cape St Claire Road, Annapolis, MD 21401; 410-757-3245; Telefax 410-757-8265.

contaminants. This is especially important in areas where radioactive particulates from environmental matrices, e.g. soils, aerosolized by wind or volatile chemicals are present. These contaminants can adversely affect sensitive chemical and radiochemical analyses as well as potentially being harmful to personnel.

The goal of the integrated laboratory system is a sample throughput of 20 samples per day, providing a full range of analyses on each sample within 16 hours (after sample preparation) with high accuracy and high quality assurance. This is much shorter than the standard 45 day turnaround time typical of commercial laboratories. In addition, shipping samples off-site is a time-consuming, paperwork-intensive process, leading to additional delays in sample analyses. The focused project support provided by the RTAL is designed to significantly accelerate characterization and remediation efforts of critical restoration projects.

A prototype RTAL system was constructed for demonstration at the DOE's Fernald Environmental Management Project (FEMP). It is being deployed at FEMP's OU-1 Waste Pits. Its performance will be evaluated with samples from these pits and with other environmental samples from the FEMP site. The prototype RTAL system will consist of 5 modules - Radioanalytical Laboratory, Organic Chemical Analysis Laboratory, Inorganic Chemical Analysis Laboratory, Aquatic Biomonitoring Laboratory, and Operations Control Center. The U.S. Army Biomedical R&D Laboratory has volunteered to provide the Inorganic Chemical Analysis Laboratory and Aquatic Biomonitoring Laboratory as part of its concurrent demonstration of Integrated Biological Assessment (IBA) technology. The demonstration of the prototype RTAL is scheduled to start late in the 1st Quarter of FY96.

The RTAL will provide the DOE with significant time and cost savings, accelerating and improving the efficiency of clean-up and remediation operations throughout the DOE complex. At the same time, the system will provide full protection for operating personnel and sensitive analytical equipment against the environmental extremes and hazards encountered at DOE sites.

INTRODUCTION

The U.S. Department of Energy (DOE) facilities around the country have, over the years, become contaminated with radionuclides and a range of organic and inorganic wastes. Many of the DOE sites encompass large land areas and were originally sited in relatively unpopulated regions of the country to minimize risk to surrounding populations. In addition, many times wastes were stored underground at the sites in 55-gallon drums, wood boxes or other containers until final disposal methods could be determined. Over the years, these containers have deteriorated, releasing contaminants into the surrounding environment. This contamination has spread, in some cases polluting extensive areas.

Remediation of these sites requires extensive sampling to determine the range of the contamination, to monitor clean-up and remediation progress, and for post-closure monitoring of facilities. Transporting these samples to a central laboratory, especially to one off-site, requires wipe tests for surface contamination before shipment and after receipt, specialized transportation containers and procedures (depending on the level of radioactivity present in the sample), and a substantial amount of additional paperwork. It can be very difficult and time-consuming to ship samples off-site from DOE facilities because of requirements established to ensure against inadvertent release of radioactive materials. The occasional improper shipment of radioactive materials from DOE facilities has led to periodic curtailment of all shipments to ensure that

proper shipping procedures are followed. Such curtailments can cause havoc to projects where accurate and timely sample analytical data is critical to decision-making and also because environmental samples degrade over time.

The DOE would benefit greatly from the use of reliable, road transportable, fully independent laboratory systems that could perform the full range of analyses required on-site. By focusing on high priority problems, such systems would accelerate clean-up and remediation efforts. They would provide critical analytical data more rapidly, and save money by eliminating handling, shipping and manpower costs associated with sample shipments.

The RTAL developed for the DOE is based on the earlier laboratories and operations control centers developed by Engineering Computer Optecnomics (ECO), Inc. for the U.S. Environmental Protection Agency, and the U.S. Departments of Defense and State. These include counter-terrorist systems for use in areas contaminated with chemical or biological warfare agents. The advances achieved in the development of these earlier systems have been incorporated into the development of the RTAL.

OBJECTIVE

The Road Transportable Analytical Laboratory (RTAL) Project covers the development and demonstration of a system to meet unique DOE needs for rapid, accurate analysis of a wide variety of hazardous and radioactive contaminants in soil, groundwater, and surface waters. This laboratory system is designed to provide the analytical equipment necessary to detect and quantify radionuclides, organics, heavy metals and other inorganics. The laboratory system consists of a set of individual laboratory modules deployable independently or as an interconnected group to meet each DOE site's specific needs.

The goal of the integrated laboratory system is a sample throughput of 20 samples per day, providing a full range of analyses on each sample within 16 hours (after sample preparation) with high accuracy and high quality assurance. This is much shorter than the standard 45 day turnaround time typical of commercial laboratories. In addition, shipping of samples off-site is a time-consuming, paperwork-intensive process, leading to additional delays in sample analyses. This focused attention on high priority needs can accelerate and improve the efficiency of clean-up and remediation operations. The RTAL will be synergistic with existing analytical laboratory capabilities by reducing the occurrence of unplanned "rush" samples which are disruptive to efficient laboratory operations.

PROJECT DESCRIPTION AND RESULTS

To meet the wide range of environmental analytical requirements at the DOE's facilities while retaining the flexibility for rapid, cost-efficient response, the RTAL was conceived as a series of individual modules that could be deployed individually or as an integrated group. After evaluating the needs of the DOE field activities and investigating alternative system designs, the modules to be included in the full RTAL are:

- Radioanalytical Laboratory
- Organic Chemical Analysis Laboratory
- Inorganic Chemical Analysis Laboratory
- Aquatic Biomonitoring Laboratory
- Field Analytical Laboratory
- Robotics Base Station
- Decontamination/Sample Screening Module
- Operations Control Center

Each module provides full protection for operators and equipment against radioactive particulates and conventional environmental contaminants. This is especially important in areas where radioactive particulates from

environmental matrices, e.g. soils, are aerosolized by wind or volatile chemicals are present. These contaminants can adversely affect sensitive chemical and radiochemical analyses as well as being potentially harmful to personnel.

Each module has the following features to ensure reliable, independent operation:

- Shock and vibration protected for road transport
- No Department of Transportation restrictions
- Filtration of incoming and exhaust air through HEPA filters
- Integral electrical generation system providing filtered power
- Uninterruptible power supply
- Heating, ventilation and air conditioning (HVAC) system capable of handling wide range of outside temperatures and humidities
- Controlled air flow from "clean" to "dirty" areas
- Insulation in walls, floor and roof
- Integral fuel tanks
- Rugged, redundant design for maximum availability
- Hardened equipment for maximum reliability
- Designed for long life
- Designed for minimum acquisition and maintenance costs
- Designed for ease of repair and maintenance
- Designed for ease of exterior decontamination
- Innocuous appearance to minimize public apprehension during transport and deployment

The continuous supply of electricity is critical to the reliability of the tests being performed. The loss of power would shut down the analytical equipment and support and control systems, critical for maintaining controlled experimental conditions. For this reason, an automatic switching circuit is provided for use when operating from an external power source. If the external power source fails, this circuit automatically starts the laboratory's electrical generator and switches all systems to this independent source of power, thus ensuring maintenance of experimental conditions.

Each module is housed in a standard 48 foot long by 8½ foot wide trailer to facilitate transport to the test sites. These units have no Department of Transportation restrictions on road transport. Wider trailers are considered "wide loads" which must have vehicular escorts, can not travel all roads, and must pay road use fees in most states. These restrictions limit the adaptability of extra-wide systems to meet the changing requirements across the DOE complex and adds significantly to their operating costs.

The use of a truck, with a dedicated engine, instead of a trailer for the laboratories was also considered. The use of a separate vehicle to move trailer-mounted modules results in higher system reliability and lower cost compared to the use of truck-mounted laboratories with a dedicated prime mover. Experience has shown that truck engines which are operated sporadically have much higher than normal breakdown frequencies. For example, the state of Maryland's truck-mounted air pollution laboratory underwent three engine overhauls within 8,000 miles of driving due to the fact that it was moved so infrequently. In addition, use of a separate prime mover saves the acquisition cost of the truck. Vehicles to move the trailers can be rented readily anywhere in the country. Since deployed modules will normally be at a single site for extended periods, the economics strongly favor setting up the modules on separate trailers rather than using a dedicated prime mover.

The chosen arrangement of RTAL modules closely follows the steps the samples and operating personnel will take, as shown in

Figure 1. The module closest to the contaminated area is the Decontamination/Sample Screening Module. This module is divided into two halves. The decontamination side is used to decontaminate personnel in protective gear who have been collecting samples or performing other duties in contaminated areas. The other side of the module is for screening of collected samples. Personnel, in appropriate protective gear, bring the samples to the sample pass-through (located on the side of the module closest to the contaminated area). The samples are passed directly into the hot cell inside the Sample Screening side of the module. The samples are screened for radiation level to determine handling requirements during subsequent testing. They are also subdivided for the analyses to follow.

The next modules behind the Decontamination/Sample Screening Module are the Robotics Base Station and the Field Analytical Laboratory. These modules provide robotically operated and hand-carried instrumentation for field determination of radioactive and chemical contamination levels. These modules are needed for initial mapping of large areas. The robotic systems, in particular, would include automated geographic positioning equipment to fix the location of each measurement. All data is transmitted to the computer in the Robotic Base Station for computerized mapping. The data provided by the robotic and field analytical systems would not meet the same high quality assurance and quality control standards as the samples analyzed in the RTAL modules. However, the data are very useful in determining the location of "hot spots," i.e. areas where personnel require protective ensembles.

The next set of modules are the four laboratories which are the heart of the RTAL system. These are the Radioanalytical, the Organic Chemical Analysis, the Inorganic Chemical Analysis, and the Aquatic Biomonitoring Laboratories. The subdivided samples from the Decontamination/Sample Screening Module are analyzed for specific analytes in the first three laboratories. The Aquatic Biomonitoring Laboratory is used for broad screening of hazardous contamination (radiological or chemical) using fish and amphibians as test organisms. Aquatic biomonitoring tests are used to detect the presence of ultra-low trace levels of contamination, i.e. below standard detection levels for specific analytes, and analytes for which there is no test. It can also be used to determine the absence of contaminants, providing a means for determining whether an environmental matrix is "clean."

The next module is the Operations Control Center, which serves as the coordinating "brain" for all RTAL operations. The entrance to the Operations Control Center provides a portal monitor for all personnel leaving the laboratory area. Even though great care will be taken to ensure that all personnel handling samples remain uncontaminated, a final check is important to ensure that there is no inadvertent contamination as a result of operations conducted within the RTAL area. If contamination is detected, a decontamination shower is located in this module adjacent to the frisking station.

This RTAL system configuration divides the overall area into three contamination zones. The first zone is the contaminated area where radioactive and chemical contaminants are expected. The second zone is the laboratory modules where contaminated samples are handled in hoods, on bench tops, and in the analytical equipment. Although these areas are designed to contain contaminants, there is always a small risk of inadvertent release. The third zone is the contaminant-free zone beyond the portal monitor in the Operations Control Center.

Personnel and samples exiting the contaminated zone must go through the

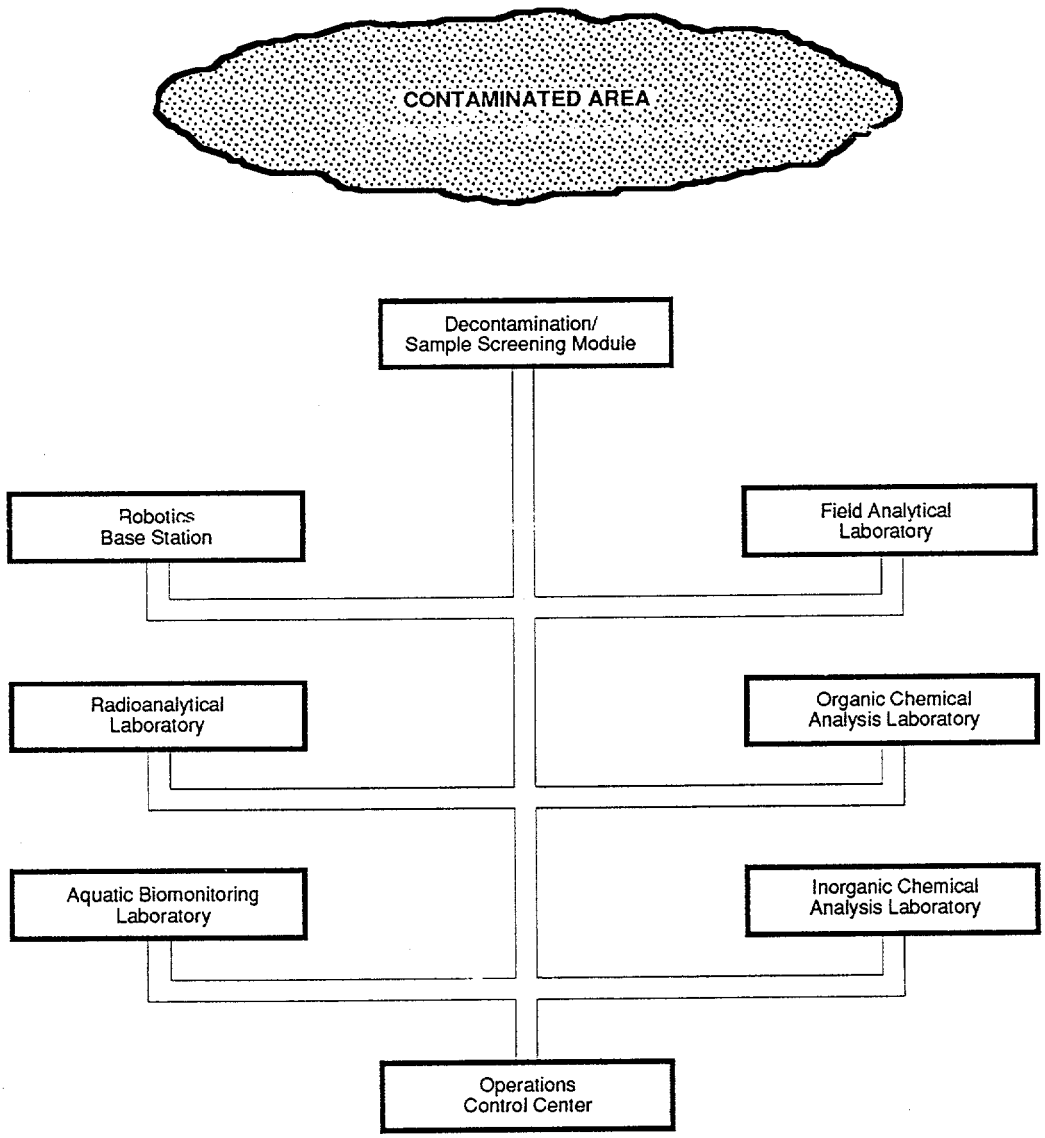

Figure 1. Road Transportable Analytical Laboratory Integrated Complex

Decontamination/Sample Screening Module. This ensures that the only contamination entering the second zone is contained within the samples. All personnel exiting the second zone must go through the Operations Control Center frisking station to ensure they are contaminant-free. This arrangement minimizes contaminant risks for all personnel, both within and outside the RTAL area.

The DOE's Office of Environmental Restoration and Waste Management is conducting a study of projected analytical needs across the DOE Complex. The study defines four levels of handling requirements based on sample radioactivity:

R1 - bench-top	<10 mR/h and <10 nCi/g alpha
R2 - hood	10-200 mR/h or <10 nCi/g alpha
R3 - hot cell	>200 mR
R4 - glove box	<200 mR/h and >10 nCi/g alpha

Preliminary results show that the vast majority (84%) of the samples projected to be collected fall in the R1 category, suitable for bench-top handling. Samples falling in the R2 category (handling in a hood) represent 14% of the total. Samples in the R3 and R4 categories (handling in a glove box or hot cell) represent a combined total of only 2% of the samples to be collected. These results clearly indicate that the RTAL system design should emphasize handling of samples on benches and in hoods. Providing the hot cells, glove boxes, and associated handling equipment necessary to perform the complete range of analyses on the 2% of the samples in the R3 and R4 categories greatly increases the cost of the RTAL modules. The RTAL's mission is to provide rapid response with high quality assurance and control for a limited number of samples. The remaining samples, not requiring rapid analysis, would be processed through central laboratories. For this reason, it was determined that the sample screening area of the Decontamination/Sample Screening Module would be designed to safely screen for all sample categories, R1 through R4, but the other laboratory modules would be designed for R1 and R2 samples only.

An additional module that can be included in the RTAL is the Protected Living Quarters. This module would be located beyond the Operations Control Center and used when personnel are needed on-site for around-the-clock operations. The need for such demanding efforts are expected to occur infrequently. However, in critical situations, the Protected Living Quarters would be very effective in supporting needed personnel in a safe environment very near the area of operations.

The RTAL incorporates cellular communications and, if desired, satellite communications. STU-III encryption devices for secure communications can also be added, if needed.

The RTAL computers are interconnected in a wireless Local Area Network (LAN). Appropriate software is included so that the computer systems within the RTAL complex can be monitored and controlled from the Operations Control Center or any of the other modules. This greatly enhances the efficiency of the operation and minimizes personnel requirements for operating the complex and performing the analyses.

The RTAL will provide the DOE with significant savings in terms of time and cost. Samples will be analyzed within about a day as opposed to the 45 day turnaround typical of commercial laboratories. In addition, off-site sample shipments will be eliminated, saving additional time and manpower. Preliminary estimates indicate that the focused, integrated approach provided by the RTAL can provide significant savings to the DOE compared to commercial laboratories. More importantly, the RTAL's rapid, high quality data response will accelerate and improve the efficiency of clean-

up and remediation operations throughout the DOE complex, resulting in major reductions in program costs.

A prototype RTAL system was constructed and delivered to the DOE's Fernald Environmental Management Project (FEMP) for demonstration. It will be deployed at FEMP's OU-1 Waste Pits. Its performance will be evaluated with samples from these pits and with other environmental samples from the FEMP site. The prototype RTAL system will consist of 5 modules - Radioanalytical Laboratory, Organic Chemical Analysis Laboratory, Inorganic Chemical Analysis Laboratory, Aquatic Biomonitoring Laboratory, and Operations Control Center. The Radioanalytical Laboratory houses two Germanium Detectors (weighing 5,000 lb. each), 24 Alpha Spectrometers, a Liquid Scintillation Counter, and a Gross Alpha/Beta Counter. The Organic Chemical Analysis Laboratory houses a Gas Chromatograph (GC)/Mass Spectrometer (MS), Purge and Trap GC/MS, GC with Flame Ionization Detector, automated Liquid/Liquid Extractor, automated Solid/Liquid Extractor, Size Exclusion Chromatograph, and Toxicity Characteristic Leachate Procedure (TCLP) Apparatus. Each laboratory also houses a sample preparation area (with hoods) in a separate room. The U.S. Army Biomedical R&D Laboratory has volunteered to provide the Inorganic Chemical Analysis Laboratory and Aquatic Biomonitoring Laboratory as part of its concurrent demonstration of Integrated Biological Assessment (IBA) technology.

FUTURE ACTIVITIES

The demonstration of the prototype RTAL is scheduled to start late in the 1st Quarter of FY96. This demonstration has several objectives:

1. Demonstrate the ability to conduct radiological, organic and inorganic chemical analyses in these field facilities with high quality assurance and control.
2. Quantify the analytical throughput of the analyses using the prototype RTAL system.
3. Quantify the turnaround time (starting from the completion of sample collection through data reporting) associated with performing analyses in the RTAL.
4. Quantify the costs (starting from the completion of sample collection through data reporting) associated with performing analyses in the RTAL.
5. Demonstrate the use of Integrated Biological Assessment to quantify hazard levels of groundwater, soils, and surface waters at DOE sites.

The demonstration tests will consist of (a) analysis of actual or surrogate samples within the RTAL radiological and chemical analytical laboratories, and (b) performance of abbreviated Integrated Biological Assessment tests using the Aquatic Biomonitoring Laboratory.

The radioanalyses will focus on total and isotopic quantification of uranium in water and soil samples since that is the radiological contaminant of concern in FEMP's environmental samples. The inorganic analyses will focus on quantification of heavy metals, and the performance of the Toxicity Characteristic Leachate Procedure (TCLP) on soils. The organic analyses will focus on volatile organic compounds (VOC) and semi-volatile organics. These tests are typical analytical requirements at DOE sites. The samples will be actual field samples, with some prepared surrogate added.

The demonstration of Integrated Biological Assessment techniques in the Aquatic Biomonitoring Laboratory will utilize ground and process discharge water. The test water will flow past aquatic organisms in a series of test tanks. The effects on the test organisms, e.g. movement and breathing frequency, will be monitored to assess the hazard level of the test water.

Acknowledgments

I am pleased to acknowledge the insightful guidance and support of Jagdish L. Malhotra, the METC Contracting Officer's Representative (COR). The period of performance is September 14, 1992 to March 31, 1996. This work is performed under the Contaminant Plume Containment and Remediation Focus Area.

4.6 Three-Dimensional Subsurface Imaging Synthetic Aperture Radar

E. Wuenschel (Mirage@rahul.net; 408-752-1600)
Mirage Systems, Inc.
232 Java Drive
Sunnyvale, CA 94089-1318

Introduction and Need

Inadequate resources, aggravated by the limited capabilities of existing site characterization technologies, require that new systems be developed to effectively aid site cleanup. The quantity, condition, and the precise location of buried waste storage containers is often unknown, and is always difficult to assess. Significant safety hazards may also be present at these sites. Therefore, new non-invasive detection techniques are needed that will be cost effective, user friendly, and have a growth path toward a system capable of accessing remote terrain. These detection methods must be economical to use and be capable of exploring large land areas quickly with minimal personnel risk. They should provide the precision for identifying the size, depth, type, and possibly the condition of the waste containers.

Objectives

The objective of this applied research and development project is to develop a system known as "3-D SISAR." This system consists of a ground penetrating radar with software algorithms designed for the detection, location, and identification of buried objects in the underground hazardous waste environments found at DOE storage sites. Three-dimensional maps of the object locations will be produced which can assist the development of remediation strategies and the characterization of the digface during remediation operations. It is expected that the 3-D SISAR will also prove useful for monitoring hydrocarbon-based contaminant migration.

Approach

The underground imaging technique being developed under this contract utilizes a spotlight mode Synthetic Aperture Radar (SAR) approach which, due to its inherent stand-off capability, will permit the rapid survey of a site and achieve a high degree of productivity over large areas. When deployed from an airborne platform, the stand-off technique is also seen as a way to overcome practical survey limitations encountered at vegetated sites.

Mirage Systems has designed and equipped a 22-foot long specially configured trailer, called the Mobile Test Vehicle (MTV), as a sensor system test platform. The MTV is being used as a mobile laboratory to house the 3-D SISAR in support of field demonstrations of this underground imaging technology. Figure 1 illustrates the technique and data collection geometry used for the test and evaluation of the concept.

In a spotlight mode SAR, the area to be surveyed is "spotlighted" or "stared at" as the

---

Research sponsored by the U.S. Department of Energy's Morgantown Energy Technology Center, under contract DE-AR21-93MC30357 with Mirage Systems, Inc., 232 Java Drive, Sunnyvale, CA 94089.

radar path forms the synthetic aperture, typically a circle. When compared to SAR strip mapping, the spotlight mode enhances spatial resolution and increases the total energy used to illuminate a patch of the ground.

The technique provides high coherent integration gain which, when combined with the inherent sensitivity of the frequency modulated, continuous wave (FMCW) signal transmission method, allows a significant improvement in imaging quality. These features are very beneficial for subsurface characterization since 1) long wavelengths, which typically produce images with limited spatial resolution, are needed to penetrate the ground, and 2) the subsurface has inherently high propagation losses requiring more available energy for effective ground penetration. The ultra-wide bandwidth of the FMCW signal provides for improved resolution in the depth dimension as well.

Project Description

A matched filter image processing algorithm has been developed for the detection and identification of buried objects. Scattering models for several types of buried objects (test spheres, barrels, barrel lids, and pipes) have been constructed from electromagnetics modeling programs for use with the matched filter algorithm.

A new radar has been developed that produces the high quality data required by the image processing algorithms. A series of tests have been performed to collect data on actual underground objects.

Preceding the software and hardware development, a series of systems engineering tasks were performed to estimate the radar requirements, to specify the desired performance, and to plan for the field tests and data collection experiments that are assisting the algorithm development.

Underground Imaging Approach Using Matched Filtering

The goal of the 3-D SISAR development is to produce a three-dimensional presentation of the near-surface underground environment that can be applied to the determination of the presence and extent of buried waste. The approach taken by Mirage for this research and development project is one that produces a representation of buried waste containers based on the unique characteristics of the scattering of electromagnetic waves. This approach has the benefit that it searches for a set of unique properties of the radar returns that characterize the shape, dimensions, and orientation of a given buried object. Once an object is located and identified, the imaging software draws a representation of that object in a three-dimensional space that defines the underground mapped region.

Figure 2 is a 3-D display of the matched filter output for a 12" diameter, 3" thick metal cylinder buried at a depth of a foot. The data shows the correlation peak produced by this test object. The center of the image response was located within 10 centimeters in all three dimensions, demonstrating the capability of the 3-D SISAR to detect and locate shallow buried objects. More information on the test results is provided in the Results section.

There are many facets to producing underground images using GPR. One of the major advantages of the matched filter approach is that it overcomes a basic difficulty with other techniques that attempt to image the underground environment directly. The difficulty results from the fact that the wavelengths used for underground imaging are on the order of the linear dimensions of the object. The scattering

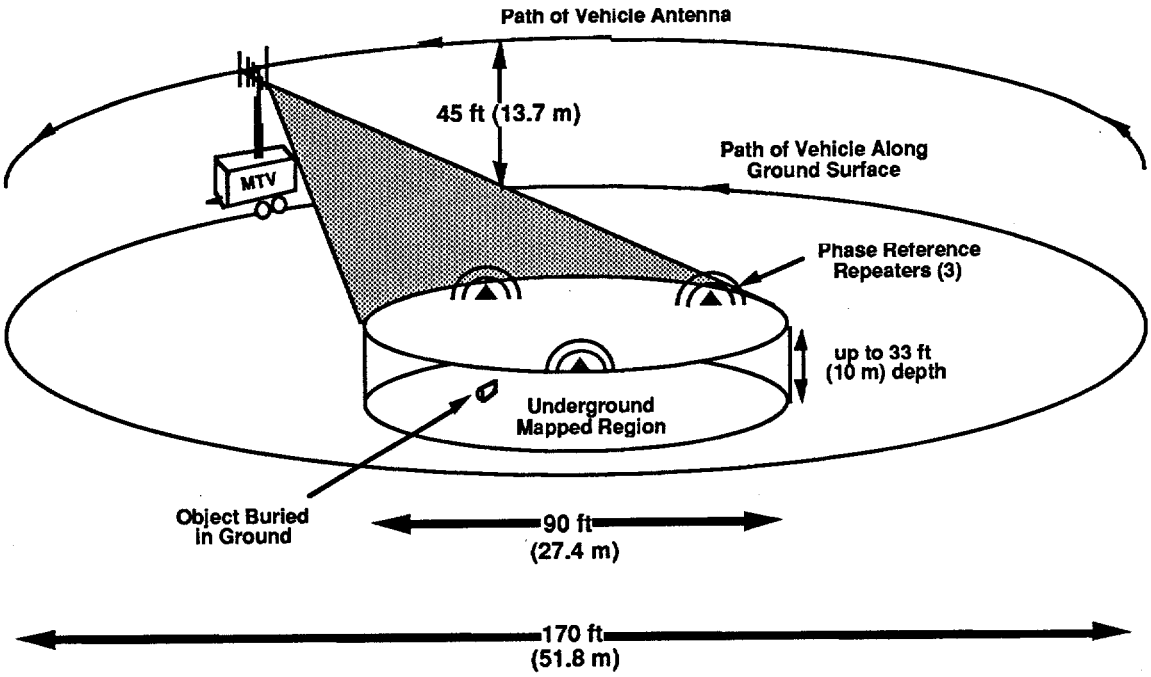

Figure 1. Site Geometry for Project Test and Evaluation

produced by such objects is in the Rayleigh regime, not the optical regime where one normally sees an image that resembles the object in shape and size. In other words, the intensity information alone from the radar return does not clearly distinguish object size and shape because the wavelengths are too long to provide much detail.

The Matched Filter technique determines the best correlation between the measured radar data and a set of potential matching functions, with each function representing an anticipated object-subsurface model. After an object is located and identified, the display program draws a representation of it at the location and depth on a 3-D display.

An advantage the customized matched filter may have over other imaging algorithms is that its performance can be greatly enhanced if the type (or characteristics) of an object is known apriori. An additional advantage is that it avoids the numerical and convergence concerns of other techniques (e.g., iterative approaches). The cost associated with these advantages is an increased processing burden. The performance robustness of the 3-D SISAR to complex underground object configurations has not yet been evaluated and will be explored during the test and evaluation task.

Radar Development

A small, lightweight radar has been developed to provide high quality data for the underground imaging algorithms. The radar is housed in a mast-mounted enclosure, with major components arranged in a compact, easy to assemble and repair layout. In function, this unit is the equivalent of nearly a full rack of equipment, mostly contained in three major subassemblies.

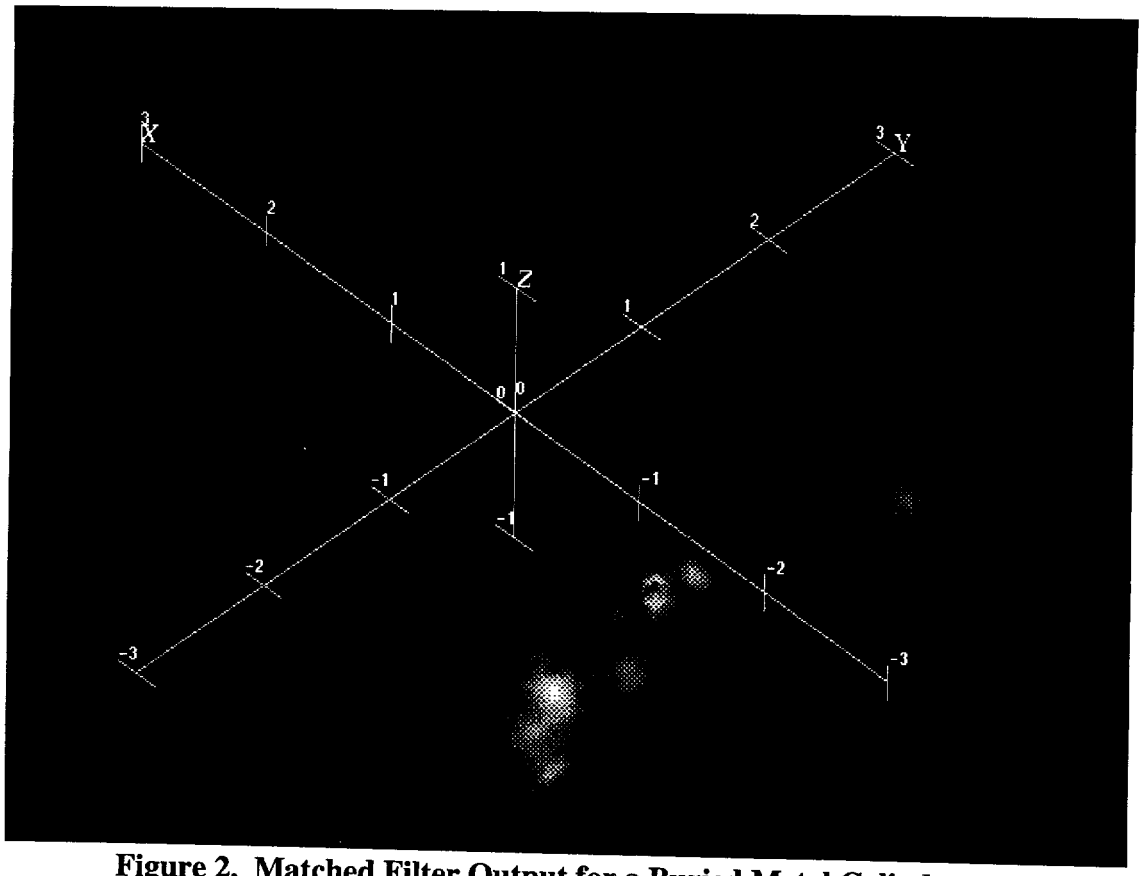

Figure 2. Matched Filter Output for a Buried Metal Cylinder

The unit is sealed from the environment, and uses an air-to-air heat exchanger so that dirt and moisture do not enter the electronics portion of the unit.

Mirage recognizes that effective imaging is key to a successful 3-D SISAR system. Mirage has provided the framework for successful imaging by including flexible spatial and frequency diversity in its data acquisition scheme. The frequency diversity is provided by the ultra-wide bandwidth of the radar, and the spatial diversity through the collection geometry and an adjustable height mast. As shown in Figure 3, the antenna and radar subassembly are located at the top of a 30 foot multi-sectioned pneumatic mast attached to the Mirage Test Vehicle. The antenna and radar are elevated to a height suitable for standoff operation, about 45 feet above ground. This configuration is being used for the field experiments and demonstrations.

The radar signal data is sent down the mast via a high speed digital link to a controller and a data collection subsystem located in the trailer. Figure 4 is a simplified block diagram of the radar and data collection subsystem. Important features of this design include provisions for adequate performance monitoring and fault isolation, and ruggedness of design to withstand the rigors of field use.

Antenna Subsystem. The antenna is a split boom log-periodic antenna, having beamwidths

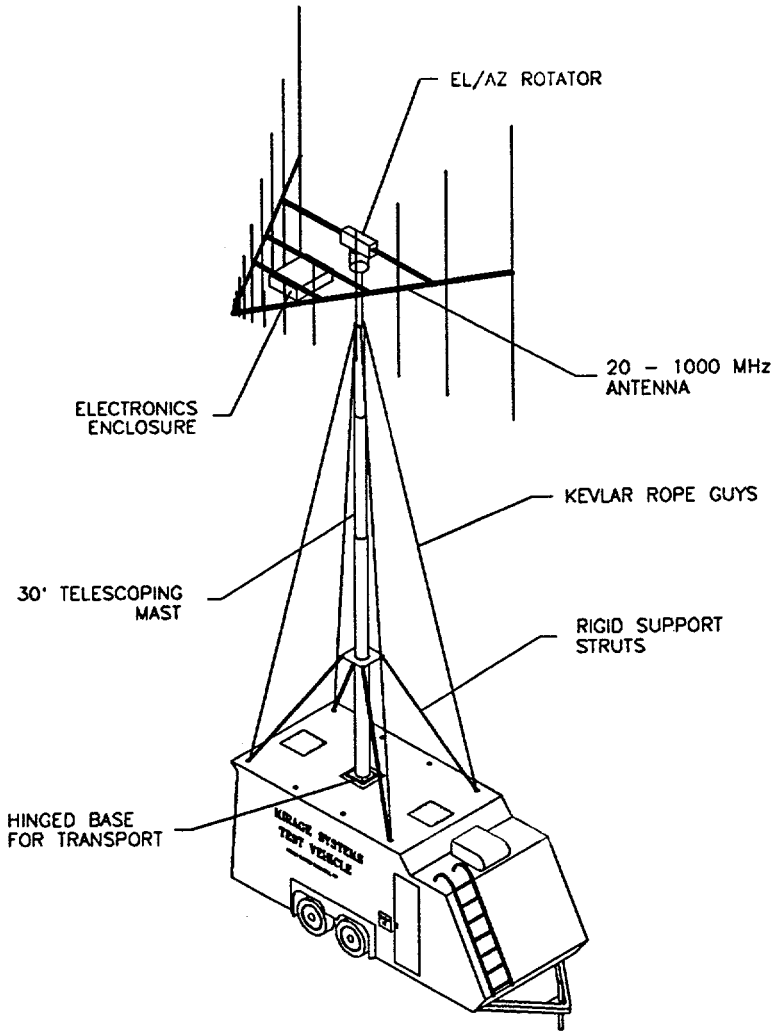

Figure 3. MTV Configured With Mast and Antenna for Test and Evaluation

in both the horizontal and vertical planes of about 70 degrees. This antenna radiation pattern optimally illuminates the underground imaging volume, and has the extended frequency coverage required for the system.

Data Acquisition Subsystem. The function of this subsystem is to control the radar operation and provide a means to display, collect, and archive the radar data. It consists of a VME-based subsystem using a Force Computers 5CE processor module running a real-time multi-tasking environment, two hard drives for storing program and radar data, a tape drive for archiving and transferring radar data files, and interfaces to the radar and calibration equipment.

Motion Compensation. Like all synthetic aperture radars, the 3-D SISAR operates by collecting a large amount of data that needs to be correlated over the dimensions of frequency, time, and space. While the frequency and time

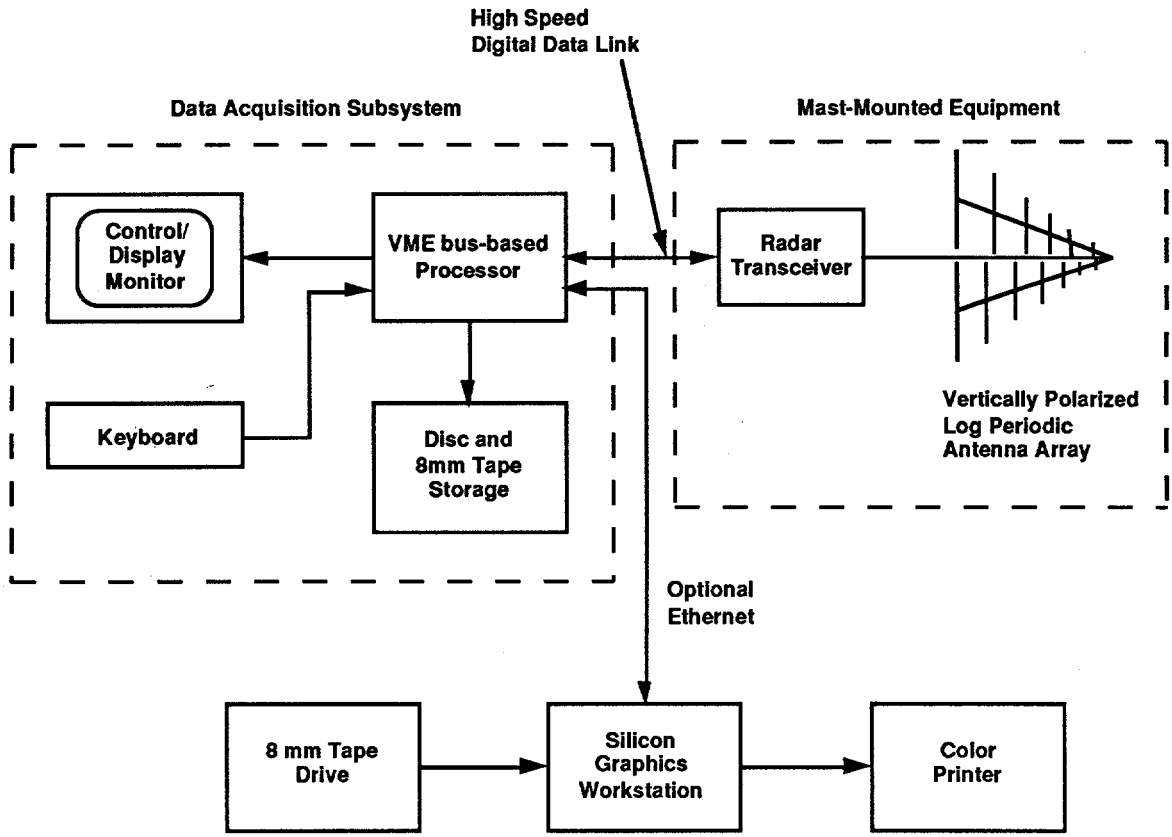

Figure 4. Simplified Block Diagram of the 3-D SISAR

correlation is an internal function of the radar, a set of three external reference repeaters are used to correlate the radar returns in the spatial dimension. The repeaters are positioned around the periphery of the surface of the imaged volume as shown in Figure 1. The signal echo from the repeaters is used to calculate the physical relationship between the radar and the imaged volume of ground. Position location accuracy of approximately 5 centimeters has been demonstrated with update rates of about 30 per second.

Graphics Display Workstation. A Silicon Graphics Indigo 2 model XZ workstation is being used both as a software development platform and as a means to display and manipulate the processed images. This workstation has the necessary processing speed and graphics capabilities to compute and display the imaging data sets. A three-dimensional digital imaging (3DDI) software program allows the operator to interact with the large data sets that comprise the images in a meaningful and efficient way. It provides the ability to render images in two and three dimensions, rotate and add perspective to images, encode image data with a range of colors, and threshold on intensity values. The program "AVS5" from Advanced Visual Systems is being used as the image display and manipulation capability.

Field Testing

Above-ground tests were performed at a large open site in order to evaluate the detection capabilities of the radar, for the development of the precision location estimation subsystem, evaluation of the motion compensation technique, and the calibration of the radar transfer function.

Below ground tests were conducted at a prepared site near Jamestown, CA in August 1995 where objects were carefully buried in a large pit. The buried objects included 55-gallon drums, an empty plastic drum, pipes, plates, a sphere, and metal cylinders of various sizes.

Remaining Tasks

The remaining tasks on this project include the completion of the analysis of the data from the field test and evaluation tasks. Additional imaging experiments will continue through the upcoming months on an as needed basis. At the completion of the experimentation, an evaluation demonstration will be scheduled for DOE personnel.

Accomplishments

To date, the experiments with the 3-D SISAR have demonstrated the detection and location of shallow buried objects with a standoff mode of operation. This is a unique accomplishment, since other standoff systems provide only one- or two-dimensional imaging, and other 3-D GPR systems employ ground contacting sensors. Objects were located to within 10 centimeters of their actual positions in three dimensions. The initial results indicate that the radar hardware and position location subsystem are working well, and providing good quality data for the SAR imaging. This also indicates that the basic assumptions underlying the imaging approach are sound.

The 3-D image of a detected buried metal cylinder was shown previously in Figure 2. Although these initial results are for shallow buried objects, work is ongoing to improve the image processing algorithms to increase the processing gain and imaging capability at greater depths. The image-to-clutter ratio for shallow buried objects has been about 10-15 dB, but this is expected to increase significantly in the near future as improvements are made to the imaging algorithms. This will result in substantial increases in depth penetration capability and clarity of the imaging.

Future Work

The funding of the current contract provides for limited testing. At the completion of the imaging algorithm development, it is envisioned that a subsequent expanded testing phase will be performed. It is suggested that additional testing be performed at a prepared DOE site. This would provide a more complete performance evaluation of the 3-D SISAR under controlled circumstances, and would provide further evaluation of the 3-D SISAR by exploring the potential of the imaging algorithms, learning about real-world remediation situations, and developing approaches for the optimal use of the 3-D SISAR during site operations.

Additional work in the image processing area consists of expanding the imaging algorithms to handle uneven ground surfaces, streamlining the processing to reduce the processing time required, a physically smaller antenna system, the integration of Global Positioning satellite data, and eventual installation aboard an airborne platform.

Acknowledgements

Support for this contract has been provided through Mr. Keith Westhusing of the METC Laramie Project Office, the project COR. The period of performance has been 9/93 through 9/95, and the EM focus areas are Contaminant Plume Containment, Remediation, and Land Stabilization.

4.7 Geophex Airborne Unmanned Survey System

I.J. Won (102173.3625@compuserve; 919-839-8515)
Dean Keiswetter (102173.3625@compuserve; 919-839-8515)
Geophex, Ltd.
605 Mercury Street
Raleigh, NC 27603-2343

Objectives

The purpose of this effort is to design, construct, and evaluate a portable, remotely-piloted, airborne, geophysical survey system. This non-intrusive system will provide "stand-off" capability to conduct surveys and detect buried objects, structures, and conditions of interest at hazardous locations.

This system permits rapid geophysical characterization of hazardous environmental sites. During a survey, the operators remain remote from, but within visual distance of, the site. The sensor system never contacts the Earth, but can be positioned near the ground so that weak geophysical anomalies can be detected.

System Approach

Geophysical surveys provide a non-intrusive means of evaluating subsurface conditions, but geophysical characterization of many environmental sites is difficult or impractical due to hazardous conditions. Ground-based surveys place personnel at risk due to the proximity of buried unexploded ordnance (UXO) items or by exposure to radioactive materials and hazardous chemicals. Use of elaborate personal protective equipment increases cost and decreases efficiency of a site characterization. These inherent problems of ground-based surveys are minimized by the use of a remotely operated geophysical survey system.

The Geophex Airborne Unmanned Survey System (GAUSS) is designed to detect and locate small-scale anomalies at hazardous sites using magnetic and electromagnetic survey techniques. The system consists of a remotely-piloted, radio-controlled, model helicopter (RCH) with flight computer, light-weight geophysical sensors, an electronic positioning system, a data telemetry system, and a computer base-station.

Figure 1 depicts a model GAUSS survey scenario in which a pilot maneuvers the radio-controlled model helicopter over a survey site. The helicopter traverses the site and positions magnetic or electromagnetic sensors close to the Earth without making contact.

Geophysical data, position data, and flight status information are telemetered from the helicopter computer to a base-station computer via a digital radio communications link. The base station records and processes the data. A cursor on the real-time graphical video display indicates the position of the moving helicopter. Each time a sensor transmits a geophysical measurement, the

Research sponsored by the U.S. Department of Energy's Morgantown Energy Tchnology Center, under Contract DE-AR21-93MC30358.

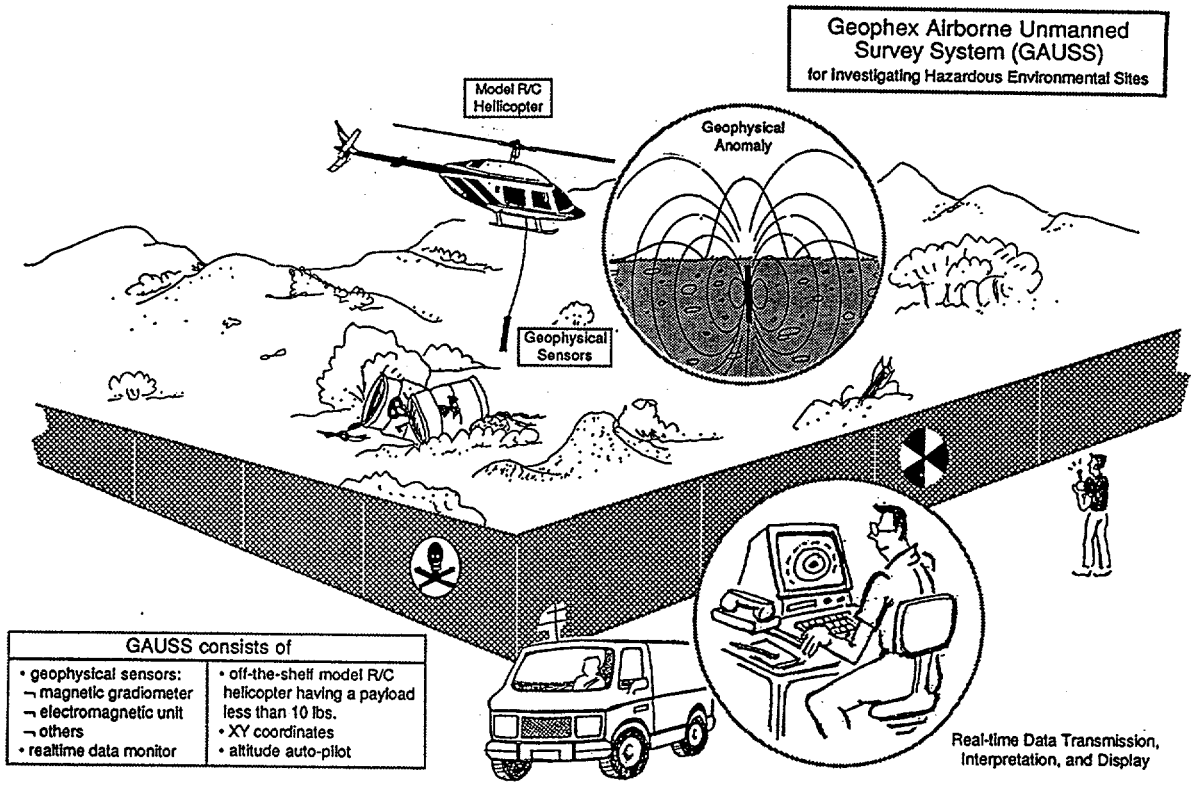

Figure 1. Geophex Airborne Unmanned Survey System (GAUSS), for characterization of hazardous environmental sites

data is displayed as a color-coded region at the location corresponding to the helicopter position.

Operators receive instant feedback regarding data content and quality via the graphical video display. Anomalies are detected, located, and characterized in real-time allowing modification of the survey to produce optimal results. For example, the survey can be modified on-the-fly to switch between a high-speed mode suitable for target detection, and a slow-speed, high data density acquisition mode for detailed target characterization.

Project Description

Goals

This project is a feasibility study to determine the applicability of RCH carried sensor systems for stand-off geophysical surveying. The emphasis is on development and demonstration of technologies for use in the airborne system.

The project is divided into two phases. The first phase requires design, construction, and testing of a hand-held pre-prototype sensor system. Specific tasks during the first phase are;

- Develop light-weight geophysical sensors with digital output.

- Develop or acquire a light-weight, two-way digital telemetry system that incorporates a communications protocol featuring error detection and correction capability.

- Develop or acquire a light-weight, real-time automatic positioning system.

- Develop software for remote instruments and for the base-station to accomplish communications, data recording, error detection, data processing and display functions.

- Integrate the components to produce a fully functional hand-carried version of the GAUSS system.

- Test and evaluate the hand-held system.

During the second phase of the project, the technology developed in the pre-prototype is applied to the airborne prototype. Tasks associated with the second phase include;

- Modify subsystems developed in phase one to maximize performance and minimize weight and size.

- Convert subsystems for use with RCH.

- Acquire a helicopter autopilot system to reduce complications during flight.

- Integrate the RCH-based survey system.

- Evaluate the efficacy of the system for geophysical surveying of environmental sites.

Project Participants

Work for this project is led by Dr. I. J. Won. Dr. Won contributes his experience and expertise to the theoretical formulation and hardware specification of geophysical sensors and flight systems. Dr. Dean Keiswetter, Deputy Program Manager of Geophysics at Geophex, Ltd. manages the daily operations and contributes in the collection, processing and analysis of geophysical data. Engineering design and development are completed by Mr. David Burgess, Mr. Joseph Seibert, and Mr. Alex Gladkov. Mr. Burgess, the Hardware Manager at Geophex, has a strong background in analog electronic systems and over twenty years experience in the field. Mr. Seibert is an electrical engineer with over eighteen years of industry experience in design and construction of custom electronics systems. Mr. Gladkov, an electrical engineer, contributes to the hardware construction.

Results

System Operation

The hand-held, pre-prototype survey system has been designed, constructed, and tested. An understanding of the acquisition system is best described by following the sequence of events that occur when a single measurement is made during a survey. A remote operator carries a geophysical sensor and the remote radio modem into the field. The base-station running GAUSS software and a local radio modem are located less than one mile from the survey site and have a clear view of the survey.

The remote operator occupies a survey location and depresses the fire button on the instrument. The instrument then makes a measurement, performs necessary calculations, and passes the datum to the remote radio modem.

The remote modem packetizes the datum, affixes error correction information to the packet, then transmits this information. The local modem receives the packet and checks for data integrity. If the information has been corrupted, the local modem discards the packet and the remote modem re-transmits the data packet. If the data packet is deemed to be uncorrupted, the local modem broadcasts confirmation to the remote modem, then makes the datum available to the base-station computer via a serial port.

The base station captures the datum from the serial port, translates to binary format, and appends it to a global data list. An error flag is attached to the data if internal errors are detected by the software. If no error condition is detected, the base-station broadcasts confirmation to the remote instrument. Radio transmission error checking is also in effect during the confirmation transmission.

Position coordinates are associated with the geophysical data and the multivalue data set is written to the base-station fixed disk. The data is scaled and displayed in color on the base-station monitor. The spatial location of the data sample is mapped to a representative location on the screen. The numerical value of the data sample determines the color.

As the survey progresses, a colored survey map is constructed on the video display. Because the geophysical map is produced in real time, anomalous areas can be re-occupied to either support, enhance, or correct suspicious results.

GAUSS Subsystems

Base-Station. A 50 MHz 80486 personal computer running DOS with VGA color display is used as the GAUSS base station. This system has sufficient power for the GAUSS software and is readily available. A pentium laptop with two serial ports and an active matrix screen is being tested as a possible replacement.

GAUSS base-station software is comprised of a suite of independent programs tied together by menu-driven DOS batch programs. These programs provide facilities to conduct automated surveys, post-process survey images, and translate the format of the survey datafiles.

The survey programs collect, record, interpret, and display sensor data in real-time; providing the functionality described in the System Operation Section. These programs have been written using the *C* language in conjunction with a real time supervisory kernel (task scheduler). The kernel utilizes interrupt driven preemptive task switching to prioritize numerous simultaneous tasks (Figure 2). Individual software tasks are indicated by rectangular borders in Figure 2, and hardware tasks are identified by an oval border. Each task is an independent programs which run simultaneously with all other tasks. The scheduler determines which task is running based upon the task's priority (indicated below each rectangular border in Figure 2), the status of the computer hardware interrupts, and software semaphores which accomplish intertask communication.

Any task has the capability to access the hardware through the associated driver, or can access the global data structure. Inter-task communication for is indicated by the arrows in Figure 2. The modular structure of this software allows flexibility during development stages and provides good performance. The magnetometer survey program has been used to receive, record, process, and display magnetometer data at rates up to 75 samples per second.

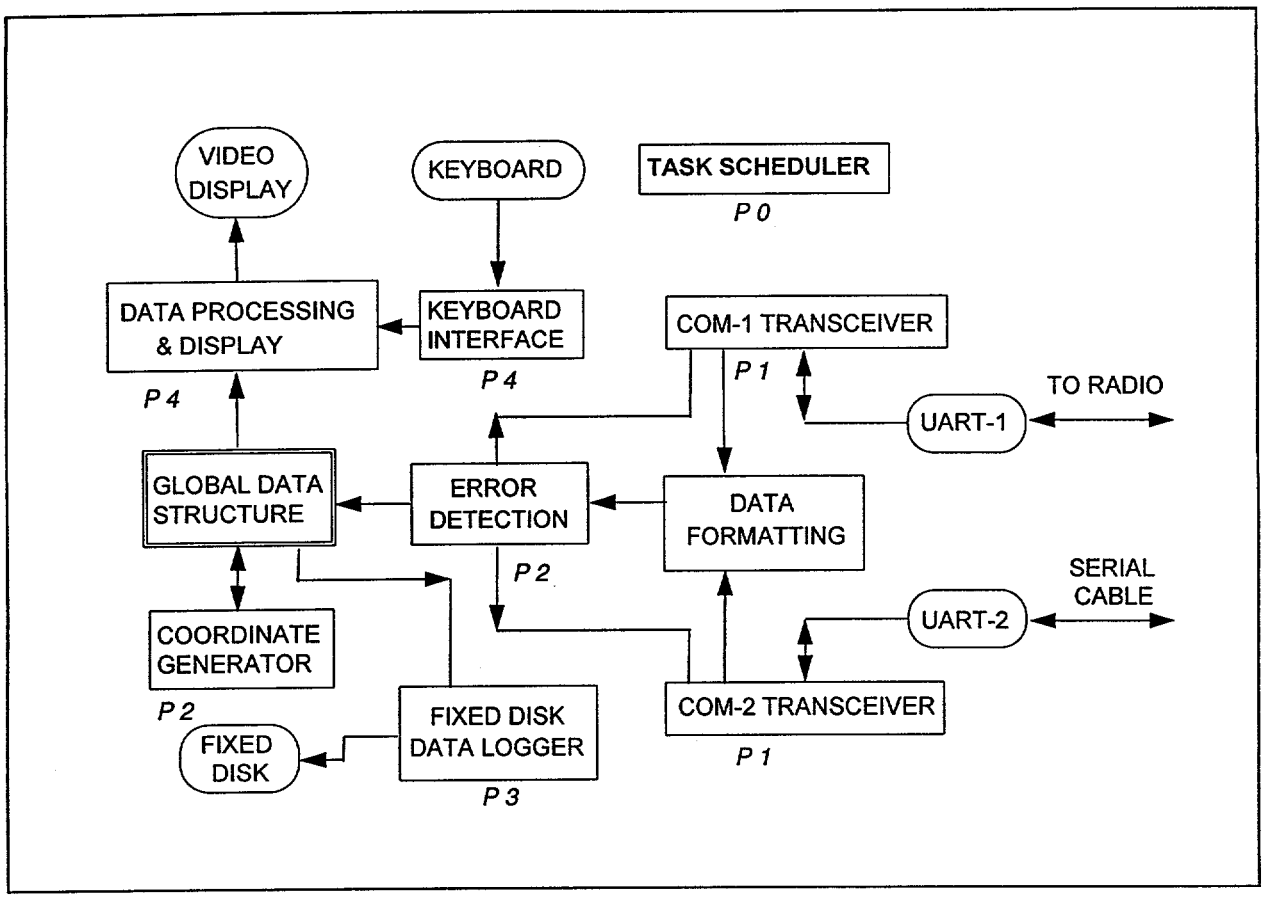

Figure 2. Software structure of the multitasking GAUSS survey module.

Sensors. GAUSS presently uses static magnetic field and induction electromagnetic sensor systems. These sensing techniques are proven and widely applicable for environmental site characterization.

The magnetic field technique is very effective at detecting magnetically permeable objects or geological formations by measuring perturbations in the Earth's natural magnetic field.

The GAUSS magnetometer subsystem uses an off-the-shelf, low noise, three axis, fluxgate magnetometer. This compact unit weighs 100 g and produces three output voltages, each proportional to the magnetic field strength in the direction of a fluxgate axis. A custom analog circuit board buffers and filters each of the three voltage signals. Three synchronized 20-bit analog to digital (A/D) converters sample the filtered signals over 9000 times per second.

A modified off-the-shelf CMOS computer controls the A/D converters and receives the vector magnetic field data at rates up to 240 data sets per second. This computer has a 2.5 by 3 inch footprint and weighs less than 50 g. The computer processes the vector data to determine

magnetic field magnitude. A tensor correction formula is used which compensates for non-orthogonality of the fluxgates and for gain differences in each of the three analog channels. The magnetometer computer then passes field magnitude data to the remote radio modem for transmission to the base station.

The induction electromagnetic survey technique detects discontinuities in the Earth's conductivity which can be caused by buried objects, contaminant plumes, groundwater, and other conditions of interest.

A block diagram of the GAUSS electromagnetic (EM) induction sensor system is shown in Figure 3. The system is comprised of electronics and a monostatic coil assembly. The custom electronics reside on a single printed circuit board which requires a unipolar supply voltage. The computer is based on the Motorola 56001 and performs control and signal processing tasks. The system functions by transmitting a trinary pulse-width modulation (PWM) bitstream to a high efficiency coil driver. The transmitter signal strength is monitored by a reference coil. The Earth's response is detected by a high-gain receiver coil. The reference and receive signals are amplified and filtered by low-noise analog electronics and then digitized by a stereo A/D converter at a rate exceeding 72 k samples/second. The computer cross correlates the receive signal with the transmitted signal to determine magnitude and phase of the anomaly response. The computer also monitors the relative gain of the receive and reference channels and compensate for thermally induced electronic drift. Figure 4 is a plot of the monostatic response of this sensor system in the vicinity of a nonferrous anomaly.

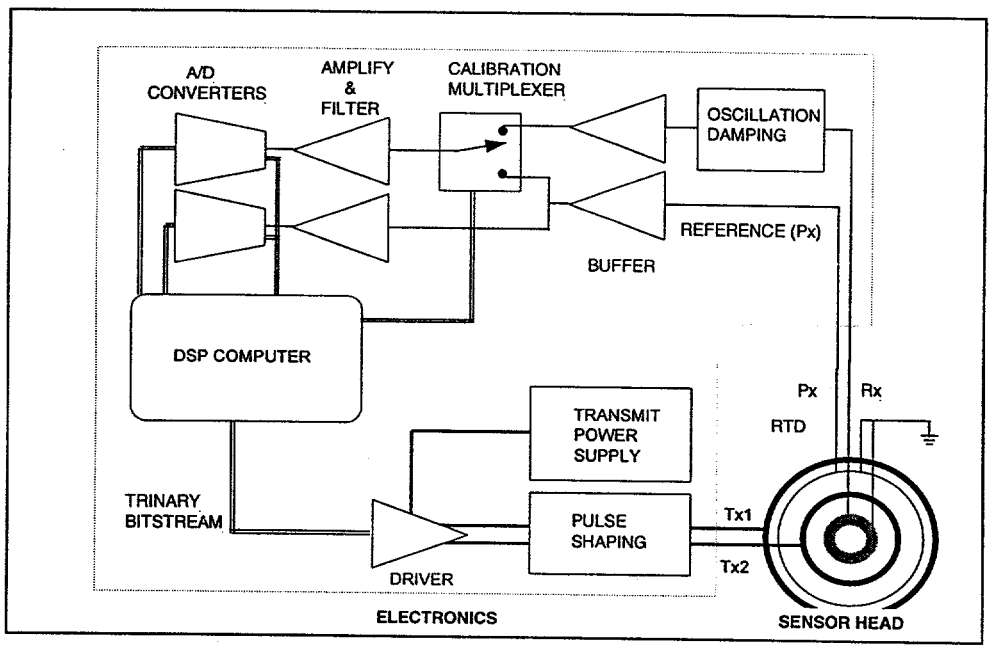

Figure 3. Block diagram of major components of the GAUSS electromagnetic sensor

Telemetry System. Radio modems are used for system telemetry. These off-the-shelf components operate at rates to 19.2 kBAUD and use checksums with handshaking to provide error free data transmission. The radios broadcast a spread-spectrum signal which can be used at any location without a radio license and allows full duplex communication. A compact OEM version is available which occupies a single printed circuit board.

Positioning System. At present, position information is acquired using a laser tracking system. Differential global positioning systems (DGPS) have been considered, but current DGPS technology does not provide sufficiently accurate real-time position data at an acceptable update rate.

Pre-prototype Test Surveys

Test surveys have been conducted using the hand-held GAUSS system with both the electromagnetic sensor and the magnetometer. Figure 5 is an eight-shade grayscale screen dump of a magnetic survey conducted over a 70 by 60 ft area located near our Raleigh Office. Magnetic data were collected on a regular 2.5 ft grid and interpolated. Filtering was used to remove the large scale effects of a metal building located seven feet south of the site and a storage shed located just off the northeast corner. Use of the data filtering capability of the GAUSS software has allowed us to detect 30 nT anomalies in the presence of a background field of 4,845 nT. The large anomaly marked with a "+" in Figure 5 is due to an exposed electrical conduit. Using this data, ferrous objects have been recovered from excavations at three locations east and north of the conduit.

Figure 6 shows a screen dump of an electromagnetic survey of a 16 by 16 ft site. Data were collected on a regular two foot grid. The

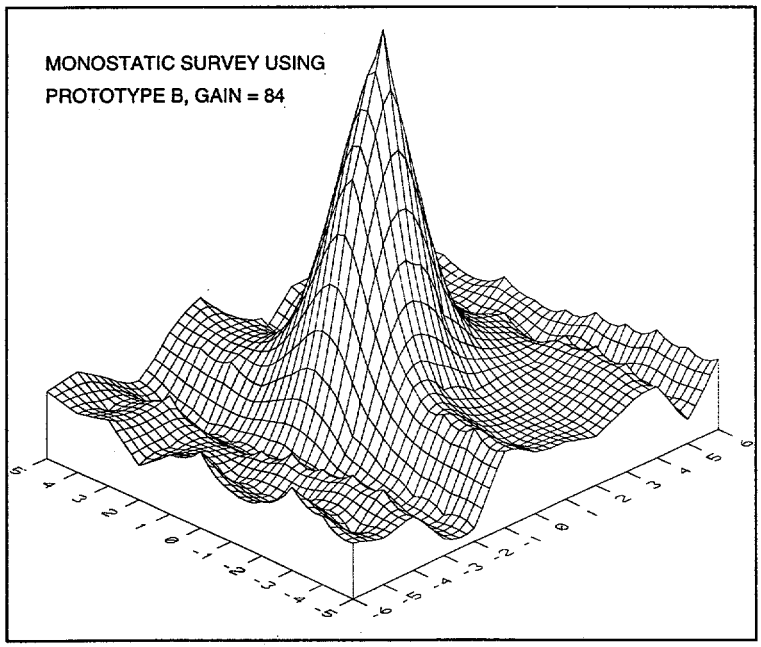

Figure 4. Monostatic response of the GAUSS electromagnetic induction sensor in the vicinity of a conductive nonferrous object

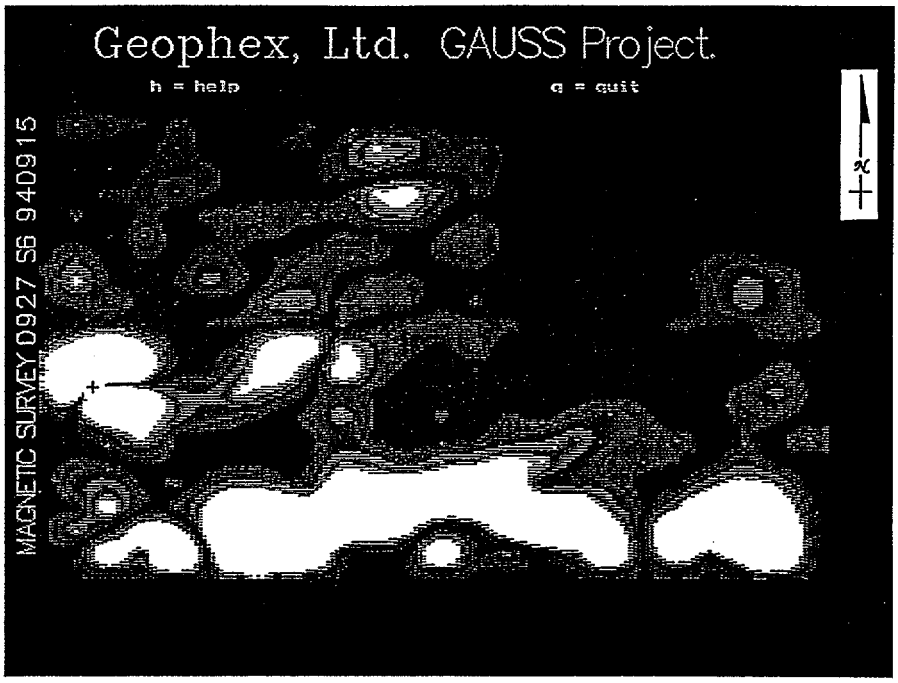

Figure 5. Screen dump of a GAUSS magnetic survey map

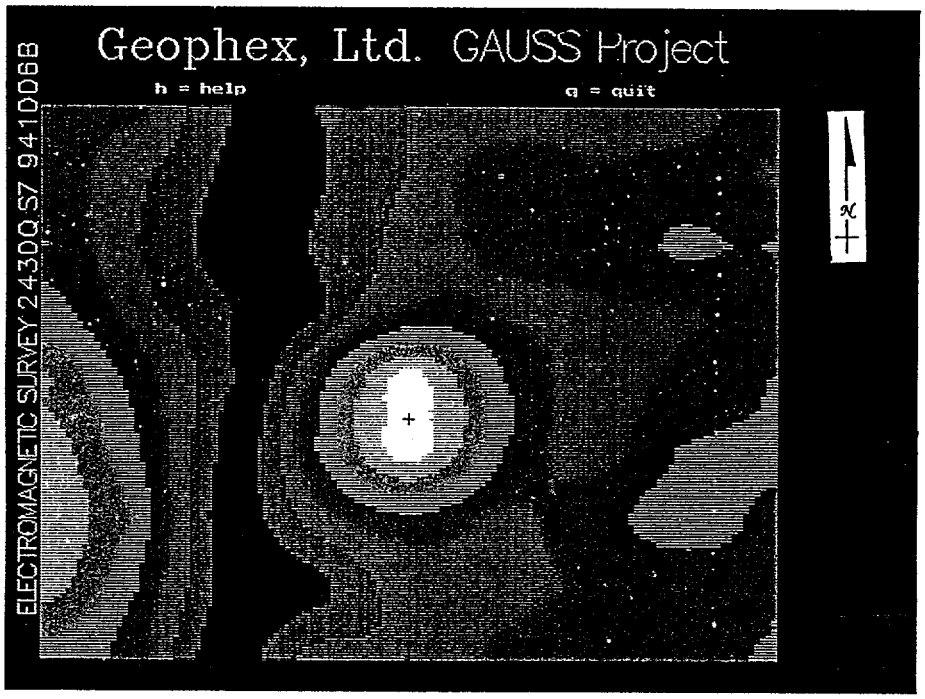

Figure 6. Screen dump of a GAUSS electromagnetic survey map

circular anomaly, marked with a "+", is caused by a vertically oriented, 5-ft steel pipe. The shallow end of the pipe is buried beneath six inches of soil.

Applications and Benefits

GAUSS allows operators to conduct geophysical surveys of hazardous environmental sites at stand-off distances which decreases the risk to personnel. The GAUSS system hovers near the ground to detect weak anomalies without direct contact with the near-surface materials. This capability is desirable in UXO remediation efforts and also mitigates the need for decontamination of equipment and personnel.

Survey systems for hazardous sites based on robotic or remotely guided ground-based vehicles have difficulty negotiating uneven terrain which can result in reduced survey speed or vehicle incapacitation. GAUSS can be used to characterize such sites (e.g. open pits or steep terrain). GAUSS can also be deployed for surveys over surf-zones, and shallow water areas where land-based or hydrographic surveys are not possible.

Existing airborne technologies typically cannot detect and locate the small-scale anomalies caused by ordnance items, explosive waste, or buried drums due to minimum sensor-height limitations. It is necessary to position sensors very close to the ground to detect and accurately locate weak anomalies. In many instances, it is not practical to attempt this with a full sized airborne system.

GAUSS provides automated data collection, processing, and display capabilities. A color map of the survey data is displayed in real time. This reduces the need for costly and time consuming post processing. The "answer" is known at the conclusion of the survey as opposed to a post processing scenario in which data quality may not be known until days after a site is abandoned. Automated data processing technology results in a cost and time savings as well as improved survey quality. This technology is applicable to surveys using any type of survey platform (e.g. ground based, model boat, etc.).

GAUSS has been designed using off-the-shelf subsystems wherever possible. As a result, costs associated with the GAUSS are minimized and maintenance is standardized.

Future Activities

We are currently completing the prototype design and have started the construction of critical subsystems. An automatic electronic positioning system has been located and is being integrated into the prototype system.

Although prototype work has begun, we continue to test the pre-prototype GAUSS system. The emphasis of these tests is the refinement of design and construction criteria necessary for the final helicopter-towed systems.

During the next year, we will complete the design, construction, and testing of the RCH-based system. Specific tasks are to 1) finalize the miniaturization of the geophysical sensor systems, 2) test the helicopter altitude autopilot system, and 3) enhance the base-station software.

Acknowledgments

We thank Carl Roosmagi, our METC Contracting Officer, for excellent support and supervision, and the Contaminant Plume Containment and Remediation and Land Stabilization Area for including our work into their program. Phase 1 of this research started in September 1993 and was completed in March 1995; phase 2 will be completed October 1996.

4.8 Field Test of a Post-Closure Radiation Monitor

Stuart E. Reed (Stu.E.Reed@RDD.McDermott.COM; 216-829-7350)
Babcock & Wilcox, Research and Development Division
1562 Beeson Street
Alliance OH 44601

C. Edward Christy (CCHRIS@METC.DOE.GOV; 304-285-4604)
U.S. Department of Energy, Morgantown Energy Technology Center
P.O. Box 880, 3610 Collins Ferry Road
Morgantown WV 26505

Richard E. Heath (Rick.Heath%EM@EM.DOE.GOV; 513-648-6291)
FERMCO
P.O. Box 538704
Cincinnati, OH 45253-8704

Abstract

The DOE is conducting remedial actions at many sites contaminated with radioactive materials. After closure of these sites, long-term subsurface monitoring is typically required by law. This monitoring is generally labor intensive and expensive using conventional sampling and analysis techniques.

The U.S. Department of Energy's Morgantown Energy Technology Center (METC) has contracted with Babcock and Wilcox to develop a Long-Term Post-Closure Radiation Monitoring System (LPRMS) to reduce these monitoring costs. The system designed in Phase I of this development program monitors gamma radiation using a subsurface cesium iodide scintillator coupled to above-ground detection electronics using optical waveguide. The radiation probe can be installed to depths up to 50 meters using cone penetrometer techniques, and requires no downhole electrical power. Multiplexing, data logging and analysis are performed at a central location.

A prototype LPRMS probe was built, and B&W and FERMCO field tested this monitoring probe at the Fernald Environmental Management Project in the fall of 1994 with funding from the DOE's Office of Technology Development (EM-50) through METC. The system was used to measure soil and water with known uranium contamination levels, both in drums and in situ at depths up to 3 meters. For comparison purposes, measurements were also performed using a more conventional survey probe with a sodium iodide scintillator directly butt-coupled to detection electronics.

This paper presents a description and the results of the field tests. The results were used to characterize the lower detection limits,

Research sponsored by the U.S. Department of Energy's Morgantown Energy Technology Center under Contract DE-AC21-92MC29103 with Babcock and Wilcox R&DD, 1562 Beeson Street, Alliance OH 44601. FAX (216) 823-0639.

precision and bias of the system, which allowed the DOE to judge the monitoring system's ability to meet its long-term post-closure radiation monitoring needs. Based on the test results, the monitoring system has been redesigned for fabrication and testing in a potential Phase III of this program. If the DOE feels that this system can meet its needs and chooses to continue into Phase III of this program, this redesigned full scale prototype system will be built and tested for a period of approximately a year. Such a system can be used at a variety of radioactively contaminated sites.

1. LPRMS Probe

Because it is intended for installation by a CPT truck, the mechanical design of the Long-Term Post-Closure Radiation Monitor (LPRMS) probe which was fabricated and tested in this program was based on the dimensional envelope of a 10 cm^2 cone penetrometer tool with a 1-7/16 inch (3.65 cm) outside diameter and a conventional 60 degree cone tip angle. The LPRMS probe consisted of a scintillation head housing the scintillator, a detection head housing the PMT and detection electronics, and several 1 meter long threaded extension sections for the push rods and lightguide. The scintillation head incorporated a 2.5 cm diameter by 25 cm long CsI(Tl) scintillator inside a 0.36 cm thick 4130 steel window section which extended slightly past the scintillator on both ends. In this design, the window material carried the push forces applied to the tool; this limited the maximum push force for this tool to about 20 tons. Although it was made in 1 meter sections for CPT installation, for these tests the probe was fully assembled above ground prior to installation and testing.

A drawing of the LPRMS probe is shown in Figure 1. The optical photons from the scintillator were transmitted by a single air-clad PMMA rod 2.5 cm OD. The optical waveguide was directly butt-coupled to the scintillator. To accommodate the waveguide, the bore of the extension sections was increased to 2.7 cm from the normal CPT rod bore of 1.6 cm. The extension sections were 1 meter in length and extended to the surface. At the surface end of the probe, the extension sections were coupled to a detection head containing a 1-1/8" head-on bialkali PMT, a voltage divider base, a pre-amp and pulse shaping electronics. The optical waveguide was directly butt-coupled to the PMT face. The PMT was operated in the pulse mode with a cathode ground (positive high voltage). This mode of operation is consistent with either photon counting or spectroscopic analysis techniques. The PMT was magnetically shielded, and operated at ambient temperature. A relatively thick stainless steel housing was used to minimize short term temperature changes of the PMT.

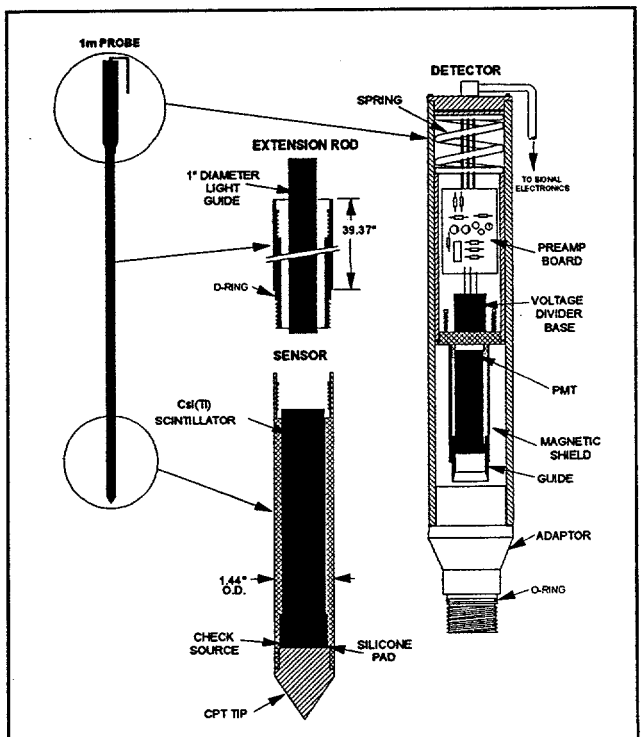

Figure 1. LPRMS Probe

2. Survey Probe

To provide performance comparison data, tests were also performed using a gamma radiation survey probe developed by B&W for radiation survey applications during site characterization and remediation. The survey probe is 1.42 inches (3.6 cm) diameter by approximately 16 inches (40 cm) long. It is designed to be lowered into a 1.5 inch diameter or larger casing on a wireline (logging mode) by hand or from a light tripod using a small hand winch. The probe contains a 1 inch (2.54 cm) diameter by 6 inch (15.3 cm) NaI(Tl) scintillator directly butt-coupled to a bialkali PMT with optical grease. The probe also contains magnetic shielding for the PMT, the voltage divider and a Cockroft-Walton high voltage power supply within a potted housing for moisture and shock resistance. A drawing of this probe is shown in Figure 2.

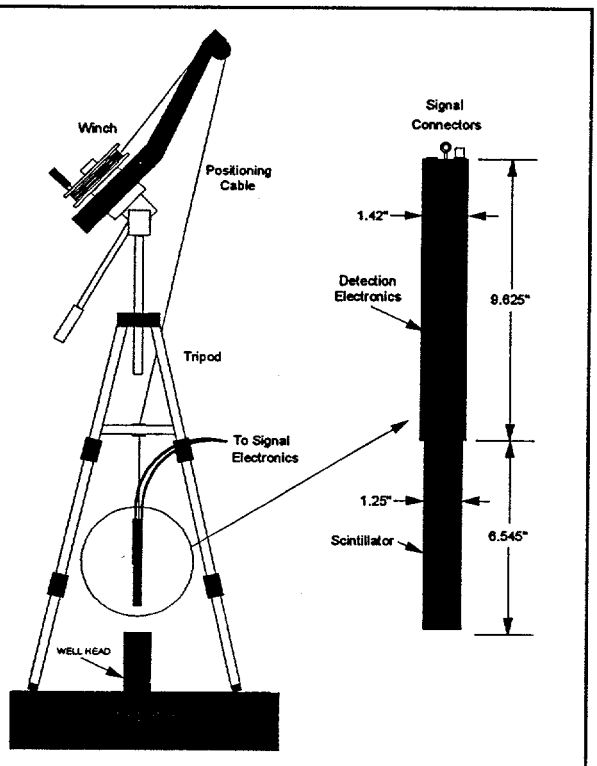

Figure 2. Survey Probe.

3. Gamma Spectrometer

The data from the two probes was acquired, analyzed, stored and printed using a commercially available PC-based two channel gamma spectrometer system. The system, manufactured by Canberra Nuclear, is comprised of two acquisition interface boards (NaI+) installed in a Gateway 486-66 PC plus gamma spectroscopy software (GENIE-PC) to provide the functions of a hardware-based MCA (multi-channel analyzer). The interface boards provide a pre-amp DC power supply, an integrated HV power supply, data amplifier and a 100 MHz Wilkinson ADC (analog to digital converter).

The functions and settings of the interface board hardware are controlled from the software through a window-style graphical user interface. The software operates under an OS-2 operating system and is a true multitasking architecture; the system can thus support simultaneous and fully independent counting and analysis procedures on the two channels. In addition to hardware control, MCA control and basic gamma spectroscopy functions (such as continuum correction and peak searches), the software also performs energy and efficiency calibrations, background subtractions, nuclide identification (interference corrected), spectrum scaling or gain stabilization, calculates weighted mean activity for the nuclides detected and the MDA (minimum detectable activity) for any specified nuclide which is not located in the spectral data. The data from a count procedure is stored in a single extensible file (a Configuration Access Method or "CAM" file) which contains the spectral data, calibration information, analysis parameters, intermediate and final analysis results, setup parameters and the complete analysis library used. The selected results, including the energy spectrum if desired, of the analysis are then output in a

user specified report format to a printer (Hewlett Packard Laserjet).

4. Calibration

To make quantitative measurements, a gamma probe needs both an energy calibration and an efficiency calibration. In normal practice, a source with known isotopic content and activity, and the same geometry as the planned measurement geometry is positioned at the detector. The source is then counted for a fixed length of time. Because the isotopic content is known, the known energy lines can be used to perform the energy calibration. Because the activity levels are known and the geometry is the same as that to be measured, the efficiency calibration can also be readily performed.

For the demonstration tests, the probe will be used inside casings, completely surrounded by contaminated soil. Soil 30 cm or more away from the casing still contributes to the measured signal, as does soil above and below the probe. To duplicate the measurement geometry, the calibration source would need to be roughly the size of a 55 gallon drum (about 2 feet in diameter and about 3 feet high). This is not an available or practical calibration source geometry. Instead, the energy calibration was performed using an Amersham QCD.1 nine nuclide disc source, positioned at the center of the scintillator, side-on. This source provides 11 known energy lines which can easily be used to perform the energy calibration in the lab or field. It is not suitable for the efficiency calibration.

The detector efficiency as a function of energy was determined by calculation in several steps. A spreadsheet model of the soil, soil moisture, casing, detector can and scintillator absorption was used to determine the gammas absorbed within the scintillator volume for known uniform activity levels in the soil. The model also accounted for the scintillation efficiency of the scintillator, optical losses due to reflection and refraction in the scintillator and lightguide, and the PMT quantum efficiency to predict the count rate at the PMT anode for a given soil activity level. This provided a first approximation of the overall efficiency in the soil measurement geometry; this approximation was then adjusted empirically based on counts of a hollow cylindrical source containing known activities of potassium, uranium and thorium. Tables of the efficiency vs energy were then stored in a computer file in the gamma spectrometer computer for use in later analysis; these efficiency values were used for the preliminary analysis of the field data.

Some of the tested soils in the field test (described below) had contamination levels that were reasonably well known, at least for the uranium isotopes. Data from these tests were analyzed and the predicted activities compared to the known activities. The analysis results consistently showed higher activity levels than the laboratory analyses indicating that the calculated efficiencies had been over-corrected by about 20%. The correction factors were then revised based on the field test data and the resulting efficiencies were used for all analyses.

The energy and efficiency calibrations permit the system to identify nuclides and calculate their activities based on a library of gamma lines and yields. To calculate nuclide activities in terms of pCi/gram, the analysis quantity in grams must be known. To determine the sample quantities for analysis, we calculated an effective radius (30 cm) and effective view angles (+- 30 deg) for the probe beyond which the contribution of additional sample material is minimal. Based on these effective dimensions, we calculated the active

sample volume for the probe in cubic centimeters. This volume is multiplied by the sample density to determine the analysis quantity.

5. Test Description

The Fernald Environmental Management Project (FEMP) site at Fernald, Ohio was the selected test site. This site is a U.S. DOE site in southwestern Ohio, approximately 17 miles from Cincinnati. Uranium isotopes are the primary contaminants of concern at this site, resulting from about 35 years of processing of uranium ore concentrates into high purity uranium metal. This test program was coordinated with three other programs: the DOE Uranium in Soils Integrated Demonstration (USID), the DOE Cone Penetrometry Demonstration (CPD) and the B&W funded Survey Tool program. The USID program provided previously characterized soils to be used in fabricating test drums with known activity levels. As part of the CPD program, two locations at the FEMP were sampled and analyzed for uranium contamination vs depth; the bores at these locations were then cased with 1.5 inch PVC casing for later measurement in our program. The B&W Survey Tool program provided the survey probe which was used to generate comparison data for each of the tests performed. All data from both probes was acquired with B&W's laboratory 2 channel gamma spectrometer.

A total of four weeks of testing were performed at the FEMP in the fall of 1994. Two types of tests were performed: tests using drummed samples with known contamination levels and in-situ (sub-surface) tests in cased boreholes at three locations at depths up to four meters. The drummed sample tests included the following types of samples:

- Homogenized soils from the USID program: eight samples with predominantly uranium contamination at known activities from 50 to about 1750 pCi/gram (three duplicates), plus one sample of clean water which was percolated into and retained in one of the samples of contaminated soil for testing;

- Water: three samples with predominantly uranium contamination at known activities from the South plume pumping station, from the storm water retention basin and from the biodenitrification facility;

- Sand matrix/water: one sample of sand matrix at background, plus one sample of water at a known activity level, which was percolated into and retained in the sand/gravel matrix for testing.

The in-situ tests were performed at three locations; one in an existing monitoring well, and two in boreholes available from the Cone Penetrometer Demonstration (CPD) test program which were subsequently cased with PVC. Over 200 counts were performed with each probe, with count times varying from 3 to 90 minutes. The system performance results presented in this paper were determined based on the counts and analyses of the drummed soil samples.

The test specimens for the drummed soils tests consisted of eight 55 gallon drums of characterized soils from the USID with five different activity levels; the nominal activity levels of the soils are listed in the table below. For each of the first 4 test specimens listed above, sufficient soil to fill the drums was taken from larger boxes of soil which had previously been sampled and analyzed for uranium isotopes. These laboratory analysis results have

Soils Samples for Drummed Soils Tests

Sample	Drum ID	Activity (pCi/gram)	Test ID
CP	F-392	51	1B
C-35	C-389	95 (two drums)	1D & 1F
C-100	D-389	146 (two drums)	1C & 1G
C-200	E-388	311 (two drums)	1E & 1H
---	P011-0380	> 1000	2A & 2B

been used for the comparisons contained in this paper; no analyses of the drummed soils were performed. The analysis results showed considerable spread over the sampling locations within the box. The analysis results thus provide only a general indication of the isotopic uranium activity of the drummed soils, not their actual content. Sample P011-0380 was taken from a similar box, but was characterized only with a single grab sample (total U greater than 1000 pCi/g); data from this sample were thus not used for the system performance.

6. Performance Results

6.1. Lower Detection Limits

The normal procedure for determining the lower detection limits (LDL) by isotope is to count and analyze the Minimum Detectable Activity (MDA) for a "blank", a sample identical to the unknowns in geometry, background nuclides (such as K-40) and absorption characteristics, but with no other isotopic activity. The count protocols and analysis parameters used are identical to those used to count and analyze unknowns. A blank soil sample was not available for the tests performed at FEMP. However, one of the test runs provided a reasonably close match to a blank: run 3A, a drum of clean sand with K-40 activity of 6.4 pCi/g.

For this sample, both the LPRMS probe and the B&W Survey Probe had been used to perform 30, 60 and 90 minute counts. The LPRMS probe was in the 1 meter configuration for test 3A. A Genie-PC nuclide library was prepared which included all of the gamma emitting isotopes from the list, prepared in Phase I, of nuclides found on DOE lands. This library included short half-life daughters which could reasonably be expected to be in secular equilibrium with the parent, with yields and half lives adjusted to provide the MDA of the parent, based on detection of the daughter. An MDA analysis was performed for both of the probes for test 3A using this library. This analysis was performed using Genie-PC, which uses the method of Currie for MDA calculation, at 95% confidence. The table below shows the MDA values for uranium isotopes from this analysis, for 30 minute and 90 minute count times. The isotopic MDA is defined as the lowest line MDA for any of the isotope's gamma lines.

This table shows that the LDLs for the LPRMS probe are generally about twice those of the survey probe, except for isotopes which only have low energy gamma lines. Both probes show LDLs for U-235, U-237 and U-238 which are potentially useful for monitoring applications; the ratio of the 30 and 90 minute count LDLs shows that the LDLs are dominated by count statistics, and that longer count times could be expected to further reduce the LDL. For reliable measurement, it's

Table 1. Lower Detection Limits: Uranium
30 and 90 Minute Counts: Test 3A

Isotope	Survey Probe		LPRMS Probe (1 m)	
	30 min	90 min	30 min	90 min
U-233	130.8	75.5 pCi/g	219.1	126.7 pCi/g
U-234	207.8	119.6 pCi/g	23320	13472 pCi/g
U-235	0.39	0.23 pCi/g	0.52	0.30 pCi/g
U-236	207.5	69.4 pCi/g	2436	1408 pCi/g
U-237	0.68	0.39 pCi/g	1.27	0.74 pCi/g
U-238	4.38	2.53 pCi/g	10.5	6.10 pCi/g

desirable for the activity to be roughly a factor of 5 to 10 or more above the lower detection limit. With the isotopic ratios typical for FEMP, this corresponds to about 50 pCi/g total U for the survey probe and about 125 pCi/g total U for the LPRMS probe for 90 minute count times (based on U-238). For 30 minute count times, the LDLs correspond to about 90 pCi/g total U for the Survey Probe and about 200 pCi/g total U for the LPRMS probe, based on U-238.

6.2. Precision and Bias

Because of the limited number of test articles and their generally low uranium activity levels, the precision values for the LPRMS and Survey probes are stated in Table 2 at isotopic activities of about 5 times the MDA, or roughly 6 to 10 times the LDL, rather than at the more typical 10 times MDA. The values listed in the table are for single 30 minute counts rather than an average of multiple counts. The activities listed in the table are isotopic activities. The precision values given are relative uncertainties; to calculate these values, the measurement uncertainty (at 1 standard deviation) for an activity determination is divided by the activity, and multiplied by 100 to give a percentage (relative precision). All of the measurement uncertainties were calculated using Genie-PC, as part of the analysis sequence.

To determine the bias of the activity measurements, the difference between the measured and known activities was divided by the known activity and the result is multiplied by 100 to give bias as a percentage (relative bias). For the tests at FEMP, the activities in the test drums were only approximately known. The bias values shown in the table below were calculated using the average isotopic activities for the boxes of USID soils as the "known" value, although there will be some unknown bias due to the sampling involved with removing the soils from the boxes and placing them in the drums, and due to the unknown uncertainties of the reference analyses themselves. The bias values were calculated for the same 30 minute counts used in the determination of precision, above.

Table 2. Precision for Detected Uranium Isotopes
Isotopic Activities at about 5 x MDA

	Survey Probe		LPRMS Probe (1 m)	
Isotope	Precision	Activity	Precision	Activity
U-235	5.6%	3.451 pCi/g	7.3%	6.693 pCi/g
U-238(Th-234)	25.0%	21.80 pCi/g	--	n/d
U-238(Pa-234m)	4.7%	155.6 pCi/g	7.4%	155.6 pCi/g

Table 3. Bias for Uranium Isotopes
Isotopic Activities at about 5 x MDA

	Survey Probe		LPRMS Probe (1 m)	
Isotope	Bias	Activity	Bias	Activity
U-235	+3.2%	3.451 pCi/g	+78.2%	6.69 pCi/g
U-238(Th-234)	+382%	21.80 pCi/g	--	n/d
U-238(Pa-234m)	+8.9%	155.6 pCi/g	+5.2%	155.6 pCi/g

7. Discussion

In general, for any given test configuration, it was more difficult for the analysis software to locate peaks for the LPRMS count data than for the survey probe. When the peaks were located in the spectra, more difficulty was encountered in identifying nuclides. For identified nuclides, the uncertainties in the calculated activities were larger. This was due primarily to the poorer resolution of the LPRMS, even though the count rates with the LPRMS probe were 10 to 40 percent higher than with the survey probe.

The effect of resolution on the energy spectrum is illustrated in Figure 3, which shows counts of a calibration source performed with the LPRMS and survey probes. The cal source and count times were the same for both probes. The resolution of the LPRMS probe is about 11.8%, the survey probe resolution is about 7.3% (at 662 keV). The peaks for the LPRMS probe (dotted line) are lower and broader than those for the survey probe (solid line), although they contain about the same or greater number of counts. The net height of the Cs-137 peak at 662 keV is roughly 7500 counts for the LPRMS probe and 12000 counts for the survey probe. The signal-to-noise ratio (net peak height/continuum) for this peak is about 4 for the survey probe and less than 2 for the LPRMS probe. This results in a significant increase in the minimum detectable activity: small peaks, either from low activities or from low yield isotopes, can't be separated from the statistical variation of the continuum count rate.

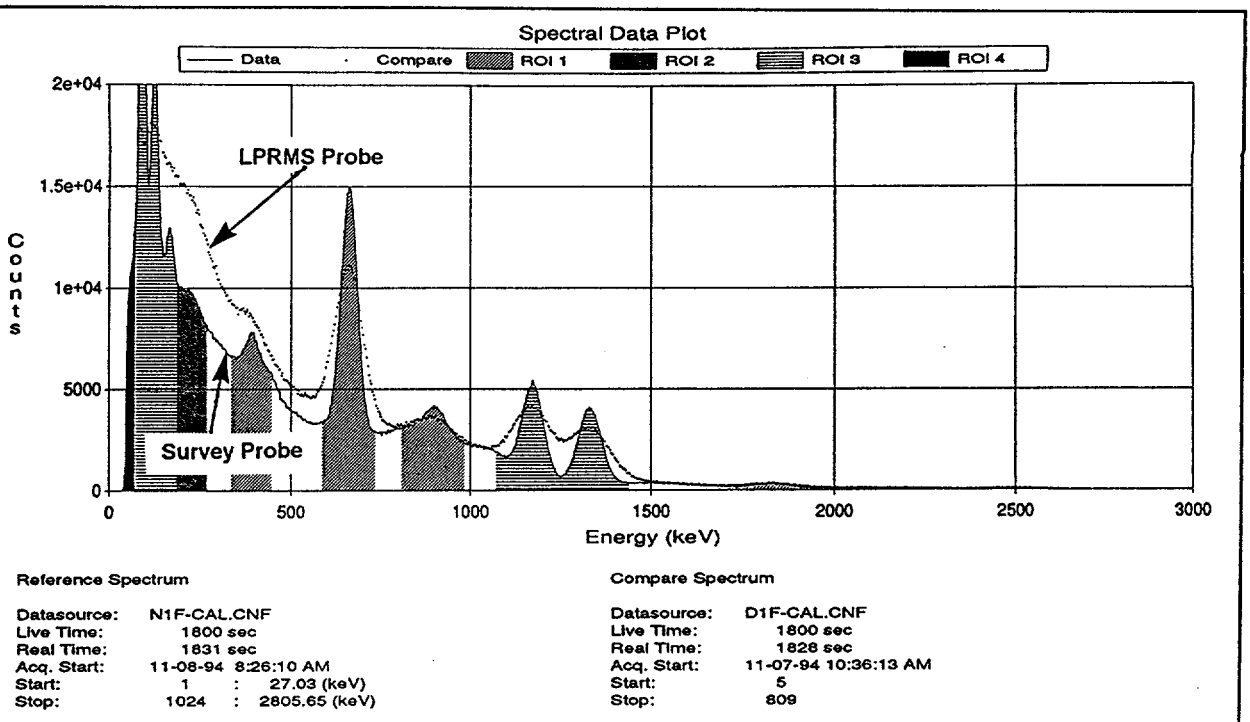

Figure 3. Comparison of Calibration Spectra

The higher FWHM results in greater uncertainty in the location of the peak centroids, making peak identification more difficult. It also results in complications in separating multiple peaks and in determining their areas. For example, the Co-60 peaks in Figure 3 are at 1173 and 1333 keV, separated by 160 keV. With the survey probe, these peaks are cleanly resolved with little overlap, and the Compton edge of the 1333 keV peak (at 1119 keV) is below the ROI for the 1173 peak. With the LPRMS probe, these two peaks have significant overlap, and the Compton edge of the 1333 keV peak is within the 1173 keV peak. While these two peaks can still be separated, simple peak height analysis algorithms will have difficulty correctly determining the peak areas because of the relatively shallow valley between them and the presence of the Compton edge of one peak within the area of the other. More complex analysis routines using interactive Gaussian fits could do a better job of analyzing these peaks, but are more expensive, slower, and can require a priori knowledge of peak locations to be effective.

The controlling factor to the achievable resolution in a PMT/scintillator combination is statistical broadening, based on the number of photoelectrons emitted from the PMT photocathode. This quantity is controlled by the number of incident optical photons/gamma event and the quantum efficiency of the photocathode. In the LPRMS, both of these factors are important. The optical losses associated with using an optical waveguide reduce the number of optical photons incident at the photocathode by about 9 dB, compared to a butt-coupled geometry. The spectral mismatch between the CsI(Tl) emission spectrum and the photocathode response spectrum introduces an additional loss of about 3.5 dB, compared to a bialkali PMT and NaI(Tl) scintillator. All other losses, such as gamma attenuation by the steel scintillator window, are minor by comparison.

The losses associated with the waveguide are primarily due to its limited view angle into the scintillator, a function of its numerical aperture. The waveguide chosen has an NA of about 0.65. Significantly increasing the lightguide numerical aperture to increase the view angle is not practical, because transparent materials with the required higher index of refraction are not readily available. The CsI(Tl) scintillator emission spectrum minimizes the throughput losses in the lightguide; changing the scintillator to improve the spectral match to a PMT would result in a greater increase in the throughput losses than could be gained in a better spectral match. Changing the waveguide to a material with lower losses in the emission spectrum of NaI(Tl) would result in a lower NA and consequently greater view angle losses than would be gained by the decrease in spectral losses.

8. Field Test Conclusions

The critical performance parameters for a post-closure monitor are the lower detection limits and precision. The performance of the LPRMS probe was consistently poorer than that of the survey probe in both of these areas. With 30 minute count times, neither of the probes tested clearly demonstrated the capability of identifying and quantifying uranium isotopes at activities near the post-closure concern levels assumed for this program (35 pCi/g total U, 17 pCi/g U- 238, 0.85 pCi/g U-235). With 90 minute or greater count times, the performance of the survey probe has marginally adequate lower detection limits for both U-235 and U-238, with precision of about 5%. To detect and monitor these isotopes at such activities, the waveguide-coupled LPRMS will require significant improvements in resolution, peak-to-total ratio, or both. A review of the options for reducing optical losses and improving the performance of this design showed that it is unlikely that the needed improvements can be obtained.

Based on the results obtained with the survey probe, it is believed that a resolution of 7.5 to 8.0% (at 662 keV) will be adequate, with some improvement in peak-to-total ratio, to reliably monitor U-235 and U-238 at the assumed post-closure concern levels, using 2 hour count times. We considered the available options to accomplish this, and concluded that a workable approach is readily available, employing a butt-coupled scintillator/PMT probe. This previously rejected approach is now practical for post-closure monitoring, because of the recent development of CPT technology to push low cost plastic casing to depths comparable to those attainable with CPT tools, opening the option for readily retrievable downhole electronic components. This approach retains the desired benefits of low installed cost, serviceability, CPT installation and minimal potential for cross-contamination both during installation and in service. A prototype system based on this approach has been proposed to DOE for demonstration in Phase III of this program; the architecture for this system is shown in Figure 4 below.

9. Cost Comparison

Based on the cost estimates obtained for the Phase III prototype system, the system installed costs have been estimated. These costs do not include any reduction in cost for quantity, marketplace competition or increased maturity of the system technology, and thus can be considered as typical of the first installed system. Costs are included for hardware, software and quality assurance, as well as project management costs for deploying the system. Costs are not included for site specific activities such as determination of monitoring

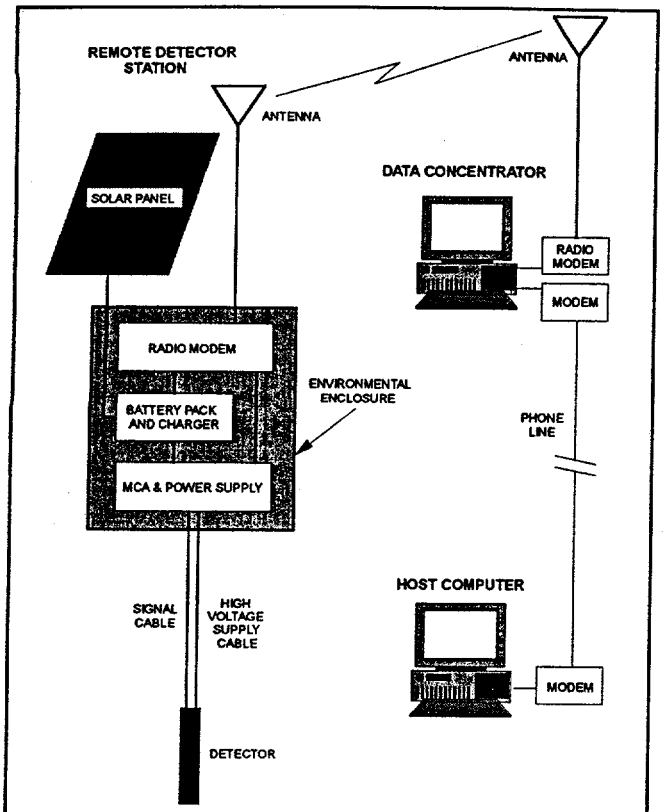

Figure 4. Phase III System Architecture

locations and depths, project specific health and safety plans, permitting and other similar activities.

The system components include those which are required for each monitoring location (PVC casing, completion, probes and remote stations), those which are required for each site monitored (transceiver and data concentrator) and those which are required for the monitoring system as a whole (host computer). For comparison purposes, a system with 12 monitoring locations at 20 meter depth has been assumed, with a maximum distance of 15 kilometers between the remote stations and the data concentrator. This system requires a single data concentrator and a single host computer. It has been assumed that the host computer is dedicated to this one system, although in actuality, a single host can provide analysis and trending for multiple sites. The total system cost for a single system to monitor 12 points with a dedicated host computer is shown below.

Table 4. Installed Costs:Monitoring System

Per Point Costs:	12 @ $20,955 = $241,860
Per Site Costs:	1 @ $38,470 = $ 38,470
Per System Cost:	1 @ $44,085 = $ 44,085
	Total System Cost = $324,415

For comparison, costs were obtained from FERMCO and Rocky Flats for conventional sampling and laboratory analysis. The total costs per sample were estimated to be about $3500 per sample, with a turnaround time of 60 to 400 days. This estimate does not include costs for project specific health and safety plans, oversight personnel, radiological control technicians, sample shipping or surveying. The costs of conventional sampling and analysis were evaluated using a simple annuity calculation (present worth) assuming an interest rate of 5%. The effects of inflation were ignored. The present worth of the cost of conventional sampling and analysis for 12 locations for 25 years is shown in Table 5 below for analysis intervals of once per year, and once per quarter. With a sampling interval of once per year, the savings with the LPRMS system are about 45%; with an interval of once per quarter, the savings are about 87%.

Table 5. Present Worth of Conventional Sampling and Analysis Costs

Once/year:	$ 591,948
Once/quarter:	$2,367,792

monitoring without significant cost impact, and eliminates the long lead time encountered with conventional sampling and laboratory analyses. Sampling error is eliminated, and each measurement is taken in the same physical location, providing an improved ability to track small changes in activity with good precision. The potential for smearing and cross contamination from sampling operations is also eliminated, as are cutting disposal and grouting. The potential for worker exposure during sampling and sample handling is also eliminated. Use of this system thus provides a faster, better, cheaper and safer means to perform long-term *in situ* monitoring for radionuclide contamination.

10. Acknowledgements

This work was supported by the Morgantown (WV) Energy Technology Center, for the Office of Technology Development (EM-50) of the U.S. Department of Energy under Contract Number DE-AC21-92MC29103. This work, performed between April 1994 and July 1995, was Phase II of a three phase contract. The METC Contracting Officer's Representative during this phase was C. Edward Christy.

Appendices

Agenda

ENVIRONMENTAL TECHNOLOGY DEVELOPMENT THROUGH INDUSTRY PARTNERSHIP
October 3-5, 1995

TUESDAY, OCTOBER 3, 1995

7:30 a.m. REGISTRATION/CONTINENTAL BREAKFAST

SESSION 1 — OPENING SESSION

Session Chair: Robert C. Bedick

8:15 a.m. *Welcome to METC*

8:25 a.m. 1.1 *Introductory Comments*
Dr. Clyde Frank
Deputy Assistant Secretary
DOE/HQ - EM Office of Science and Technology

8:50 a.m. 1.2 *EM Technology Development - METC Perspective*
Thomas F. Bechtel
Director
Morgantown Energy Technology Center

9:15 a.m. 1.3 *Mixed Waste Characterization, Treatment, and Disposal Focus Area Perspective*
Christine J. Bonzon
DOE Idaho Operations Office

9:35 a.m. 1.4 *High-Level Waste Tank Remediation Focus Area Perspective*
Dennis Brown
DOE Richland Operations Office

9:55 a.m. BREAK

10:15 a.m. 1.5 *Contaminant Plume Containment and Remediation Focus Area Perspective*
James Wright
DOE Savannah River Operations Office

10:35 a.m.	1.6	*Landfill Stabilization Focus Area Perspective* James Brown DOE Savannah River Operations Office
10:55 a.m.	1.7	*Decontamination and Decommissioning Focus Area Perspective* Paul Hart Morgantown Energy Technology Center
11:15 a.m.	1.8	*Crosscutting Technologies Focus Area Perspective - Characterization* Caroline B. Purdy DOE/HQ - EM Office of Science and Technology
11:30 a.m.	1.9	*Crosscutting Technologies Focus Area Perspective - Separations* Teresa B. Fryberger DOE/HQ - EM Office of Science and Technology
11:45 a.m.	1.10	*Crosscutting Technologies Focus Area Perspective - Robotics* Linton W. Yarbrough DOE/HQ - EM Office of Science and Technology
12:00 noon	1.11	*The GETE Approach to Facilitating the Commercialization and Use of DOE-Developed Environmental Technologies* Thomas N. Harvey Global Environment & Technology Foundation
12:20 p.m.	LUNCH	
1:20 p.m.	POSTER SESSION I	

Session Chair: Jagdish L. Malhotra

PI.1	*Electromagnetic Mixed Waste Processing System for Asbestos Decontamination* Raymond S. Kasevich KAI Technologies, Inc.
PI.2	*Electrokinetic Decontamination of Concrete* Henry L. Lomasney ISOTRON Corporation
PI.3	*Decontamination of Process Equipment Using Recyclable Chelating Solvent* John M. Jevec Babcock & Wilcox R&DD

PI.4 *Alpha Detection in Pipes Using an Inverting Membrane Scintillator*
C. David Cremer
Science and Engineering Associates, Inc.

PI.5 *Rapid Surface Sampling and Archive Record System*
Elizabeth Barren
GE Corporate Research and Development Center

PI.6 *Portable Sensor for Hazardous Waste*
Lawrence G. Piper
Physical Sciences Inc.

PI.7 *Protective Clothing Based on Permselective Membrane and Carbon Adsorption*
Doug Gottschlich
Membrane Technology & Research

PI.8 *Coherent Laser Vision System (CLVS)*
Richard L. Sebastian
Coleman Research Corporation

PI.9 *Multisensor Inspection and Characterization Robot for Small Pipes*
Eric Byler
Lockheed Martin

PI.10 *Mixed Waste Treatment Using the ChemChar Thermolytic Detoxification Technique*
Daniel J. Kuchynka
Mirage Systems

PI.11 *Automated Baseline Change Detection*
Peter A. Berardo
Lockheed Martin Missiles & Space

PI.12 *Electrodialysis-Ion Exchange for the Separation of Dissolved Salts*
Charles J. Baroch
WASTREN, Inc.

PI.13 *Decontamination Systems Information and Research Program*
Echol E. Cook
West Virginia University

PI.14 *Environmental Management Technology Demonstration and Commercialization*
Edward N. Steadman
Energy & Environmental Research Center

PI.15 *VAC*TRAX — Thermal Desorption for Mixed Wastes*
Michael J. McElwee
Rust Federal Services

SESSION 2 — MIXED WASTE CHARACTERIZATION, TREATMENT, AND DISPOSAL FOCUS AREA

Session Chair: Clifford P. Carpenter, II

2:45 p.m. 2.1 *Development Studies of a Novel Wet Oxidation Process*
Terry W. Rogers
Delphi Research, Inc.

3:10 p.m. 2.2 *Innovative Vitrification for Soil Remediation*
Norman W. Jetta
Vortec Corporation

3:35 p.m. BREAK

3:50 p.m. 2.3 *Catalytic Extraction Processing of Contaminated Scrap Metal*
Bashar M. Zeitoon
Molten Metal Technology, Inc.

4:15 p.m. 2.4 *Waste Inspection Tomography*
Richard T. Bernardi
Bio-Imaging Research, Inc.

4:40 p.m. 2.5 *A Robotic End Effector for Inspection of Storage Tanks*
Gregory Hughes
Oceaneering Space Systems

5:05 p.m. ADJOURN

6:00 p.m. SOCIAL

7:00 p.m. DINNER
West Virginia University Erickson Alumni Center

WEDNESDAY, OCTOBER 4, 1995

7:45 a.m. REGISTRATION/CONTINENTAL BREAKFAST

8:15 a.m. *Welcome Back to METC*
DOE/METC

8:20 a.m. **PANEL DISCUSSION — MIXED WASTE CHARACTERIZATION, TREATMENT, AND DISPOSAL ISSUES**

Session Chair: William J. Huber

Christine J. Bonzon
DOE Idaho Operations Office

Bill Owca
DOE Idaho Operations Office

Tom Anderson
DOE/HQ - EM Office of Science and Technology

James Brown
DOE Savannah River Operations Office

10:00 a.m. BREAK

SESSION 3 — DECONTAMINATION AND DECOMMISSIONING FOCUS AREA

Session Chair: Steven J. Bossart

10:20 a.m. 3.1 *Advanced Worker Protection System*
Bruce Caldwell
Oceaneering Space Systems

10:45 a.m. 3.2 *Characterization of Radioactive Contamination Inside Pipes with the Pipe Explorer™ System*
C. David Cremer
Science and Engineering Associates, Inc.

11:10 a.m. 3.3 *Laser-Based Coatings Removal*
Joyce Freiwald
F2 Associates Inc.

11:35 a.m.	3.4	*Concrete Decontamination by Electro-Hydraulic Scabbling* Victor Goldfarb Textron Defense Systems
12:00 noon	3.5	*Advanced Technologies for Decontamination and Conversion of Scrap Metal* Alan L. Liby Manufacturing Sciences Corporation
12:30 p.m.	LUNCH	
1:30 p.m.	3.6	*Floor Decontamination and Waste Minimization with ROVCO$_2$* Andrew M. Resnick Oceaneering International, Inc.
1:55 p.m.	3.7	*Mobile Worksystems for Decontamination and Dismantlement* Jim "Oz" Osborn Carnegie Mellon University
2:20 p.m.	3.8	*Interactive Computer Enhanced Remote Viewing System* John Tourtellott Mechanical Technology Incorporated
2:45 p.m.	3.9	*Three Dimensional Characterization and Archiving System (3D-ICAS)* Richard L. Sebastian Coleman Research Corporation
3:10 p.m.	BREAK	
3:25 p.m.	3.10	*BOA: Pipe-Asbestos Insulation Removal Robot System* Hagen Schempf Carnegie Mellon University
3:50 p.m.	3.11	*An Intelligent Inspection and Survey Robot* Joseph S. Byrd University of South Carolina
4:10 p.m.	3.12	*Intelligent Mobile Sensor System for Autonomous Monitoring and Inspection* Eric Byler Lockheed Martin
4:35 p.m.	3.13	*Houdini: Reconfigurable In-Tank Robot* Adam D. Slifko RedZone Robotics, Inc.

5:00 p.m. POSTER SESSION II

Session Chair: Vijay P. Kothari

PII.1 *THE LASI High-Frequency Ellipticity System*
Ben K. Sternberg
University of Arizona

PII.2 *Analyze Imagery and Other Data Collected at the Los Alamos National Laboratory*
N. A. David
Environmental Research Institute of Michigan (ERIM)

PII.3 *Surfactant-Enhanced Aquifer Remediation at the Portsmouth Gaseous Diffusion Plant*
Richard E. Jackson
INTERA Inc.

PII.4 *Laboratory "Proof of Principle" Investigation for the Acoustically Enhanced Remediation Technology*
Joe L. Iovenitti
Weiss Associates

PII.5 *Measuring Fuel Contamination Using High Speed Gas Chromatography and Cone Penetration Techniques*
S. Farrington
Applied Research Associates, Inc.

PII.6 *Miniature GC for In-Situ Monitoring of Volatile Organic Compounds Within a Cone Penetrometer*
Henry Wolhjen
Microsensor Systems

PII.7 *Development of an On-Line Real-Time Alpha Radiation Measuring Instrument for Liquid Streams*
Keith Patch
Thermo Power Corp., Tecogen Division

PII.8 *Fiber Optic/Cone Penetrometer System for Subsurface Heavy Metals Detection*
Steven Saggese
Science and Engineering Associates, Inc.

PII.9 *Radioactivity Measurements Using Storage Phosphor Technology*
Y. T. Cheng
NeuTek

PII.10 *Surfactant-Modified Zeolites as Permeable Barriers to Organic and Inorganic Groundwater Contaminants*
Robert S. Bowman
New Mexico Institute of Mining and Technology

PII.11 *Barometric Pumping With a Twist: VOC Containment and Remediation Without Boreholes*
William E. Lowry
Science and Engineering Associates, Inc.

PII.12 *Measurement of Radionuclides Using Ion Chromatography and Flow-Cell Scintillation Counting with Pulse Shape Discrimination*
Robert A. Fjeld
Clemson University

PII.13 *Development of HUMASORB™, a Lignite Derived Humic Acid for Removal of Metals and Organic Contaminants fromGroundwater*
H. G. Sanjay
Kailash Srivastava
ARCTECH, Inc.

PII.14 *Field Raman Spectrograph for Environmental Analysis*
John W. Haas, III
EIC Laboratories, Inc.

PII.15 *An Advanced Open-Path Atmospheric Pollution Monitor for Large Areas*
Lyle H. Taylor
Westinghouse Science & Technology Center

PII.16 *Nitrate to Ammonia Ceramic (NAC) Bench-Scale Stabilization Study*
W. Jon Caime
Rust - Clemson Tech Center

6:30 p.m. ADJOURN

THURSDAY, OCTOBER 5, 1995

7:45 a.m. REGISTRATION/CONTINENTAL BREAKFAST

8:15 a.m. *Welcome Back to METC*
DOE/METC

8:20 a.m. **PLUME PANEL DISCUSSION —**
HOW GOOD IS GOOD ENOUGH?
The Application, Evaluation, and Acceptance of In-Situ and Ex-Situ Plume Remediation Technologies

Session Chairs: Kelly D. Pearce
Jim Wright

Carol Eddy-Dilek
Westinghouse Savannah River Company

Richard Jackson
Intera

Bob Siegrist
Colorado School of Mines

Sa V. Ho
Monsanto Company

Dane McKinney
University of Texas

Andrew Paterson
Environmental Business Partners

Thomas Brouns
PNL

10:00 a.m. BREAK

SESSION 4 — CONTAMINANT PLUME CONTAINMENT AND REMEDIATION, AND LANDFILL STABILIZATION FOCUS AREAS

Session Chair: C. Eddie Christy

10:20 a.m.	4.1	*Field Portable Detection of VOCs Using a SAW/GC System* Edward Staples Electronic Sensor Technology
10:45 a.m.	4.2	*Field-Usable Portable Analyzer for Chlorinated Organic Compounds* William J. Buttner Transducer Research, Inc.
11:10 a.m.	4.3	*Development of the Integrated In Situ Lasagna Process* Sa V. Ho Monsanto Company
11:35 a.m.	4.4	*Steerable/Distance Enhanced Penetrometer Delivery System* Ali Amini UTD Incorporated
12:00 noon	4.5	*Road Transportable Analytical Laboratory (RTAL) System* Stanley M. Finger Engineering Computer Optecnomics, Inc.
12:30 p.m.	LUNCH	
1:30 p.m.	4.6	*Three-Dimensional Subsurface Imaging Synthetic Aperture Radar* Ed Wuenschel Mirage Systems, Inc.
1:55 p.m.	4.7	*Geophex Airborne Unmanned Survey System* Dean Keiswetter Geophex, Ltd.
2:20 p.m.	4.8	*Field Test of a Post-Closure Radiation Monitor* Stuart E. Reed Babcock & Wilcox, R&DD
2:45 p.m.	CLOSING REMARKS	
3:00 p.m.	METC SITE TOUR	

Meeting Participants

Tim Adams
Vice President
ICF Consulting Group
9300 Lee Highway
Fairfax, VA 22031-1207
703-934-3637; fax: 703-934-3083

Michael Akard
Research Chemist
Chromatofast Inc.
912 N. Main, Ste. No. 14
Ann Arbor, MI 48104
313-662-3410; fax: 313-662-3462

Brian Albers
BDM Federal
555 Quince Orchard Rd., Ste. 400
Gaithersburg, MD 20878
301-212-6220; fax: 301-212-6251

Ed Alperin
Dir., Tech Applications Lab
IT Corporation
312 Directors Drive
Knoxville, TN 37923
423-690-3211; fax: 423-694-9573

Ali Amini
Vice President
UTD Incorporated
8560 Cinderbed Road
P.O. Box 8560, Ste. 1300
Newington, VA 22122
703-339-0800; fax: 703-339-6519

Carl Anderson
Dir., Radioactive Waste Mgmt.
National Research Council
2001 Wisconsin Ave., N.W.
Washington, DC 20007
202-334-3066; fax: 202-
334-3077CANDERS@NAS.EDU

Jon B. Anderson
Program Mgr., Research & Design
UTD Incorporated
8560 Cinderbed Road
P.O. Box 8560, Ste. 1300
Newington, VA 22122
703-339-0800; fax: 703-339-6519

Thomas D. Anderson
Deputy Director, R&D
U.S. Department of Energy
19901 Germantown Road
Germantown, MD 20874-1290
301-903-7295; fax: 301-903-7618

Rodney Anderson
Physical Scientist
Morgantown Energy Technology Center
U.S. Department of Energy
P.O. Box 880, MS-A03
Morgantown, WV 26507-0880
304-285-4709; fax: 304-285-4403
RANDER@METC.DOE.GOV

Richard A. Bajura
Dir., NRCCE
West Virginia University
P.O. Box 6064
Morgantown, WV 26506
304-293-2967; fax: 304-293-3749

Rita A. Bajura
Assoc. Dir., OPTM
Morgantown Energy Technology Center
U.S. Department of Energy
P.O. Box 880, MS-B06
Morgantown, WV 26507-0880
304-285-4109, fax: 304-285-4292
RBAJUR@METC.DOE.GOV

Richard Baker
Dir., Environmental Mgmt. Div.
U.S. Department of Energy
9800 S. Cass Avenue
Argonne, IL 60439
708-252-2647; fax: 708-252-2750

Leona C. Bares
Product Manager, D&D Systems
Redzone Robotics, Inc.
2425 Liberty Ave.
Pittsburgh, PA 15222
412-765-3064; fax: 412-765-3069
LBARES@REDZONE.COM

Elizabeth Barren
Chemist
GE Corporate R&D
1 River Road, P.O. Box 8
Schenectady, NY 12301-0008
518-387-7712; fax: 518-387-5592
BARRENE.LRD.GE.COM

Richard J. Bateman
Mgr., Tech Integ.
Kaiser-Hill, LLC
P.O. Box 464
Golden, CO 80402-0464
303-966-5746; fax: 303-966-4235

Terry Bates
Vice President
Energetics, Inc.
7164 Gateway Drive
Columbia, MD 21046
410-290-0370; fax: 410-290-0377

Tia Maria Beatty
Engineering Scientist
West Virginia University
P.O. Box 6103
Morgantown, WV 26505
304-293-3031; fax: 304-293-7109
BEATTY@CEMR.WVU.EDU

Thomas F. Bechtel
Director
Morgantown Energy Technology Center
U.S. Department of Energy
P.O. Box 880, MS-C02
Morgantown, WV 26507-0880
304-285-4511, fax: 304-285-4292
TBECHT@METC.DOE.GOV

Robert C. Bedick
Product Manager, EWM
Morgantown Energy Technology Center
U.S. Department of Energy
P.O. Box 880, MS-D01
Morgantown, WV 26507-0880
304-285-4505, fax: 304-285-4403
RBEDIC@METC.DOE.GOV

David Bennett
Director, Systems Tech.
Schilling Robotic Systems
1632 Da Vinci Ct.
Davis, CA 95616
916-753-6718; fax: 916-753-8092
DAVID@EMAIL.COM

Peter A. Berardo
Senior Staff Scientist
Lockheed Martin
3251 Hanover St., 9230B250
Palo Alto, CA 94306
415-424-2137; fax: 415-424-2854
BERARDO@LMSC.LOCKHEED.COM

James Berger
Mgr., Tech. Integration
Westinghouse Hanford Co.
P.O. Box 1970
Richland, WA 99352
509-376-9942; fax: 509-376-9746

Richard T. Bernardi
V.P. of Business Development
Bio-Imaging Research, Inc.
425 Barclay Blvd.
Lincolnshire, IL 60069
708-634-6425; fax: 708-634-6440

Samit K. Bhattacharyya
Assoc. Dir. Tech. Development
Argonne National Laboratory
9700 S. Cass Ave., Bldg. 207
Argonne, IL 60439
708-252-3293; fax: 708-252-4007
BHATT@TD.ANL.GOV

Amilcare Biancheria
Project Mgmt. - Environmental
AWK Consulting Engineers
1225 Rodi Road
Turtle Creek, PA 15145
412-823-8331; fax: 412-823-6987

David Biancosino
Program Manager
U.S. Department of Energy
19901 Germantown Road
Germantown, MD 20874
301-903-7961; fax: 301-903-7234

Lindsey Bierer
Program Manager
U.S. Department of Energy
CDM Federal Programs
3760 Convoy St., Suite 210
San Diego, CA 92111
619-268-3383; fax: 619-268-9677

Dave Black
Manager
Argonne National Laboratory
9700 S. Cass Avenue
Argonne, IL 60439
708-252-6030; fax: 708-252-1774

Roseanne Black
Communication Specialist
Waste Policy Institute
1872 Pratt Dr., Suite 1600
Blacksburg, VA 24060
540-231-9848; fax: 540-231-3968
ROSEANNEBLACK@WPI.ORG

Christine Bonzon
Manager
U.S. Department of Energy
785 DOE Place
Idaho Falls, ID 83402
208-526-3752; fax: 208-526-0160
BONZONCJ@INEL.GOV

John D. Borgman
Assoc. Dir., Robotics
The University of Texas
PRC MER 1.206 R 9925
Austin, TX 78712
512-471-3039; fax: 512-471-3987
JBORGMAN@MAIL.UTEXAS.EDU

Steve Bossart
Project Manager
Morgantown Energy Technology Center
U.S. Department of Energy
P.O. Box 880, MS-E06
Morgantown, WV 26507-0880
304-285-4643, fax: 304-285-4403
SBOSSA@METC.DOE.GOV

Stanley S. Borys
V.P., Environmental Prog. Dev.
Institute of Gas Technology
1700 S. Mt. Prospect Road
Des Plaines, IL 60018
708-768-0522; fax: 708-768-0516
BORYS@IGT.ORG

Joseph F. Boudrfaux
Research Associate
Florida International Univ.
University Park
Miami, FL 33199
305-348-3727; fax: 305-348-1932
(JOSEPHB)@ENG.FIU.EDU

Robert S. Bowman
Dir./Professor of Hydrology
New Mexico Tech.
Dept. of Earth & Environ. Sci.
Socorro, NM 87801
505-835-5992; fax: 505-835-6436
BOWMAN@PRISM.NMT.EDU

Gerald Boyd
Assoc. Deputy to Asst. Sec.
U.S. Department of Energy, EM 50
Washington, DC 20545
301-903-7260; fax: 301-903-7618

Taz Bramlette
Mgr., Environmental Programs
Sandia National Laboratories
7011 East Ave., MS 9410
Livermore, CA 94550
510-294-2299; fax: 510-294-2999
TTBRAML@SANDIA.GOV

Albert Brennsteiner
Post Doctoral Fellow
West Virginia University
Dept. of Chemical Engineering
P.O. Box 6102
Morgantown, WV 26506
304-293-2111

Marvin S. Brooks
Project Manager
Waste Policy Institute
555 Quince Orchard Road, Ste. 600
Gaithersburg, MD 20878-1437
301-990-3125; fax: 301-990-6150

Thomas Brouns
Program Manager
Pacific Northwest Laboratory
3200 Q Avenue
Richland, WA 99352
509-372-6265; fax: 509-372-6268

Dennis A. Brown
Program Manager
U.S. Department of Energy
Richland Operations Office
3230 Q Ave.
Richland, WA 99352
509-372-4030; fax: 509-372-4037
DENNIS_A_BROWN@RL.GOV

Jim Brown
LSFA Manager
DOE - Savannah River
P.O. Box A
Aiken, SC 29802
803-725-1027; fax: 803-725-2123
JPERR.3L.BROW@SRS.GOV

Alan Browne
Program Manager
Energetics, Inc.
7414 Cranberry Square
Morgantown, WV 26505
304-594-1450; fax: 304-594-1486

Dwight L. Burns
Chief, Engineering Div.
U.S. Army Corps of Engineers
502 Eighth St.
Huntington, WV 25701-2070
304-529-5254; fax: 304-529-5960

William J. Buttner
Sr. Principal Scientist
Transducer Research, Inc.
999 Chicago Avenue
Naperville, IL 60540
708-357-0004; fax: 708-357-1055

Eric Byler
Lockheed Martin
P.O. Box 179
Denver, CO 80201
303-977-3000

Joseph S. Byrd
Professor
University of South Carolina
301 South Main St.
3A38 Swearingen Eng. Cnt.
Columbia, SC 29208
803-777-9569; fax: 803-777-8045
JSBYRD@ECE.SCAROLINA.EDU

Jon Caime
Environmental Engineer
RUST-Clemson Technical Center
100 Technology Drive
Anderson, SC 29625
803-646-2413; fax: 803-646-5311

Bruce Caldwell
Program Manager
Oceaneering Space Systems
1665 Space Center Blvd.
Houston, TX 77058
713-488-9080; fax: 713-488-2027

Pat Cannon
Customer Service Manager
EG&G/TSWV
P.O. Box 880, MS-L02
Morgantown, WV 26507-0880
304-285-5450; fax: 304-285-4403
PCANNO@METC.DOE.GOV

James K. Carey
Program Director
Energetics
7164 Gateway Drive
Columbia, MD 21046
301-290-0370; fax: 301-290-0377

Cliff Carpenter
Project Manager
Morgantown Energy Technology Center
U.S. Department of Energy
P.O. Box 880, MS-E06
Morgantown, WV 26507-0880
304-285-4041, fax: 304-285-4403
CCARPE@METC.DOE.GOV

Ismail Celik
Professor
West Virginia University
Mechanical & Aerospace Engineering
Morgantown, WV 26506-6106
304-293-3111; fax: 304-293-6689

Texas Chee
Technical Advisor
U.S. Department of Energy
19901 Germantown Road
EM 521 - Cloverleaf
Germantown, MD 20874
301-903-7933; fax: 301-903-7238

Sam C. Cheng
D&D Team Leader
U.S. Department of Energy
Miamisburg Area Office
1 Mound Road, P.O. Box 66
Miamisburg, OH 45343-0066
513-865-4778; fax: 513-865-4489

Yu-Tarng Cheng
Neutek
13537 Scottish Autumn Lane
Darnestown, MD 20878-3990
301-975-6216; fax: 301-948-6427
YJZC51A@PRODIGY.COM

Roger F. Christensen
Dir., Technology Develop. Div.
U.S. Department of Energy
Richland Operations Office
Richland, WA 99352
509-372-4030; fax: 509-372-4037

C. Edward Christy
Project Manager
Morgantown Energy Technology Center
U.S. Department of Energy
P.O. Box 880, MS-E06
Morgantown, WV 26507-0880
304-285-4604, fax: 304-285-4403
CCHRIS@METC.DOE.GOV

Sheila A. Cleary
Corp. Counsel/Dir. of Contracts
Waste Policy Institute
555 Quince Orchard Rd.
Gaithersburg, MD 20878
301-990-3023; fax: 301-990-6150

Cindy Cobb
President
Global Initiatives, Inc.
7010 Little River Turnpike, Ste. 330
Annandale, VA 22003
703-750-3934; fax: 703-750-5438
CINDY.COBB@GNET.ORG

E. E. (Bud) Cook
Professor
West Virginia University
Civil & Envir. Engineering
Morgantown, WV 26505
304-285-4657; fax: 304-285-4469

Steve Cooke
Project Manager
Morgantown Energy Technology Center
U.S. Department of Energy
P.O. Box 880, MS-E01
Morgantown, WV 26507-0880
304-285-5437, fax: 304-285-4403
SCOOKE@METC.DOE.GOV

Marc Cordes
President
Nexi Nuclear Expertise, Inc.
10461 White Granite Drive
Oakton, VA 22124
703-352-4912; fax: 703-352-4915
102072.611@COMPUSERVE.COM

C. David Cremer
Senior Scientist
Science & Engineering Assoc.
6100 Uptown Blvd., Ste. 700
Albuquerque, NM 87110
505-884-2300; fax: 505-884-2991
SEAENTEC@USA.NET

Eric Crivella
Nuclear/Hazmat Specialist
Pentek, Inc.
1026 Fourth Ave.
Coraopolis, PA 15108
412-262-0725; fax: 412-262-0731

Floyd W. Crouse
Div. Dir., EWM
Morgantown Energy Technology Center
U.S. Department of Energy
P.O. Box 880, MS-E06
Morgantown, WV 26507-0880
304-285-4535, fax: 304-285-4403
FCROUS@METC.DOE.GOV

Geoff Cunliffe
Program Manager
Spar Aerospace Ltd.
9445 Airport Road
Brampton, Ontario L6S-4J3
Canada
905-790-2800; fax: 905-790-4506
GCUNLIFF@SPAR.CA

Ember Curry
Engineering Assistant
GPU Nuclear Corp.
P.O. Box 480, Route 441 S.
Mail Stop NOB-2
Middletown, PA 17057
717-948-8592; fax: 717-948-8313

Dan Daly
Geologist
Energy & Environ. Research Ctr.
P.O. Box 9018
Grand Forks, ND 58202
701-777-5000; fax: 701-777-5181

Kamal Das
Project Manager
Morgantown Energy Technology Center
U.S. Department of Energy
P.O. Box 880, MS-C05
Morgantown, WV 26507-0880
304-285-4065, fax: 304-285-4403
KDAS@METC.DOE.GOV

Nancy A. David
Manager NM Operations
ERIM
1701 Old Pecos Trail
Santa Fe, NM 87505
505-982-9180; fax: 505-982-0322
NDAVID@ERIM.ORG

S. Ladd Davies
Energetics, Inc.
7414 Cranberry Square
Morgantown, WV 26505
304-594-1450; fax: 304-594-1486

Richard Dennis
Project Manager
Morgantown Energy Technology Center
U.S. Department of Energy
P.O. Box 880, MS-C04
Morgantown, WV 26507-0880
304-285-4515, fax: 304-285-4403
RDENNI@METC.DOE.GOV

Arthur Desrosiers
V.P., Special Projects
Bartlett Services, Inc.
60 Industrial Park Road
Plymouth, MA 02360
508-746-6464; fax: 508-830-3616
BARTLETT@BARTLETTNUCLEAR.COM

Miles C. Dionisio
Program Manager
U.S. Department of Energy
20400 Century Blvd.
Germantown, MD 20874
301-903-7639; fax: 301-903-7457
MILES.DIONISIO@EM.DOE.GOV

Holmer Dugger
Program Manager
ICF Kaiser Hanford Co.
1200 Jadwin
Richland, WA 99352
509-376-3297; fax: 509-376-6698

Abdul R. Dulloo
Senior Engineer
Westinghouse Electric Corp.
Science & Technology Center
Pittsburgh, PA 15235
412-256-2140; fax: 412-256-1222
DULLO@CIS.PGH.WEC.COM

Dale S. Dutt
Manager
Westinghouse Hanford Co.
P.O. Box 1970, MSIN N121
Richland, WA 99352
509-376-7439; fax: 509-376-7327
DALE_S_DUTT%CCMAIL@PNL.GOV

Thomas O. Early
Lockheed Martin
P.O. Box 2008, MS-6400
Oak Ridge, TN 37831-6400
423-576-2103; fax: 423-576-3989
EOT@ORNL.GOV

Ali Ebadian
Professor & Chairperson
Florida International Univ.
Hemisphere Center
Environmental Technology
Miami, FL 33199
305-348-2569; fax: 305-348-4176

Steve Einan
Program Analyst
U.S. Department of Energy
Cloverleaf Bldg., EM-52
Germantown, MD 20874
301-903-7947; fax: 301-903-1530
STEVEN.EINAN@EM.DOE.GOV

William D. Ellis
Environmental Chemist
SAIC
Waste Policy Institue
1262 Pineview Drive
Morgantown, WV 26505
800-997-7293; fax: 304-598-9392
BILL_ELLIS@CCMAIL.GMT.SA

Michael Elo
Nuclear Engineer
Burns & Roe Environ. Services
20201 Century Blvd.
Germantown, MD 20874
301-916-7265; fax: 301-916 7272

Donald L. Erich
Manager/Dir. VIT Research Lab
Clemson University
342 Computer Court
Anderson, SC 29625
803-656-0772; fax: 803-656-0672
DERICH@ESE.CLEMSON.EDU

L. Dean Eyman
President & CEO
Waste Policy Institute
1700 Kraft Drive, Ste. 2400
Blacksburg, VA 24060
540-231-3471; fax: 540-231-3481
DEYMAN@WPI.ORG

Stephen P. Farrington
Staff Engineer
Applied Research Associates
Box 120A Waterman Road
S. Royalton, VT 05068
802-763-8348; fax: 802-763-8283
SFARRINGTON@NED.ARA.COM

Stanley M. Finger
Vice President
ECO, Inc.
1356 Cape, St. Claire Rd.
Annapolis, MD 21401
410-757-3245; fax: 410-757-8265

Robert Fjeld
Professor
Clemson University
342 Computer Ct.
Anderson, SC 24625
803-656-5569; fax: 803-656-0672
FJELD@ESE.CLEMSON.EDU

Eugene L. Foster
President Emeritus
UTD Incorporated
8560 Cinderbed Road
P.O. Box 8560, Suite 1300
Newington, VA 22122
703-339-0800; fax: 703-339-6519

Clyde Frank
Deputy Asst. Sec., Tech. Dev.
U.S. Department of Energy
1000 Independence Ave., S.W.
EM-50
Washington, DC 20585
202-586-6382; fax: 202-586-6773

Brian Frankhouser
Project Manager
Morgantown Energy Technology Center
U.S. Department of Energy
P.O. Box 880, MS-N03
Morgantown, WV 26507-0880
304-285-4847, fax: 304-285-4403
BFRANK@METC.DOE.GOV

Joyce Freiwald
President
F2 Associates Inc.
1708 Soplo Road, S.E.
Albuquerque, NM 87123-4485
505-271-0260; fax: 505-271-1437
JFREIWALD@AOL.COM

Karl-Heinz Frohne
Project Manager
Morgantown Energy Technology Center
U.S. Department of Energy
P.O. Box 880, MS-E06
Morgantown, WV 26507-0880
304-285-4412, fax: 304-285-4403
KFROHN@METC.DOE.GOV

Teresa B. Fryberger
Program Manager
U.S. Department of Energy
HQ-EM-53, Office Tech. Dev.
19901 Germantown Road
Germantown, MD 20874-1290
301-903-7688; fax: 301-903-7450

Andrew D. Gabel
Environ. Restor. Prog. Mgr.
U.S. Department of Energy
Chicago Operations Office
9800 S. Cass Avenue
Argonne, IL 60439
708-252-2213; fax: 708-252-2361

Richard E. Gannon
Director, Business Development
Textron Defense Systems
2385 Revere Beach Parkway
Everett, MA 02149
617-381-4630; fax: 617-381-4160

Victor E. Gatto
V.P., Government Affairs
Molten Metal Technology, Inc.
51 Sawyer Road
Waltham, MA 02154
617-487-7642; fax: 617-487-7870

Rodney Geisbrecht
Project Manager
Morgantown Energy Technology Center
U.S. Department of Energy
P.O. Box 880, MS-C05
Morgantown, WV 26507-0880
304-285-4658, fax: 304-285-4403
RGEISB@METC.DOE.GOV

Kurt Gerdes
Program Manager
U.S. Department Energy
19901 Germantown Rd., CL-EM-54
Germantown, MD 20874-1290
301-903-7289; fax: 301-903-7234

Madhav R. Ghate
Dir., Technology Base Project Mgmt.
Morgantown Energy Technology Center
U.S. Department of Energy
P.O. Box 880, MS-C05
Morgantown, WV 26507-0880
304-285-4135, fax: 304-285-4403
MGHATE@METC.DOE.GOV

Tom Gibb
Chief Operating Officer
Waste Policy Institute
555 Quince Orchard Road, Ste. 600
Gaithersburg, MD 20878-1437
301-990-7200; fax: 301-990-6150

Roger L. Gilchrist
Senior Consultant
Westinghouse Hanford Co.
P.O. Box 1970, L5-62
Richland, WA 99352
509-376-5310; fax: 509-376-9964

Gary Goken
Lab Manager
3M Center
Bldg. 209-1W-24
St. Paul, MN 55144
612-733-6030; fax: 612-737-4538

Victor Goldfarb
Principal Research Scientist
Textron Defense Systems
2385 Revere Beach Parkway
Everett, MA 02149
617-381-4325; fax: 617-381-4160

Bruce S. Goldwater
Deputy Division Manager
Quest Integrated, Inc.
21414 68th Avenue, South
Kent, WA 98032
206-872-9500; fax: 206-872-0690

Morgan Gopnik
Asst. Director, CGER
National Research Council
2101 Wisconsin Ave., N.W.
Washington, DC 20418
202-334-3066; fax: 202-334-3362
MGOPNIK@NAS.EDU

Doug Gottschlich
Applications Engineer
Membrane Technology & Research
1360 Willow Road, No. 103
Menlo Park, CA 94025
415-328-2228; fax: 415-328-6580

Gerald Groenewold
Director
Energy & Environ. Research Ctr.
P.O. Box 9018
Grand Forks, ND 58202
701-777-5131; fax: 701-777-5181

John Haas
Sr. Scientist
EIC Laboratories, Inc.
111 Downey St.
Norwood, MA 02062
617-769-9450; fax: 617-551-0283

Dennis C. Haley
Section Head
Oak Ridge National Lab
P.O. Box 2008, Bldg. 7601
Oak Ridge, TN 37831-6304
423-576-4388; fax: 423-576-2081
H6Y@ORNL.GOV

Jerry L. Harness
Program Manager, D&D Focus Area
U.S. Department of Energy
Oak Ridge Operations Office
P.O. Box 2001
Oak Ridge, TN 37831-8620
423-576-6008; fax: 423-576-5333
X96@ORNL.GOV

Alison E. Harrington
Mgr., R&D and Marketing
Molten Metal Technology, Inc.
51 Sawyer Road
Waltham, MA 02154
617-487-5810; fax: 617-487-7870

Paul Hart
Project Manager
Morgantown Energy Technology Center
U.S. Department of Energy
P.O. Box 880, MS-E06
Morgantown, WV 26507-0880
304-285-4358, fax: 304-285-4403
PHART@METC.DOE.GOV

Tom Harvey
Chairman and CEO
Global Environment & Tech.
7010 Little River Turnpike
Annandale, VA 22003
703-750-6401; fax: 703-750-6506
TOM.HARVEY@GNET.ORG

Michael Heeb
U.S. Department of Enegy
20400 Germantown Road
Germantown, MD 20874-1290
301-903-7954

James E. Helt
Dir., EM Program Off.
Argonne National Laboratory
9700 S. Cass Ave.
Argonne, IL 60439
708-252-7335; fax: 708-252-5912
HELT@CMT.ANL.GOV

John Hendrikson
Assistant to the Director
Energy & Environ. Research Ctr.
P.O. Box 9018
Grand Forks, ND 58202
701-777-5000; fax: 701-777-5181

Donald Herman
Mgr., Technology Development
FERMCO
P.O. Box 538704, MS 81-2
Cincinnati, OH 45253-8704
513-648-6555; fax: 513-648-6915

Steve Hightower
President
Hi-Mark Group
3589 Commerce Drive
Franklin, OH 45005
513-423-4272; fax: 513-423-5750

Sa V. Ho
Principle Investigator
Monsanto Company
800 N. Lindbergh Blvd.
Mailzone U4E
St. Louis, MO 63167
314-694-5170; fax: 314-694-1531

Larry Holcombe
Project Manager
Radian Corporation
1093 Commerce Park Dr.
Oak Ridge, TN 37830
615-483-9870; fax: 615-483-9061
LARRY_HOLCOMBE@RADIAN.COM

James Hooper
Center Director
Marshall University
Environmental Center
400 Hal Greer Blvd.
Huntington, WV 25755
304-696-5453; fax: 304-696-5454
HOOPER@MARSHALL.EDU

L. John Hoover
President
UTECH, Inc.
11160-E South Lakes Dr., Ste. 363
Reston, VA 22091
703-476-4835; fax: 703-476-1021
LJOHNH@AOL.COM

Philip H. Horton
Mgr., Nuclear Operations
Rockwell
6633 Canoga Ave.
Canoga Park, CA 91303
818-586-5383
PHHORTON@RDYNE.ROCKWELL.COM

William J. Huber
Project Manager
Morgantown Energy Technology Center
U.S. Department of Energy
P.O. Box 880, MS-E06
Morgantown, WV 26507-0880
304-285-4663, fax: 304-285-4403
WHUBER@METC.DOE.GOV

Gregory Hughes
Senior Engineer
Oceaneering Space Systems
10665 Space Center Blvd.
Houston, TX 77058
713-488-9080; fax: 713-488-2027

Jerry M. Hyde
D&D Program Manager
U.S. Department of Energy
19901 Germantown Rd., EM 541
Germantown, MD 20874-1290
301-903-7914; fax: 301-903-7234

Joe Iovenitti
Principal Geologist
Weiss Associates
5500 Shellmound St.
Emeryville, CA 94608-2411
510-450-6141; fax: 510-547-5043
JLI@WEISS.COM

Richard E. Jackson
Mgr., Chemical Hydrogeology
Intera Inc.
6850 Austin Center Blvd., Ste. 300
Austin, TX 78731
512-346-2000; fax: 512-346-9436

Andrew Jarabak
Mgr., Program Development
Westinghouse Electric Corp.
1310 Beulah Road
Pittsburgh, PA 15235
412-256-2881; fax: 412-256-1948

Lisa Jarr
Patent Advisor
Morgantown Energy Technology Center
U.S. Department of Energy
P.O. Box 880, MS-A03
Morgantown, WV 26507-0880
304-285-4555, fax: 304-285-4403
LJARR@METC.DOE.GOV

Joseph L. Jarvis
President
Icon Image Inc.
200 Fairmont Avenue
Fairmont, WV 26554
304-367-9858; fax: 304-367-9884
JJARVIS@PIPELINE.COM

John M. Jevec
Babcock & Wilcox
1562 Beeson St.
Alliance, OH 44601
216-829-7588; fax: 216-829-7831

John D. Johns
Dir., Market Development
ECO Purification Systems Inc.
8813 Waltham Woods Rd., Ste. 304
Baltimore, MD 21234
410-882-1566; fax: 410-882-2910

James O. Johnson
Environmental Engineer
U.S. Department of Energy
Miamisburg Area Office
P.O. Box 66
Miamisburg, OH 45343-0066
513-847-5234; fax: 513-865-4489
JOHNJO@DOE-MD.GOV

Peter M. Jones
Chairman
Alias Group, Inc.
4617 Brookside Drive
Alexandria, VA 22312-1408
703-941-2485; fax: 703-941-8345
ALIAS@CAIS.COM

H. C. Jordan
2006 Dry Creek Road
Roberts, MT 59070
406-445-2416; fax: 406-445-2488

Trina Karolchik
Assoc. Dir., NRCCE
West Virginia University
Evansdale Drive, Box 6064
Morgantown, WV 26506
304-293-2867; fax: 304-293-3749

Raymond S. Kasevich
President
KAI Technologies, Inc.
175 N. New Boston Street
P.O. Box 3059
Woburn, MA 01801
617-932-3328; fax: 617-932-0927

Ken Kasper
1202 Willow Woods Drive
Aiken, SC 29803
803-643-3203

Regina Kaupanger
Butte Program Manager
Basic Technologies Intl.
P.O. Box 3462
Butte, MT 59702
406-494-7401; fax: 406-494-7463

Dean Keiswetter
Dep. Prog. Mgr., Geophysics
Geophex, Ltd.
605 Mercury St.
Raleigh, NC 27603-2343
919-839-8515; fax: 919-839-8528
102173.3625@COMPUSERVE

Mark D. Kessinger
Project Manager
U.S. Army Corps of Engineers
502 Eighth St.
Huntington, WV 25701-2070
304-529-5083; fax: 304-529-5960

Thomas E. Kiess
Staff Officer
National Research Council
2001 Wisconsin Ave., N.W.
Washington, DC 20007
202-334-3074; fax: 202-334-3077
TKIESS@NAS.EDU

Patricia A. Kirk
Vice President Marketing
Spintek
16421 Gothard St., Unit A
Huntington Beach, CA 92647
714-848-3060; fax: 714 848-3034

C. A. Komar
Staff Engineer
Morgantown Energy Technology Center
U.S. Department of Energy
P.O. Box 880, MS-B05
Morgantown, WV 26507-0880
304-285-4107, fax: 304-285-4403
CKOMAR@METC.DOE.GOV

Vijay Kothari
Project Manager
Morgantown Energy Technology Center
U.S. Department of Energy
P.O. Box 880, MS-E06
Morgantown, WV 26507-0880
304-285-4579, fax: 304-285-4403
VKOTHA@METC.DOE.GOV

Richard Kouzes
Dir., Program Development
West Virginia University
Research Office
P.O. Box 6201, Stuart Hall
Morgantown, WV 26506
304-293-8281; fax: 304-293-7498

Matthew Kozak
Principal Staff Consultant
Intera Information Tech.
3609 South Wadsworth Blvd.
Denver, CO 80235
303-985-0005; fax: 303-980-5900
MKOZAK@AOL.COM

Daniel J. Kuchynka
Environmental Programs Dir.
Mirage Systems, Inc.
232 Java Dr.
Sunnyvale, CA 94089
408-744-3262; fax: 408-334-8845
MIRAGE@RAHUL.NET

Roger Kuhl
Venture Development Mgr.
Thermo Technology Ventures Inc.
P.O. Box 1625, MS-3821
Idaho Falls, ID 83415-3821
208-526-7573; fax: 208-526-4492
BOGG@INEL.GOV

Leonel E. Lacos
Research Associate
Florida International Univ.
University Park
Miami, FL 33199
305-348-3727; fax: 305-348-1932

Robert B. Lacount
Professor of Chemistry
Waynesburg College
51 West College Street
Waynesburg, PA 15370
412-852-3286; fax: 412-852-2615

Wu K. Lan
Project Manager
Morgantown Energy Technology Center
U.S. Department of Energy
P.O. Box 880, MS-C05
Morgantown, WV 26507-0880
304-285-4044, fax: 304-285-4403
WLAN@METC.DOE.GOV

Paul Lauterbach
EHS Administration
Pittsburgh Energy Technology Center
P.O. Box 18288
Pittsburgh, PA 15236
412-892-5811; fax: 412-892-4726
LAUTERBA@PETC.DOE.GOV

Will Laveille
Technical Program Officer
U.S. Department of Energy
PM & CD, P.O. Box A
Aiken, SC 29802
803-725-7663; fax: 803-725-3616

Robb Lenhart
Dir., Business & Development
Ctr. Hazardous Materials Res.
320 William Pitt Way
Pittsburgh, PA 15238
412-826-5321; fax: 412-826-5552

James Lexo
Secretary
Nexi Nuclear Expertise, Inc.
10461 White Granite
Oakton, VA 22124
703-352-4912; fax: 703-352-4915
102072.611@COMPUSERVE.COM

Alan Liby
President
Manufacturing Sciences Corp.
804 Kerr Hollow Road
Oak Ridge, TN 37830
615-481-0455; fax: 615-481-3142

Michael J. Lineberry
Director, Tech. Dev. Div.
Argonne National Laboratory
P.O. Box 2528
Idaho Falls, ID 83403-2528
208-533-7434; fax: 208-533-7735
MICHAEL.LINEBERRY@ANL.GOV

Akhtar Lodgher
Mgr., Info. Tech. Programs
Marshall University
Environmental Center
400 Hal Greer Blvd.
Huntington, WV 25755
304-696-2695; fax: 304-696-5454
LODGHER@MARSHALL.EDU

Hsue-Peng Loh
Chemical Engineer
Morgantown Energy Technology Center
U.S. Department of Energy
P.O. Box 880, MS-E01
Morgantown, WV 26507-0880
304-285-4546, fax: 304-285-4403
HLOH@METC.DOE.GOV

Henry L. Lomasney
President
Isotron Corporation
13152 Chef Menteur Hwy.
New Orleans, LA 70129
504-254-4624; fax: 504-254-5172
CLAMASNEY@ATTMAIL.COM

James Longanbach
Project Manager
Morgantown Energy Technology Center
U.S. Department of Energy
P.O. Box 880, MS-C04
Morgantown, WV 26507-0880
304-285-4659, fax: 304-285-4403
JLONGA@METC.DOE.GOV

William E. Lowry
Senior Engineer
Science & Engineering Assoc.
1570 Pacheco St., Ste. D-1
Santa Fe, NM 87505
505-983-6698; fax: 505-983-5868
SEA@ROADRUNNER.COM

Rudi Luyendijk
Mgr., Research Development
Waste Policy Institute
1872 Pratt Dr., Ste. 1600
Blacksburg, VA 24060-6363
703-231-3324; fax: 703-231-3968

Valerie MacNair
Project Manager
Manufacturing Sciences Corp.
804 Kerr Hollow Road
Oak Ridge, TN 37830
615-481-0455; fax: 615-481-3142

Jeet Malhotra
Project Manager
Morgantown Energy Technology Center
U.S. Department of Energy
P.O. Box 880, MS-E06
Morgantown, WV 26507-0880
304-285-4053, fax: 304-285-4403
JMALHO@METC.DOE.GOV

Harry Mann
Waste Mgmt. Consultant
8250 Greenwood Place
Niwot, CO 80503
303-652-2492

Jennifer Marek
Program Manager
U.S. Department of Energy
Savannah River Operations
P.O. Box A
Aiken, SC 29802
803-725-9596; fax: 803-725-3616
JENNI.MAREK@SRS.GOV

Kenneth E. Markel, Jr.
Assoc. Dir., OPM
Morgantown Energy Technology Center
U.S. Department of Energy
P.O. Box 880, MS-E02
Morgantown, WV 26507-0880
304-285-4364, fax: 304 285-4432
KMARKE@METC.DOE.GOV

James Marsh
Physical Scientist
Morgantown Energy Technology Center
U.S. Department of Energy
P.O. Box 880, MS-E02
Morgantown, WV 26507-0880
304-285-4064, fax: 304-285-4403
JMARSH@METC.DOE.GOV

Tom Martin
Contract Specialist
Morgantown Energy Technology Center
U.S. Department of Energy
P.O. Box 880, MS-I07
Morgantown, WV 26507-0880
304-285-4087, fax: 304-285-4403
TMARTI@METC.DOE.GOV

Douglas M. Maynor
Technology Transfer Engineer
U.S. Department of Energy
Ohio Field Office
P.O. Box 3020
Miamisburg, OH 45343-3020
513-865-3986; fax: 513-865-4402

Michael J. McElwee
Engineer
RUST Federal Services
100 Technology Dr.
Anderson, SC 29625
803-646-2413; fax: 803-646-5311

John McFee
IT Coporation/RFETS
P.O. Box 464
Golden, CO 80402-0464
303-966-4340; fax: 303-966-4235

Dane McKinney
Assistant Professor
University of Texas
10100 Burnet Rd., Bldg. 119
Austin, TX 78712
512-471-8772; fax: 512-471-0072

Kliss McNeel
Project Manager
U.S. Department of Energy
Mixed Waste Focus Area
P.O. Box 1625, MS 3875
Idaho Falls, ID 83415-3875
208-526-7925; fax: 208-526-1061

James McNeil
Life Cycle Environmental
1 Poston Road, Suite 300
Charleston, SC 29407
803-556-7110; fax: 803-556-2621
JIMM@LCECHAS.USA.COM

William P. McQuiggan, Jr.
Senior Scientist
Global Environment & Tech.
7010 Little River Turnpike, Ste. 300
Annandale, VA 22003
703-750-6401; fax: 703-750-6506
BILL.MCQUIGGAN@GNET.ORG

Sam Meacham
Executive Vice President
Global Environment & Tech.
7010 Little River Turnpike, Ste. 300
Annandale, VA 22003
703-750-6401; fax: 703-750-6506

Edward W. Merz
Program Manager
Waste Policy Institute
555 Quince Orchard Rd.
Gaithersburg, MD 20872
301-990-3115; fax: 301-990-6150

John B. Meyers
Develop. District Manager
Babcock & Wilcox
Nuclear Environmental Services
1359 Silver Bluff Rd., Ste. A-7
Aiken, SC 29804
804-948-4726; fax: 804-948-4801

Howard W. Mielke
Associate Professor
Xavier Univ. of Louisiana
7325 Palmetto Street
New Orleans, LA 70125
504-483-7523; fax: 504-488-3108

Joel Miles
President/CEO
CER Corporation
955 Grier Dr., Suite A
Las Vegas, NV 89119
702-361-2700; fax: 702-361-7766
CERCORP@TERMINUS.INTERMIND.NET

Tom Miller
Division Manager
United Energy Services Corp.
1113 Poplargrove Ct.
Mt. Airy, MD 21771
301-903-1642; fax: 301-903-7020

Don Moak
Vice President
Water Development Hanford
P.O. Box 4194
West Richland, WA 99353
509-377-3977; fax: 509-377-3980

Darren Mollot
Project Manager
Morgantown Energy Technology Center
U.S. Department of Energy
P.O. Box 880, MS-C04
Morgantown, WV 26507-0880
304-285-5447, fax: 304-285-4403
DMOLLO@METC.DOE.GOV

Kurt Myers
GTS Duratek
8955 Guilford Rd., Ste. 200
Columbia, MD 21046
410-312-5100; fax: 301-621-3211

Neil Naraine
Project Engineer
U.S. Department of Energy
1000 Independence Ave.
Washington, DC 20015
301-903-8175; fax: 301-903-3175
NEILNARAMINE@EM.DOE.GOV

Bill Newton
Environmental Engineer
Aberdeen Test Center
STEAL - EU 633
Aberdeen Prov. Ground, MD 21005-5059
410-278-5294; fax: 410-278-9353

Mark W. Noakes
Development Engineer
Oak Ridge National Lab
P.O. Box 2008, Bldg. 7601
Oak Ridge, TN 37831-6304
423-574-5695; fax: 423-576-2081
MON@ORNL.GOV

Kimberly Nuhfer
Senior Engineer
Energetics, Inc.
2414 Cranberry Square
Morgantown, WV 26505
304-594-1450; fax: 304-594-1485

Charles O'Connor
Director
EEMRI
Chemistry Dept./UNO
New Orleans, LA 70148
504-286-6846; fax: 504-286-6860
CJOCM@UNO.EDU

Donald Oakley
Chief Scientist
Waste Policy Institute
555 Quince Orchard Blvd.
Gaithersburg, MD 20878
301-990-3138; fax: 301-990-6150

Joseph P. Ondek
Chief, Environmental Office
Aberdeen Test Center
CDR, USAATC, STEAC-EV, Bldg. 633
Aberdeen Prov. Ground, MD 21005-5059
410-278-5294; fax: 410-278-9353

James Orr
Vice President
GTS Duratek
8955 Guilford Rd., Ste. 200
Columbia, MD 21046
410-312-5100; fax: 301-621-8211

Jim "Oz" Osborn
Senior Project Scientist
The Robotics Institute
Carnegie Mellon University
5000 Forbes Avenue
Pittsburgh, PA 15213
412-268-6553; fax: 412-268-5895
OZ@CMU.EDU

William K. Overbey
BDM Federal Inc.
1199 Van Voorhis Road
Morgantown, WV 26505

William Owca
General Engineer
DOE - Idaho
850 Energy Drive
Idaho Falls, ID 83401-1562
208-526-1983; fax: 208-526-5964
OWCAWA@INEL.GOV

George A. Pappas
Program Manager
Electronic Sensor Technology
2301 Townsgate Road
Westlake Village, CA 91361
805-495-9388; fax: 805-495-1550

Bob Parkins
General Manager
AE Environmental Service
Route 5, Box 5
Wheeling/Ohio County Airport
Wheeling, WV 26003
304-277-5503; fax: 304-277-5505

John Parkinson
Assistant Director
SRI International
1611 N. Kent St.
Arlington, VA 22209
703-247-8472; fax: 703-247-8569
PARKINSO@WDC.SRI.COM

Keith Patch
Program Manager
TECOGEN
45 First Ave., P.O. Box 8995
Waltham, MA 02554-8995
617-622-1400; fax: 617-622-1025
PATCH@TECOGEN.COM

Andrew Paterson
Partner
Environ. Business Partners
4452 Park Blvd., Suite 306
San Diego, CA 92116
619-295-7685; fax: 619-295-5743

John S. Patten
Mgr., Government Programs
Vortec Corporation
3770 Ridge Pike
Collegeville, PA 19426-3158
215-489-2255; fax: 215-489-3185

Brian Payea
Dir., R&D Management
Molten Metal Technology
51 Sawyer Road
Waltham, MA 02154
617-487-7681; fax: 617-487-7870
BPAYEA@MMT.COM

Kelly D. Pearce
Project Manager
Morgantown Energy Technology Center
U.S. Department of Energy
P.O. Box 880, MS-E06
Morgantown, WV 26507-0880
304-285-5424, fax: 304-285-4403
KPEARC@METC.DOE.GOV

Leon Petrakis
Senior Scientist
Brookhaven National Laboratory
P.O. Box 5000
Upton, NY 11973-5000
516-282-3037; fax: 516-282-4130
PETRAKIS@BNL.GOV

Lawrence G. Piper
Physical Sciences, Inc.
20 New England Business Center
Andover, MA 01810
508-689-0003; fax: 508-689-3232
PIPER@PSICORP.COM

John E. Plunkett
Mgr., Scientific & Engineering
EG&G/TSWV
P.O. Box 880, MS M02
Morgantown, WV 26507-0880
304-285-4605; fax: 304-285-4403
JPLUNK@METC.DOE.GOV

James A. Poston
Project Manager
Morgantown Energy Technology Center
U.S. Department of Energy
P.O. Box 880, MS-N04
Morgantown, WV 26507-0880
304-285-4635, fax: 304-285-4403
JPOSTO@METC.DOE.GOV

Mary Poulton
Assistant Professor
University of Arizona
MGE Dept., Mines 229
Tucson, AZ 85721
520-621-8391; fax: 520-621-8330
MARY@MGE.ARIZONA.EDU

Rod Prodonovich
Business Development
Fenix Systems, Ltd.
31500 W. 13 Mile, Ste. 220
Farmington Hills, MI 48334
810-855-1090; fax: 810-855-1096

John C. Propeck
Mgr., Nuclear Site Services
Oceaneering Hanford
660 Swift Blvd., Suite D
Richland, WA 99352
509-946-5170; fax: 509-946-5261
JPROPECK@AOTECH2.OCEANEERING.COM

Caroline B. Purdy
Program Manager, CMST-CP
U.S. Department of Energy
HQ-EM Office of Tech Dev.
19901 Germantown Road
Germantown, MD 20874-1290
301-903-7672; fax: 301-903-7457

John Quaranta
Engineering Scientist
West Virginia University
P.O. Box 6101, ESB
Morgantown, WV 26506-6101
304-293-3031; fax: 304 293-7109
QUARANTA@CEMR.WVU.EDU

Stephen Rattien
Dir. Commission on Geosciences
National Research Council
2101 Constitution Ave.
Washington, DC 20418
202-334-3600; fax: 202-334-3362
SRATTIEN@NAS.EDU

Brian Reed
Asst. Professor Civil Engineering
West Virginia University
Box 6103
Morgantown, WV 26506
304-293-3031

Stuart E. Reed
Senior Principal Engineer
Babcock & Wilcox
1562 Beeson St.
Alliance, OH 44601
216-829-7350; fax: 216-823-0639
STU.E.REED@RDD.MCDERMOTT.COM

William Rees
Manager, Commercial Develop.
MSE, Inc.
P.O. Box 4078
Butte, MT 59702
406-723-8213; fax: 406-723-8328

Dennis W. Reisenweaver
Sr. Dept. Manager
NES, Inc.
44 Shelter Rock Road
Danbury, CT 06810
203-796-5382; fax: 203-792-3168
DENNIS@ANL.COM

Scott Renninger
Project Manager
Morgantown Energy Technology Center
U.S. Department of Energy
P.O. Box 880, MS-E06
Morgantown, WV 26507-0880
304-285-4790, fax: 304-285-4403
SRENNI@METC.DOE.GOV

Andrew Resnick
Program Manager
Oceaneering Technologies
501 Prince Georges' Blvd.
Upper Marlboro, MD 20774
301-249-3300; fax: 301-390-1309
RESNICK@ADTECH1.OCEANEERING.COM

D. Denise Riggi
Contract Specialist
Morgantown Energy Technology Center
U.S. Department of Energy
P.O. Box 880, MS-I07
Morgantown, WV 26507-0880
304-285-4241, fax: 304-285-4403
DRIGGI@METC.DOE.GOV

Rodrigo V. Rimando, Jr.
D&D Program Manager
DOE - Savannah River
P.O. Box A
Aiken, SC 29802
803-725-4118; fax: 803-725-7548

Pamela Rogers
Delphi Research, Inc.
701 Haines Ave., N.W.
Albuquerque, NM 87102
505-243-3111; fax: 505-243-3188

Terry W. Rogers
President
Delphi Research, Inc.
701 Haines Ave., N.W.
Albuquerque, NM 87102
505-243-3111; fax: 505-243-3188

Michael A. Rollor
Pres. & Chief Operating Off.
Alaron Corporation
17 West Jefferson St., Ste. 104
Rockville, MD 20850
301-340-9622; fax: 301-340-9623

Robert M. Rosselli
Asst. Mgr. for Tech. Mgmt.
U.S. Department of Energy
P.O. Box 550, K8-50
Richland, WA 99352
509-372-4005; fax: 509-372-4549
ROBERT_M_ROSSELLI@RL.GOV

Steven Saggese
Senior Scientist
Science & Engineering Assoc.
2878 Camino Del Rio South, Ste. 315
San Diego, CA 92108
619-294-6982; fax: 619-294-3567
SSAGGESE@SEASD.COM

Lou Salvador
Deputy Director
Morgantown Energy Technology Center
U.S. Department of Energy
P.O. Box 880, MS-A05
Morgantown, WV 26507-0880
304-285-4147, fax: 304-285-4403
LSALVA@METC.DOE.GOV

Jack Saluja
President
Viking Systems International
2070 William Pitt Way
Pittsburgh, PA 15238
412-826-3355; fax: 412-826-3353
JACKSALUJA@AOL.COM

Robert Sameski
Mgr., Business Dev. DOE
M4 Environmental Mgmt. Inc.
1000 Clearview Court
Oak Ridge, TN 37830
615-220-5017; fax: 615-220-5046

H. G. Sanjay
Research Engineer
Arctech, Inc.
14100 Park Meadow Dr.
Chantilly, VA 22021
703-222-0280; fax: 703-222-0299

James Santoianni
Process Development Manager
Vortec Corporation
3770 Ridge Pike
Collegeville, PA 19426
610-489-2255; fax: 610-489-3185

Hagen Schempf
Systems Scientist
Carnegie Mellon University
5000 Forbes Ave., FRC 201
Pittsburgh, PA 15213
412-268-6884; fax: 412-268-5895
HAGEN+@CMU.EDU

Shara Schenck
Assistant to Director
Hemispheric Ctr. Envir. Tech.
Florida International Univer.
University Park Campus
Miami, FL 33199
305-348-3585

Marc Schneckenberger
Industrial Process Manager
Ecology & Environment, Inc.
368 Pleasantview Dr.
Lancaster, NY 14086
716-684-8060; fax: 716-684-0844

John Seaman
Research Associate
SREL/AACES
Drawer E
Aiken, SC 29802
803-725-3981; fax: 803-725-3309
SEAMAN@SREL.EDU

Richard Sebastian
Vice President
Coleman Research Corp.
6551 Loisdale Court, Ste. 800
Springfield, VA 22150
703-719-9200; fax: 703-719-9229
RICHARD_SEBASTIAN@MAIL.CRC.COM

Richard E. Seif
Dep. Mgr., Econ. Dev. Div.
Westinghouse Savannah River Co.
227 Gateway Drive
Aiken, SC 29803
803-652-1830; fax: 803-652-1848
RES@SRS.GOV

James T. Semrau
Senior Technical Manager
Triodyne Inc.
5950 West Touhy Avenue
Niles, IL 60714-4610
708-677-4730; fax: 708-647-2047
TRIODYNE@NSLSILUS.ORG

Sanjiv Shah
Environmental Engineer
SAIC, WPI
1262 Pineview Drive
Morgantown, WV 26505
304-598-9383; fax: 304-598-9392
SANJIV_SHAH@CCMAIL.GMT.SAIC.

Richard C. Shank
Mgr., Technology Integration
Westinghouse Savannah River Co.
139 Darlington Drive
Aiken, SC 29803
803-644-4912; fax: 803-644-4916

Richard B. Sheldon
Field Project Leader
GE Corporate Research & Dev.
Building K-1, Room 3B35
P.O. Box 8
Schenectady, NY 12301
518-382-6565; fax: 518-387-5604
SHELDON@CRD.GE.COM

Robert Sheneman
Environ. Restoration Manager
Princeton Plasma Physics Lab.
P.O. Box 451
Princeton, NJ 08543
609-243-3392; fax: 609-243-3366
RSHENEMA@PPPL.GOV

Mel Shupe
Manager
U.S. Department of Energy
P.O. Box 3462
Butte, MT 59702
406-494-7205; fax: 406-494-7290

Bob Siegrist
Research Associate Professor
Colorado School of Mines/ORNL
Coolbaugh Hall, Room 112
Golden, CO 80401-1887
303-273-3490; fax: 303-273-3413
BS7@ORNL.GOV

Claire H. Sink
Special Asst. for Tech Policy
U.S. Department of Energy
19901 Germantown Road
Germantown, MD 20874
301-903-7928; fax: 301-903-1530

Adam Slifko
Mechanical Engineer
Redzone Robotics, Inc.
2425 Liberty Avenue
Pittsburgh, PA 15222
412-765-3064; fax: 412-765-3069
SLIFKO@REDZONE.COM

Wilkins Smith
Mgr., Morgantown Operations
Energetics, Inc.
2414 Cranberry Square
Morgantown, WV 26505
304-594-1450; fax: 304-594-1485

Kailash Srivastava
Vice President
Arctech, Inc.
14100 Park Meadow Dr.
Chantilly, VA 22021
703-222-0280; fax: 703-222-0299

Edward J. Staples
Vice Pres., Engineering
Electronic Sensor Technology
2301 Townsgate Road
Westlake Village, CA 91361
805-495-9388; fax: 805-495-1550

Ron Staubly
Project Manager
Morgantown Energy Technology Center
U.S. Department of Energy
P.O. Box 880, MS-C04
Morgantown, WV 26507-0880
304-285-4991, fax: 304-285-4403
RSTAUB@METC.DOE.GOV

Edward Steadman
Deputy Associate Director
Energy & Environ. Research Ctr.
P.O. Box 9018
Grand Forks, ND 58202
701-777-5000; fax: 701-777-5181

John L. Steele
Mgr., Focus Area Programs
Westinghouse Savannah River
Building 773-A, Room A-208
Aiken, SC 29808
803-725-1830; fax: 803-725-8136

Ben K. Sternberg
Professor
University of Arizona
MGE Dept., Bldg. No. 12
Tucson, AZ 85721
602-621-2434
BKS@MGE.ARIZONA.EDU

Lorin R. Stieff
Vice President
RAD Elec. Inc.
5714-C Industry Lane
Frederick, MD 21701
301-694-0011; fax: 301-694-0013

Albert J. Sturm, Jr.
Manager, Robotics Group
Par Systems, Inc.
899 Highway 96 West
Shoreview, MN 55126
612-484-7261; fax: 612-483-2689
ASTURM@PAR.COM

Ginger Swartz
President
Swartz & Associates, Inc.
4171 Piedra Place
Boulder, CO 80301
303-440-3527; fax: 303-440 3527

John Swope
Deputy Project Manager
Arrey Industries Corp.
10461 White Granite Dr., Ste. 100
Oakton, VA 22124
703-352-6337

Lyle Taylor
Fellow Scientist
Westinghouse STC
1310 Beulah Road
Pittsburgh, PA 15235-5098
412-256-1650; fax: 412-256-1661
TAYLOR@CIS.PGH.WEC.COM

Delbert Tesar
Professor
Univ. of Texas at Austin
Robotics Research Group
PRC, Mail Code R9925
Austin, TX 78712-1100
512-471-3039; fax: 512-471-3987

Karyanil T. Thomas
Senior Staff Officer
National Research Council
2001 Wisconsin Ave., N.W.
Washington, DC 20007
202-334-3066; fax: 202-334-3077
KTHOMAS@NAS.EDU

Cheryl K. Thornhill
Program Manager
Pacific Northwest Laboratory
P.O. Box 999, MSIN K9-14
Richland, WA 99352
509-375-2532; fax: 509-375-5963
CK_THORNHILL@PNL.GOV

Richard K. Thorpe
Assistant Vice President
SAIC
555 Quince Orchard Rd., Ste. 500
Gaithersburg, MD 20878
301-924-6152; fax: 301-924-4594

John Tourtellott
Program Manager
Mechanical Technology
968 Albany-Shaker Road
Latham, NY 12110
518-785-2181; fax: 518-785-2420

Richard Turton
Professor
West Virginia University
Dept. of Chemical Engineering
Morgantown, WV 26506-6102
304-293-2111; fax: 304-293-4139
TURTON@CEMR.

Sandra P. Ulbricht
Principal Chemist
Babcock & Wilcox
1562 Beeson Street
Alliance, OH 44601
216-829-7715; fax: 216-829-7831

Nancy Ulerich
Mgr., Technology Development
Westinghouse STC
1310 Beulah Road
Pittsburgh, PA 15238
412-256-2198; fax: 412-256-1222

Robert Vagnetti
Project Manager
Waste Policy Institute
1262 Prineview Drive
Morgantown, WV 26505
304-598-9383; fax: 304-598-9372

John G. Vanosdol
Mechanical Engineer
Morgantown Energy Technology Center
U.S. Department of Energy
P.O. Box 880, MS-A04
Morgantown, WV 26507-0880
304-285-5446, fax: 304-285-4403
JVANOS@METC.DOE.GOV

Venkat K. Venkataraman
Project Manager
Morgantown Energy Technology Center
U.S. Department of Energy
P.O. Box 880, MS-C05
Morgantown, WV 26507-0880
304-285-4105, fax: 304-285-4403
VVENKA@METC.DOE.GOV

Gary Voelker
COO
Thermochem, Inc.
10220-H Old Columbia Rd.
Columbia, MD 21046
410-312-6300; fax: 410-312-6303

David K. Walker
Associate Professor
Marshall University
400 Hal Greer Blvd.
Huntington, WV 25755
304-696-2691; fax: 304-696-4646
WALKER@MARSHALL.EDU

Jeffrey S. Walker
Program Manager
U.S. Department of Energy
19901 Germantown Road
Germantown, MD 20874-1290
301-903-7966; fax: 301-903-7234

Lewis Walton
Mgr., Technical Support
B&W Nuclear Environ. Services
2220 Langhorne Road
Lynchburg, VA 24502
804-948-4647; fax: 804-948-4801

Terry Walton
Senior Program Manager
Pacific Northwest Laboratory
3200 Q Avenue
Richland, WA 99352
509-372-6265; fax: 509-372-6268

Kung K. Wang
Professor
West Virginia University
Dept. of Chemistry
Morgantown, WV 26506
304-293-3068; fax: 304-293-4904

Ed Wannemacher
Mgr., Business Development
RUST-Clemson Technical Center
100 Technology Drive
Anderson, SC 29625-6540
803-646-2413; fax: 803-646-5311

Steve Webber
V.P./General Manager
Coleman Research Corp.
6551 Loisdale Ct., Suite 800
Springfield, VA 22150
703-719-9200; fax: 703-719-9229
STEVE.WEBBER@MAIL.CRC.COM

Greg Weber
Senior Research Manager
Energy & Environ. Research Ctr.
P.O. Box 9018
Grand Forks, ND 58202
701-777-5000; fax: 701-777-5181

C. Brooks Weingartner
Environmental Engineer
DOE - Idaho
785 DOE Place
Idaho Falls, ID 83402
208-526-1366; fax: 208-526-6249
WEINGACB@INEL.GOV

Roger Wetzel
Mgr., Technical Assessment
Energetics, Inc.
2414 Cranberry Square
Morgantown, WV 26505
304-594-1450; fax: 304-594-1485

David W. White
Director of Business Develop.
Redzone Robotics, Inc.
2425 Liberty Ave.
Pittsburgh, PA 15222
412-765-3064; fax: 412-765-3069
DWHITE@REDZONE.COM

Paul Wieber
Associate Director, OID
Morgantown Energy Technology Center
U.S. Department of Energy
P.O. Box 880, MS-A03
Morgantown, WV 26507-0880
304-285-4544, fax: 304-285-4403
PWIEBE@METC.DOE.GOV

Carl Williams
Vice Pres., Engineering
Nexi Nuclear Expertise, Inc.
10461 White Granite Drive
Oakton, VA 22124
703-352-4912; fax: 703-352-4915
102072.611@COMPUSERVE.COM

Eric Williams
Deputy Manager
U.S. Department of Energy
Mixed Waste Focus Area
P.O. Box 1625, MS 3875
Idaho Falls, ID 83415
208-526-8089; fax: 208-526-1061

Dwayne A. Wilson
Dir., Business Development
Fluor Daniel, Inc.
3333 Michelson Dr.
Irvine, CA 92730
714-975-3889; fax: 714-975-4793

John S. Wilson
Operations Director
Waste Policy Institute
1262 Pineview Drive
Morgantown, WV 26505
304-598-9383; fax: 304-598-9392

Tom Wrenn
Customer Service Manager
EG&G/TSWV
P.O. Box 880, MS K07
Morgantown, WV 26507-0880
304-285-4749; fax: 304-285-4403
TWRENN@METC.DOE.GOV

James Wright
Lead Mgr., Plume Focus
DOE - Savannah River
Road One, Bldg. 703-46A
Aiken, SC 29802
803-725-9718; fax: 803-725-2123

Edward F. Wuenschel
Project Manager
Mirage Systems, Inc.
232 Java Drive
Sunnyvale, CA 94089-1318
408-752-1600; fax: 408-734-8845
MIRAGE@RAHUL.NET

Christopher Wyatt
Senior Engineer
Energetics, Inc.
2414 Cranberry Square
Morgantown, WV 26505
304-594-1450; fax: 304-594-1485

Ben Yamagata
Van Ness Feldman, P.C.
1050 Thomas Jefferson St., N.W.
Washington, DC 20007
202-298-1857; fax: 202-338-2416

Linton W. Yarbrough
Program Manager, Robotics
U.S. Department of Energy
HQ-EM Office of Tech Dev.
19901 Germantown Road
Germantown, MD 20874
301-903-7923; fax: 301-903-7457
LINTON.YARBROUGH@EM.DOE.GOV

Thomas J. Yule
Manager, D&D
Argonne Natational Laboratory
9700 S. Cass Ave., TD-207
Argonne, IL 60439
708-252-6740; fax: 708-252-1774
TJYULE@ANL.GOV

Bashar M. Zeitoon
Program Manager
Molten Metal Tech, Inc.
51 Sawyer Road
Waltham, MA 02154
617-487-5831; fax: 627-487-7870
BZIETOON@MMT.COM

John Zondlo
Professor
West Virginia University
P.O. Box 6102
Morgantown, WV 26506-6102
304-293-2111

Michael Zuber
Senior Petroleum Engineer
S.A. Holditch & Associates
1310 Commerce Drive
Pittsburgh, PA 15275
412-787-5403; fax: 412-787-2906

William F. Zuroff
Engineer
Westinghouse Hanford Co.
P.O. Box 1970, R1-49
Richland, WA 99352
509-373-1003; fax: 509-373-7226

Author Index

W

X, Y, Z

Organization Index

V, W

* U.S. GOVERNMENT PRINTING OFFICE: 1996-709-136